Elucidation of mechanisms of antibiotic subversion in mycobacteria

Krupa Naran

Division of Medical Microbiology
Department of Clinical Laboratory Sciences

A thesis submitted to the Faculty of Health Sciences, University of Cape Town, in fulfilment of the requirements for the degree of Doctor of Philosophy.
February 2015.

There was a beginning of time.
There was a time
before the beginning of time.
There was a time before the time
before the beginning of time.
There is being.
If there is being,
there must be non-being.
If there is non-being,
There must have been a time
when even non-being didn't exist.
Suddenly there was non-being.
But can any non-being really exist,
And can being not-exist?

I just said something,
But did what I just said really
Say anything, or not?

—Chuang-tzu

Declaration

I declare that this thesis is my own unaided work. It is being submitted for the degree of Doctor of Philosophy at the University of Cape Town. It has not been submitted for any degree or examination at any other university.

Signed by candidate

Krupa Naran

16 February 2015

Date

Abstract

The intrinsic resistance of *Mycobacterium tuberculosis* (*Mtb*) to antibiotics is generally attributed to multiple factors, most significantly the low permeability of the mycobacterial cell wall, the operation of various drug inactivating systems, and the activity of efflux pumps. This study aimed to investigate the role of various components of the "intrinsic resistome" that limit the efficacy of antitubercular agents.

The DNA damage response: the SOS response was hypothesized to play a role in antibiotic-mediated cellular death, and that disabling the mycobacterial SOS response, by generating non-cleavable LexA mutants (*lexA*$^{Ind-}$), could be used as a tool to validate antibiotic-mediated cell death. To this end, the *M. smegmatis* (*Msm*) cleavable LexA was shown to be essential for induced mutagenesis and damage tolerance and that an intact DNA damage repair system is required to respond to antibiotic-mediated DNA damage. In contrast, *Mtb* cleavable LexA was required for induced mutagenesis but not necessarily damage sensitivity. In addition, the *Mtb* SOS response does not contribute significantly to remediation of antibiotic-mediated DNA damage. Collectively, these data suggest that DNA repair mechanisms differ between the mycobacterial species and despite effectively inactivating the LexA-dependent DNA repair mechanism(s) in *Msm* and *Mtb*, these organisms are able to circumvent this pathway and successfully remediate damaged DNA sustained under various conditions. Furthermore, *Mtb* auto-bioluminescent reporter strains were generated by introducing the *lux* operon downstream of the *recA* or *radA* promoters. Analysis of a panel of antimicrobials against these strains allowed for the identification of true DNA-damaging agents and the evaluation of the kinetics of the DNA-damage response, in a concentration- and time-dependent manner.

Efflux-mediated drug resistance: This study aimed to evaluate the interactions between pairwise combinations of selected antimicrobials and efflux pump inhibitors (EPIs), *in vitro* and *ex vivo*, and to identify a novel verapamil (VER)-analogue with improved efficacy against *Mtb*. Subsequently, a candidate EPI was identified, with equivalent *in vitro* synergistic effects to VER when used in combination with various antibiotics but with reduced cytotoxic effects, *ex vivo*, when compared to VER.

Mycothiol-mediated protection: It was hypothesized that undetectable levels of mycothiol (MSH) in *Mtb* would potentiate the use of current antibiotics. To investigate the contribution of the cellular antioxidant, MSH, to the mitigation of antimicrobial efficacy, this study aimed to disrupt MSH production by conditionally knocking-down expression of the essential gene, *mshC*. The *mshC* knock-down mutants (in all configurations) were not anhydrotetracycline (ATC)-regulatable in liquid or on solid medium, which was subsequently validated with quantitative gene expression analysis. These data suggest that a tetracycline (Tet)-based conditional expression system may not be applicable to *mshC*.

In conclusion, *Mtb* has a multitude of inherent mechanisms to subvert the effects of antimicrobial treatment. This study has contributed to the understanding of certain aspects of the intrinsic resistome and in doing so, established tools that can be used in future drug discovery programmes.

Acknowledgements

I am grateful for funding received from the **Carnegie Corporation of New York**, the German Academic Exchange Service (**DAAD**)/National Research Foundation (**NRF**), and the University of Cape Town (**UCT**). I wish to acknowledge **AstraZeneca India** for the 3-month exchange opportunity, funded by the **WIPO** Research Initiative, and Bioventures for Global Health (**BVGH**) and facilitated by the Medical Research Council (**MRC**).

To my beloved parents, **Harry** and **Meera**, words alone cannot describe my gratitude to you both. I thank you for giving your children the freedom to dream, for all your sacrifices, understanding, unshakeable faith and enduring love. My journey is your journey, my achievements are yours. You are my heart. My brother, **Ravi**, through you I have learnt what it means to persevere and that no dream is unattainable. You are my hope. To **Seema** and **Rajen**, you've shown me that success is achievable through balance in life. You are my strength. My nieces, **Rhea** and **Aaral**, may I always live up to your standards. You are my moral compass.

To my supervisor and mentor, **Assoc. Prof. Digby Warner**, you have taught me to go beyond my perceived capabilities and expectations and to make the unimaginable and impossible just another day in Wonderland. I thank you for adopting this once orphaned Master's student, and for guiding, motivating and inspiring me. We are the reflection of those that have the greatest influence in our lives; I am grateful to you for your part.

To my co-supervisor and mentor, **Prof. Valerie Mizrahi**, your astounding knowledge never fails to amaze and inspire me. I thank you for your unwavering guidance and support. You are and will be a role model for generations to come.

To my colleagues at the **MMRU**, you are each special and worthy of every success that may come your way. I thank you all for your assistance, support and for making this a truly memorable experience.

To our collaborator, **Prof. Kelly Chibale**, and colleagues from the UCT Department of Chemistry, I thank you for teaching me to "think like a chemist". Our collaboration has shown me that the mind is pliable and it's never too late to learn something new.

Publications from this thesis

Li, Y., de Kock, C., Smith, P. J., Guzgay, H., Hendricks, D. T., **Naran, K.,** Mizrahi, V., Warner, D. F., Chibale, K. and Smith, G. S. (2012). Synthesis, characterization, and pharmacological evaluation of silicon-containing aminoquinoline organometallic complexes as antiplasmodial, antitumor, and antimycobacterial agents. *Organometallics* 32(1): 141-150.

Tukulula, M., Sharma, R.-K., Meurillon, M., Mahajan, A., **Naran, K.,** Warner, D., Huang, J., Mekonnen, B. and Chibale, K. (2012). Synthesis and antiplasmodial and antimycobacterial evaluation of new nitroimidazole and nitroimidazooxazine derivatives. *ACS medicinal chemistry letters* 4(1): 128-131.

Mjambili, F., Njoroge, M., **Naran, K.,** De Kock, C., Smith, P. J., Mizrahi, V., Warner, D. and Chibale, K. (2014). Synthesis and biological evaluation of 2-aminothiazole derivatives as antimycobacterial and antiplasmodial agents. *Bioorganic & medicinal chemistry letters* 24(2): 560-564.

Singh, K., Kumar, M., Pavadai, E., **Naran, K.,** Warner, D. F., Ruminski, P. G. and Chibale, K. (2014). Synthesis of new verapamil analogues and their evaluation in combination with rifampicin against *Mycobacterium tuberculosis* and molecular docking studies in the binding site of efflux protein *Rv1258c*. *Bioorganic & medicinal chemistry letters* 24(14): 2985-2990.

Naran, K., Singh, K., Kumar, M., Chibale, K. and Warner, D. F. (2015). Identification of a novel verapamil-analogue with improved *in vitro* and *ex vivo* profiles against *Mycobacterium tuberculosis*. In preparation.

Naran, K., Ioerger, T.R., Wasuna, A., Chibale, K., Sacchettini, J.C. and Warner, D.F. (2015). Identification of a novel nitroimidazole with potent activity against *Mycobacterium tuberculosis.* In preparation.

Table of Contents

List of Figures

List of Tables

Chapter 1: General Introduction

1.1 Tuberculosis

Mycobacterium tuberculosis (*Mtb*), the aetiological agent of tuberculosis (TB), is a Gram positive, facultative intracellular pathogen that infects and persists within its obligate human host. *Mtb* infection is initiated upon inhalation of the tubercle bacilli, which are immediately phagocytosed by cells of the innate immune system, principally resident alveolar macrophages. A granuloma develops as lymphocytes, monocytes, and fibroblasts are recruited as a result of a proinflammatory response from the infection of naive alveolar macrophages and dendritic cells (Stallings & Glickman 2010). The bacilli successfully evade both innate and adaptive host immunity by various mechanisms including inhibition of phagosome maturation, resistance to innate bactericidal mechanisms and cytokine-mediated host defences, as well as inhibition of antigen presentation (Harding & Boom 2010). This ability to evade elimination by the host immune system results in primary infection with *Mtb* which is highly successful and subsequently leads to widespread dissemination of the bacilli to most organs in the body (Stallings & Glickman 2010). However, *Mtb* infection is usually asymptomatic in immunocompetent hosts and rarely leads to progressive TB (Philips & Ernst 2012). Based on immunological tests, up to one third of the world's population is thought to be infected with this highly successful pathogen, yet latent and persistent infection is the predominant outcome (Carvalho *et al.,* 2011). This unique ability of *Mtb* to cause latent TB infection (LTBI) creates a huge reservoir of potential cases of reactivation disease and subsequent transmission of the bacillus (Chao & Rubin 2010).

There were an estimated 9 million new cases and 1.5 million TB-related deaths in 2013 (WHO 2014). As such, TB remains a major cause of morbidity and mortality worldwide, more so than any other bacterial infection, despite the existence of both chemotherapeutic interventions as well as vaccine prophylaxis. South Africa is ranked in the top ten countries with the highest incident rates, where about 1 person in every 100 develops active TB (WHO 2014). The Human Immunodeficiency Virus (HIV) pandemic has exacerbated the high burden of TB disease as the virus weakens the immune system, increasing the risk of not only reactivating LTBI, but also rapid progression to active TB soon after infection (Godfrey-Faussett & Ayles 2003; Sharma *et al.,* 2005). In addition, the emergence of resistant *Mtb*

strains, both multidrug resistant (MDR) and extensively drug resistant (XDR), poses a major threat to control of TB worldwide: in 2013, there were an estimated 480 000 cases of MDR-TB (defined as resistance to the two frontline drugs, isoniazid [INH] and rifampicin [RIF]) and 9% of these were classified XDR-TB (MDR-TB plus additional resistance to a fluoroquinolone and any of the second-line injectable agents). Existing preventative measures include the *M. bovis*-derived bacille Calmette–Guérin (BCG) vaccine, which offers inconsistent protection (young children are protected against disseminated TB but protection against pulmonary TB in adolescents and adults remains variable) – and whose efficacy has been unequivocally demonstrated only in low-burden settings (Fine 1995; Trunz *et al.,* 2006). Dishearteningly, a recent phase IIb trial in South African infants showed no efficacy against TB with the candidate vaccine, MVA85A (Tameris *et al.,* 2013). There is, however, much optimism as there are several vaccine candidates at various stages of clinical trials, in a pipeline that was virtually empty in the early 1990s (Andersen & Kaufmann 2014). Until such preventative measures are established, management of the current TB global health crisis is massively dependent on therapeutic intervention in active TB disease.

1.2 Antimycobacterial chemotherapy

Following the discovery of penicillin in 1928, a significant number of antibiotics were discovered in the subsequent years, many of which were used for the treatment of Gram positive infections. Since Waksman's discovery of streptomycin (STM) as the first antimycobacterial drug in 1944, the history of TB chemotherapy has evolved dramatically (Janin 2007; Da Silva & Palomino 2011). Shortly after its introduction as an effective chemotherapy, reports of STM-resistant (STM^R) *Mtb* surfaced, and were later shown to be the result of STM monotherapy (Da Silva & Palomino 2011). By 1955, following the discovery of several drugs with antimycobacterial activity, multidrug therapy became the standard treatment for TB and a regimen of STM, para-aminosalysilic acid (PAS) and INH was developed, and shown to clear TB disease following 18–24 months of therapy (Lienhardt *et al.,* 2012). The major breakthroughs in the treatment of TB came with the discovery in the late 1960s of RIF, which is inhibitory to both actively growing and slowly metabolizing bacilli, and the rediscovery of the antimycobacterial activity of pyrazinamide (PZA), which inhibits semi-dormant bacilli in acidic environments. These drugs ultimately replaced STM,

shortening the duration of treatment considerably, to 9 months (Jawahar 2004; Da Silva & Palomino 2011). Following the resurgence of TB in the 1990's, driven largely by the HIV pandemic, a global TB control policy (*d*irectly *o*bserved *t*herapy, *s*hort course – DOTS) was launched which centred on the direct supervision of drug intake by patients. This strategy relies on a complex regimen of administering several different drugs simultaneously. These include a two-month treatment (the so-called "intensive phase") comprising four drugs – INH, RIF, PZA and ethambutol (EMB) – which is then followed by four months (the "continuation phase") of INH and RIF. This regimen of first-line drugs is highly efficacious, with cure rates of around 90% in HIV-negative patients (WHO 2014). However, as described below, the extended therapy does pose several major challenges, especially in terms of public health resourcing and patient adherence.

1.3 Limitations of current treatment regimens

Several problems are associated with the current treatment for TB that has led to the widespread emergence of drug resistance. *Mtb* has an unusual propensity to down-regulate its metabolism and enter a state of non-replication (Chao & Rubin 2010). This phenomenon, referred to as non-replicating persistence or dormancy, is thought to be induced in response to various stresses (nutritional, hypoxic, nitrosative and acidic) and underlies the need for a long duration of treatment, to ensure sterilization. However, the lengthy and complex regimen leads to complications with patient adherence, resulting in high relapse rates which perpetuate the epidemic (Connolly *et al.,* 2007; Cohen *et al.,* 2013). Furthermore, irregular drug supply, inappropriately prescribed drugs, delayed or limited drug-susceptibility testing as well as the financial burden of treatment and the side effects associated with extensive drug therapy can, in many cases, result in "effective monotherapy". In turn, this leads to emergence of drug resistance (Chatterjee 1997; van Helden *et al.,* 2006; Guy & Mallampalli 2008; Zhang & Yew 2009). The problem is intensified by the subsequent transmission of resistant *Mtb* strains from the index patient to others (Zhang & Yew 2009).

Resistance has evolved to every antibiotic ever introduced into clinical practice (Figure 1.1) (Walsh 2003). *Mtb* acquires MDR and XDR through a step-wise accumulation of chromosomal mutations, each of which confers resistance to individual drugs (Trauner *et al.,* 2014). In the early 1990s, several converging features led to the emergence of MDR-TB

(Sandgren *et al.,* 2009). The perceived threat of MDR-TB is enormous as TB control has been put in jeopardy and the cost of treating MDR-TB patients is extremely high relative to treatment for patients carrying drug-sensitive strains (Dye & Williams 2000). Furthermore, treatment of MDR-TB is currently limited to second-line drugs which are significantly more expensive, less effective as evidenced by the low cure rate, more toxic with serious side effects, and treatment is for at least 18-24 months (Williams & Duncan 2007; WHO 2014). In addition to MDR-TB, reports of XDR-TB have exacerbated this health emergency. In South Africa, XDR-TB is considered endemic: a 2006 outbreak in the small town of Tugela Ferry, KwaZulu-Natal, highlighted the scale of the problem (Gandhi *et al.,* 2006). This study reported that of the 221 patients diagnosed with MDR-TB, 53 of the cases were identified as XDR-TB (Gandhi *et al.,* 2006; Singh *et al.,* 2007), and the mortality rate among patients co-infected with HIV was 98% (Gandhi *et al.,* 2006). Since the Tugela Ferry study, over 100 countries had reported cases of XDR-TB by the end of 2013 (WHO 2014).

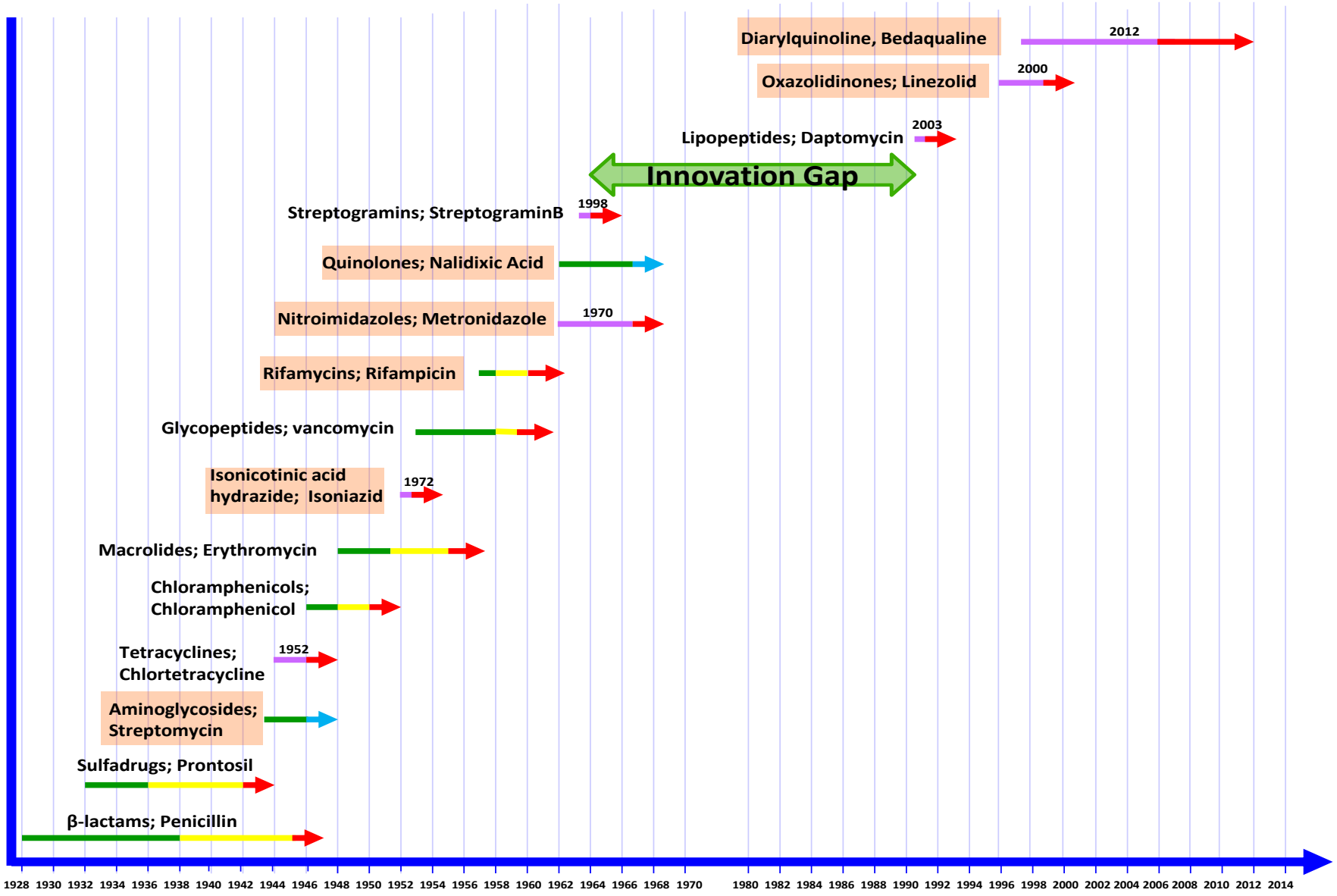
Diarylquinoline, Bedaqualine
2012
Oxazolidinones; Linezolid
2000
Lipopeptides; Daptomycin
2003
Innovation Gap
Streptogramins; StreptograminB
1998
Quinolones; Nalidixic Acid
Nitroimidazoles; Metronidazole
1970
Rifamycins; Rifampicin
Glycopeptides; vancomycin
Isonicotinic acid hydrazide; Isoniazid
1972
Macrolides; Erythromycin
Chloramphenicols; Chloramphenicol
Tetracyclines; Chlortetracycline
1952
Aminoglycosides; Streptomycin
Sulfadrugs; Prontosil
β-lactams; Penicillin
1928 1930 1932 1934 1936 1938 1940 1942 1944 1946 1948 1950 1952 1954 1956 1958 1960 1962 1964 1966 1968 1970 1980 1982 1984 1986 1988 1990 1992 1994 1996 1998 2000 2002 2004 2006 2008 2010 2012 2014
Discovery and Development
Clinical Introduction
Resistance
Clinical Introduction and Resistance (same year)
Laboratory-induced Resistance identified before (year) Clinical Introduction

Figure 1.1: Timeline of the discovery and introduction of antibiotics Resistance has developed against every antibiotic placed into clinical practice. Highlighted antimicrobial classes indicate those that have been approved for the treatment of TB (susceptible and/or resistant strains). Adapted from (Lewis 2013).

Current efforts to control TB focus primarily on treatment of infectious cases, yet 95% of infection exists in an asymptomatic latent form (Young *et al.,* 2009). Treatment of latent infection comprises a lengthy course of INH preventative therapy (IPT) for 9 months or more, but a more rapid and effective treatment is required (WHO 2014). An additional complication is co-infection with HIV: besides the well documented drug-drug interactions between TB drugs and anti-retroviral (ARV) medication, in which RIF causes cytochrome P450 induction and consequently decreases the levels of HIV protease inhibitors, several difficulties associated with TB/HIV combination therapy include high pill burdens (average of 15 pills for 6-22 months), drug toxicities, immune reconstitution inflammatory syndrome (IRIS) directed specifically towards mycobacterial antigens, co-morbid diseases as well as the emergence of both drug resistant TB and drug resistant HIV (Pepper *et al.,* 2007; Lawn *et al.,* 2013).

The limitations of current efforts to control TB necessitates the need for either a constant supply of novel compounds, ideally with novel mechanisms of action (MoAs) that are shorter-acting and active against non-replicating mycobacteria. In addition, there is growing interest in the complementary approach of potentiating existing antibiotics by identifying (non-essential) targets for increasing susceptibility to specific antimicrobials, either in the host (Hawn *et al.,* 2013) or the bacillus (Brynildsen *et al.,* 2013).

1.4 Drug Discovery

Drug discovery has evolved into a multidisciplinary endeavour that includes a consolidation of genomic sciences, molecular biology, combinatorial and medicinal chemistry, pharmacology, and automated high-throughput screening (HTS) whereby “hits”, or compounds that respond positively in a specific assay, give rise to “leads”, or compounds that continue to respond positively in more complex downstream applications (Drews 2000). In this way, the drug discovery pipeline is constantly being replenished with new hits and leads. The success of this drug discovery paradigm is evident in the availability of 10

new or repurposed drugs, at various stages of clinical trials, in the current TB drug development pipeline (NewTBDrugs.org 2015).

1.4.1 Approaches to drug discovery

The search for new antimicrobial compounds can be broadly divided into 2 strategies: the target-based or "rational" approach and the whole-cell, empiric or phenotypic approach.

1.4.1.1 Target-based approaches

The completion of the *Mtb* genome sequence in 1998 provided the possibility of systematically identifying novel drug targets (Cole *et al.,* 1998). Thus began the exploitation of the target-based approaches in which inhibitors were designed to specifically target enzymes known to be essential in vital biosynthetic pathways (Coxon *et al.,* 2012; Lechartier *et al.,* 2014). Following validation of the specific enzyme target, molecular modelling and structural biology form the starting point of this approach. Briefly, structure-based molecular modelling of the target protein, such as high-resolution X-ray crystallography, is exploited to identify new ligands or dock compounds which in turn will guide medicinal chemists in generating compound libraries (Coxon *et al.,* 2012). The target-based approach is advantageous as it aims to ensure that the compound of interest inhibits cellular function in a target-specific manner and so molecular selectivity is achieved. However, the success of this approach relies on the quality of the target as well as the level of validation (Balganesh *et al.,* 2008). In TB drug discovery, several inhibitors have been successfully identified by rational drug design, whether structure-, ligand- or fragment-based (Coxon *et al.,* 2012). However, in the general field of anti-infective drug development, this approach has been largely disappointing, as the majority of the rationally chosen targets were intractable, undruggable, non-essential during disease (due to lack of chemical validation), and/or compromised by the failure to translate potent, selective enzyme activity into whole-cell activity (Payne *et al.,* 2006; Lechartier *et al.,* 2014). In addition, the single-target approach is questionable, as there is increasing evidence that many antibacterials have multiple targets.

1.4.1.2 Phenotypic-based approaches

Through the phenotypic-based approach, compounds are identified that exhibit activity against the whole organism, as opposed to engineering inhibitors for a specific target in a cell-free system. Large libraries of compounds are assessed at known concentrations for their ability to kill *Mtb* under specific growth conditions (Coxon *et al.,* 2012). The identification of several promising drug candidates, including the diarylquinoline, TMC207 (bedaquiline – BDQ); the nitroimidazoles, PA-824 (pretonamid) and OPC-67683 (delamanid); the imidazopyridine amide compound, Q203; the diethylamine, SQ-109; and the benzothiazinone, BTZ043, testifies to the success of whole-cell screening approaches (Lechartier *et al.,* 2014). The major advantage of this approach is that compounds that are able to penetrate the cell wall are selected *a priori* (Williams & Duncan 2007). In addition, phenotypic screening enables early identification of compounds with cidal activity in different metabolic states of the pathogen and thus circumvents a major challenge early in the drug discovery pathway (Balganesh *et al.,* 2008). The obvious disadvantage of this strategy is that the site(s) of action may not be known, and failure to identify the target may limit the ability to generate structure-activity relationships (SARs), whereby the on-target activity and selectivity of analogues based on the lead compound cannot be ensured (Coxon *et al.,* 2012). However, whole-genome sequencing (WGS) to identify mechanisms of resistance (and, in some cases, the MoA), can alleviate this challenge. This is best demonstrated by the recent identification of the targets of BDQ (ATP synthase), the FadD32-targeting diarylcoumarins, and the indolcarboxamides, NITD-304 and NITD-349, which appear to inhibit MmpL3 (Mdluli *et al.,* 2014). An added disadvantage to this approach for TB discovery is the long generation time of *Mtb* (~24 hours) and its limitations on assay development as well as the stringent biosafety requirements that govern experimental manipulation of the bacillus (Williams & Duncan 2007; Coxon *et al.,* 2012).

1.4.2 Challenges with the TB drug discovery paradigm

In 2012, the diarylquinoline BDQ (TMC-207, Sirturo™ from Janssen) became the first new anti-TB drug to be approved by the US Food and Drug Administration (FDA) in more than 40 years. Then, in 2013, delamanid (OPC-67683, Deltyba™ from Otsuka) was approved by two committees. Both drugs are reserved for the treatment of MDR-TB (Mdluli *et al.,* 2014; WHO 2014); therefore, despite the unquestionable significance of these events, enthusiasm is

tempered by the knowledge that the current TB drug pipeline is still not sufficient to curb the pandemic. Concerted efforts to increase the numbers of compounds at all stages of early dug discovery have prompted comprehensive analyses of the methodologies adopted in TB drug discovery programmes globally, in order to define “best practice”; that is, to identify a standard set of optimized assays for the evaluation of compounds against *Mtb* (Franzblau *et al.,* 2012). It is evident that a number of significant challenges have hindered the process of early drug discovery, including the recurrent identification of hits structurally related to current anti-TB drugs or chemotypes with recognized anti-mycobacterial activity; for example, imidazo[1, 2-a]pyridine-3-carboxamides, and tetrahydropyrazolo[1, 5-a]pyrimidine-3-carboxamides, from different small-molecule libraries by various organizations. This has been attributed to the bias imposed by the screening strategies (*in vitro* assay parameters such as oxygen tension, growth medium, *etc.*) as well as similarities between the libraries (Manjunatha & Smith 2014; Mdluli *et al.,* 2014).

In addition, there is a growing appreciation that screening and target identification programmes repeatedly identify the same set of “promiscuous” targets” (Goldman 2013) – that is, molecular targets to which multiple pharmacophores bind, but not necessarily at the same site. These include Ddn, DprE1, MmpL3, AtpE, and QcrB (Lechartier *et al.,* 2014). The reasons for this are not clearly understood, but it may be due to the inherent properties of these targets that make them more accessible and vulnerable to the screening conditions and compound libraries used (Goldman 2013; Lechartier *et al.,* 2014; Mdluli *et al.,* 2014). This bias for membrane-localized targets correlates with compound lipophilicity and an average logP of 4.0, in contrast to current anti-TB drugs that were discovered more than 40 years ago, and which are characterized by average logP values of -1.0 (Goldman 2013). Importantly, lipophilicity impacts pharmacokinetic (PK) parameters, toxicology properties and positively correlates with off-target promiscuity (Tarcsay & Keserű 2013), which severely limits the prospects for advancing highly lipophilic compounds through the development pipeline.

Thus, the screening approach as well as the paucity of novel structural scaffolds may predispose the outcome and limit downstream applications such as the identification of novel targets and the development of screening hits into leads and candidate clinical

compounds. The key questions remain: how will new TB drugs be identified and where to look for them?

1.4.3 Strategies to overcome limitations in TB drug discovery

1.4.3.1 Revising screening approaches and platforms

Diversifying current screening approaches to include the identification of inhibitors of latency, exploitation of conditional knock-down mutants of *Mtb*, siRNA screens, and targeting host functions by immunomodulation and pharmacological manipulation may divulge additional, novel targets (Lechartier *et al.,* 2014). The identification of produgs - compounds that are activated intracellularly by bacteria-specific enzymes and may also have the potential to eradicate dormant persisters – offers an additional screening approach (Lewis 2013). The potential of the pro-drug approach is evident in the success of INH, PZA and ethionamide (ETH), the first two of which constitute the core of TB treatment, although none of these targets persisters.

Target-based whole-cell screening (TB-WCS) overcomes the limitations of the two traditional approaches (target- *versus* phenotype- based screening) by bridging the two and combining the specificity of the target-based approach with the cell-permeation advantage that phenotypic screening provides (DeVito *et al.,* 2002; Young *et al.,* 2006). TB-WCS exploits conditional mutants that underexpress essential genes, as well as various counterscreens for validation of on-target inhibition. Thus, small molecule inhibitors against defined biochemical targets (PanC) or pathways (biotin biosynthesis or pH homeostasis) are identified, as demonstrated recently (Abrahams *et al.,* 2012; Darby *et al.,* 2013; Park *et al.,* 2014).

A species-specific platform is attractive and has had much success with anti-TB drug discovery. The option of screening against the surrogate *Mycobacterium smegmatis* (*Msm*), not only evades the limitation of *Mtb*'s long generation time, but identifies potential hits targeting enzymes conserved among mycobacteria. The success of this approach is evidenced by the discovery of BDQ, which was initially identified from a library screen against *Msm*. It can be argued that screening against surrogate models may delay the development process, as all compounds will eventually be screened against *Mtb*, however a

more focused subset of compounds are selected for evaluation against *Mtb*, which surely expedites the hit triage process (Coxon *et al.,* 2012).

Before reaching their intended molecular target in the bacterial cell, anti-TB drugs need to permeate several barriers: from the blood vessels into the interstitial space of granulomas, followed by diffusion and accumulation in immune cells – including phagolysosomes in which the tubercle bacilli reside – or, in the case of necrotic granulomas and cavities, diffusion though the caseum and, finally, permeation of the lipid-rich mycobacterial cell envelope (Dartois 2014). Given the importance of drug concentration in the plasma and drug penetration in tissue, the PK and pharmacodynamics (PD) parameters should be considered during the lead-compound discovery and lead-compound optimization stages of early drug discovery and can be easily implemented with medium-throughput *in vitro* assays (Franzblau *et al.,* 2012). Novel methods such as the MALDI mass spectrometry imaging (MALDI–MSI) and positron emission tomography (PET) using ^{11}C-or ^{18}F-labelled drugs have recently been used to quantify drug distribution and image drug penetration, respectively (Dartois 2014).

1.4.3.2 Identifying novel chemical scaffolds

The "golden era" of antibiotic discovery from 1940-1960 was dominated by natural products which further proved excellent scaffolds for remodelling and reengineering by medicinal chemists to create subsequent generations of semi-synthetic derivatives (Newman *et al.,* 2003). However, drug discovery programs have gradually shifted away from natural products and replaced these with high-throughput combinatorial chemistry methodologies in which large libraries of synthetic compounds are generated and optimized (Walsh 2003). Owing to limited structural diversity, combinatorial libraries were predicted to be unlikely sources of novel antibiotics when hits only ranging within 1 – 10 µM were identified. This prediction has proven accurate to some extent, as the experience of Novartis attests following a massive undertaking of 3 phenotypic HTS campaigns over a 5 year period with ~2.2 million compounds (Walsh 2003; Manjunatha & Smith 2014). One solution offered to increase the structural diversity of combinatorial libraries is to introduce architectural complexity or functional group density approaching that of natural products. Interestingly, CPZN-45, spectinamides, and macrolides are natural product-derived chemical series that

are currently undergoing lead optimization, while a multitude of natural products themselves have been reported to possess novel structural architecture and exhibit activity against susceptible and MDR strains of *Mtb* (García *et al.,* 2012; Mdluli *et al.,* 2014). This suggests that the reinvestigation of natural product libraries using novel approaches may prove to be promising, as only a small portion of microbes are culturable, while 90-99% of the metagenome is yet to be discovered (Walsh 2003; Ling *et al.,* 2015).

The structural bias in current small-molecule libraries is also likely to be a contributing factor in the repeated identification of the same membrane-bound targets by multiple drug screening programmes. The empirical guidelines currently used to predict oral bioavailability and, by extension, cell permeability, address targets in human eukaryotic cells which have distinct membrane architectures compared to bacterial membranes (Veber *et al.,* 2002; Lipinski *et al.,* 2012). Therefore, the structural and physicochemical properties that govern compound permeability in *Mtb* may differ greatly. Recently, a systematic approach using quantitative tools was developed to evaluate the permeability of diverse small molecules in bacteria with distinct cell envelopes. Accumulation in *Msm* was not shown to correlate with size (molecular weight and surface area) but more weakly correlated with hydrophobicity and polarity. Analytical tools such as these provide a platform for the prediction of permeability of small molecules during the early stages of drug discovery (Davis *et al.,* 2014).

1.5 Mechanisms of drug resistance

1.5.1 Acquired drug resistance

Mtb is thought to be isolated in an ecologically sterile host niche for the bulk of its natural "lifecycle". Therefore, unlike most other bacterial pathogens where horizontal gene transfer by mobile genetic elements such as plasmids, transposons or integrons, mediates acquired drug resistance, in *Mtb* the evolution of resistant strains is driven mainly by the sequential acquisition and accumulation of spontaneous mutations in chromosomal genes (Sandgren *et al.,* 2009; Da Silva & Palomino 2011; Trauner *et al.,* 2014). These mutations alter the drug target and thereby interfere with drug binding, compromise prodrug activation, or cause over-expression of the target (Sandgren *et al.,* 2009; Trauner *et al.,* 2014). RIF resistance (RIF^R) is primarily associated with single-nucleotide substitution mutations in *rpoB*, the gene encoding the β-subunit of the DNA-dependent RNA polymerase, and results in

conformational changes that decrease the affinity for the drug (Da Silva & Palomino 2011). Resistance to fluoroquinolones is associated with amino acid substitutions in the putative fluoroquinolone binding region in *gyrA* and, rarely, in *gyrB*, for clinical isolates (Takiff *et al.,* 1994). EMB resistance (EMB^R) is most often found in association with missense mutations at codon 306 of *embB* which encodes arabinosyl transferase (Starks *et al.,* 2009). However, resistance to EMB has recently been reported to occur through the multistep acquisition of mutations in the *embCAB* operon (Safi *et al.,* 2013; Korkegian *et al.,* 2014). Missense mutations or deletions in the *pncA* gene constitute the main mechanism of PZA resistance (PZA^R), by decreasing the pyrazinamidase activity (Scorpio *et al.,* 1997). Resistance to INH (INH^R) is complex and is associated with mutations in several genes including *ahpC, kasA* and *ndh*, however mutations in *katG* (resulting in a decrease or total loss of catalase/peroxidase activity) and in the *inhA* promoter region (causing overexpression) have been identified as the main molecular mechanisms of resistance (Zhang *et al.,* 1992; Rawat *et al.,* 2003; Da Silva & Palomino 2011).

The mutation rate per base pair (bp) is inversely proportional to the genome size. For many anti-TB drugs, this is estimated at a rate of 10^{-9} mutations per cell division. Since mutations resulting in drug resistance are unlinked, combination therapy reduces the probability of developing resistance to three drugs to 10^{-27} (Da Silva & Palomino 2011). No single pleiotropic mutation has been associated with a MDR phenotype; instead, *Mtb* acquires MDR and XDR through a step-wise accumulation of chromosomal mutations, each of which confers resistance to individual drugs (Motiwala *et al.,* 2010). In addition, drug resistance is also influenced by phenomena such as epistasis – the interaction between genes, where the phenotypic effect of one mutation is determined by the presence of one or more other mutations – and bacterial fitness – that is, where mutation(s) may impact growth rate, virulence, and transmissibility (Koch *et al.,* 2014; Trauner *et al.,* 2014).

1.5.2 Intrinsic drug resistance

It is now generally accepted that the molecular mechanisms that perpetuate antibiotic resistance in a clinical setting are not limited to a single resistance mechanism, but to the combined effect of both intrinsic and genetic resistance mechanisms (Viveiros *et al.,* 2012). These intrinsic mechanisms include the permeability barrier of the mycobacterial cell wall,

mycothiol (MSH)-mediated protection, transcriptional regulation of multidrug resistance, the SOS response, drug modification and degradation and efflux-mediated resistance. These do not function as discrete mechanisms, but rather in a complex and overlapping interplay that constitutes the intricate, dynamic network termed the "intrinsic resistome."

1.5.2.1 The permeability barrier provided by the mycobacterial cell wall

The mycobacterial cell wall is distinct from other microorganisms and presents a formidable permeability barrier to hydrophobic and hydrophilic compounds, a trait attributable to its structural complexity, molecular composition and architectural arrangement. Multiple layers of unique components enable this structure to efficiently impede entry of various antibiotics and also contribute to the survival of the organism under harsh conditions by providing resistance to chemical injury and dehydration (Niederweis *et al.,* 2010). The cell envelop includes an inner plasma membrane, the mycobacterial cell wall core composed of the mycolyl arabinogalactan–peptidoglycan (mAGP) complex, the outer membrane which is covalently linked to the arabinogalactan and a capsule which forms the outermost layer. Interspersed in the outer membrane bilayer, are cell wall proteins and the "free" (non-covalently linked) lipids: phosphatidylinositol mannosides (PIMs), the phthiocerol-containing lipids (PDIM and PGL), lipomannan (LM), and lipoarabinomannan (LAM) (Brennan 2003; Jackson 2014) (Figure 1.2).

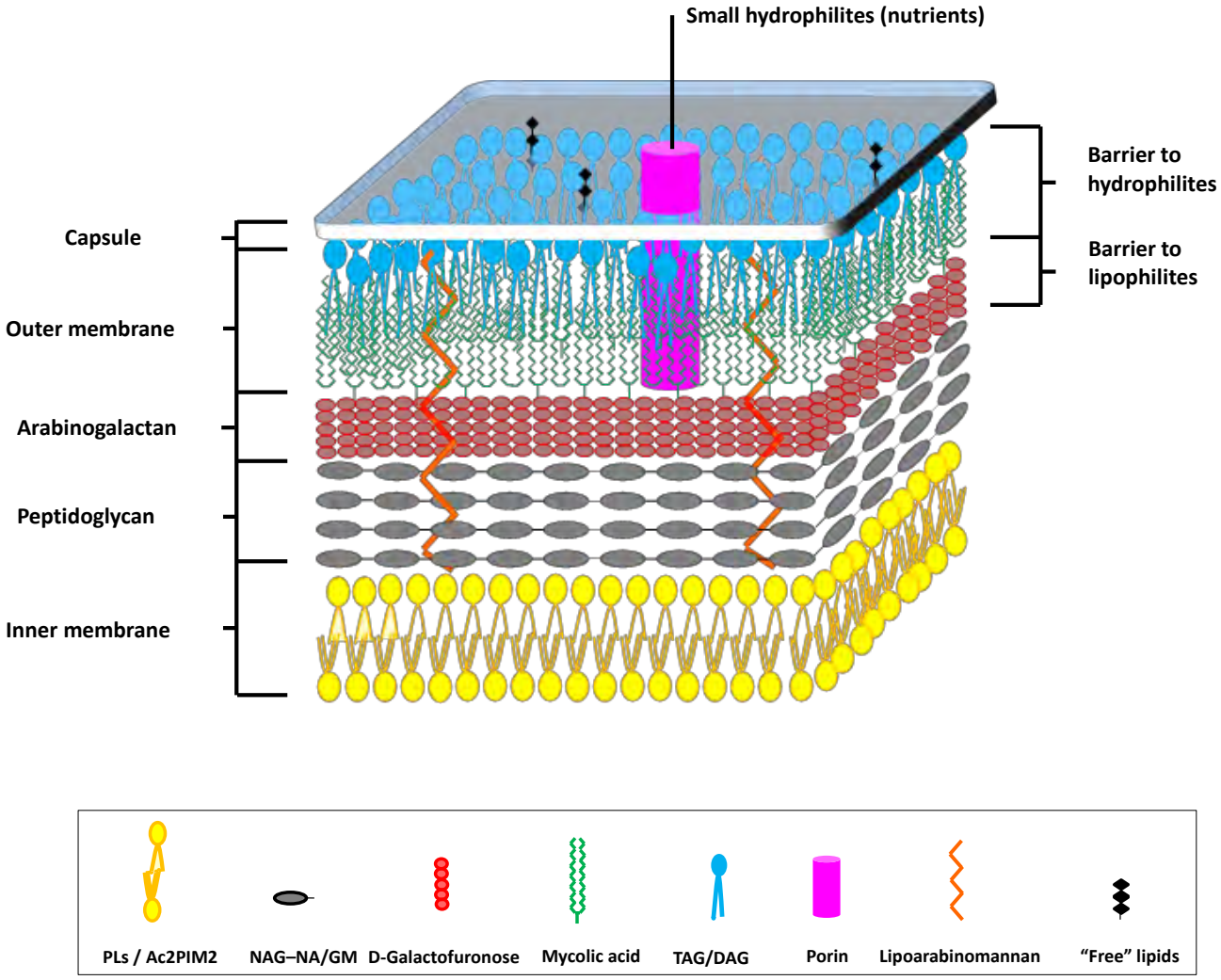

Figure 1.2: The mycobacterial cell envelope. The inner membrane is composed of diacyl phosphatidylinositol dimannoside, which contains four fatty acyl chains within a single molecule. Peptidoglycan consists of repeated alternating sugars N-acetyl glucosamine (NAG) and NA/GM (muramic acid with or without the glycolyl modification), which are cross-linked to a pentapeptide side chain and functions to maintain the shape and size of the cell. Arabinogalactan is the major cell wall polysaccharide and limits the entry of large hydrophobic molecules. Together, these structures form the mycolyl arabinogalactan–peptidoglycan (mAGP) complex. The *Corynebacterineae*–specific cell wall lipid, mycolic acid, comprises 40-60% of the cell's dry weight and is a major permeability barrier to hydrophilic compounds. Triacylglycerols (TAGs), diacyl gycerols (DAGs) and free mycolic acids form an outer leaflet that together with the inner leaflet of mycolic acids are arranged as an outer membrane. Nutrients and small hydrophilite uptake is facilitated by porins (Brennan 2003; Nguyen & Thompson 2006; Bansal-Mutalik & Nikaido 2014) the identity of which remains largely unknown in *Mtb.* Adapted from (Niederweis *et al.,* 2010; Bansal-Mutalik & Nikaido 2014).

The lipids, proteins and lipoglycans of the outer membrane function as signalling and effector molecules during the disease process, while the cell wall core is essential for viability (Brennan 2003). The current mycobacterial cell wall ultrastructure is based on a model suggested by Minnikin which proposed that an asymmetrical bilayer is fashioned by an inner leaflet of mycolic acids and an outer leaflet of free lipids that either intercalate with the mycolates (Minnikin 1982) or form a defined interlayer plane (Rastogi *et al.,* 1991). The hypothesis of a mycobacterial outer membrane was disputed for many years due to contrasting results utilizing different techniques such as freeze-fracture experiments and electron microscopy of ultrathin sections (Puech *et al.,* 2001; Etienne *et al.,* 2005). The first breakthrough validating the existence of an outer membrane was achieved by the use of cryo-electron tomography (CET) and microscopy (CEM) of ultrathin cryosections in *M. smegmatis*, *M. bovis* BCG, and *Corynebacterium glutamicum*, to reveal that the outermost layer of the cell envelope exists as a morphologically symmetrical lipid bilayer (Hoffmann *et al.,* 2008). Mutalik and Nikaido (2014) recently used the unique technique of reverse micellar solution (RMS) extraction to isolate and characterize the outer membrane lipids (Bansal-Mutalik & Nikaido 2014) and thus validated the lipid bilayer structure. In addition, despite the well-established architecture of the inner membrane, it has also been shown that this layer comprises of an unusual lipid, diacyl phosphatidylinositol dimannoside, which contains four fatty acyl chains within a single molecule and thus creates a bilayer environment of unusually low fluidity (Bansal-Mutalik & Nikaido 2014). The existence of two bilayers contributes to the function of the mycobacterial cell wall as a permeability barrier.

The presence or absence of a capsule surrounding the outer membrane has also been a source of controversy (Daffe & Etienne 1999). This structure appears as an electron-transparent zone in conventional electron microscopy preparations as the outermost compartment of the cell envelope. However, CET and CEM of vitreous sections failed to identify this structure, questioning its existence (Chapman *et al.,* 1959; Hoffmann *et al.,* 2008; Zuber *et al.,* 2008). This layer consists of a mixture primarily of polysaccharide and protein, and insignificant amounts of lipid and is considered to have a different molecular composition in pathogenic and non-pathogenic species (Ortalo-Magne *et al.,* 1995; Lemassu *et al.,* 1996; Daffe & Etienne 1999). Recently, it has been shown by a plunge freezing CEM technique that pathogenic mycobacteria produce a thick capsule, only present under

unperturbed growth conditions and easily removed by mild detergents. In addition, the capsule has been reported to play a role in mycobacterial pathogenicity by enhancing the Mycobacterium-macrophage interaction and dampening the pro-inflammatory cytokine response (Sani *et al.,* 2010).

Mycolic acids are a specific and distinct cell wall component of all organisms classified within the *Corynebacterineae* suborder. These lipids represent the key permeability determinant, the hallmark of the mycobacterial cell envelope, and account for up to 40-60% of the cell's dry weight. Mycolic acids covalently associate into a tight, closely packed lipid bilayer and thus form the primary hydrophobic barrier (Chatterjee 1997; Lambert 2002; Gebhardt *et al.,* 2007). They are long chain (C_{70} – C_{90}), α-alkyl branched, β-hydroxy fatty acids and disruption of biosynthesis of these lipids by antibiotic treatment or chemical mutagenesis dramatically alters hydrophobicity, permeability and morphology in *Msm* (Liu & Nikaido 1999; Wang et al., 2000). In addition, the composition and amounts of mycolic acids have been shown to affect the virulence, growth rate, colony morphology, permeability, cording and persistence of *Mtb* (Liu *et al.,* 1996; Glickman *et al.,* 2000). These lipids create a natural fluidity gradient such that the outside surface of the bacillus is the most fluid, providing for the promiscuous association of membrane peripheral components (Liu *et al.,* 1996). Additionally, alterations of mycolyl-arabinogalactan properties affect the natural hydrophilicity of the membrane, while the cell wall integrity influences the surface exposure of the lipids, carbohydrates and proteins. The structure of mycolic acids is functionally important as mutations that affect modification or the length of these fatty acids results in phenotypic variations that affect the permeability properties.

Essentiality of mycolic acids varies amongst the Actinobacteria as mutations that lead to complete loss are lethal to mycobacteria but not to corynebacteria; a mycolic-acid deficient mutant of the latter does not have an outer membrane bilayer and is more permeable to antibiotics, thus highlighting the significance of the outer membrane as a permeability barrier (Liu *et al.,* 1996; Glickman *et al.,* 2000; Gebhardt *et al.,* 2007; Hoffmann *et al.,* 2008; Zuber *et al.,* 2008). There are three types of mycolic acids including α-mycolate, methoxymycolate, and ketomycolate, however, only pathogenic mycobacteria produce significant amounts of cyclopropanated mycolic acids (Barkan *et al.,* 2009). In bacteria and plants, cyclopropanation is a common membrane modification, and although the exact

physiological function is poorly defined, it has a significant effect on membrane fluidity and permeability in various organisms, including *Mtb* (Nagamachi *et al.,* 1991; George *et al.,* 1995; Grogan & Cronan 1997; Yuan *et al.,* 1998). Cyclopropanation of mycolic acids is mediated by methyltransferases which synthesize the cyclopropane rings and methyl branches, and have been shown to be essential for *Mtb* viability, cell wall structure and intrinsic resistance to antibiotics. Recently, Barkan *et al*., 2009 demonstrated the chemical inhibition of multiple mycolic acid methyltransferases with a single compound, resulting in lethal dysregulation of membrane homeostasis.

The exact mechanism by which many antimicrobials enter the mycobacterial cell wall remains unclear; however, passive diffusion, active transport, and facilitated uptake represent the three most common routes. The hydrophobic nature of the cell membrane allows the direct diffusion of lipophilic compounds which then equilibrate with the outside concentration unless there is a binding sink within the cell (Goldman & Scaglione 2004). Cooperative binding has been suggested as a mechanism by which drugs are restricted to the cell membrane, while still allowing diffusion and rotation within the membrane, thereby enhancing the interaction of the drugs with the specific membrane-bound targets. In addition, small, hydrophobic compounds partition into the phospholipid bilayer and then diffuse laterally through the membrane and inhibit metabolic function by interacting with a specific membrane protein (Goldman 2013). In Gram-negative bacteria, antimicrobials from the β-lactam, tetracycline and fluoroquinolone classes have been shown to use porins – proteins that comprise water-filled pores that allow the diffusion of small (typically < 600 kDa) hydrophilic molecules through the barrier (Nikaido 1994; Jap & Walian 1996). Knowledge of porins in slow-growing mycobacteria remains limited, but based on the amphiphilic beta-barrel structure of Gram-negative outer membrane proteins (OMPs), bioinformatics approaches have led to the prediction of several OMP-like porins of *Mtb* (Song *et al.,* 2008; Mah *et al.,* 2010). The exploitation of pore-forming channels as a mechanism of entry for hydrophilic molecules through the cell wall of *Mycobacterium chelonae* was first described by (Trias *et al.,* 1992). Subsequently, two classes of channel-forming outer membrane proteins were defined in mycobacteria: OmpA-like porins in slow-growing mycobacteria and MspA-like porins in fast-growing mycobacteria (Senaratne *et al.,* 1998; Niederweis *et al.,* 1999). OmpA has since been disputed as a channel protein in the

outer membrane of *Mtb*, as deletion of *ompA* did not confer the expected increased drug resistance. Additionally, structural and functional studies have failed to reconcile the suggested porin activity of OmpA (Teriete *et al.,* 2010; Song *et al.,* 2011). A number of studies have subsequently shown a physiological role of OmpA in the adaptation of *Mtb* to an acidic environment, and thus contributing to the role of *Mtb*'s cell wall in pathogenicity (Raynaud *et al.,* 2002; Song *et al.,* 2011). In contrast, the role of the *Msm mspA*-encoding porin, which constitutes 70% of all pores in the *Msm* cell wall, has been established in *mspA*-deletion mutants which displayed reduced uptake of hydrophilic fluoroquinolones, chloramphenicol, β-lactams and, surprisingly, vancomycin (VAN), erythromycin (ERY), and RIF, molecules thought to be too large to diffuse through the MspA pore (Stahl *et al.,* 2001; Stephan *et al.,* 2004; Danilchanka *et al.,* 2008). In general, mycobacteria have 45-fold lower number of pores and 2.5-fold longer pore channels compared to *E. coli*, two determinants that are likely to have contributed to the species-specific, 100-1000-fold less efficient porin pathway for drug uptake (Jarlier & Nikaido 1990; Chambers *et al.,* 1995; Stahl *et al.,* 2001; Engelhardt *et al.,* 2002).

Several pathogenic mycobacteria, including *Mtb* and *M. leprae*, produce two structurally related groups of diesters called phthiocerol dimycocerosates (PDIMs) and phenolic glycolipids (PGLs) which are nonconvalently bound to the outer leaflet of the mycobacterial outer membrane. Earlier studies showed that loss of PDIMs in PGL-deficient *Mtb* strains correlates with reduced virulence in animal models (Camacho *et al.,* 2001). In direct contradiction to these findings, a recent study in which H37Rv strains from several laboratories were whole-genome sequenced, showed that PDIM deficient strains are fully virulent in mice; however, it is possible that compensatory mutation(s) may play a role in retaining virulence (Ioerger *et al.,* 2010). In addition, PGL production has been implicated in the emergence of Lineage 2 (Beijing) *Mtb* strains, in particular the increased likelihood of developing drug resistance (Reed *et al.,* 2007). Thus, PDIMs and PGLs might be considered potentially fruitful drug targets. The first PGL biosynthesis inhibitor was described in 2008 (Ferreras *et al.,* 2008) and was shown to inhibit PGL production in *Mtb* and other pathogenic mycobacteria. Additionally, through comprehensive genetic experimentation, Chavadi *et al*., (2011) demonstrated the role of *M. marinum tesA* (encoding a type II thioesterase) in PDIM and PGL biosynthesis and that inhibition of this enzyme results in hypersusceptibility to

various antibiotics *in vitro* (Chavadi *et al.,* 2011). Reduction of PDIM and PGL in the outer leaflet of the mycobacterial outer membrane by *tesA* deletion results in structural or fluidity alterations which consequently influence the outer-membrane permeability.

In addition to the ingenious architectural design of the mycobacterial cell wall, there are various cell wall-associated molecular components that contribute to the permeability barrier, many of which may prove to be rewarding drug targets in the future. These include the MtrAB two-component system, the only signal transduction system known to be essential in *Mtb* (Zahrt & Deretic 2000). MtrAB contributes to multiple cellular processes including cell wall and cell division homeostasis and alterations in expression of the two-component regulator leads to variations in cell morphology, reduced antibiotic resistance and attenuated virulence (Möker *et al.,* 2004; Fol *et al.,* 2006). Classical two-component systems consist of a transmembrane sensor histidine kinase (HK) and a cytoplasmic response regulatory (RR) protein which are often genetically linked. The sensor kinase recognises specific stimuli and autophosphorylates one of the histidine residues in its cytoplasmic domain which transfers the phosphate group to an aspartate residue of the cognate RR. Phosphorylation activates the RR and modulates expression of RR-regulated genes resulting in alterations of cell behaviour in response to the stimuli (Nguyen *et al.,* 2010). In other organisms, mutations in this system have multiple downstream effects including alterations to cell wall permeability, antibiotic resistance, lipid integrity, biofilm formation, cellular morphology, osmotic stress and virulence (Martin *et al.,* 1999; Liu *et al.,* 2006; Senadheera *et al.,* 2007). In *Mtb*, the *mtrA*-encoded RR is constitutively expressed and transcription is regulated by the virulence σ factor C (*sigC*) (Sun *et al.,* 2004). One of the genes upregulated by *mtrA* overexpression includes *dnaA*, a key component in cell division. Recently, it has been shown that the lipoprotein LpqB modulates MtrB activity through interaction with the extracellular domain, thereby altering MtrA phosphorylation which in turn affects the promoter activity of *dnaA*. Thus, in *Mtb*, cytokinetic and cell wall homeostatic processes are coordinated by a three-component system that includes LpqB, MtrB and MtrA (Nguyen *et al.,* 2010).

1.5.2.2 Overcoming the permeability barrier

Strategies to increase permeation include the identification of cell-penetrating peptides (CCPs), which have been shown to penetrate most biological cell membranes, even when attached to various cargos and acting as drug delivery vehicles (Pujals *et al.,* 2006). Recently, a covalently linked conjugate of the CCP octaarginine and the antimalarial fosmidomycin was shown to reverse resistance of *Mycobacteria* to fosmidomycin (Sparr *et al.,* 2013). It remains to be determined if octaarginine-antibiotic conjugates are effective against *Mtb* and even more interestingly, against non-replicating *Mtb* bacilli which have been shown to undergo cell wall structural alterations which affect the permeability of drugs (Boshoff & Barry III 2006). Thus, the development of novel strategies that improve delivery and bioavailability - and thereby permeation - of existing or novel drugs aims to significantly increase efficacy and/or reduce toxicity effects via dose reduction. In addition, polyamines are naturally occurring aliphatic cations, endogenous to prokaryotic and eukaryotic cells. Although the exact function of these molecules remains unclear, they have recognized functions in various biological processes and are essential for cell growth and proliferation (Tabor & Tabor 1985). Recently, polyamines have been shown to reduce the permeability of the mycobacterial outer membrane to fluoroquinolones by inhibiting drug uptake. In addition it was shown that polyamines increase the survival of the bacillus following fluoroquinolone exposure, suggesting that these molecules may contribute towards the development of drug resistance of intracellular *Mtb* (Sarathy *et al.,* 2013). Thus, targeting polyamines, which has been shown to be effective for cancer prevention, appears to be an interesting approach for increasing permeability of anti-TB drugs (Babbar & Gerner 2011).

1.5.2.2 Transcriptional regulation of multidrug resistance

In addition to the assault of antimicrobial treatment, *Mtb* is exposed to a multitude of environmental stresses, including hypoxia, nutrient starvation and oxidative and genotoxic stress (Hingley-Wilson *et al.,* 2003). To survive these hostile environments, it is imperative for *Mtb* to sense and respond to these conditions appropriately. *Mtb* has complex and extensive regulatory pathways, including σ-factors, two component systems, protein kinases and > 150 transcription factors (TFs), that respond to signals from the changing environment by mediating gene expression (Bowman & Ghosh 2014; Minch *et al.,* 2015). Given the significance of transcriptional regulation and its role in antimicrobial tolerance or intrinsic

drug resistance (Colangeli *et al.,* 2007), a systems-level framework was developed in which the *Mtb* TF-controlled gene regulatory network was mapped and validated by the identification of *furA,* the transcriptional regulator of *katG,* derepression of which results in reduced susceptibility to INH (Rustad *et al.,* 2014). Resources such as this will facilitate the identification of additional components of transcriptional regulation and their role in *Mtb*'s intrinsic resistome, and suggest the potential for systems biology approaches to elucidate the factors which contribute to intrinsic resistance which might be considered an emergent property of a functioning mycobacterial cell.

Members of the *whiB* gene family are exclusive to the Actinomycetes. Seven *whiB*-like genes have been identified in *Mtb* and these perform critical roles in cell division, redox homeostasis, virulence and antibiotic resistance (Morris *et al.,* 2005; Geiman *et al.,* 2006; Singh *et al.,* 2009). Deletion of *whiB7* in various mycobacterial species results in a multidrug-sensitive phenotype *in vitro*, suggesting that WhiB7 is an ancestral multidrug resistance determinant. Gene expression profiling analyses have shown that *whiB7* determines drug resistance by activating the expression of at least eight genes, the functions of some of which are associated with intrinsic drug resistance (e.g. the efflux pump, *tap*, and a ribosome modifying enzyme, *erm37*) (Philalay *et al.,* 2004; Morris *et al.,* 2005). In addition, upon antibiotic treatment, *whiB7* induces the *eis* (enhanced intracellular survival) gene suggesting that WhiB7 activation not only contributes to drug resistance, but to enhanced mycobacterial tolerance to host immunity. Thus, targeting WhiB7 might result in preventing the emergence of drug resistant bacilli as well as effective sterilization. Recently, it has been shown that upon antibiotic treatment, the transcriptional activation of *whiB7*-dependent intrinsic drug resistance is induced upon a reductive shift of redox metabolism in response to the inhibition of diverse cellular targets (in particular, inhibition of protein biosynthesis) (Burian *et al.,* 2012). WhiB7 is activated in response to a metabolic shift to increased reducing potential. During normal growth conditions, *whiB7* plays a key role in maintaining a reduced cytoplasmic environment by directly or indirectly regulating the MSH concentration. Upon antibiotic treatment, the oxidized form of MSH, mycothione (MSSM), decreases to undetectable levels, suggesting that *whiB7* contributes in regulating MSSM reduction (Burian *et al.,* 2012) (The role of MSH detoxification in *Mtb*'s intrinsic resistome is discussed further in Chapter 6).

In response to antibiotic treatment, *Mtb* generates a specific and coordinated transcriptional response. Certain antibiotic-induced transcriptional changes contribute to the adaptation of *Mtb* as they induce antimicrobial tolerance or intrinsic drug resistance. Of course, factors that regulate the expression of genes are also potentially significant. Lsr2 is a small histone-like protein which is highly conserved among mycobacteria and has been shown to regulate antibiotic-induced expression of the multidrug efflux pump-encoding *iniBAC* operon and *efpA* gene. Lsr2 was shown to repress a wide variety of DNA-interacting enzymes suggesting transcriptional regulation of several important pathways in mycobacteria (Colangeli *et al.,* 2007). In addition to its role as a global transcriptional regulator, electron microscopy and DNA binding studies suggest that Lsr2 binds to DNA and physically protects it from reactive intermediates (Colangeli *et al.,* 2009). Therefore, while the essentiality of the *lsr2* remains controversial, its established role as a significant contributor to *Mtb*'s intrinsic resistome suggests it is a potential drug target.

1.5.2.3 Drug modification and degradation

Mycobacteria are able to inactivate antibiotics by chemical modifications, and this provides another mechanism for intrinsic resistance. A well-established example is the inactivation of aminoglycosides via three known chemical modifications: acetylCoA-dependent N-acetylation of amino groups, catalysed by aminoglycoside acetyltransferases (AACs); ATP-dependent phosphorylation of hydroxyl groups by aminoglycoside phosphotransferases (APHs); and ATP-dependent O-adenylation by aminoglycoside nucleotransferases (ANTs) (Wright 2005). In *Mtb*, limited data exist on the role of these enzymes in the intrinsic resistome: of the four predicted enzymes in the genome, only the *Rv0262c*-encoded AAC has been biochemically validated as a functional aminoglycoside-modifying enzyme, although it does not contribute to clinically relevant aminoglycoside resistance (which is uniquely attributed to point mutations in 16S rRNA) (Hegde *et al.,* 2001; Draker *et al.,* 2003). Interestingly, structural analyses of *Mtb*'s AAC suggest that this enzyme may play a role in MSH biosynthesis by regulating the flux of MSH precursors via acetylation and deacetylation (Vetting *et al.,* 2003). Similarly, while resistance to RIF results primarily from mutations in *rpoB,* approximately 5% of clinical RIF-resistant *Mtb* isolates do not have mutations in this gene, suggesting a role for an alternative resistance mechanism (Telenti *et al.,* 1993). Three mechanisms of RIF inactivation by chemical modifications have been described:

phosphorylation, glucosylation and ribosylation. Inactivation by ribosylation, catalysed by adenosine diphosphate (ADP) ribosyltransferase, has only been detected in *Mycobacterium* and closely related taxa (Dabbs *et al.,* 1995; Tanaka *et al.,* 1996).

β-lactams are a class of antibiotics that inhibit cell wall biosynthesis, specifically via inhibition of peptidoglycan-modifying peptidases (D,D-penicillin binding proteins, PBPs, and the L,D-transpeptidases) (Zapun *et al.,* 2008). Following β-lactam exposure, a number of molecular pathways to cell death have been identified including autolysis, induced autolysis, holin: antiholin and oxidative damage pathways (Wivagg *et al.,* 2014). Consequently, there exist a number of mechanisms by which resistance to β-lactams is acquired, of which two are considered the principal mechanisms: decreasing the effective concentration of β-lactams at the general site of action, and modification of the PBPs such that sufficient transpeptidase activity remains to permit survival even in the presence of the β-lactam. Alterations to β-lactam concentrations result from modifications to outer membrane permeability, changes in β-lactamase activity and changes in efflux pump activity. *Mtb* is highly resistant to β-lactams as a result of a strong, constitutive β-lactamase (encoded by *blaC*) that binds and degrades these antibiotics. The co-administration of β-lactams with β-lactamase inhibitors, such as clavulanate or sublactam, or β-lactams which are resistant to β-lactamases such as the carbapenems with clavulanate has been shown to circumvent this resistance mechanism (Hugonnet & Blanchard 2007; Hugonnet *et al.,* 2009). Therefore, resistance to β-lactams offers an instructive example of the interplay between intrinsic mechanisms by which permeability, drug inactivation by β-lactamase activity, and active efflux by multidrug pumps, each or in combination contribute to the resistance profile.

1.6 Aims and objectives of this study

In addition to the low permeability of the mycobacterial cell wall, transcriptional regulation and the operation of various drug inactivating/modifying systems, there are three major mechanisms that contribute to the intrinsic resistome of *Mtb* and that limit the efficacy of anti-TB agents. This study aimed to investigate the roles of the DNA damage (or SOS) response, efflux-mediated drug resistance, and MSH-mediated protection as integral mechanisms of *Mtb*'s intrinsic resistome to subvert antibiotic efficacy. In conjunction with examining the physiological functions of these mechanisms, various tools were developed to aid drug discovery platforms in the search for novel agents that may inhibit these systems and so disarm the protective effect of the mycobacterial intrinsic resistome.

Chapter 2: General Materials and Methods

2.1 Strains and growth conditions

Details on study-specific strains and plasmids are described in the relevant Chapters, with general strains and plasmids listed here (Table 2.1). All bacterial strains utilized in this study were stored at -80°C in 30% glycerol (v/v).

Table 2.1: General bacterial strains used in this study

Strain	Description/ Genotype	Reference/ Source
***Escherichia coli* (*E. coli*)**		
DH5α	*supE44 ΔlacU169* (*F80 lacZΔM15*) *hsdR17 recA1 endA1 gyrA96 thi-1 relA1*	Promega
***Mycobacterium smegmatis* (*Msm*)**		
mc^2155	High frequency transformation mutant of *Msm* ATCC 706	(Snapper *et al.,* 1990)
***Mycobacterium tuberculosis* (*Mtb*)**		
H37RvMA	Virulent reference laboratory strain of *Mtb* ATCC 27294	(Ioerger *et al.,* 2010)

E. coli. All strains were cultured overnight on Luria-Bertani (LB) Agar (IncoTherm Incubator, Labotec) or in LB Broth IncoShake Incubator, Labotec) at 37°C. Alternatively, strains harbouring large plasmids (≥ 8 kbp) were cultured at 30°C (IncoCool Incubator, Labotec) for 48 hr to minimize plasmid rearrangements.

Msm. Unless otherwise indicated, all strains were cultured on Middlebrook 7H10 (Difco™) supplemented with 0.5% glycerol and 10% (v/v) Middlebrook Oleic Acid Dextrose Catalase (OADC) enrichment (Difco™) (7H10/OADC), or in Middlebrook 7H9 supplemented with 0.2% glycerol, 10% (v/v) Middlebrook OADC, and 0.05% Tween80 (7H9/OADC). Liquid cultures were cultured in Erlenmeyer flasks at 37°C shaking (IncoShake Incubator, Labotec). For negative selection of transformants carrying the *sacB* gene, 2% (w/v) sucrose was used. For

positive selection, 2 mg/ml X-gal (5-bromo-4-chloro-3-indolyl-beta-D-galacto-pyranoside) was utilized.

Mtb. Unless otherwise indicated, all strains were cultured on solid 7H10/OADC or in liquid 7H9/OADC. Liquid cultures were grown at 37°C in tissue culture flasks that were placed flat. All culturing and manipulations of *Mtb* strains were performed in a Biosafety Level 3 laboratory, in a Class II flow cabinet at negative pressure (160 - 170 kPa). Negative and positive selection of transformants was performed as described for *Msm.*

2.2 Antimicrobial agents

For *E. coli*, liquid and solid media were supplemented with antibiotics at the following concentrations: kanamycin (KAN), 50µg/ml; ampicillin (AMP), 200µg/ml; hygromycin (HYG), 200 µg/ml; and Gentamycin (GEN), 20µg/ml. For *Msm* and *Mtb* strains, antibiotics were used at the following concentrations: KAN, 20 µg/ml; HYG, 50 µg/ml; GEN, 2.5 µg/ml. Antimicrobial stock solutions were stored at 4°C.

Selection of transformants. For negative selection of *E. coli* and mycobacterial clones that carry the *sacB* gene, 5% (w/v) and 2% (w/v) sucrose (Suc), respectively, was used in solid media. For positive selection by disruption of *lacZ*, 50 µl X-gal (5-bromo-4-chloro-3-indolyl-β-D-galactopyranoside; 20 mg/ml in deionised dimethyl formamide) was utilized per 25 ml plate.

2.3 DNA Extraction

2.3.1 Plasmid DNA extraction and purification from *E. coli*

Small-scale plasmid preparation. Cultures were grown overnight (37°C) or over 48 hr (30°C) and harvested by centrifugation at room temperature (Eppendorf 5415D; 15000 *× g* for 1 min). The supernatant was discarded and the pellet was resuspended in 100 µl Lysis Solution I (0.5 M glucose, 50 mM Tris-HCl pH 8.0, 10 mM EDTA), followed by the addition of 200 µl Solution II (0.2 M NaOH, 1% SDS) and mixed gently. After a 5 min incubation at room temperature, 150 µl of neutralization Solution III (3 M potassium acetate, pH 5.5) was added and gently mixed followed by centrifugation at 15000 *× g* for 5min at room temperature. The supernatant was collected and treated with RNase A (1 µl of 10 µg/ml stock solution;

Sigma Aldrich) for 10 min at 37°C. Plasmid DNA was precipitated by adding 350 µl of isopropanol, incubation for 10 min at room temperature and centrifuging at 15000 × *g* for 10 min. The pelleted DNA was washed with 70% ice cold ethanol and dried at 40°C in a vacuum centrifuge (MiVac DNA concentrator, GeneVac). The plasmid DNA was resuspended in 20 µl of sterile distilled water (sdH_2O).

Large-scale plasmid preparation. Cultures were grown overnight or over 48 hr in 50 ml of LB broth and harvested by centrifugation at 3901 × *g* for 10 min (Beckmann Allegra X-22R). Thereafter, the extraction method was as described for the small-scale extraction except that the solution volumes were increased by a factor of 10. The plasmid DNA was resuspended in 500µl dsH_2O and precipitated with $1/10^{th}$ volume sodium acetate (3M). Equal volumes of phenol/chloroform (1:1; v/v) solution was added to purify the DNA, followed by vigorous mixing and centrifugation 15000 × *g* for 10 min (Eppendorf 5415D Centrifuge) at room temperature. The aqueous phase was collected and an equal volume of chloroform: isoamyl alcohol (24:1; v/v) was added, mixed vigorously, and centrifuged at 15000 × *g* for 10 min at room temperature. The aqueous phase was collected and the plasmid DNA was further precipitated by adding 2.5 volumes of ice-cold 100% ethanol. The solution was incubated for 45 min at -20°C and the precipitated DNA was collected by centrifugation at 15000 × *g* for 20 min at room temperature. The DNA pellet was washed with ice cold 70% ethanol, dried in a vacuum centrifuge and resuspended in 50 µl sdH_2O.

2.3.2 Chromosomal DNA extraction and purification from mycobacteria

Msm. Chromosomal DNA was isolated using a modified cetyltrimethylammonium bromide (CTAB) method (Larsen 2000). Briefly, cells were heat killed at 65°C for 20 min and harvested by centrifugation at 16100 × *g* for 1 min. The pellet was resuspended in 500 µl TE buffer (10mM Tris-HCl pH 8.0, and 1mM EDTA) and 50µl lysozyme (10 mg/ml) was added. After overnight incubation at 37°C, 70 µl 10% SDS and 6 µl proteinase K (10 mg/ml) were added and the mixture incubated for 2 hr at 65°C in a Thermomixer Compact (Eppendorf) set to 400 rpm. Thereafter, 80 µl pre-warmed CTAB (10% CTAB prepared in 0.7M NaCl) and 100µl 5M NaCl were added and the mixture was further incubated for 10 min at 65°C. An equal volume of chloroform:isoamyl alcohol (24:1 v/v) was added to degrade residual proteins and mixture was centrifuges for 5 min at 16100 × *g*. The aqueous phase was collected and added to an equal volume of ice cold isopropanol and incubated on ice for 30

min. The precipitated DNA was collected by centrifugation at 16100 × *g* for 20 min at room temperature and the pellet was washed with ice cold 70% ethanol, dried in a vacuum centrifuge and resuspended in 100 µl sdH_2O.

Mtb. The CTAB method used for *Mtb* DNA extraction was similar to that described for *Msm*. All procedures prior to the overnight lysozyme step were performed in a Biosafety Level 3 laboratory, in a Class II flow cabinet at negative pressure (160 - 170 kPa). Minor deviations from the previously described method were carried out. Briefly, *Mtb* cells were harvested by centrifugation at 3901 × *g* for 10 min and the pellet was resuspended in 500 µl TE buffer followed by heat kill at 80°C for 1 hr and 50 µl lysozyme treatment (10 mg/ml), overnight at 37°C. The following day, 70 µl of 10% SDS and 50 µl of proteinase K (10 mg/ml) were added to the mixture and incubated 65°C for 2 hr in a Thermomixer Compact (Eppendorf) set to 400 rpm. Thereafter, 100 µl pre-warmed 10% CTAB and 100µl 5M NaCl were added and incubated for 15 min at 65°C (Thermomixer). The mixtures were placed at -70°C for 15 min, then removed and allowed to thaw before a further incubation at 65°C for 15 min in the Thermomixer. An equal volume of chloroform:isoamylalcohol (24:1) was added to the mixture and tubes were inverted several times to mix, then harvested by centrifugation at 16100 × *g* for 10 min. The aqueous phase was collected and added to an equal volume of ice cold isopropanol and incubated overnight at 4°C. The following day, precipitated DNA was collected by centrifugation at 16100 × *g* for 20 min at room temperature and the pellet was washed with ice cold 70% ethanol, dried in a vacuum centrifuge and resuspended in 55 µl sdH_2O.

2.3.3 Small-scale chromosomal DNA extraction from mycobacteria

The colony boil method was used for the isolation of genomic DNA for PCR screening. Colonies were picked from agar plates and resuspended in 100 µl of TE buffer (10 mM Tris·HCl pH 8.0, 0.1 mM EDTA). For reference, 10 µl of the suspension was spotted onto an agar plate. The remaining 90 µl was heat-killed at 95°C for 20 min. An equal volume of chloroform was added, and the mixture centrifuged at 16100 × *g* for 5 min. The aqueous phase was carefully extracted into fresh microfuge tubes and 2 µl was used as the DNA template for PCR.

2.4 DNA manipulations

All DNA manipulations were and molecular biology techniques were performed according to standard protocols (Sambrook *et al.,* 1989; Sambrook & Russell 2001)

Agarose gel electrophoresis. Standard electrophoretic techniques were used. High molecular weight DNA fragments were separated on 1% agarose gels while low molecular weight fragments were separated on 2% gels. Gels were prepared with 1xTAE (40 mM Tris-acetic acid, 1 mM Na_2EDTA pH 8.0), agarose powder (Sigma-Aldrich) and 0.5 µg/ml ethidium bromide. DNA samples were loaded with tracking dye (0.025% bromophenol blue in 30% glycerol). Fragment sizes were assessed using lambda DNA molecular weight markers (III-VI; Roche Applied Science, Germany). Gels were electrophoresed in a Mini-Sub Cell GT mini gel horizontal submarine unit (Bio-Rad) at 80-100 volts and visualized under UV-light using the Gel Doc (WealTeach Keta Imaging System).

Recovery of DNA fragments form agarose gels and quantification. DNA fragments were excised from the agarose gels and purified using the Nucleospin Extract II Kit (Macherey-Nagel) as per the manufacturer‘s instructions. DNA was eluted in 30 µl sdH_2O and quantified by agarose gel electrophoresis (by comparison to DNA molecular weight markers) or on a NanoDrop ND-1000 Spectrophotometer (Thermo Scientific).

Restriction digests. Restriction enzymes were purchased from New England Biolabs Inc. (The Scientific Group) or Fermentas (Thermo Scientific). All restriction enzyme digests were performed at 37°C unless otherwise required by the manufacturer. Plasmid DNA (1 µg) was digested for 2 hr (or overnight) and mycobacterial DNA (5 µg) was digested overnight with the appropriate reaction buffer(s). For confirmation of point mutation/ restriction site, purified PCR fragments were digested for 2-3 hr with the appropriate reaction buffer(s). Digested DNA fragments were separated and analysed on agarose gels (as described previously).

Dephosphorylation of vector DNA. To prevent vector re-ligation**,** linearized plasmid DNA was treated with Antarctic Alkaline Phosphatase (New England Biolabs Inc.) to ensure removal of the 5‘-phosphate. The dephosphorylation reaction was performed at 37°C for 1

hr after followed by heat inactivation of the enzyme at 65°C for 20 min (as per the manufacturer's instructions).

Ligations of DNA fragments. Ligation reactions were carried out using the Fast-link™ ligation kit (Epicentre® Biotechnologies) as per the manufacturer's instructions. Following inactivation of the ligase at 70°C for 15 min, competent *E. coli* DH5α cells were transformed with the entire reaction.

Polymerase Chain Reaction (PCR). To generate fragments to be used in subsequent cloning procedures, DNA was amplified with Phusion High-Fidelity DNA polymerase (Finnzymes), due to the low error rate of this polymerase (4.4×10^{-7}). As per the manufacturer's instructions, 20-50 µl reactions contained: 1 × HF reaction buffer, 200 µM of each dNTP, 0.5 µM of each primer, 3% DMSO, 0.02 U/µl of DNA polymerase and 10-100 ng of plasmid or genomic DNA. DNA amplifications were performed using the following parameters: initial denaturation at 98°C for 3 min, followed by 30 cycles of denaturation (98°C for 10 s), annealing (for 30 s), extension (72°C for 30s/kb), and final extension at 72°C for 7 min. The annealing temperature varied according to the melting temperature (Tm) of individual primer sets (according to the manufacturer's instructions). For screening purposes, DNA was amplified using FastStart Taq (Roche) as per the manufacturer's instructions. Briefly, 20-50 µl reactions contained 10-100 ng of plasmid or genomic DNA 1 × PCR reaction buffer (includes $MgCl_2$), 200 µM of each dNTP, 0.5-1.0 µM of each primer, 1 × GC-rich solution, and 2U/50 µl of DNA polymerase. The following thermal cycler parameters were used: initial denaturation at 95°C for 4 min, followed by 30 cycles of denaturation (95°C for 30 s), annealing (60°C for 30 s), extension (72°C for 60s/kb), and a final extension at 72°C for 7 min. All PCR reactions were carried out in the MyCycler™ thermal cycler (Bio-Rad) with oligonucleotide primers purchased from Integrated DNA Technologies (IDT).

2.5 Bacterial transformation

2.5.1 Chemical transformation of *E. coli*

Preparation of competent cells. The rubidium chloride method obtained from Dr P. Stolt was used to prepare competent cells. Briefly, 1 ml of an overnight culture of *E. coli* DH5α was inoculated into 100 ml LB and grown to an OD_{600} of 0.4-0.5. The cells were kept on ice

for 15 min then harvested by centrifugation at 3901 × *g* for 5 min at 4°C. The pellet was resuspended in 20 ml transformation buffer (Tfb) I (30 mM potassium acetate, 100 mM rubidium chloride, 10 mM calcium chloride, 50 mM manganese chloride, and 15% v/v glycerol; pH 5.8). The mixture was chilled on ice for 15 min and harvested by centrifugation (3901 × *g* for 5 min at 4°C). The pellet was resuspended in 2 ml TfbII (10 mM MOPS, 75 mM calcium chloride, 10 mM rubidium chloride and 15% v/v glycerol; pH 6.5). Aliquots of 500 µl were flash-frozen in ethanol and stored at -80°C until required.

Transformation with plasmid DNA. Competent *E. coli* DH5α cells were thawed on ice and 100 µl aliquots were incubated with up to 1 µg plasmid DNA on ice for 20 min. Thereafter, cells were heat-shocked at 42° for 90 s, immediately placed on ice for 1-2 min and rescued in 500 µl of 2TY (Tryptone Yeast broth) for 1 hr at 37°C. Cells were plated on LA plates containing the appropriate antibiotics, and incubated overnight at 37°C (Sambrook *et al.,* 1989; Sambrook & Russell 2001) or for two days at 30°C, for plasmids larger than 8 kbp (Parish & Stoker 2000).

2.5.2 Transformation of mycobacteria by electroporation

Mycobacteria were electroporated with plasmid DNA according to (Larsen 2000; Gordhan & Parish 2001).

***Msm*.** Briefly, 100 ml of 7H9/OADC medium was inoculated with an overnight culture and grown to an OD_{600} of 0.8-1.0 at 37°C. Cells were harvested by centrifugation at 3901 *× g* for 10 minutes at 4°C and washed three times in pre-chilled 10% glycerol (v/v). After the final wash, cells were resuspended in 2 ml 10% glycerol (v/v). Four hundred µl aliquots were incubated briefly on ice with 1-5 µg of plasmid DNA in pre-chilled electroporation cuvettes (0.2 cm electrode gap, Bio-Rad) and pulsed once in a GenePulser™ (Bio-Rad) set at 2.5 kV, resistance 1000 Ω, capacitance 25 µF. Cells were rescued immediately after pulsing with 1 ml Middlebrook 7H9/OADC, transferred to a clean microcentrifuge tube and incubated for 3 hr at 37°C. The electroporation reactions were plated on 7H10/OADC agar containing the appropriate antibiotics and incubated for 3-5 days at 37°C.

***Mtb*.** Electroporation of *Mtb* was similar to that described for *Msm*, except that all manipulations were performed at room temperature (Wards & Collins 1996). Briefly, 1 ml of a log-phase pre-culture was inoculated into 100 ml of 7H9/OADC and grown to an OD_{600} of

0.8-1.0. Cells were harvested by centrifugation at 3901 × *g* for 10 min and then washed twice in 10% glycerol (v/v) and resuspended in 2-5 ml of 10% glycerol (v/v). Plasmid DNA (1-5 µg) was mixed with 400 µl of competent cells in electroporation cuvettes (0.2 cm electrode gaps, Bio-Rad) and pulsed once in a GenePulser™ (Bio-Rad) set at 2.5 kV, resistance 1000 Ω, capacitance 25 µF. Cells were rescued immediately after pulsing in 1 ml 7H9/OADC and incubated overnight at 37°C. The following day, electroporation reactions were plated on 7H10/OADC agar containing the appropriate antibiotics and incubated for 21-28 days at 37°C.

2.6 Sequencing

All sequencing of plasmid constructs or PCR products was performed as a pay-for-service by the Central Analytical Sequencing Facility at Stellenbosch University. Whole-genome sequencing (WGS) of resistant mutant strains was performed by Professors Tom R. Ioerger and James C. Sacchettini (Texas A&M University, Texas, USA).

2.7 Southern blot analysis

Electroblotting. Genomic DNA (5 µg) was digested overnight with the appropriate restriction enzyme(s) at 37˚C after which the DNA was separated by electrophoresis on a 1% agarose gel at 80 V,and viewed and photographed with a fluorescent ruler with the Gel Doc (WealTeach Keta Imaging System). The agarose gel was shaken gently in depurination buffer (0.25M HCl) for 15 min, followed by denaturation buffer (1.5 M NaCl/0.5M NaOH) for 25 min and finally neutralization (1.5 M NaCl, 5 M Tris·HCl, pH 7.5) for 30 min. The DNA was transferred to a nitrocellulose membrane (Hybond™-N+ membrane, Amersham) using a vacuum blotter (Model 785, Bio-Rad). Once transferred, the DNA was cross-linked to the membrane by irradiation in a UV Stratalinker 1800 (Stratagene) at 1200 mJ/cm^2, and membranes were hybridized immediately.

Synthesis and labelling of probes. All probes used for Southern blot analyses were synthesized by PCR using the oligonucleotides indicated in each Chapter. The ECL Direct Nucleic Acid Labelling and Detection System protocol (Amersham) was used to label probes. Briefly, 100 ng of probe DNA in a total volume of 10 µl was denatured by boiling for 5 min at 95˚C in a water-bath and immediately chilled on ice for 5 min. Equal volumes of DNA

labelling agent and gluteraldehyde (Amersham) were added to the probe, mixed gently and incubated for 15 min at 37˚C. Following incubation, the labelled probe was added to the hybridization buffer.

Hybridization. The ECL Direct Nucleic Acid Labelling and Detection System protocol (Amersham) was used to prepare the hybridization buffer. Briefly, for membranes 10cm^2 in size, 20 ml of hybridization buffer, 5% w/v blocking agent and 0.5 M NaCl was combined and stirred at room temperature for 1 hr and then at 42°C for 1 hr. Subsequent to cross-linking, the membrane was pre-hybridized in roller bottles in the Hybridisation oven/shaker SI3OH (Stuart) for 1 hr at 42°C, after which the labelled probe was added and the membrane was hybridized overnight at 42°C.

Detection. Following overnight hybridization, the membrane was washed twice in primary wash buffer (6 M Urea, 0.4% SDS, 0.5 × SSC) for 20 min each, at 42°C, and then twice for 5 min at room temperature in secondary wash buffer (0.5 × SSC). Thereafter, detection reagents 1 and 2 (Amersham) were mixed in equal quantities transferred to the membrane and incubated for 1 min at room temperature. The membrane was then drained to remove excess detection reagent, saran wrapped and exposed to X-ray film (Amersham Biosciences) in a cassette for time periods ranging from 1 min to 2 hr at room temperature before developing.

Development of X-ray film. Membrane exposure and subsequent development of the X-ray film (High performance chemiluminescence film, Amersham Hyperfilm™ECL) was carried out in a dark room with red-light facilities. Immediately after exposure, for the appropriate time, the X-ray film was submerged in developer solution (GBX Developer, Carestream® Kodak®, Sigma-Aldrich) for 3 min, rinsed briefly in H_2O and submerged in fixer solution (GBX Fixer, Carestream® Kodak®, Sigma-Aldrich) for 3 min. X-ray films were air-dried completely before being photographed.

2.8 Quantitative gene expression analysis

RNA isolation. 30 ml cultures were grown to mid-log phase (OD_{600} of 0.5) and subsequently split into 2 × 15 ml volumes, to which one was treated with the drug and the other left untreated for the specified times. Total RNA was extracted using a FastRNA ProBlue Kit (MP

Biomedicals) per the manufacturer's instructions. Briefly, cells were harvested at 1500 × *g* for 15 min at 4°C. The supernatant was removed and the pellet resuspended in 1 ml of RNApro™Solution and transferred to tubes containing Lysing MatrixB, provided in the kit. The samples were processed in the FastPrep®Instrument 3x at the following settings: set 6.0, time: 40; samples were kept at 4°C for 5 min between each cycle. Samples were centrifuged at 13000 × *g* for 5 min at 4°C, after which the liquid (~750 µl) was transferred to a new microcentrifuge tube and incubate at room temperature for 5 min. Chloroform, 300 µl was then added to the sample and incubated at room temperature for 5 min. Samples were centrifuged at 13000 × *g* for 5 min at 4°C. The aqueous phase transferred to a new microcentrifuge tube, to which 500 µl of cold absolute ethanol was added. RNA was precipitated overnight at -20°C. RNA was harvested by centrifugation at 13000 × *g* for 5 min at 4°C, washed with 500 µl of cold 70% ethanol (made with DEPC-H_2O, provide with the kit) and dried for no longer than 5 min in vacuum centrifuge (MiVac DNA concentrator, GeneVac). RNA was resuspended in 30 µl DEPC- H_2O, overnight at 4°C. A NanoDrop ND-1000 Spectrophotometer (Thermo Scientific) was used to quantify the RNA. RNA was stored at -80°C.

DNase treatment. Two rounds of DNase I treatment of RNA were carried out using Turbo DNase (Ambion). In the first round, the reaction contained 2 µg of RNA, 2 µl DNase, 2 µl 10 × Buffer and sdH_2O to a final volume of 20 µl. The reaction was incubated at 37°C, for 45 min followed by purification of the RNA. The reaction was made up to a total volume of 100 µl with sdH_2O, to which 100 µl of acid phenol: chloroform: isoamylalchol (25:24:1) was added. After vortexing briefly, the sample was centrifuged at 15000 × *g* for 5 min. the aqueous phase was then collected (~80 µl) and the RNA was precipitated with 1/10^{th} volume sodium acetate (3M) and 2.5 volumes of ice-cold 100% ethanol. The RNA was incubated at -80°C for 1 hr and then centrifuged at 15000 × *g* for 15 min, The supernatant was discarded the RNA pellet was washed with room temperature70% ethanol(prepared in DEPC-H_2O), dried in a vacuum centrifuge (MiVac DNA concentrator, GeneVac)for no longer than 5 min and resuspended in 11 µl DEPC-H_2O. Following incubation overnight at 4°C, RNA was quantified and followed by a second round of DNase treatment, as described. Removal of DNA contamination was confirmed with conventional PCR and samples were kept at 4°C to prevent degradation.

cDNA synthesis. For cDNA synthesis, iScript™cDNA Synthesis Kit (Bio-Rad) was used, in which 100 ng of DNase-treated RNA was used as template with 1 µl iScript reverse transcriptase and 4 µl of 5 × iScript reaction mix and DEPC-H_2O to a final reaction volume of 20 µl. Reverse transcription was performed in a conventional T100 Thermal Cycler (Bio-Rad) at the following conditions: 5 min at 25°C, 30 min at 42°C and 5 min at 85°C. cDNA synthesis was confirmed by conventional PCR and all samples were kept at 4°C.

Droplet Digital™ PCR (dd-PCR™). Primers and TaqMan minor groove binder (MGB) probes were designed using Primer Express software version 3.0.1. To facilitate multiplexing, TaqMan MGB probes homologous to the target gene were labeled with 6-carboxyfluorescein (FAM), and the reference gene, *sigA*, was labelled with 4,7,20-trichloro-7'-phenyl-6-carboxyfluorescein (VIC). Primers-probe amplification conditions for duplex PCR were first optimized by gradient PCR, however all reactions worked optimally at 60°C Reaction mixtures (20 µl) containing 1 ng of RNA-equivalent cDNA, 1 × dd-PCR Supermix for probes (Bio-Rad), 500 nM of each primer, and 250 nM of each TaqMan probe were emulsified with droplet generator oil using a QX200 Droplet Generator (Bio-Rad). PCR amplification was performed using a two-step thermocycling protocol (95c for 10 min, 40 cycles at 94°C for 30 s and 60°C for 60 s, and 98°C for 10 min) in a conventional T100 Thermal Cycler (Bio-Rad). The droplets were then analyzed using a QX200 Droplet Reader (Bio-Rad). Controls included a negative control (H_2O) as well as 1 ng of each DNase-treated RNA sample (DNA contamination control). Three technical replicates of each gene were performed. The QuantaSoft Software version 1.4.0.99 (Bio-Rad) provided the absolute number of gene copies, normalized to *sigA*. Standard deviations were calculated using Microsoft Excel 2010.

2.9 Drug susceptibility testing by broth microdilution

The broth microdilution method (Collins & Franzblau 1997; Collins *et al.,* 1998) allows a range of antibiotic concentrations to be tested, on a single 96-well microtitre plate, to determine the minimum inhibitory concentration (MIC). Briefly, a 10 ml culture of *Mtb* or *Msm* was grown to an OD_{600} of 0.6 – 0.7. The culture was then diluted 1:500 in 7H9/OADC. In a 96- well, U-bottom microtitre plate (PGRE650180, Lasec, SA), 50 µl of 7H9/OADC was added to all wells from Rows 2-12. The antimicrobials to be tested were added to Row 1 at a

final concentration of 8 × MIC_{90} and serially diluted, 2-fold, using a multichannel pipette, by transferring 50 µl of the liquid in Row 1 to Row 2 and aspirating to mix. Fifty µl of the liquid in Row 2 was transferred to Row 3 and aspirated. The procedure was repeated until Row 12 was reached, where 50 µl of the liquid in Row 12 was discarded to bring the final volume in these wells to 50 µl. Finally, 50 µl of the diluted culture was added to all the wells. The microtitre plate was stored in a secondary container and incubated at 37°C for 3 days (*Msm*) and 14 days (*Mtb*). On Day 3 (*Msm*) and Day 14 (*Mtb*) alamarBlue® (BUF012B, Celtic Molecular Diagnostics) was added to each well and plates were incubated at 37°C for 6 hr or 24 hr, respectively. The lowest concentration of drug which prevented the colour change of alamar blue (from blue to pink) was considered the MIC that inhibited more than 90% of the bacterial population (MIC_{90}).

Chapter 3: The role of the SOS response in subversion of antibiotic efficacy

3.1 Introduction

3.1.1 The bacterial SOS response

The existence in the Gram-negative *E. coli* of an inducible, global response to DNA damage was first hypothesized by Miroslav Radman in the 1970s (Radman 1974). The naval distress signal "Save Our Souls" was aptly invoked to describe this response, as subsequent extensive characterization established the SOS response as a system that involves the induction of more than 40 unlinked genes following exposure to exogenous or endogenous DNA-damaging agents (Courcelle *et al.,* 2001; Erill *et al.,* 2007). In most bacterial systems, the proteins LexA and RecA have been shown to be the key regulatory components of the SOS response (Erill *et al.,* 2007). LexA is a repressor protein which binds to a specific sequence, termed the SOS box, that is located upstream of the start codon of LexA-regulated genes, including *lexA* itself and *recA* (Figure 3.1) (Butala *et al.,* 2009). LexA is widely distributed across the Bacterial Domain and has been shown *in silico* to regulate 10 – 40 genes in different species. There are, however, some exceptions: some *Pseudomonadaceae* and *Xanthomonadaceae* have two functional, independent, copies of *lexA* while *Streptococci* have none; neither of the two *lexA* homologues encoded by *Deinococcus radiodurans* regulates *recA* (suggesting that an alternative regulatory mechanism coordinates resistance to γ radiation), whereas the *lexA* homologue of *Spirochaete L. interrogans* regulates *recA,* but not itself; and, *lexA*-like genes have been identified in green nonsulfur bacteria, *Cyanobacteria* and all *Proteobacteria* subclasses except for *Epsilonproteobacteria* (Abella *et al.,* 2004; Erill *et al.,* 2007; Butala *et al.,* 2009). RecA is highly conserved and found in virtually all bacteria, with the only known exception to be certain endosymbionts (Cox 2007).

In addition to regulating multiple genes, the expression of LexA is autoregulated by a feedback mechanism which enables a rapid response to even small amounts of inducing signal (Butala *et al.,* 2009). The degree of identity with the consensus SOS motif determines the affinity of LexA binding and consequently, the level, timing and duration of induction. Differential derepression of certain genes may occur in response to the internal pH, which affects the DNA binding affinity of LexA, or even minor endogenous DNA damage, as LexA binds some operators more weakly than others (Butala *et al.,* 2009). In *E. coli*, the SOS

response is not only induced upon exposure to exogenous DNA damaging agents, but can also be stimulated by DNA damage from metabolic intermediates or mistakes in replication, recombination and chromosome segregation (Foster 2007). The timing of gene repression and subsequent synthesis of the SOS-induced proteins varies for individual genes. In *E.coli*, SOS boxes that bind LexA weakly are the first to be derepressed (Janion 2008). These include *lexA* itself, *uvrAB, cho* and *uvrD* (involved in nucleotide excision repair – NER), *ruvAB* (recombinational DNA repair), the DNA polymerases Pol II, Pol IV, as well as *recA* and *recN* (recombination and recombinational repair). If these proteins are not sufficient to repair the damage, LexA is further degraded, enabling the expression of genes with stronger SOS boxes such as *sulA* which inhibits cell division and thereby prolongs the time during which the DNA may be repaired, as well as assembly of the components, $UmuD'_2C$, of the error-prone DNA polymerases Pol V, which results in mutagenic repair (Janion 2008).

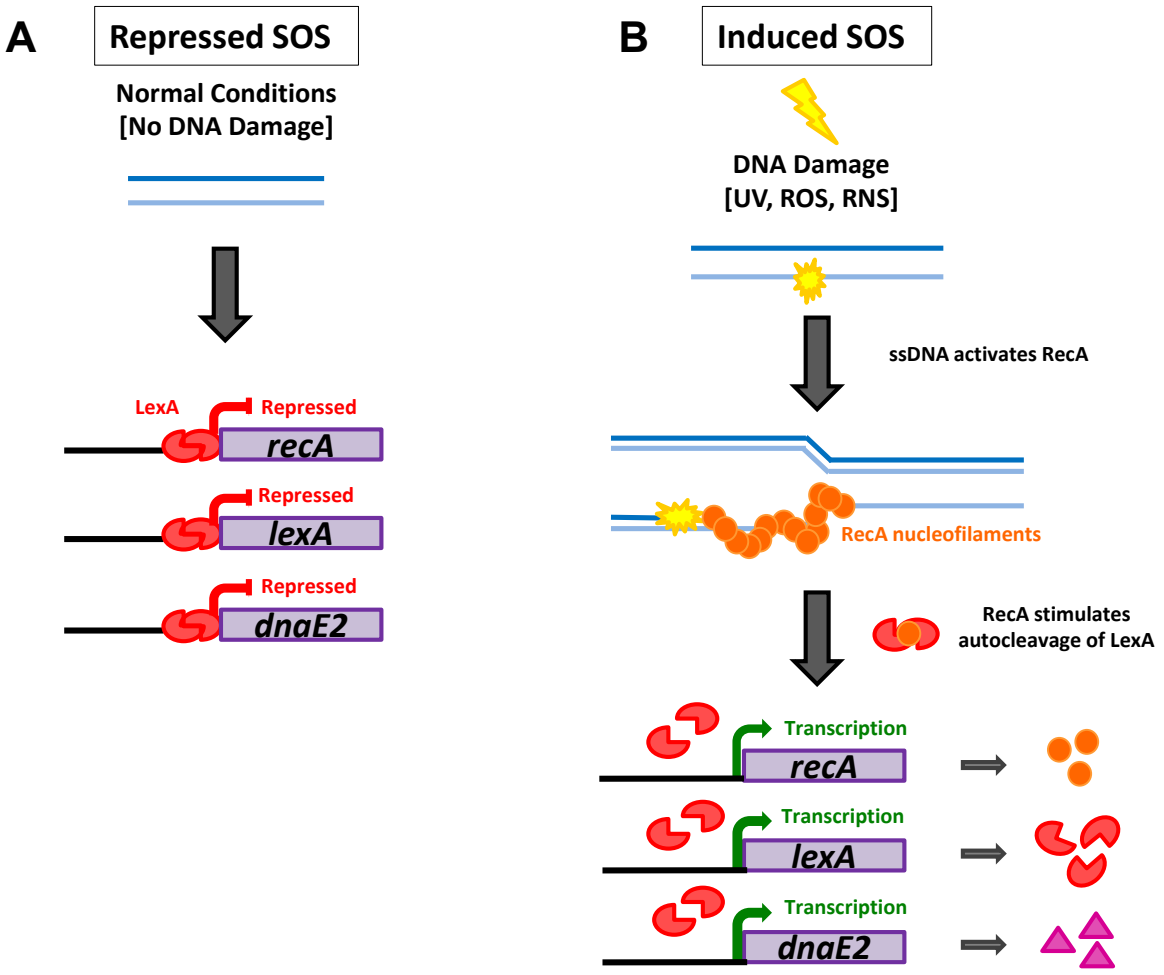

Figure 3.1: The SOS response. A) During normal growth, SOS genes are negatively regulated by the LexA repressor, which binds to the SOS box in the promoters of SOS-regulated genes and thereby inhibits their expression. B) Following genotoxic damage (UV; reactive oxygen or nitrogen species, ROS/RNS), RecA protein binds to single-stranded DNA (ssDNA) at sites of DNA lesions and replicon arrest, to form nucleoprotein filaments. The RecA nucleoprotein filaments interact with LexA which stimulates the cleavage of LexA in an autocatalytic reaction that de-represses the SOS regulon genes. As DNA damage is repaired, the co-protease activity of the RecA filament disappears, allowing functional LexA to re-accumulate and bind to the SOS boxes and subsequently switch off the response (Rand *et al.,* 2003; Butala *et al.,* 2009). Schematic adapted from (Nohmi 2006).

3.1.2 The mycobacterial DNA-damage response

The regulation of *recA* in a RecA/LexA-independent manner was initially reported in *Acinetobacter calcoaceticus* (Rauch *et al.,* 1996) and subsequent homology studies suggest that a range of DNA damage response mechanisms, different from the typical SOS response, exists in all members of this genus *Acinetobacter* (Hare *et al.,* 2006; Hare *et al.,* 2012). Mycobacteria are intriguing in that there are two mechanisms associated with the regulation of DNA repair genes: a small number of genes are regulated by the classic SOS or RecA/LexA-dependent mechanism (referred to as the SOS response), while a larger subset of genes are regulated by an alternate, RecA/LexA-independent mechanism (referred to as the RecA-ND mechanism/response) (Figure 3.2) (Durbach *et al.,* 1997; Rand *et al.,* 2003; Gamulin *et al.,* 2004; Smollett *et al.,* 2012). During normal mycobacterial growth - or the "uninduced state" – binding of LexA to the SOS box restricts LexA expression and the expression of at least 25 other SOS regulon genes (Smollett *et al.,* 2012). Comparative analyses with other bacteria enabled the identification of the consensus SOS box sequence TCGAAC(N4)GTTCGA in *Mtb* (Davis *et al.,* 2002). Studies have shown that *Mtb*'s *recA* gene is inducible independently of RecA and LexA (Davis *et al.,* 2002) and that expression is driven off two different promoters (Gopaul *et al.,* 2003). The two *recA* promoters have been studied extensively: there is a distal RecAp2 promoter which is a typical sigma70 (σ^{70})-like promoter, and this overlaps with a LexA-binding site and a proximal RecAp1 promoter which lacks an apparent LexA-binding site (Gopaul *et al.,* 2003). Interestingly, both promoters are inducible upon DNA damage, despite the lack of a LexA-binding site within RecAp1 (Davis *et al.,* 2002). Subsequently, a promoter motif was identified in the upstream regions of genes induced independently of RecA and LexA in *Mtb*, termed the RecA non-dependent promoter (RecA-NDp) (Gamulin *et al.,* 2004). The majority of RecA-ND genes (e.g., *radA, lhr, alkA, ahpC*, and mobile elements) are induced in the macrophage environment to a significant level (Schnappinger *et al.,* 2003; Gamulin *et al.,* 2004). In addition, genes that are involved in the basic DNA damage response as well as oxidative stress were shown to be regulated by this alternate mechanism (Gamulin *et al.,* 2004). Some genes, including *recA*, possess the RecA-ND motif as well as an SOS box, suggesting the two DNA damage response mechanisms may partially overlap (Rand *et al.,* 2003; Gamulin *et al.,* 2004; Smollett *et al.,* 2012). The identified motif includes two consensus sequences tTGTC(G/A)gtg and TAnnnT, separated by eight nucleotides and are similar to σ^{70} recognition elements (Gamulin *et al.,*

2004). Recently, *in vitro* electrophoretic mobility shift assays and *in vivo* chromatin immunoprecipitation was used to show that the *Rv2745c*, and the *Msm* homolog *MSM*EG_2694, encode the ClgR transcriptional regulator that specifically binds to RecA-NDp and may play an essential role in inducing expression of DNA repair genes in *Mtb* and *Msm*, respectively (Wang *et al.,* 2011). In addition, ClgR, which acts as a regulator of the ATP-dependent Clp protease system, has been shown to be essential for *Mtb* replication in macrophages and is implicated in diverse regulatory networks in response to a multitude of stress conditions, including intraphagosomal redox stress, hypoxia, reaeration, cell wall stress and heat shock (Estorninho *et al.,* 2010; Mehra *et al.,* 2010; Sherrid *et al.,* 2010; McGillivray *et al.,* 2014).

Owing to its genetic composition, the SOS response can be an error-prone or mutagenic pathway that results in genetic diversity of the organism and thereby enables survival through adaptive evolution. In *Mtb*, this occurs by inducible mutagenesis and damage tolerance mediated by the upregulation of the low fidelity, or "mutator," polymerase DnaE2 (Boshoff *et al.,* 2003). In addition, *uvrB* contributes significantly to *Mtb's* resistance to UV irradiation *in vitro,* and to reactive nitrogen and oxygen intermediates (RNI and ROI) *in vivo* (Darwin & Nathan 2005). Furthermore, recent biochemical evidence supports the critical role of the entire UvrABC complex in repair of UV-damaged DNA via the NER pathway (Mazloum *et al.,* 2011).

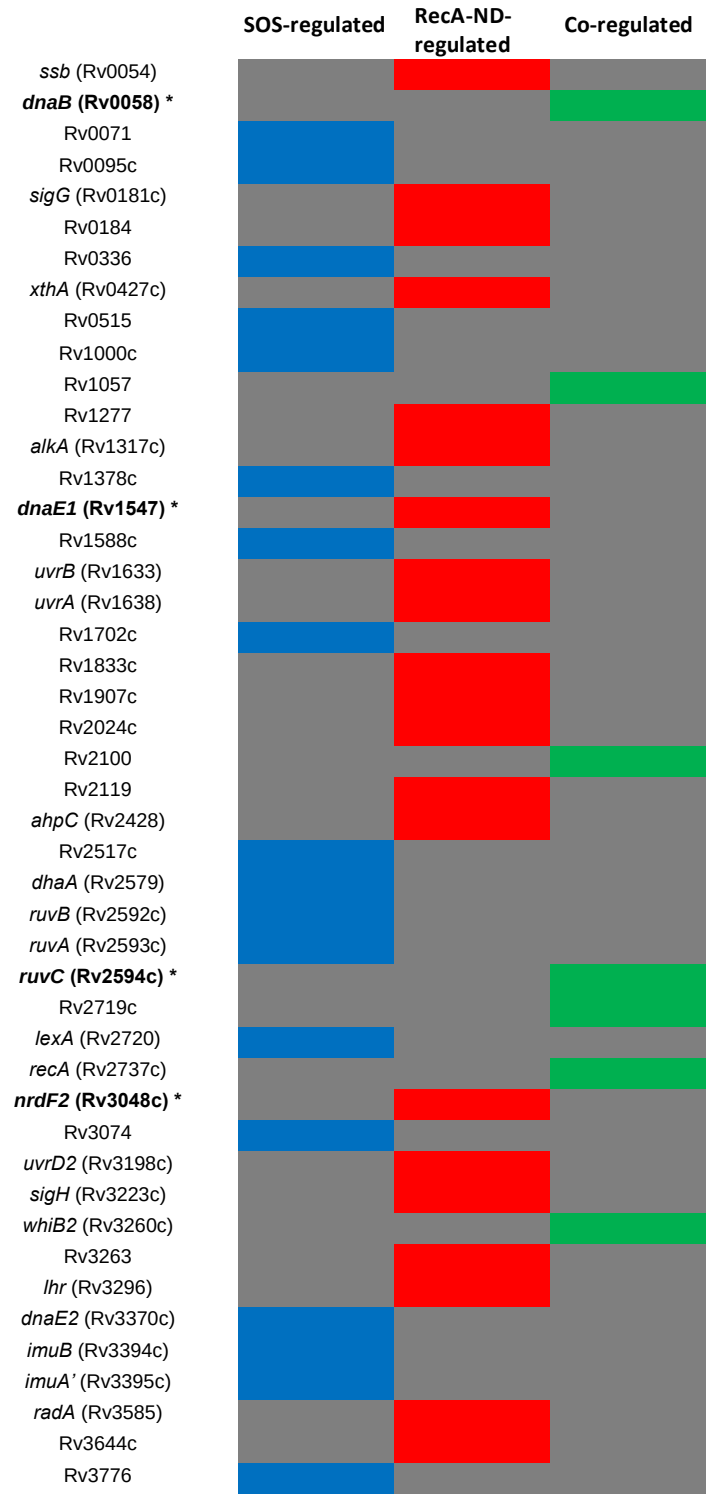

Figure 3.2: Regulation of DNA repair and associated genes in *Mtb*. Multiple genes are regulated in the classical RecA/LexA-dependent (SOS response) manner and have are identifiable by the presence of the SOS box, TCGAAC(N4)GTTCGA . However, the majority of DNA repair genes are regulated independently of RecA and LexA (RecA-ND response) and have the characteristic tTGTCRgtg(N8)TA(N3)T (or RecA-NDp) motif in their promoters. In addition, a subset of genes is co-regulated as both motifs have been identified in the promoters of these genes (Gamulin *et al.,* 2004; Smollett *et al.,* 2012). *Essential genes (Sassetti *et al.,* 2003).

3.1.3 A common mechanism of cell death

It has been proposed that a common mechanism underlies antibiotic-mediated cell death in bacteria (Kohanski *et al.,* 2007; Keren *et al.,* 2013; Liu & Imlay 2013). Since the "universal mechanism" is independent of drug-target interaction, the proposal has met with considerable controversy (Keren *et al.,* 2013; Liu & Imlay 2013; Dwyer *et al.,* 2014). Nevertheless, there are aspects of the model which have been recapitulated in multiple systems, including *Mtb* (Grant *et al.,* 2012). In essence, this mechanism centres on the generation in antibiotic-exposed cells of ROS such as superoxide, hydrogen peroxide and highly deleterious hydroxyl radicals ($OH^{\cdot}$) (Kohanski *et al.,* 2007; Dwyer *et al.,* 2014). ROS are highly toxic and will readily damage proteins, membrane lipids and DNA. In addition, studies in *E. coli* suggest that antibiotic-mediated cell death results from the oxidation of the guanine nucleotide pool and subsequent incorporation of toxic oxidation products (8oxo-dG) into nucleic acids (Foti *et al.,* 2012). This is consistent with other evidence implicating the SOS response in intrinsic resistance to antibiotics including β-lactams, the ribonucleotide reductase inhibitor trimethoprim, and fluoroquinolones (Miller *et al.,* 2004; Cirz & Romesberg 2007; Kohanski *et al.,* 2007). To date, clofazimine, pretonamid and delamanid are the only anti-tuberculars which have been shown to generate ROS and/or RNS as their presumed mechanism of action against *Mtb* (Mdluli *et al.,* 2014). Mycobacteria possess DNA repair systems such as HR (homologous recombination), BER (base excision repair), NER as well as a system for NHEJ (nonhomologous end-joining) (Gorna *et al.,* 2010; Warner 2010). However, unlike other prokaryotes, mycobacteria do not possess mechanisms known to be required for MMR (mismatch repair) (Mizrahi & Andersen 1998). Bacteria appear to incur DNA damage unceasingly (partially attributable to normal aerobic cellular metabolism) as almost half of the *Mtb* DNA repair genes are continuously expressed during exponential phase growth in broth and similar findings have been reported in *E.coli* (Fu & Fu-Liu 2007; Pennington & Rosenberg 2007).

3.2 Aims and objectives

Several lines of evidence implicate the SOS response in intrinsic resistance to antibiotics through its role in adaptive mutagenesis (Drlica & Zhao 1997; Miller *et al.,* 2004; Cirz & Romesberg 2007; Kohanski *et al.,* 2007). The SOS response and, as such, DNA damage responses, subsequently induce the synthesis of error-prone DNA polymerases upon exposure to sub-lethal doses of some commonly used antibiotics (Foster 2007). These include trimethoprim, the dihydrofolate reductase inhibitor that arrests DNA replication; the DNA topoisomerase inhibitor, ciprofloxacin; the RNA polymerase inhibitor, rifampicin; and, surprisingly, β-lactams, the cell wall inhibitors (Butala *et al.,* 2009). Therefore, antibiotics can drive evolution by inducing the SOS response and subsequently accelerating mutagenesis, for example, by acquiring point mutations that result in inactivation or efflux of the drug. Consequently, antibiotic therapy can be counteracted at many levels by the SOS response.

Numerous studies have utilized gene-deleted *recA* mutants in order to better understand the SOS response. However, RecA is not only involved in the SOS response but is central to the processes of recombination and replication restart (Cox *et al.,* 2000; Cox 2003). Thus, abrogation of RecA function is likely to have pleiotropic effects not solely related to the SOS response. To date, a *lexA*$^{Ind-}$ mutant has not been constructed in *Msm* or *Mtb*. Davis *et al*. (2002) were not able to construct a *Mtb lexA* null (deletion) mutant (Griffin *et al.,* 2011, recently demonstrated the essentiality of *lexA*, *in vitro*), but instead expressed a non-cleavable *Mtb* LexA protein from a plasmid in *Msm* and used this strain to infer DNA damage-induced regulation of the *recA* promoter independently of LexA. In addition, the strain that was characterized not only had two copies of *lexA,* the native *Msm lexA* and the *Mtb lexA*^{S141A}, but was also a marked mutant in that a hygromycin-resistance gene was present.

Against this background, the overall aim of this study was to investigate the role of the SOS response in limiting the efficacy of antitubercular agents. It was hypothesised that the SOS response plays a role in antibiotic-mediated cellular death in mycobacteria and that disabling the mycobacterial SOS response could be used as a tool to validate antibiotic-mediated cell death. The specific objectives were:

1. To generate unmarked *Msm* and *Mtb* *lexA*$^{Ind-}$ mutants that each possess a single copy of the mutated gene.

2. To evaluate phenotypically the extent to which the SOS response contributes to remediation of DNA damage, and to determine whether this impacts antibiotic-mediated cellular death in mycobacteria.

3.3 Materials and Methods

3.3.1 Mycobacterial strains, plasmids, and probes

The strains used in this study are detailed in Table 3.1, plasmids are listed in Table 3.2, and primers in Table 3.3.

Table 3.1: Strains used in this study

Strain	Description/ Genotype	Reference/ Source
Msm		
mc^{2}155	High frequency transformation mutant of *Msm* ATCC 706	(Snapper *et al.,* 1990)
Δ*dnaE2*	*dnaE2* knockout mutant of mc^{2}155	Edith E. Machowski, MMRU
Δ*recA*	*recA* deletion mutant of mc^{2}155	(Machowski *et al.,* 2007)
lexA^{S167A}	*lexA* S167A point mutant of mc^{2}155	This study
lexA^{K204A}	*lexA* K204A point mutant of mc^{2}155	This study
Mtb		
H37RvMA	Virulent reference laboratory strain of *Mtb* ATCC 27294	(Ioerger *et al.,* 2010)
Δ*dnaE2*::*hyg*	*dnaE2* knockout mutant of H37Rv, HYG^R	(Boshoff *et al.,* 2003)
lexA^{Ind-}	*lexA* S141A point mutant of H37RvMA; *lexA*-non-inducible	This study

Table 3.2: Plasmids used in this study

Plasmid	Description	Reference/ Source
p2NIL	Cloning vector, KAN^R	(Parish & Stoker 2000)
pGOAL19	Plasmid carrying *hyg*, *lacZ* and *sacB* genes as a *Pac*I cassette; AMP^R	(Parish & Stoker 2000)
p2NIL::*MsmlexA*	p2NIL harbouring 1957 bp PCR product containing 732 bp of mc^2155 *lexA* plus 1225 bp flanking sequence; KAN^R	This study
p2NIL::S167A	p2NIL::*MsmlexA* site-directed mutagenesis vector carrying *Msm* $lexA^{S167A}$ allele, KAN^R	This study
p2NIL::K204A	p2NIL::*MsmlexA* site-directed mutagenesis vector carrying *Msm* $lexA^{K204A}$ allele, KAN^R	This study
p2NIL::S167A-P19	p2NIL::S167A vector containing the *Pac*I cassette from pGOAL19; KAN^R, HYG^R, Suc^S	This study
p2NIL::K204A-P19	p2NIL::K204A vector containing the *Pac*I cassette from pGOAL19; KAN^R, HYG^R, Suc^S	This study
p2NIL::*MtblexA*	p2NIL harbouring 2345 bp PCR fragment containing 654 bp H37Rv *lexA* plus 1691 bp flanking sequence; KAN^R	This study
p2NIL::S141A	p2MIL::*MtblexA* site-directed mutagenesis vector carrying *Mtb* $lexA^{S141A}$ allele, KAN^R	This study
p2NIL::S141A-P19	p2S141A vector containing the *Pac*I cassette from pGOAL19; KAN^R, HYG^R, Suc^S	This study

Table 3.3: Primers used in this study

Name	Sequence 5'-3'	Comments ★
***Msm lexA*$^{Ind-}$ point mutants**		
*Msm*LexAF	GATCGGGCGAAGCTTCGACGCGCGGGACATCAGGA	1957 bp; *MSM*EG_2740 including 1225 bp flanking sequence with introduced *Hin*dIII sites
*Msm*LexAR	CCGGCGAGGACCAAGCTTAGAACCCCGAAGAGCCGGCGCA	
LexAS167A	GACGCCATGGTCGACGCCGCGATCTGCGAT	277 bp when used with LexAMegR; mutagenic forward primer with introduced *Sty*I site and S167A mutation
LexAK204A	ACGGTCGCGACCTTCAAGCGCGCACGCGGTC	159 bp when used with LexAMegR; mutagenic forward primer with introduced *Nru*I site and K204A mutation
2740MegR	CCCGCACGAACGGATTCGTACGGGCGA	Reverse primer to generate megaprimer with LexAS167A or LexAK204A *;* introduced *Bsi*WI site
2740MegF	GGGATGTCGAGGATGGCCATCTGACT	1025 bp; forward primer used with megaprimer LexAS167A/ 2740MegR or LexAK204A/ 2740MegR; introduced *Bsa*BI site
2740Fsp	ATAGAACGGGGTACCGAC	1130 bp; forward and reverse primers for screening
2740Rsp	ACGCGGCGATCGAATTCG	
*Msm*Fprobe	CTTGCGGATGACGGT	558 bp; probe for Southern blot
*Msm*Rprobe	CGAGAGATCGGCGAC	

***Mtb lexA*$^{Ind-}$ point mutant**

*Mtb*LexAF	CGCCACTAAGCTTGACTACG	2345bp; *Rv2720* including 1691 bp flanking sequence with introduced *Hin*dIII sites
*Mtb*LexAR	GCCGAGAAGCTTCCGGGT	
LexAS141A	CGGTGACGCCATGGTCGA	254 bp megaprimer; mutagenic forward primer with introduced *Sty*I and reverse primer with introduced *Bsa*BI site
2720MegR	ACGCGGATCAGCATCAGA	
2720MegF	CGAGCGGGCCCCGCAGATT	1032 bp; forward primer used with megaprimer LexAS141A/ 2720MegR; introduced *Apa*I site
2720Fsp/ 2720Meg	CGAGCGGGCCCCGCAGATT	1211 bp; forward and reverse primers for screening
2720Rsp	CTGCCGCTCGAGGACCCAT	
*Mtb*Fprobe	GCAGGAACAGGGTGCCCT	260 bp; probe for Southern blot
*Mtb*Rprobe	GCACCAGCTGCGCACCCT	

★Restriction sites are underlined

3.3.2 Construction of suicide delivery vectors carrying *lexA* point mutations

Msm: Site-directed mutagenesis (SDM) was used to mutate the key catalytic residues (S167A and K204A), and thereby interrupt the self-cleavage reaction of LexA. Briefly, the entire *lexA* gene, *MSMEG_2740* (732 bp), including the 1225 bp flanking sequence, was amplified by PCR (oligonucleotides specified in Table 3.3). The resulting amplicon was purified and digested with *Hin*dIII and subsequently ligated with *Hin*dIII-linearized p2NIL (p2NIL::*MsmlexA* construct) and transformed into competent *E. coli* DH5α cells. Following confirmation of the construct, by restriction analysis, it was used as the template DNA for subsequent megaprimer-based mutagenesis for introduction of point mutations (Kammann *et al.,* 1989). Briefly, two rounds of PCR were performed, using two flanking oligonucleotides and one internal mutagenic oligonucleotide. In the first round of PCR, the internal mutagenic forward primer and the flanking reverse primer were used and the resultant product was the "megaprimer", 277 bp. The megaprimer was then used as the reverse primer with the second flanking forward primer to generate the complete DNA sequence with the desired mutation, 1055 bp (Datta 1995; Tyagi *et al.,* 2004). This PCR product was then digested with *Bsa*BI and *Bsi*WI, two unique restriction sites that were introduced in the flanking forward and reverse primers respectively and ligated into *Bsa*BI/*Bsi*WI-digested p2NIL::*MsmlexA* to generate p2NIL::S167A or p2NIL::K204A. In this way, the wilt type (Wt) *lexA* allele is replaced with an allele with the desired point mutation. The *Pac*I cassette from pGOAL19 was then cloned into the p2NIL::S167A and p2NIL::K204 constructs and positive constructs were confirmed as blue, KAN–resistant (KAN^R), HYG–resistant (HYG^R), sucrose–sensitive (Suc^S) and included the respective point mutations S167A – *Sty*I site; K204A – *Nru*I site – confirmed with restriction digest (detailed below). Both constructs were further confirmed by Sanger sequencing of the *lexA* locus.

Mtb: Similarly, the key catalytic residue Ser-141 of *Mtb lexA*, *Rv2720*, was mutated to Ala by SDM. The entire *lexA* gene of 654 bp plus 1691 bp flanking sequence was PCR amplified and subsequently cloned into p2NIL (using *Hin*dIII), to generate the template construct for SDM (p2NIL::*MtblexA*). The S141A megaprimer was generated (254 bp) using a mutagenic forward primer and the flanking reverse primer, including the *Bsa*BI restriction site. The S141A megaprimer was used as the reverse primer with the flanking forward primer that includes an *Apa*I restriction site, to generate the insert (1033 bp) with the desired point

mutation. This PCR product was then digested with *Apa*I and *Bsa*BI, and ligated into *Apa*I/*Bsa*BI -digested p2NIL::*MtblexA* to generate p2NIL::S141A. Similar to the *Msm* suicide delivery vectors, the *Pac*I cassette was introduced and positive constructs were confirmed as blue, KAN^R, HYG^R and Suc^S and included the point mutation S167A – *Sty*I site, which was further confirmed by restriction digest (detailed below) and Sanger sequencing of the *lexA* locus.

3.3.3 Screening of *lexA* point mutants

To aid in the screening process, the Ser-Ala and Lys-Ala point mutations were engineered so as to introduce the unique restriction sites *Sty*I and *Nru*I, respectively. The screening was done in a two-step process: first, the *lexA* gene was amplified using the primer pair 2740Fsp/2740Rsp or 2720Fsp/2720Rsp (Table 3.3), which generated a 1130 bp or 1211 bp fragment respectively. Then, in the second step the PCR product was digested with *Sty*I (Ser-Ala) or *Nru*I (Lys-Ala), and positive transformants that harboured the point mutations yielded two fragments of 668 bp and 462 bp (S167A), 778 bp and 352 bp (K204A) and 791 bp and 420 bp (S141A).

3.3.4 Damaging treatments of mycobacteria

3.3.4.1 UV irradiation

Msm: For DNA damage by UV, 40 ml cultures were grown to an OD600 of 0.6–0.8. Cells were concentrated by centrifugation at 3901 × *g* for 10 min (Beckmann Allegra X-22R) and suspended in 5 ml and aliquoted into in 90 mm petri dishes. Open petri dishes were irradiated with 20 mJ/cm^2 (UV Stratalinker 1800, Stratagene), after which cultures were rescued in final volumes of 40 ml for 3 hr at 37°C. Cultures were then plated on solid 7H10/OADC without antibiotic (for viable CFU evaluation) or containing 200 µg/ml RIF (for determination of RIF^R frequencies). Plates were incubated for 3 days for CFU determination and 5–6 days for RIF^R determination, at 37°C.

Mtb: UV-induced mutagenesis was performed similarly to *Msm*, except that cultures were recovered for 24 hr at 37°C before plating for CFU and RIF^R frequencies determination. Plates were incubated for 21 days for CFU determination and 4–5 weeks for RIF^R determination, at 37°C.

3.3.4.2 Survival assay

Msm: 10 ml cultures were grown to an OD_{600} of 0.6–0.8, after which 10-fold serial dilutions were prepared and 5 µl of each dilution was spotted onto solid 7H10/OADC (untreated control) and MMC (0.02 µg/ml and 0.04 µg/ml). Plates were incubated for 3–4 d at 37°C.

Mtb: As executed for *Msm*, except plates were incubated for 10–12 d at 37°C.

3.3.5 Antimicrobial agents

RIF; INH; KAN; STR; vancomycin (VAN); novobiocin (NOV); 5-fluorouracil (5-FU); norfloxacin (NOR); ofloxacin (OFX); ciprofloxacin (CIP); gatifloxacin (GAT); moxifloxacin (MOX); levofloxacin (LEV) and mitomycin C (MMC) were purchased from Sigma Aldrich. bedaqualine (BDQ) was purchased from Asclepia MedChem Solutions (Belgium, www.asclepia.com). For stock solutions, antimicrobials were all dissolved in the following solvents: INH; KAN; STR; VAN; NOV; 5-FU; GAT; MOX; LEV and MMC in nuclease-free water (Qiagen), CIP in 0.1N hydrochloric acid and RIF; NOR; OFX; and BDQ in dimethyl sulfoxide (DMSO – Sigma Aldrich). Antimicrobial stock solutions were stored at 4°C.

3.3.6 Quantitative RT-PCR of *Mtb* genes in response to MMC treatment

Primers and probes used for droplet digital PCR (dd-PCR) were designed using the Primer3 programme (http://frodo.wi.mit.edu/cgi-bin/primer3/primer3_www.cgi) (Table 3.4). All primers were designed to amplify DNA fragments internal to the coding sequence of the relevant genes with the same annealing temperatures (60°C).

Table 3.4: Primers and probes used for dd-PCR used in this study

	Primer 5'-3'		**Probe 5'-3' ⋆**
dnaE2	Rv3370RTF	CGCGAAAAGGTCATCCAGTAC	TCTACCACAAATACGGCC (FAM)
	Rv3370RTR	GACTACGCCGCCCAGGT	
radA	Rv3585RTF	GTCGACGTTGTGCTGCATTT	CTGCGGATGGTCC (FAM)
	Rv3585RTR	AGGAGGAAACATCCGACTTCATC	
recA	Rv2737RTF	GGCGCGCTGAATAATTCG	CACCACGGCGATCT (FAM)
	Rv2737RTR	CGCGGAGCTGGTTGATG	
sigA	sigARTF	CGAGCCGATCTCGTTGGA	ACGAGGGCGACAGC (VIC)
	sigARTR	TTCGATGAAATCGCCAAGCT	

⋆ TaqMan minor groove binder (MGB) probes were either labelled with 6- carboxyfluorescein (FAM) or with 4,7,2'-trichloro-7'-phenyl-6- carboxyfluorescein (VIC)

3.4 Results

3.4.1 Disabling the *Msm* SOS response by mutating the key catalytic residues of LexA.

Slilaty and Little (1987) showed that changing either Serine-119 or Lysine-156 to Alanine in *E. coli* LexA resulted in two mutant proteins that had normal repressor function and, apparently, normal structure, but were completely deficient in cleavage (Slilaty & Little 1987). That is, the S119A and K156A alleles prevent LexA-dependent induction of the SOS response, effectively resulting in an SOS-deficient mutant. To determine the feasibility of adopting a similar approach in *Msm* and *Mtb*, an alignment of LexA was performed to compare the amino acid sequences of the *E. coli*, *Msm* and *Mtb* LexA proteins. This analysis revealed a high degree of conservation between the LexA proteins and, importantly, confirmed the conservation of the *E.coli* S-119 and K-156 residues among these organisms (Figure 3.3).

Based on this analysis, site directed mutagenesis (SDM) was used to generate equivalent *Msm* LexA (*MSMEG_2740*) point mutants by changing S-167 and K-204 to A, respectively. The final constructs, p2NIL::S167A-P19 and p2NIL::-K204A-P19, were subsequently electroporated into mc^2155 to generate the strains $lexA^{S167A}$ and $lexA^{K204A}$ (jointly referred to as $lexA^{Ind-}$). The presence of the mutations in the constructs as well as after genomic integration (single-cross-overs, SCOs and double-cross-overs, DCOs) following electroporations, was confirmed by restriction digest of the PCR-amplified *lexA* gene (Figure 3.4). In addition, introduction of the S167A and K204A mutations was further confirmed by DNA sequencing of the PCR-amplified *lexA* genes (plasmid vectors and allelic exchange mutants).

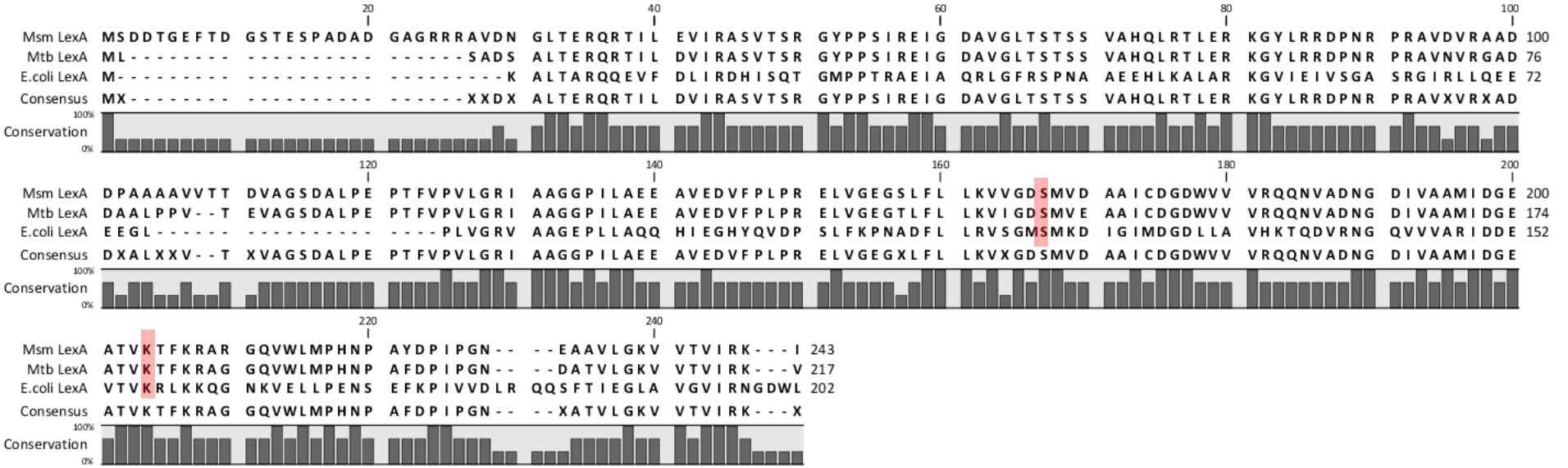

Figure 3.3: LexA protein alignment. The *E. coli* S-119 and K-156 residues are conserved between *Msm* and *Mtb* and correspond to S-167 and K-204 and S-141 and K-178, respectively (highlighted) (CLC DNA Workbench 6.0.1).

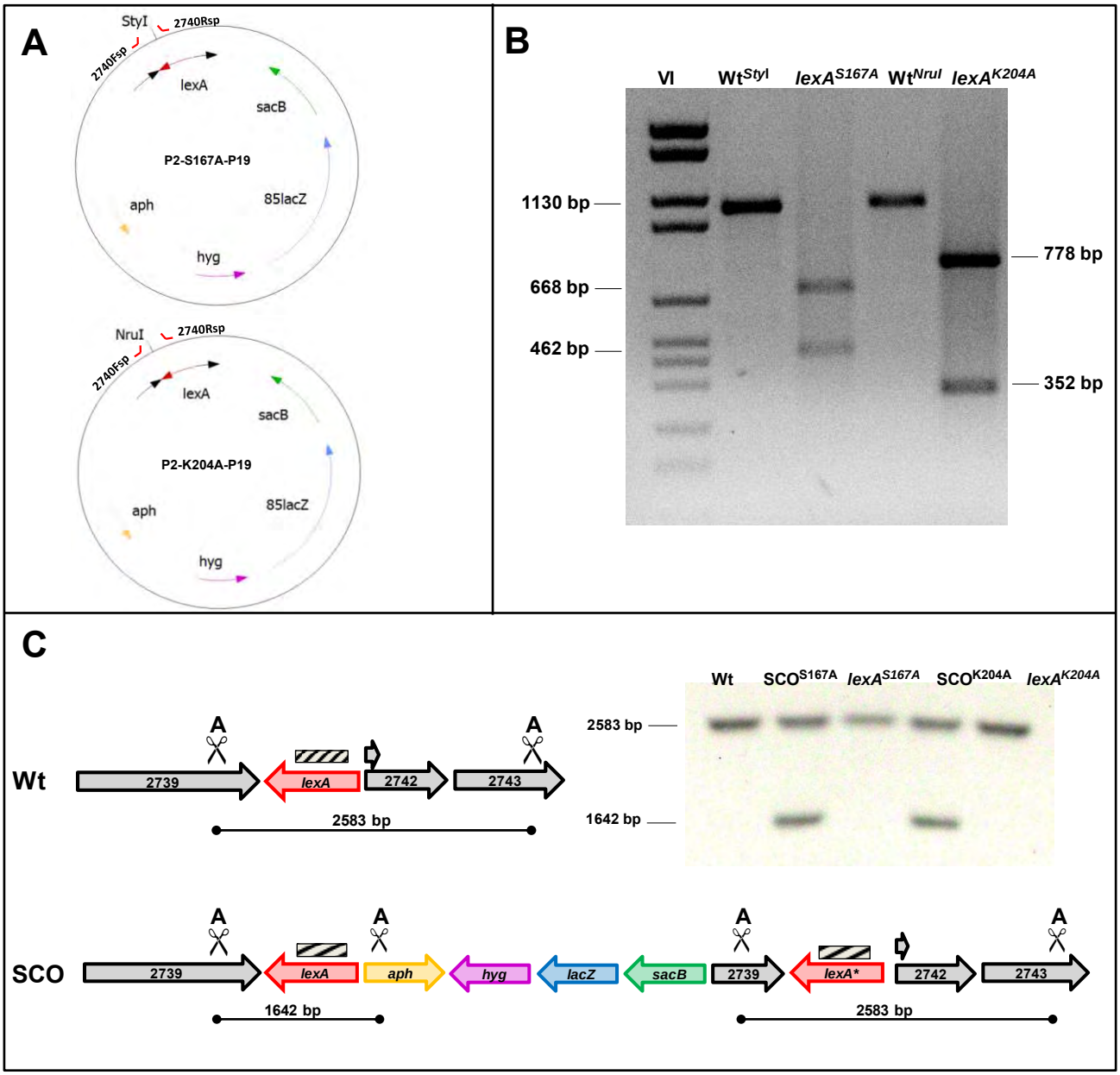

Figure 3.4: Construction and genotypic characterisation of the *lexA*^{S167A} and *lexA*^{K204A} mutants of *Msm*. (**A**) Schematic representation of the p2NIL::S167A-P19 and p2NIL::-K204A-P19 suicide vectors in which the key catalytic residues of *Msm* LexA were mutated by site-directed mutagenesis. (**B**) To confirm the presence of the mutation, the PCR-amplified (using primer set 2740Fsp/2740Rsp, as depicted in **A**) *lexA* gene product from each strain was digested at the unique restriction site that was introduced concurrently with the mutation: *lexA*^{S167A} digested with *StyI* yields two fragments of 668 bp and 462 bp, *lexA*^{K204A} digested with *NruI* yields two fragments of 778 bp and 352 bp, and Wt *lexA* remains undigested (1130 bp) by *StyI* and *NruI*; molecular weight marker VI (Roche) is shown in lane1. (**C**) Genotypic confirmation by Southern blot analysis. *Alu*I-digested genomic DNA was hybridized to the 558 bp probe, depicted as the lined box (not drawn to scale). The merodiploid strains (SCOs) carry both Wt and mutant versions of the *lexA* gene whereas the parental Wt and allelic exchange mutants have either one or the other. The mutant *lexA* allele in *lexA*^{S167A} and *lexA*^{K204A} was confirmed, as shown in panel A.

3.4.2 Cleavable LexA is required for induced mutagenesis and damage tolerance in *Msm.*

In other bacterial systems, it has been shown that a disabled SOS response renders the organism susceptible to DNA damage (Kohanski *et al.,* 2007). Therefore, to validate that mutating S167 and K204 to A in *Msm* disables the SOS response, we evaluated induced mutagenesis by exposing a panel of *Msm* strains, including Wt, Δ*dnaE2* (Boshoff *et al.,* 2003), Δ*recA* (Machowski *et al.,* 2007), and the *lexA*$^{Ind-}$ mutants (*lexA*^{S167A} and *lexA*^{K204A}), to UV irradiation to induce mutations that confer rifampicin resistance (RIF^{R}) (Table 3.5). This technique has been used extensively in *E. coli* and has been validated as an appropriate tool to study induced mutagenesis in mycobacteria (Boshoff *et al.,* 2003; Warner *et al.,* 2010). However, the possibility of pre-existing mutants in the population provides an inherent inaccuracy to this assay; one that can be overcome by fluctuation analysis of the mutation rate whisch is more accurate and reproducible (Rosche & Foster 2000). Subsequently, the mutation frequencies of mc^{2}155 (Wt), Δ*dnaE2* and Δ*recA* were consistent with those previously reported (Boshoff, 2003). The *lexA*$^{Ind-}$ mutants displayed decreased mutation frequencies, phenocopying Δ*recA*, and confirming that either S167A or K204A mutation in LexA disables the *Msm* SOS response.

Table 3.5: UV-induced mutation frequencies to rifampicin resistance (RIF^{R}). The *lexA*$^{Ind-}$ mutants and the Δ*recA* mutant show decreased UV-dependent mutation frequency compared to Wt and Δ*dnaE2*. ⋆

Strain	**CFU/ml**†	**Number of RIF^{R} colonies**	**Mutation frequency**
Wt	3.6×10^{6}	201	5.6×10^{-6}
Δ*dnaE2*	3.4×10^{6}	73	2.1×10^{-6}
Δ*recA*	4.0×10^{6}	0	0
lexA^{S167A}	3.7×10^{6}	0	0
lexA^{K204A}	3.8×10^{6}	0	0

⋆ Data are from a representative experiment performed in triplicate.
† CFU/ml – colony forming units/ml

To evaluate the tolerance to DNA damage of these mutants, survival assays were performed in which the sensitivity was determined to mitomycin C (MMC), a DNA damaging agent that forms crosslinks between the complementary strands of DNA preventing their separation and inhibiting DNA replication (Tomasz 1995). Briefly, $\log_{10}$-fold dilutions of 10^6 CFU/ml cultures were spotted onto MMC-supplemented (0.02 µg/ml or 0.04 µg/ml) or unsupplemented media (Figure 3.5). For both concentrations, it appeared that the *lexA* non-cleavable mutants were unable to tolerate, and thus unable to survive, the DNA damage induced by MMC, as reflected by the hypersensitivity to the agent. This is consistent with the Δ*recA* phenotype but contrary to Wt, which shows significant resilience to the effects of DNA damage. As observed previously (Warner *et al.,* 2010 and Boshoff *et al.,* 2003), the Δ*dnaE2* mutant showed reduced, not abrogated, growth (4-fold and 8-fold growth reduction at 0.02 µg/ml and 0.04 µg/ml, respectively).

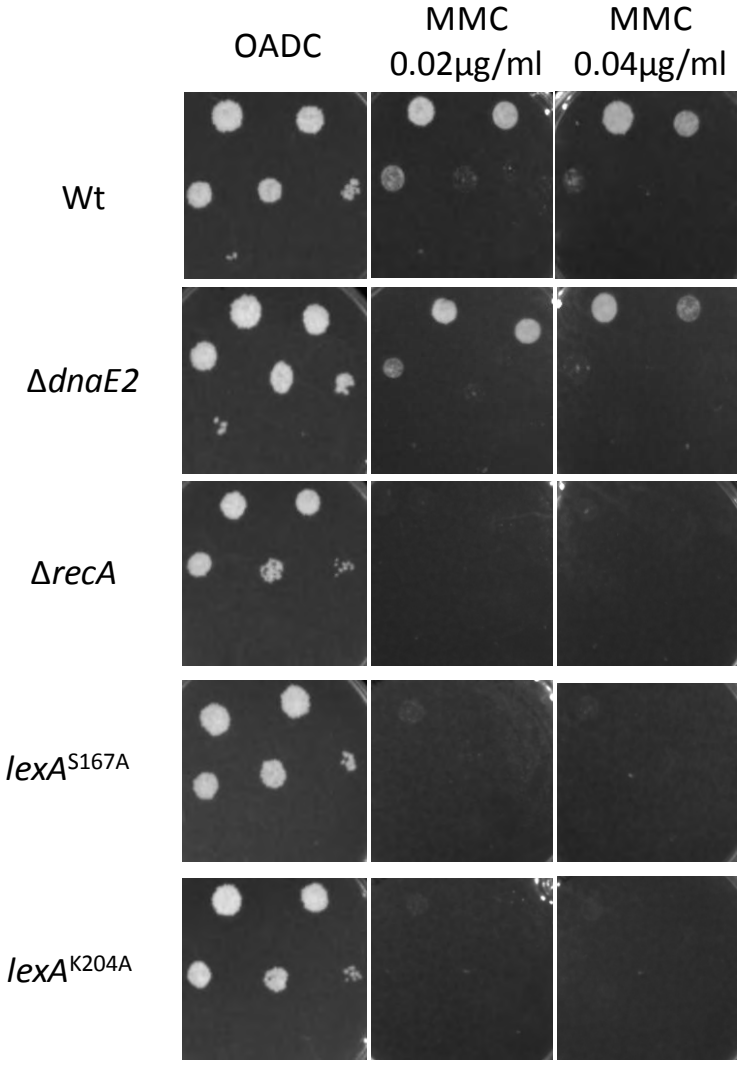

Figure 3.5: *Msm* cleavable LexA is required for damage tolerance. Log_{10}-fold dilutions of mc^2155 (Wt), Δ*dnaE2*, Δ*recA*, *lexA*^{S167A} and *lexA*^{K204A} were plated on standard OADC medium or medium containing MMC at 0.02 µg/ml or 0.04 µg/ml. Cultures were also plated onto standard 7H10/OADC to enumerate CFU/ml, to ensure equivalent numbers of cells were spotted (10^6 CFU/ml). The *lexA*^{S167A} and *lexA*^{K204A} mutants phenocopy Δ*recA*, as all three strains show hypersensitivity to DNA damage and are unable to grow in the presence of MMC (0.02µg/ml or 0.04µg/ml). On the contrary, Wt is resilient to the effects of DNA damage, while Δ*dnaE2* shows reduced, not abrogated growth. Data are from a representative experiment performed in triplicate.

3.4.3 An intact *Msm* DNA damage repair system is required to respond to antibiotic-mediated DNA damage.

In *E. coli*, it has been shown that an intact DNA damage repair system mitigates the effects of antibiotic-mediated DNA damage (Kohanski *et al.,* 2007). Therefore, it was determined whether disabling the mycobacterial SOS response could potentiate antibiotic efficacy. To this end, we subjected the panel of strains to a series of antibiotics from various classes (inhibitors of cell wall, transcription, *etc.*) and determined the MIC_{90} (Figure 3.6). In general, when compared to the Wt MIC_{90}, the *lexA*$^{Ind-}$ mutants displayed increased sensitivity (≤ 4-fold) to established compounds from the quinolone class of drugs which target DNA gyrase, resulting in lethal DNA double-strand breaks (Malik *et al.,* 2006). Surprisingly, only a 2-fold increase in MIC_{90} was observed for the fourth-generation fluoroquinolones, MOX and GAT. In addition, a 2-fold increase in susceptibility was also observed for RIF and 5-FU. Hypersusceptiblity (16-fold) of the the *lexA*$^{Ind-}$ mutants to MMC was observed, consistent with the damage tolerance assay (Figure 3.5). The Δ*recA* strain displayed a similar MIC_{90} profile to the *lexA*$^{Ind-}$ mutants, although increased susceptibility was observed against certain antimicrobials (RIF, CIP, MOX, and GAT). Finally, the Δ*dnaE2* strain displayed comparable MIC_{90} to Wt, with the exception of certain quinolones.

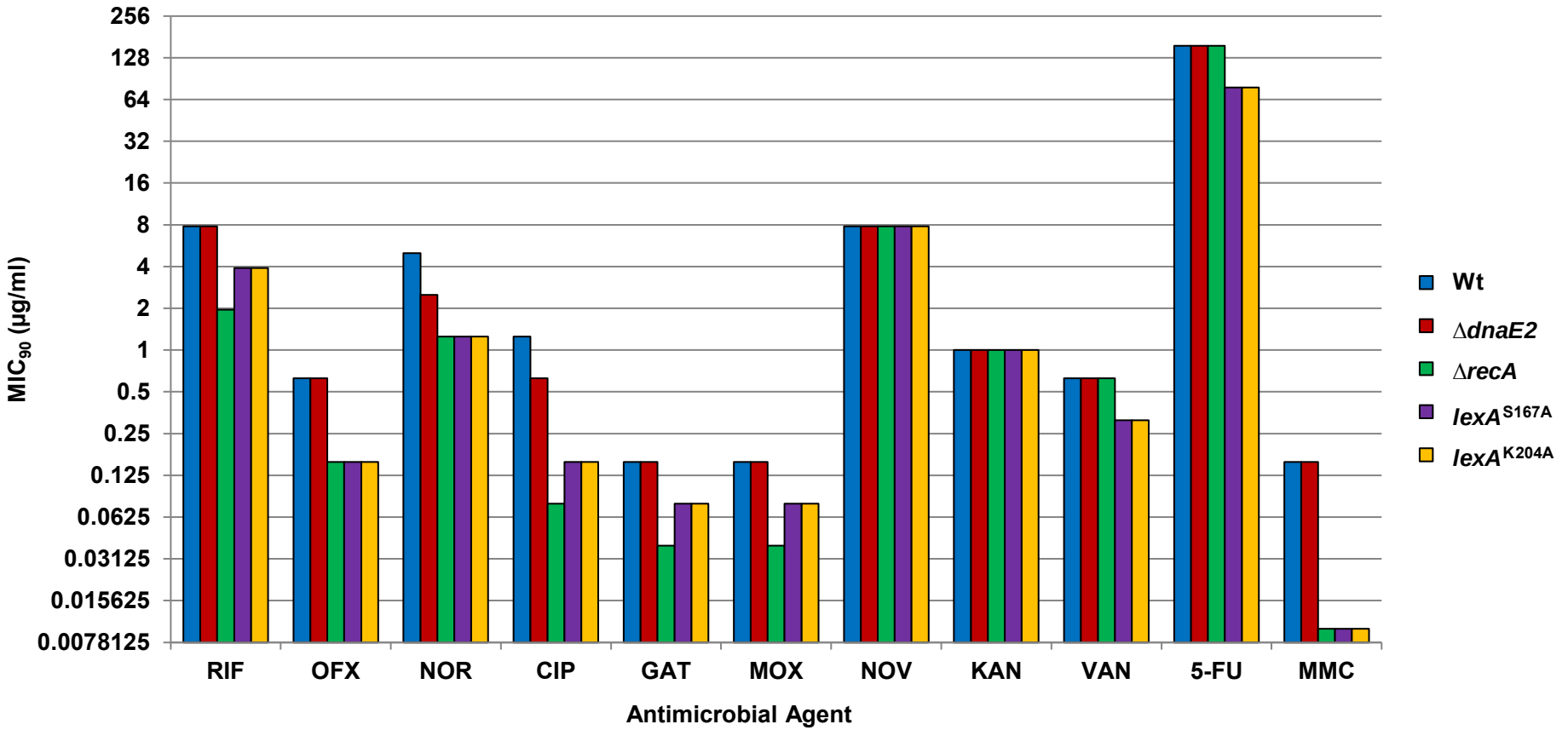

Figure 3.6: Susceptibility to DNA-damaging agents. The *lexA*$^{Ind-}$mutants and the Δ*recA* mutant show increased sensitivity to the quinolone class of drugs, compared to Wt and Δ*dnaE2*. In addition, hypersensitivity to MMC complements the results from the MMC survival assay (Figure 3.5). Data are from a representative experiment performed in triplicate.

3.4.5 Disabling the *Mtb* SOS response by mutating the catalytic Ser-141 residue in LexA.

Characterization of the *Msm lexA*$^{Ind-}$ mutants showed that S167A phenocopies K204A under all conditions assayed. Given the equivalence of these mutations, we generated a single *Mtb* mutant in which the Ser-141 catalytic residue (equivalent to *Msm* LexA S167A and *E. coli* LexA S119, Figure 3.7) was mutated by SDM, using the same approach as described for *Msm*. In addition, introduction of the S141A mutation was further confirmed by DNA sequencing of the PCR-amplified *lexA* genes (plasmid vector and allelic exchange mutants).

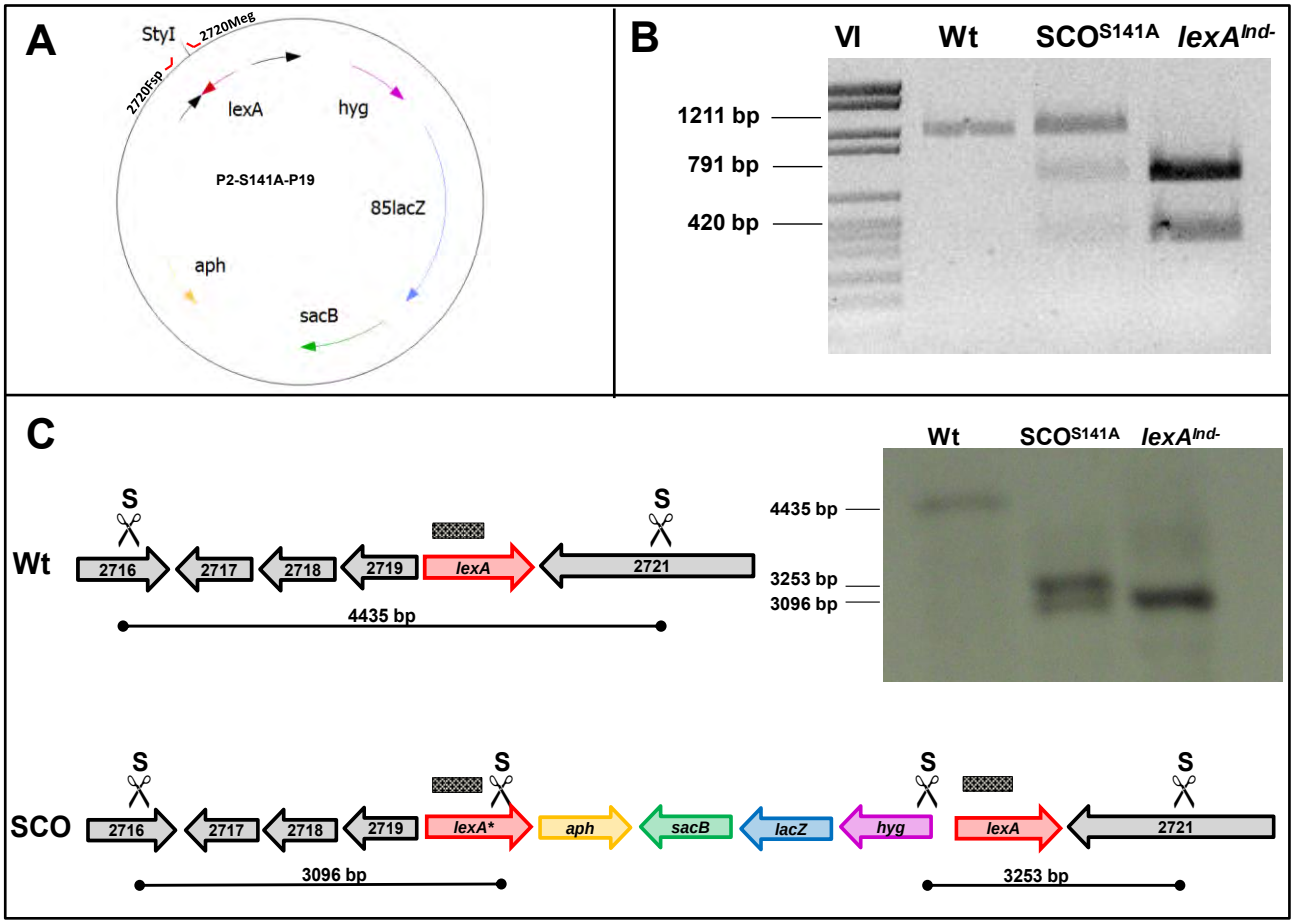

Figure 3.7: Construction and genotypic characterisation of the *lexA*$^{Ind-}$ mutant of *Mtb*. (**A**) Schematic representation of the p2NIL::-S141A-P19 suicide vector in which the key catalytic Ser-141 residue is mutated to an Ala by site-directed mutagenesis. (**B**) To confirm the presence of the mutation, the PCR-amplified (using primer set 2720Fsp/2720Meg, depicted in **A**) *lexA* gene product from Wt, the merodiploid (SCO) and the *lexA*$^{Ind-}$allelic exchange mutant was digested at the unique restriction site (*StyI)* that was introduced concurrently with the mutation: Wt *lexA* remains undigested (1211 bp), the SCO yields three fragments of 1211 bp, 791 bp and 420 bp (as two copies of *lexA* are present in this strain) and the *lexA*$^{Ind-}$ mutant yields two fragments of 791 bp and 420 bp; molecular weight marker VI (Roche) is shown in lane1. (**C**). Schematic illustration of the Southern blot strategy in which *Sty*I-digested genomic DNA hybridized to the 260 bp probe, depicted as the patterned box (not drawn to scale).

3.4.6 Cleavable LexA is required for induced mutagenesis but not necessarily for damage tolerance in *Mtb*.

The *Mtb lexA*$^{Ind-}$ mutant (S141A) was then characterized using an analogous set of assays to those employed in *Msm*. Inactivation of the SOS response was validated by evaluating induced mutagenesis: a small panel of *Mtb* strains, H37Rv (Wt), Δ*dnaE2* and *lexA*$^{Ind-}$, was exposed to UV irradiation to induce lesion-targeted, base-substitution mutations that confer rifampicin resistance (RIF^R) (Table 3.6). An increased mutation frequency in Wt was observed, whereas the number of mutants was reduced significantly in Δ*dnaE2* consistent with previous reports (Boshoff *et al.,* 2003). The *lexA*$^{Ind-}$ mutant displayed hypersensitivity to UV irradiation, confirming that the S141A mutation in LexA disables the SOS response. Although the number of RIF^R colonies and subsequent mutation frequency of Wt and Δ*dnaE2* was lower than previously reported (Boshoff *et al.,* 2003), the overall trend was replicated. The discrepancy is likely due to the use here of 2-fold $\log_{10}$ lower CFU/ml in the initial cultures pre-UV irradiation, compared to previous reports.

Table 3.6: UV induced mutation frequencies to rifampicin resistance (RIF^R). The *lexA*$^{Ind-}$ mutant shows hypersensitivity to UV irradiation, compared to Wt and Δ*dnaE2*. ⋆

Strain	**CFU/ml**	**Number of RIF^R colonies**	**Mutation frequency**
Wt	4.2×10^6	27	6.4×10^{-6}
Δ*dnaE2*	4.2×10^6	0	0
lexA^{Ind-}	4.0×10^6	0	0

⋆ Data are from a representative experiment performed in triplicate.

Tolerance of the *lexA*$^{Ind-}$ mutant to DNA damage was evaluated by damage survival assay: $\log_{10}$-fold dilutions of Wt, Δ*dnaE2* and *lexA*$^{Ind-}$ were plated on standard OADC medium or medium containing MMC at 0.02 μg/ml or 0.04 μg/ml (Figure 3.8). Consistent with reported data, Wt and Δ*dnaE2* are able to tolerate MMC exposure, i.e. ability to survive in the presence of the DNA-damaging agent (Boshoff *et al.,* 2003). A less pronounced phenotype was observed for the *Mtb* mutant compared to *Msm* (Figure 3.5): only a slight increase was detected in the sensitivity of *Mtb lexA*$^{Ind-}$ to MMC exposure (~1 $\log_{10}$ and 2 $\log_{10}$, at 0.02

µg/ml and 0.04 µg/ml, respectively), compared to absence of growth with *Msm lexA*$^{Ind-}$ mutants at the same MMC concentrations. Nevertheless, this suggested a damage tolerance phenotype of the *Mtb lexA*$^{Ind-}$ mutant.

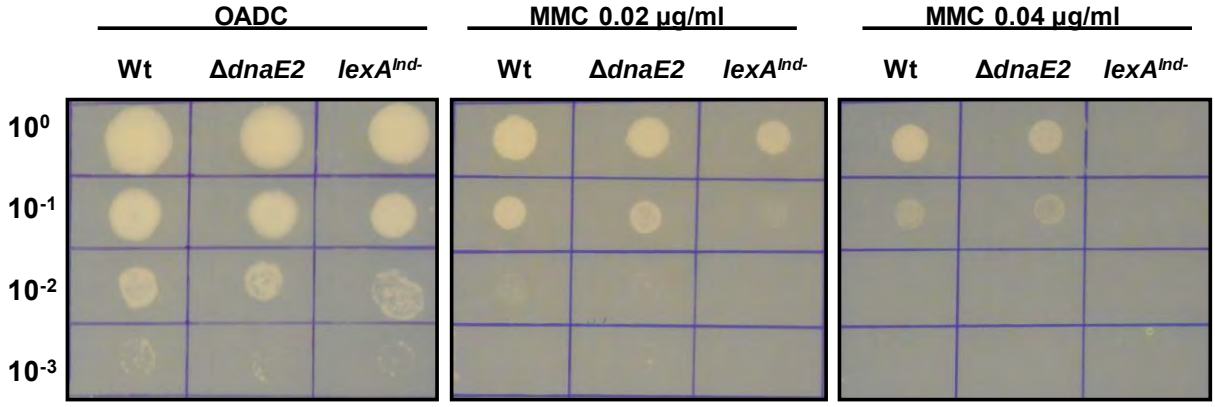

Figure 3.8: Tolerance of *Mtb lexA*$^{Ind-}$ to DNA damage. Log_{10}-fold dilutions of H37Rv (Wt), Δ*dnaE2*, and *lexA*$^{Ind-}$were plated on standard OADC medium or medium containing MMC at 0.02 µg/ml or 0.04 µg/ml. Cultures were also plated onto standard 7H10/OADC to enumerate CFU/ml, to ensure equivalent numbers of cells were spotted (10^6 CFU/ml). Wt and Δ*dnaE2* are resilient to the damaging effects of MMC, in comparison to the *Mtb lexA*$^{Ind-}$ mutant which is 2-fold and 4-fold more sensitive at 0.02 µg/ml and 0.04 µg/ml, respectively. Data are from a representative experiment performed in triplicate.

3.4.7 The *Mtb* SOS response does not contribute to remediation of antibiotic-mediated DNA damage.

It was hypothesised that an intact SOS response in *Mtb* might mitigate the effects of antibiotic-mediated DNA damage and that inactivation of LexA would potentiate the efficacy of agents that target DNA metabolism, as observed in *Msm* (Figure 3.9). To investigate the impact of disabled SOS function on *Mtb*, the MIC_{90} was evaluated by subjecting a panel of strains to a series of antibiotics, both current anti-TB drugs as well as novel drugs in various clinical phases of development, from different drug classes. The Δ*dnaE2* strain displayed comparable MIC_{90} to Wt, with the exception of VAN, BDQ, OFX and MMC (2-fold increase in sensitivity). The *lexA*$^{Ind-}$ mutant displayed slightly increased sensitivity (2-fold) to all compounds tested from the quinolone class of drugs and hypersensitivity (16-fold) to MMC only. Furthermore, a 2-fold increase in sensitivity was also observed for NOV, 5-FU and BDQ in the *lexA*$^{Ind-}$ mutant.

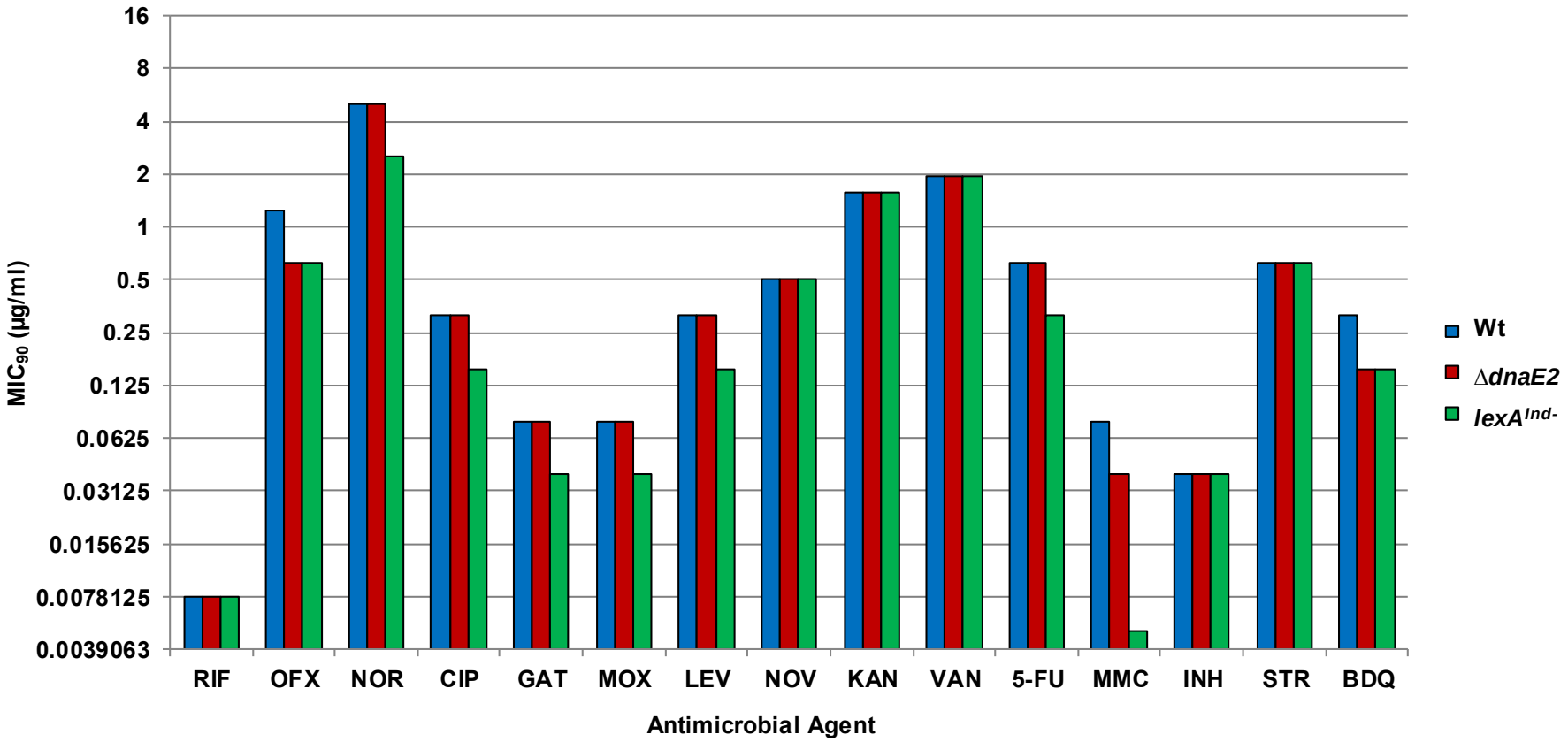

Figure 3.9: Susceptibility to DNA-damaging agents. The *lexA*$^{Ind-}$ mutant shows a moderate increase in sensitivity to the quinolone class of drugs and more profound hypersensitivity to MMC compared to Wt and Δ*dnaE2*. Data are from a representative experiment performed in triplicate.

3.4.8 A RecA-ND mechanism remains functional in the *Mtb lexA*$^{Ind-}$ mutant and contributes significantly to DNA repair.

The hypersusceptibilty of *Msm lexA*$^{Ind-}$ mutants to various quinolones (Figure 3.6) compared to the moderate susceptibility of the *Mtb lexA*$^{Ind-}$ mutant to those same agents (Figure 3.9) suggested that, while the same two DNA damage-repair pathways have been identified in *Msm* and *Mtb* (SOS response and RecA-ND) (Gamulin *et al.,* 2004), they might not contribute equally within the two organisms. To investigate this possibility, droplet digital (dd)-PCR was used to analyse the expression levels of three *Mtb* genes, each differentially regulated in response to DNA damage according to the presence of either a SOS box, the RecA-NDp motif, or both in the upstream regulatory region: *dnaE2* is SOS-inducible, *radA* is a RecA-ND regulon gene, and *recA* has both an SOS box and a RecA-NDp motif (Figure 3.2). MMC was selected as the DNA damage inducer as hypersusceptibility to this agent, relative to other DNA damaging agents, had been observed (Figure 3.9). In addition to analysing expression levels in Wt and the *lexA*$^{Ind-}$ mutant, the Δ*dnaE2* mutant was included as a control (Figure 3.10). As expected, all three genes were upregulated in Wt upon MMC treatment. Interestingly, a substantial level of *recA* transcript was present, even before DNA damage, which is consistent with the function of RecA in multiple replication and repair pathways. In the *lexA*$^{Ind-}$ mutant, *dnaE2* levels were low relative to WT, and remained low upon MMC treatment. This confirmed that the SOS pathway had been disabled in this strain and, further, suggested that *Mtb* experiences constitutively low levels of DNA damage under normal growth conditions *in vitro*. In contrast, significant levels of *radA* and *recA* were detected in the untreated *lexA*$^{Ind-}$ and were induced substantially upon exposure to MMC, consistent with reported data (Davis *et al.,* 2002). This suggests that the RecA-ND pathway is functional and genes regulated entirely or partially by this mechanism are able to remediate the damage sustained by MMC treatment and possibly others types of DNA damage, consistent with observations from both the tolerance assay (Figure 3.8) and MIC determinations (Figure 3.9). Interestingly, upon treatment, there was a 2.3-fold upregulation of *dnaE2* in the *lexA*$^{Ind-}$ mutant which contradicts previous evidence that *dnaE2* is solely SOS regulated (Boshoff *et al.,* 2003; Rand *et al.,* 2003), and raises the possibility that an alternative mechanism(s) can regulate *dnaE2* levels in response to genotoxic stress.

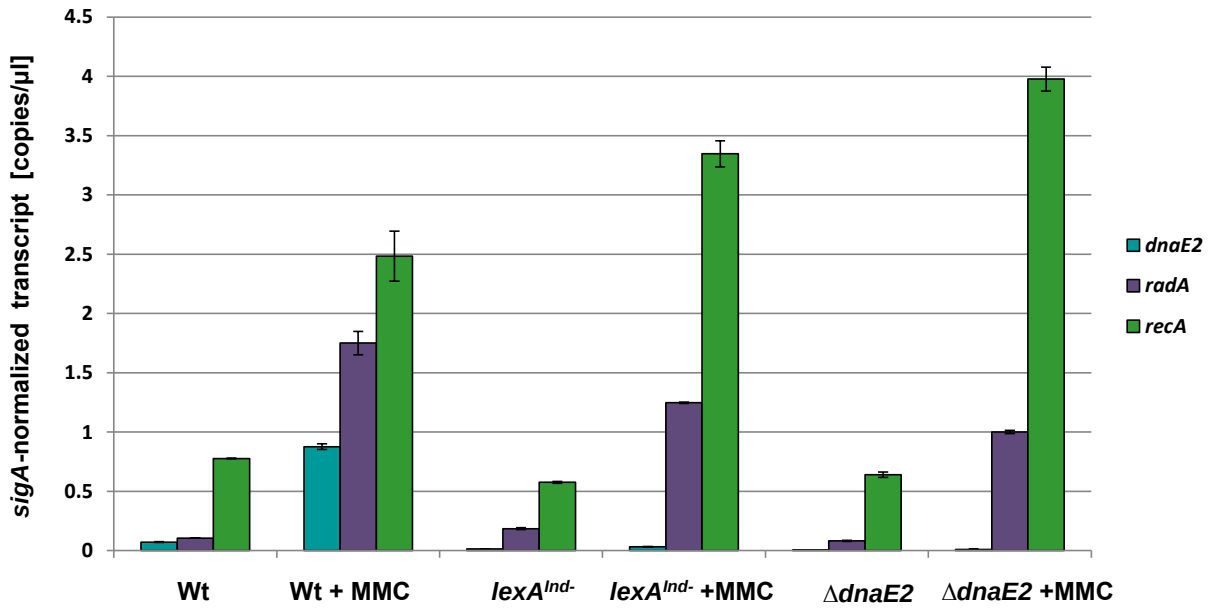

Figure 3.10: Effect of *lexA*$^{Ind-}$ on transcriptional responses of *Mtb* to DNA damage. dd-PCR analysis of *dnaE2, radA* and *recA* expression in *Mtb* Wt, *lexA*$^{Ind-}$ and Δ*dnaE2* after exposure to MMC (0.6 µg/ml for 6 hr), or untreated. Data are from a single experiment comprising three technical replicates. Error bars indicate standard deviations, calculated from the mean of triplicate samples.

3.5 Discussion

The SOS response has an established role in remediation of DNA damage by various mechanisms, including cell cycle arrest, upregulation of detoxification proteins, DNA repair and damage tolerance (Butala *et al.,* 2009). Therefore, recent evidence implicating a universal ROS-dependent mechanism in cell death in turn suggests that the SOS response should be considered part of the intrinsic resistome (Kohanski *et al.,* 2007). Given the existence of an alternative DNA damage response in mycobacteria (Rand *et al.,* 2003; Gamulin *et al.,* 2004), corresponding *Mtb* and *Msm lexA*$^{Ind-}$ (SOS-uninducible) mutants were generated to evaluate how the SOS pathway specifically contributes to antibiotic-mediated DNA damage tolerance and induced mutagenesis. This study is the first to report the construction of *lexA*$^{Ind-}$ mutants in both *Msm* and *Mtb*.

To investigate the role of the SOS response in damage tolerance, UV irradiation-induced mutagenesis and MMC sensitivity of the *lexA*$^{Ind-}$ mutant were evaluated. UV irradiation of cellular DNA results primarily in cyclobutane pyrimidine dimers and pyrimidine (6–4) pyrimidine photoproducts, in which two adjacent pyrimidines are covalently linked (Janion 2008). In addition, UV can also damage bases, producing cytosine hydrate and thymine glycol (Gorna *et al.,* 2010). MMC damages DNA by specifically crosslinking the guanine nucleoside in the sequence 5'-CpG-3' (Tomasz 1995). The SOS response induces specialized DNA polymerases that are able to catalyse translesion synthesis (TLS) across these sites of damage (Friedberg *et al.,* 2002; Goodman 2002; Boshoff *et al.,* 2004a). In *Mtb*, the DnaE2 polymerase mediates TLS-catalysed DNA repair, and, importantly, has been shown to be regulated by the SOS mechanism in response to DNA damage (Boshoff *et al.,* 2003). For these reasons, a Δ*dnaE2* mutant was used a control throughout the study. Given the profound phenotypes associated with loss of DnaE2 function (Boshoff *et al.,* 2003; Warner *et al.,* 2010), and based on the fact that *dnaE2* is included in the mycobacterial *lexA*/*recA*-dependent SOS response, it was expected that the *lexA*$^{Ind-}$ mutants might phenocopy the Δ*dnaE2* mutant in the induced mutagenesis assay. Indeed, both the *Msm* and *Mtb lexA*$^{Ind-}$ mutants were severely impaired for UV-induced mutagenesis (Table 3.5 and Table 3.6, respectively). This might be attributable to loss of DnaE2 function, a conclusion that is supported by transcriptional analyses (Figure 3.10) which detected constant, low-level

dnaE2 expression in the *Mtb lexA*$^{Ind-}$ mutant under standard conditions and elevated expression after MMC exposure.

In contrast to UV-induced mutagenesis, differential abilities to tolerate MMC-mediated damage distinguished *Mtb* and *Msm*: whereas the *Mtb lexA*$^{Ind-}$ mutant appeared only 2 $\log_{10}$ more susceptible to MMC compared to Wt, the *Msm lexA*$^{Ind-}$ mutants exhibited marked hypersensitivity as demonstrated by complete growth inhibition at the higher MMC concentration (Figure 3.8 and Figure 3.5, respectively). The observation that the phenotype of the *Mtb* mutant was mild relative to *Msm* suggests a role for an alternate mechanism of repair that is regulated in a RecA-ND manner. Although this was not tested in this study, it seems reasonable to speculate that this "alternate mechanism" is likely to be NER and/or HR as repair of inter-strand crosslinks is mediated by these mechanisms (Noll *et al.,* 2006). Furthermore, NER-related genes *uvrA*, *uvrB* and *uvrD2* are regulated by the RecA-ND mechanism, while RecA-mediated HR is co regulated by the SOS response as well as the RecA-ND mechanism (Gamulin *et al.,* 2004; Smollett *et al.,* 2012). Although both mechanisms have been identified in *Msm* (Gamulin *et al.,* 2004) not nearly enough is known about the RecA-ND mechanism in this organism to explain the differential sensitivities of *Msm* and *Mtb lexA*$^{Ind-}$ mutants to genotoxic agents. As expected, a minor (4-fold and 8-fold growth reduction) effect was observed on the DNA damage sensitivity to MMC of the Δ*dnaE2* mutant (Boshoff *et al.,* 2003) However, abrogation of the SOS response in a *lexA*$^{Ind-}$ mutant not only affects the expression of *dnaE2*, but also every other gene in the regulon – which includes proteins involved in DNA repair and cell cycle arrest. Therefore, the markedly increased sensitivity of the *lexA*$^{Ind-}$ mutants compared to Δd*naE2* is intuitive.

As remediation of damaged DNA by SOS-regulated repair systems has been reported to mitigate the damaging effects of the antibiotics in *E. coli* (Kohanski *et al.,* 2007), this study set out to evaluate the effect of an inactivated SOS response on antibiotic-mediated mycobacterial cell death. To this end, the *lexA*$^{Ind-}$ mutants were exposed to antibiotics with various MoAs to examine the possibility that "a common mechanism" of cell death, regardless of the drug-target interaction, was prevalent in mycobacteria. With the existence of two damage response pathways in mycobacteria, it might equally be expected that different regulons respond to specific types of damage stress, especially given the limited overlap in gene composition, or that the regulons are redundant. Previous evidence

suggests that deletion of *recA* or key damage response components *uvrB* or *dnaE2*, results in hypersusceptibilty to some genotoxins (Boshoff *et al.,* 2003; Rand *et al.,* 2003; Darwin & Nathan 2005). Therefore, hypersensitivity of *Msm lexA*$^{Ind-}$ mutants to DNA-damaging agents (MMC and quinolones) indicates a crucial role of the SOS response in remediation (and tolerance) of damage in this organism. In contrast, in *Mtb* the type of DNA damage appears to determine the response induced. For example, previous reports have shown differential SOS gene expression profiles in response to CIP and MMC (O'sullivan *et al.,* 2008). In support of this, the *Mtb lexA*$^{Ind-}$ mutant in this study displayed hypersensitivity to MMC, which damages DNA by crosslinking the guanine nucleoside, and moderate susceptibility to various fluoroquinolones, which cause lethal double-strand breaks (DSBs) by targeting the Type II DNA topoisomerase subunit, GyrA (Drlica *et al.,* 2008). DSBs are repaired by NHEJ and HR, of which the LigD, Ku and RecBCD pathway components are fully functional in mycobacteria (Gorna *et al.,* 2010). From transcriptional (Boshoff *et al.,* 2003; Rand *et al.,* 2003; Smollett *et al.,* 2012) and bioinformatic (Gamulin *et al.,* 2004) analyses, none of these repair mechanisms appears to be subject to SOS or RecA-ND regulation in response to DNA damage. This suggests an alternative mechanism for repairing DSBs, possibly the single-strand annealing (SSA) pathway (Gupta *et al.,* 2011). Furthermore, equivalent susceptibilities were observed for the *lexA*$^{Ind-}$ mutants and Wt to NOV, a coumarin which, unlike fluoroquinolones, targets the GyrB subunit without causing DSBs and therefore does not induce the SOS response (Boshoff *et al.,* 2004a). This finding supports the notion that the type of DNA damage incurred determines the response induced. Moreover, the data also suggest that, unlike *E. coli*, inactivation of the SOS response does not sensitize mycobacteria to general antibiotic-mediated cell death.

3.5.1 Evaluation of the RecA-ND mechanism

Unlike *Msm*, an uncleavable LexA in *Mtb* does not increase susceptibility to fluoroquinolones which suggests that the RecA-ND mechanism is the major contributor to remediation of fluoroquinolone-induced damage, or that the RecA-ND response is able to compensate for loss of the canonical SOS. As ClgR has been proposed as the transcriptional regulator of the RecA-ND response (Wang *et al.,* 2011), it might be proposed that inactivation or deletion of this gene in the *lexA*$^{Ind-}$ background will generate a strain with a crippled ability to induce DNA-repair systems in response to DNA-damage. Application of a

ClgR-deficient mutant in the same assays described in this study might therefore allow the comprehensive evaluation of the proposed common mechanism of cell death in mycobacteria, as has been demonstrated in other organisms (Dwyer *et al.,* 2007).

A global analysis of the transcriptional profile of the *Mtb lexA*$^{Ind-}$ mutant following treatment with various DNA damaging agents may provide some insight into the key players of the LexA-independent DNA repair mechanism. An alternative option for evaluating the RecA-ND mechanism would be the assessment of an *Mtb lexA* null mutant. In *E. coli*, a *lexA* null mutation causes lethal filamentation, which can be prevented by creating the *lexA* deletion in a *sulA* mutant background. SulA is *lexA*-regulated and is an inhibitor of cell division, resulting in long, filamentous structures (Drlica & Zhao 1997). A *lexA* deletion mutant has not been described in *Mtb* and may not be possible to construct as the gene has been predicted to be essential *in vitro* (Griffin et al. 2011). However, evidence suggests that *Rv2719c*, a potential regulator of cell division in *Mtb* may be a SulA-orthologue. In addition multiple parallels can be drawn between SulA and *Rv2719c*, including divergent transcription from *lexA*, induction by DNA damage, and regulation in a RecA-ND manner (Brooks *et al.,* 2006; Chauhan *et al.,* 2006). Therefore, it may be possible to delete *Mtb*'s *lexA* by deleting/ mutating the non-essential *Rv2719*c (Griffin *et al.,* 2011).

In summary, the DNA damage response in mycobacteria might be considered as comprising of damage tolerance (including error-prone TLS) and DNA repair (error-free) pathways (Figure 3.11). LexA plays a crucial role in damage tolerance via induction of DnaE2-mediated TLS. Overall, it is evident that DNA repair mechanisms differ between the mycobacterial species investigated in this study and, despite effectively inactivating the LexA-dependent SOS response in *Msm* and *Mtb*, these organisms are able to circumvent this pathway and successfully remediate damaged DNA induced under various conditions.

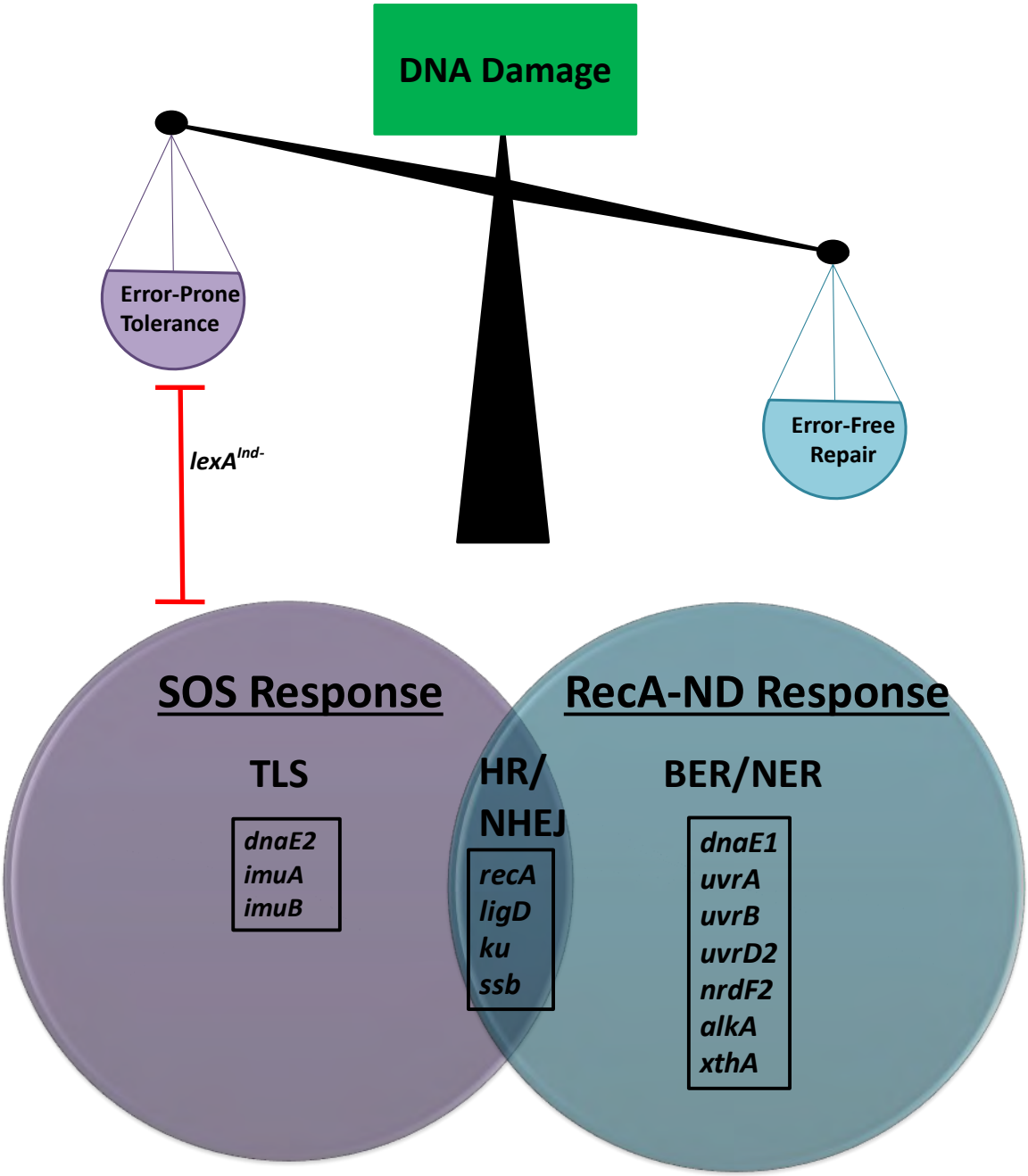

Figure 3.11: The DNA damage response in mycobacteria. A balance exists between error-prone damage tolerance and error-free DNA repair to maintain genome integrity following DNA damage. The error-prone damage tolerance mechanism is mediated via translesion synthesis (TLS), specifically the SOS-regulated genes. High fidelity DNA repair is governed by base-excision repair (BER) and nucleotide excision repair (NER) mechanisms which comprise of RecA-ND-regulated genes. In addition, homolgous recombination (HR) and non-homologous end-joining (NHEJ) repair mechanisms are co-regulated by the SOS response and RecA-ND response. The *lexA*$^{Ind-}$ mutants generated in this study have an inactivated SOS response, but fully functional RecA-ND and co-regulated responses. Thus, error-prone damage tolerance (TLS) is compromised in these strains, but error-free DNA repair (BER/NER) and repair of double-strand breaks (DSBs, HR/NHEJ) remains functional.

Chapter 4: Construction and validation of auto-bioluminescent DNA-damage reporter strains for *Mtb* whole-cell screening

4.1 Introduction

The identification of the molecular target of novel antimicrobials during the early stages of the drug discovery process is essential for progression of hit compounds or series towards a promising clinical candidate. The increasingly wide availability of next generation sequencing platforms has enabled WGS of bacteria to become high-throughput and affordable, and results are usually obtained promptly. In drug discovery, WGS is used extensively for target identification of hit compounds (Lechartier *et al.,* 2014). Briefly, log-phase cultures are plated onto solid agar media containing the hit compound at a range of concentrations that extend well above the minimum inhibitory concentration (MIC). The plates are incubated for 4-6 weeks, after which spontaneous drug-resistant mutants are isolated. Following DNA extraction, WGS is applied to identify single nucleotide polymorphisms (SNPs) or other mutations that confer resistance. The locus of resistance is often assumed to be the target gene/s (Ioerger *et al.,* 2013); however, while in many cases the drug-target pair can be reliably interpreted from these results, in others, the resistance mutation might provide information regarding MoA without elucidating the direct target (especially where the compound functions as a pro-drug) (Manjunatha *et al.,* 2006; Ioerger *et al.,* 2013). There is a further category, too: that is, where resistance mutations map to "non-specific"' cellular mechanisms, such as efflux (Ioerger *et al.,* 2013). In addition to some of the difficulties associated with interpreting mutation data, related limitations to this technique include: (i) the fact that it is labour intensive and time consuming, especially where there are multiple hit compounds and active series, and, of course (ii) the risk of contamination as a consequence of the long incubation time required for resistant colonies to emerge on solid media.

Cell-based reporter assays or bacterial biosensors offer a useful alternative for MoA studies of potent whole-cell active compounds (Alland *et al.,* 2000; Boshoff *et al.,* 2004b). Using this approach, multiple targets may be screened, enabling simultaneous identification of the pathway and/or target before extensive medicinal chemistry efforts are undertaken (Balganesh *et al.,* 2008; Fan *et al.,* 2014). At the inception of the current study, it was proposed that monitoring the response of antibiotics in real-time with high sensitivity might represent an efficient approach to be applied in addition to the traditional agar-based method for cases in which the target is novel and not readily resolved. Bioluminescence has

been profitably exploited to generate reporter mutants that can provide a rapid, sensitive and quantitative real-time readout of the mycobacterial response to antibiotics (Andreu *et al.,* 2010; Andreu *et al.,* 2012; Singh *et al.,* 2014b). Therefore, the overall goal of this study was to generate novel bioluminescence-based reporters to detect the activation of the DNA damage response in *Mtb*.

A remarkably diverse set of organisms possess the capacity for bioluminescence including bacteria, dinoflagellates, fungi, fish, insects, shrimp and squid. Luciferases are the enzymes that catalyse the bioluminescence reactions and in most cases, the substrates are designated luciferins (Meighen 1991). Bioluminescent bacteria are categorized into four genera: *Photobacterium, Vibrio, Photorhabdus* and *Altermonas*. The light-emitting reaction in bacteria involves the oxidation of reduced riboflavin phosphate ($FMNH_2$) and a long-chain fatty aldehyde by luciferases with the concomitant emission of blue-green light at 490 nm. The bacterial Lux operon, *luxCDABE*, encodes the luciferase as well as the aldehyde substrate. Luciferase is a heterodimeric enzyme composed of α and β subunits encoded by *luxA* and *luxB*, respectively. The aldehyde for the bioluminescence reaction is synthesized by a multienzyme complex containing three proteins: a reductase (*luxC*), a transferase (*luxD*), and a synthetase (*luxE*) (Meighen 1991).

4.2 Aims and objectives

Studies in various organisms have utilized reporter assays, in particular green fluorescent protein (GFP)-based assays, for the determination of MoA (Hutter *et al.,* 2004; Fan *et al.,* 2014). In mycobacteria, bioluminescence-based approaches have been used for the evaluation of drug and vaccine efficacy *in vitro* and *in vivo* (Andrew & Roberts 1993; Cooksey *et al.,* 1993; Hickey *et al.,* 1996; Al-Attiyah *et al.,* 2006; Andreu *et al.,* 2010; Andreu *et al.,* 2012). Thus, reporter strains using pathway-specific promoters may provide a better alternative to currently available methods for MoA determination by allowing a limited screening of compounds interfering with only a particular metabolic pathway.

This study aimed to utilize the *Photorhabdus luminescens*-derived luminescence system to exploit DNA metabolism as a target to identify novel genotoxins. The main advantage of this system is that exogenous luminescence substrate is not required. The specific objectives therefore included:

1. Introduction of the *lux* operon under the transcriptional control of *Mtb* promoters that are known to be DNA-damage-inducible, specifically *recA* and *radA*.
2. Development and validation of an assay that measures the SOS-dependent induction of luminescence in a dose-dependent and time-dependent manner.
3. Testing of novel compounds from an existing drug discovery platform in the DNA damage Lux assay.

4.3 Materials and Methods

4.3.1 Construction of the Lux reporter strains

Andreu *et al*., 2010 previously reported the development of auto-luminescent mycobacteria in which exogenous substrate is not required to generate a luminescence signal. Their pMV306*lux* vector was purchased from Addgene Inc. and the putative promoter regions of *Mtb* H37Rv *recA* (*Rv2737c*), P_{recA}, and *radA* (*Rv3585*), P_{radA}, (481 bp and 487 bp, respectively) were synthesized by GeneWiz Inc, Sigma. Promoter replacement of P_{hsp60} was performed by ligating *Not*I/*Nco*I- digested P_{recA} or P_{radA} with *Not*I/*Nco*I – digested pMV306*lux* to generate pMV306RecA and pMV306RadA, respectively (Table 4.1). Following selection on KAN, positive constructs were validated by restriction analysis. The constructs were then electroporated into *Mtb* H37Rv (Wt) and the *Mtb lexA*$^{Ind-}$ backgrounds (described in Chapter 3) to generate strains described in Table 4.2.

Table 4.1: Plasmids used in this study

★ P_{hsp60} and P_{G13} are strong promoters derived from *M. bovis* BCG and *M. marinum*, respectively (Andreu *et al.,* 2010).

Plasmid	Description ★	Reference/ Source
pMV306*hsp*Lux	Mycobacterial integrating vector, with *luxAB* under P_{hsp60} regulation and *luxCDE* under P_{G13} regulation, KAN^R	(Andreu *et al.,* 2010)
pMV306*radA*	Mycobacterial integrating vector, with *luxAB* under P_{radA} regulation and *luxCDE* under P_{G13} regulation; KAN^R	This study
pMV306*recA*	Mycobacterial integrating vector, with *luxAB* under P_{recA} regulation and *luxCDE* under P_{G13} regulation; KAN^R	This study

Table 4.2: Strains used in this study

Strain	Description/ Genotype	Reference/ Source
Wt::p*recA*-*lux*	H37RvMA derivative carrying an integrating reporter vector in which the *luxABCDE* operon is fused downstream of the *recA* promoter, KAN^R	This study
Wt::p*radA*-*lux*	H37RvMA derivative carrying an integrating reporter vector in which the *luxABCDE* operon is fused downstream of the *radA* promoter, KAN^R	This study
lexA^{Ind-}::p*recA*-*lux*	*Mtb lexA*$^{Ind-}$ mutant carrying an integrating reporter vector in which the *luxABCDE* operon is fused downstream of the *recA* promoter, KAN^R	This study
lexA^{Ind-}::p*radA*-*lux*	*Mtb lexA*$^{Ind-}$ derivative carrying an integrating reporter vector in which the *luxABCDE* operon is fused downstream of the *radA* promoter, KAN^R	This study

4.3.2 Screening of transformants

To test for bioluminescence, 10 randomly selected transformants on 7H10/OADC + KAN^{20} were isolated and grown to an OD_{600} of 0.3 in 7H9/OADC +KAN^{20}. Cultures were treated with CIP or MMC at sub-MIC_{90} concentrations for 24 hr and aliquoted into 96-well microtitre plates for measurement of luminescence (described below). Positive isolates were sub-cultured into larger volumes of media for archiving as freezer stocks.

4.3.3 Antimicrobial agents

RIF; INH; KAN; 5-FU; CIP; MMC; nitrofurazone (NFZ); 5-FU; 4-nitroquinoline-1-oxide (4NQO); D-cycloserine (DCS) and fusidic acid (FA) were purchased from Sigma Aldrich. For stock solutions, antimicrobials were all dissolved in the following solvents: INH; KAN; 5-FU and MMC in H_2O, CIP in 0.1M hydrochloric acid and RIF; NFZ, 4NQO and FA in DMSO. Antimicrobial stock solutions were stored at 4°C

4.3.4 Bioluminescence Assay

The standard broth microdilution method (described in Chapter 2) was adopted to evaluate induction of DNA damage by various compounds. The protocol was adapted to include additional controls. The outermost wells of each 96-well microtitre plate (Greiner, white plates with clear lids– Lasec, P1PLA045W-000096ST) were used for controls: Media + cells (0% luminescence); Media only (contamination control) and Media + CIP (½ × MIC) + Cells

(100% luminescence) (Figure 4.1). All media used in this assay contained KAN (20 µg/ml) to maintain the pMV306 plasmid. *Mtb* Lux strains were grown to OD_{600} of 0.5 – 0.6. Cultures were diluted to an OD_{600} of 0.05 before inoculation of 96-well plates, such that final volume in each well was 100 µl. Plates were incubated in airtight containers at 37°C for 14 days. The FLUOstar OPTIMA (BMG LABTECH) plate reader was used to measure luminescence (recorded as Relative Luminescence Units, RLU) every 24 hr. The following settings were applied: measurement interval time for 1.0 s after a positioning delay of 0.2 s; top optic was used with an empty lens emission filter, gain adjustment of 4095 and plates were shaken for 5 s at 120 rpm, before plate reading.

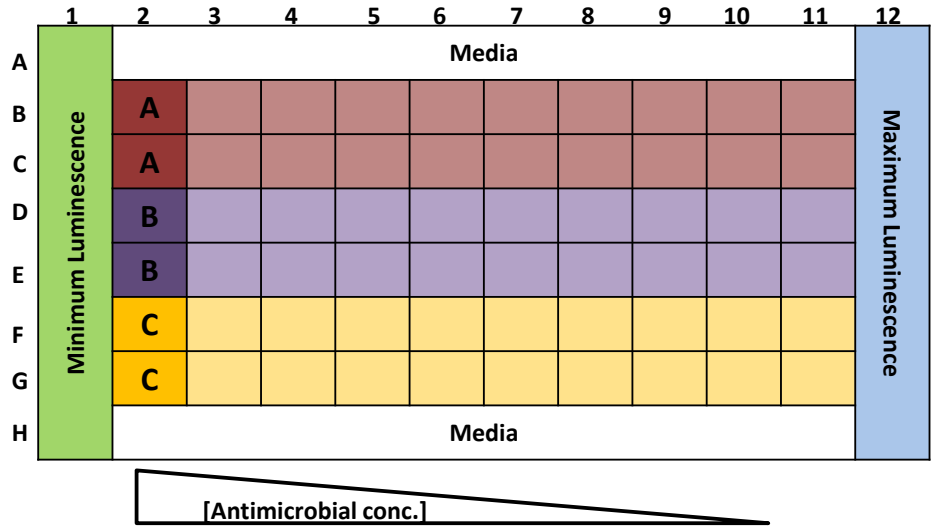

Figure 4.1: Bioluminescence assay plate layout. The outer wells were used for controls - Column 1 for the minimum luminescence control (media +cells), Column 12 for maximum luminescence (media + cells +CIP at ½ × MIC_{90}) and Row A and H for media only. Three antimicrobials were tested per plate, each in duplicate (**A**, **B** and **C**). Antimicrobials were added to Column 2 and serially diluted, 2-fold, to Row 11.

4.3.4 Data analysis

Raw RLU data were provided by the MARS Data Analysis Software. All RLUs were normalized to the 100% luminescence sample to generate a fold-induction value for each treatment time-point. Values were then adjusted to take into account the 0% luminescence control resulting in the final % luminescence value. As each antimicrobial was tested in duplicate, the final % luminescence values were averaged and plotted as 3D surface charts (Microsoft Excel 2010) against concentration and time.

4.4 Results

4.4.1 *Mtb* autoluminescent DNA damage reporter strains

Andreu *et al.,* 2010 previously reported the development of auto-luminescent mycobacterial mutants in which exogenous substrate is not required to generate the luminescence signal. Promoter replacement of P_{hsp60} in their pMV306hsp+LuxAB+G13+CDE vector (referred to as pMV306*lux* in this study) with the putative promoter regions of *Rv2737c* (*recA*) or *Rv3585* (*radA*) resulted in two new DNA damage-responsive bioluminescent reporters: pMV306*recA* and pMV306*radA* (Figure 4.2). The constructs were confirmed by restriction analysis and electroporated into *Mtb* Wt and *Mtb* $lexA^{Ind-}$ backgrounds (described in Chapter 3) to generate the strains Wt::p*recA-lux*, Wt::p*radA-lux,* $lexA^{Ind-}$::p*recA-lux* and $lexA^{Ind-}$::p*radA-lux*, respectively.

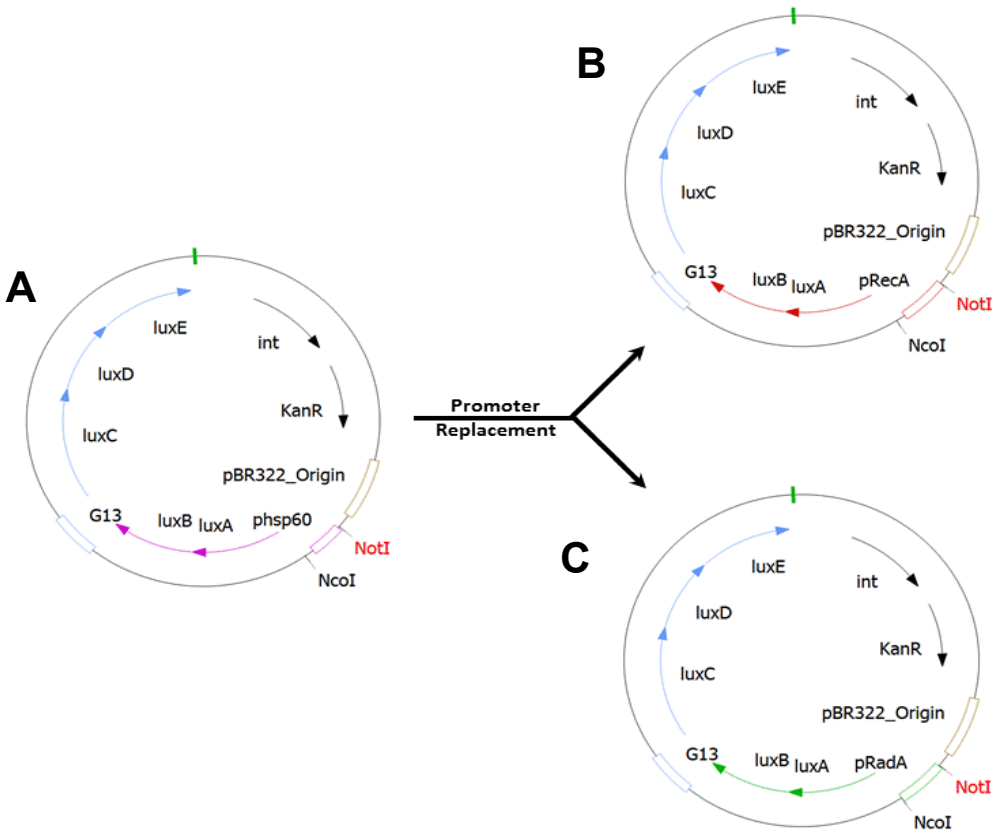

Figure 4.2: Construction of vectors for DNA damage-inducible autoluminescence. (**A**) pMV306*lux*::P_{hsp60} drives the expression of the luciferases (encoded by the *luxAB* genes), and the strong promoter P_{G13} drives the expression of the long-chain aldehyde substrate (encoded by *luxCDE*). The vector also carries a KAN^R marker for maintenance and selection (Andreu et al., 2010). Using the enzymes *Nco*I and *Not*I, P_{hsp60} was replaced with either the 481 bp upstream region of *recA* (**B**) or the 487 bp upstream region of *radA* (**C**) to generate pMV306*recA* and pMV306*radA*, respectively.

4.4.2 Assay development and validation

RecA is the hallmark component of the DNA damage response in the majority of organisms and is induced by known DNA inhibitors in *Mtb* (Chapter 3). In addition, the same DNA inhibitors have been shown to induce expression of *radA*, which is regulated by the RecA-ND response (Boshoff *et al.,* 2003; Rand *et al.,* 2003; Smollett *et al.,* 2012) (Chapter 3, Figure 3.2). Therefore, the *recA* and *radA* promoters were selected to identify inhibitors of DNA metabolism that result in genotoxic stress. The broth microdilution method was used to measure the induction of luminescence in a concentration-dependent manner at 24 hr intervals. Initially, 10 randomly selected transformants from each strain were selected and tested for induction of luminescence (described in section 4.3.2). The transformation efficiency varied between the different promoter constructs as well as between the two strains (Table 4.3). As no transformants were isolated for the *lexA*$^{Ind-}$ strains, only the Wt stains were selected for further assay development. The inability to isolate *lexA*$^{Ind-}$::*lux* strains may be attributable to the low transformation efficiency in general. As the Lux constructs were only electroporated once in the *lexA*$^{Ind-}$ background and only 10 putative transformants were initially selected for screening of luminescence, electroporations will be repeated and considerably more colonies need to be screened in the future. From a research interest, characterization of the Wt Lux strains was of priority and due to time constraints the *lexA*$^{Ind-}$::*lux* strains were re-prioritized to future work.

Table 4.3: Transformation efficiency of Lux constructs in *Mtb* H37Rv (Wt) and the *Mtb* *lexA*$^{Ind-}$ backgrounds

	Wt::p*recA*-*lux*	**Wt::p*radA*-*lux***	***lexA*$^{Ind-}$::p*recA*-*lux***	***lexA*$^{Ind-}$::p*radA*-*lux***
Number of transformants*	7	2	0	0

*Number of transformants out of 10 that displayed induction upon exposure to CIP or MMC, as a measure of luminescence.

Evaluation of the raw data highlighted a significant difference in the level of induction of the two promoters in response to CIP, as indicated by the ~38-fold higher induction of the *recA* "maximum luminescence" control (row 12), compared to that of *radA* (as a measure of RLU) (Figure 4.3).

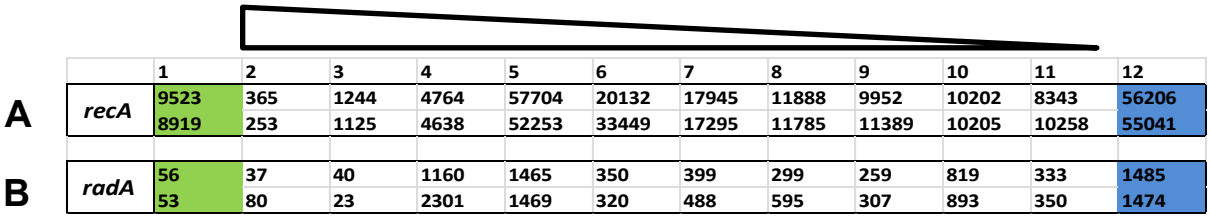

		1	2	3	4	5	6	7	8	9	10	11	12
A	*recA*	9523	365	1244	4764	57704	20132	17945	11888	9952	10202	8343	56206
		8919	253	1125	4638	52253	33449	17295	11785	11389	10205	10258	55041
B	*radA*	56	37	40	1160	1465	350	399	299	259	819	333	1485
		53	80	23	2301	1469	320	488	595	307	893	350	1474

Figure 4.3: Raw relative luminescence unit (RLU) data of Wt::*lux* strains in response to ciprofloxacin (CIP). Column 1 indicates the minimum luminescence (green) and Column 12 indicates the maximum luminescence (blue). CIP was serially diluted, 2-fold from column 2 to column 11, in duplicate. Induction of *recA* (**A**) was significantly higher than induction of *radA* (**B**), as indicated by the RLUs.

CIP was selected as the maximum luminescence control as preliminary data indicated immediate (within 24 hr) and sustained (up to 12 d) induction (Figure 4.4). During initial screening of transformants, CIP was not the most potent DNA-damage inducer, therefore it was selected as the representative threshold inducer, to which compounds that induce significantly more or less could be compared. With such a large amount of data generated for each antimicrobial compound, representation of the normalized data presented a challenge. After some experimentation with visualization styles, 3-D plots were selected, as they incorporated concentration, time and RLU in a single image. The "bird's eye view" representation (Figure 4.4A) was ultimately chosen as the standard format for presenting data in this study.

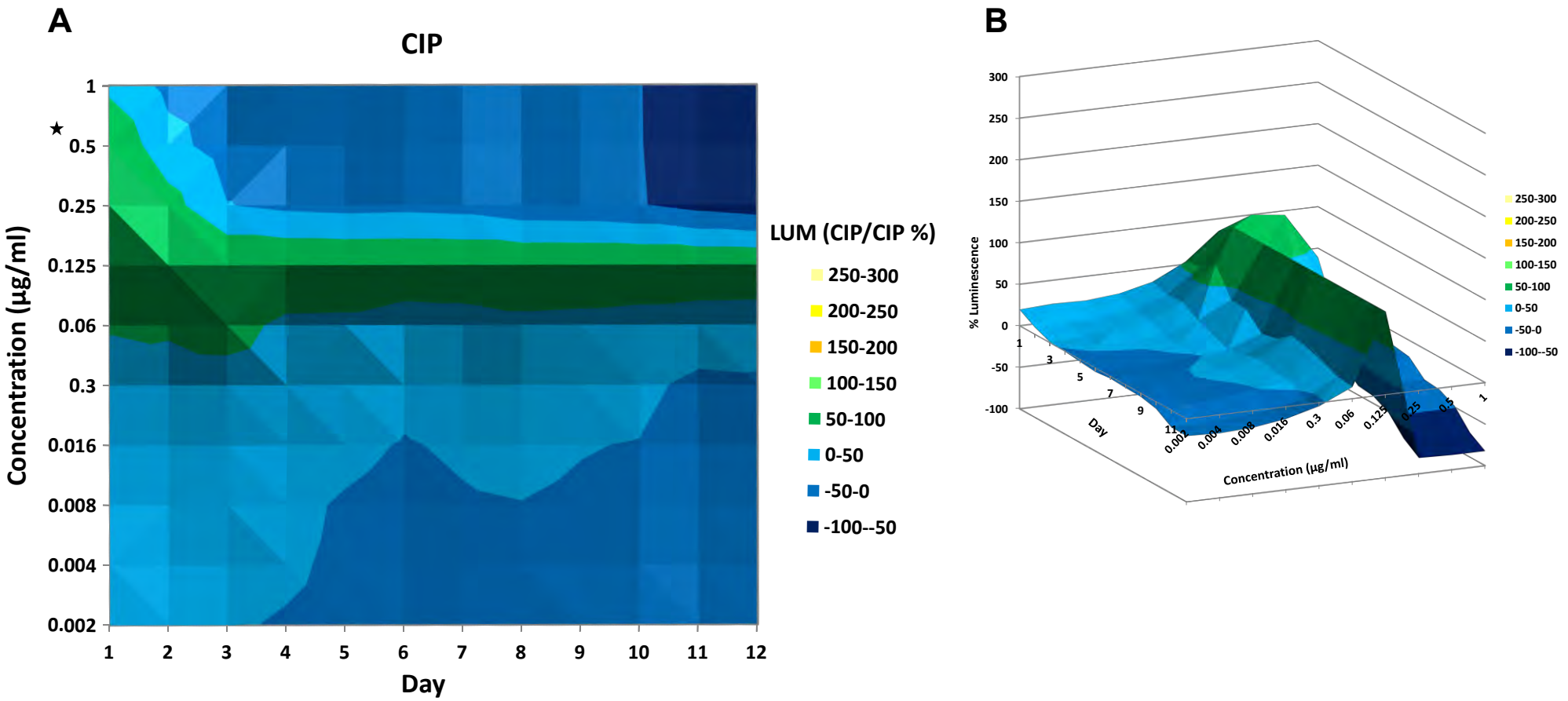

Figure 4.4: Kinetics of Wt::p*recA-lux* induction in response to ciprofloxacin (CIP). A bird's eye view (**A**) and 3-D surface (**B**) representation of *recA* induction in response to CIP, as a measure of luminescence (reported as % luminescence, normalized to CIP) at 10 different concentrations over a 12-day period. The colour gradient indicates low to no induction (-100 – 49%, blue), induction (50 – 149%, green), and elevated induction (150 – 300%, yellow). Data were normalized to CIP's maximum % luminescence, such that CIP induction only ever reached a maximum of 100% luminescence. CIP induced *recA* within 24 hr and throughout the time course up to day 12 .The MIC_{90} is indicated by an asterisk (★). Data are representative of at least 3 biological replicates.

To validate the assay, a panel of established DNA inhibitors including CIP, MMC, NFZ and 4NQO, was selected and tested against Wt::p*recA*-*lux* and Wt::p*radA*-*lux*. The luminescence signal detected in response to all antimicrobials was assayed with both strains, and normalized to CIP as the DNA-damage control. That is, CIP was assigned the maximum of 100% luminescence (Figure 4.4). MMC exhibited the greatest induction of all antimicrobials assayed. Significant induction was observed within 24 hr of exposure, which then decreased slightly over the following 4 days, and then increased exponentially between days 7 and 12, with maximum induction observed at days 10 and 11 (Figure 4.5A). Interestingly, NFZ, a DNA-damaging agent that forms adducts at the N^2 -position of deoxyguanosine (dG) (Jarosz *et al.,* 2007), appeared to induce expression only after day 6. This suggests that NFZ might be required to accumulate to a certain level before sufficient genotoxic stress is achieved to trigger induction of *Mtb recA* (Figure 4.5B). In addition, 4NQO, a DNA-damaging agent that also forms dG lesions carrying adducts at the N^2 position (Jarosz *et al.,* 2007), exhibited moderate induction initially, which then tapered off by day 7 (Figure 4.5C). This suggests that this antimicrobial doesn't induce significant genotoxic stress in *Mtb*, or that exposure to 4NQO induces the DNA damage response by a mechanism alternate to *recA*; the latter possibility was further examined by the *radA* response.

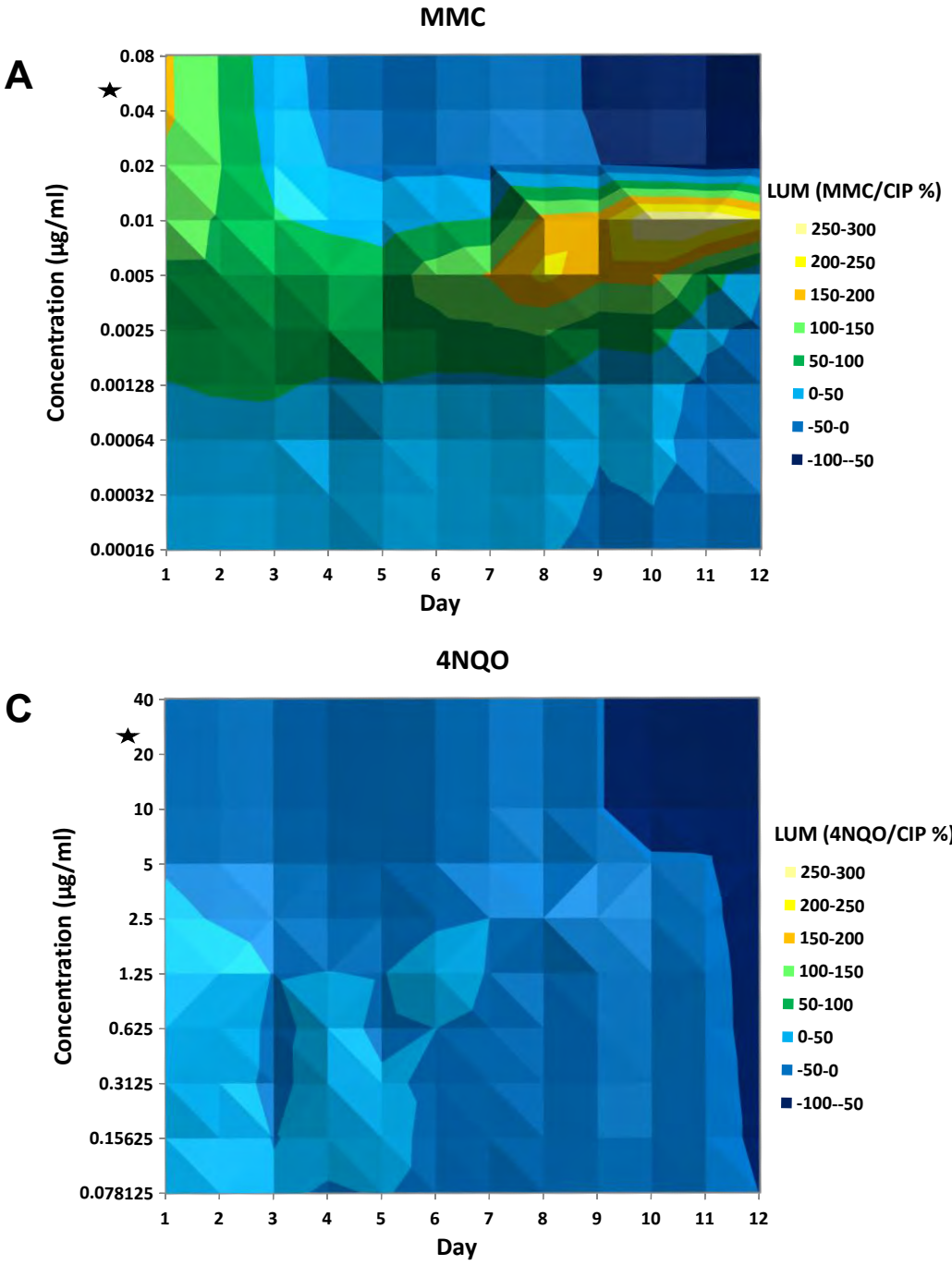
A
MMC
Concentration (µg/ml)
0.08
0.04
0.02
0.01
0.005
0.0025
0.00128
0.00064
0.00032
0.00016
1 2 3 4 5 6 7 8 9 10 11 12
Day
LUM (MMC/CIP %)
250-300
200-250
150-200
100-150
50-100
0-50
-50-0
-100--50
B
NFZ
Concentration (µg/ml)
256
128
64
32
16
8
4
2
1
0.5
1 2 3 4 5 6 7 8 9 10 11 12
Day
LUM (NFZ/CIP %)
250-300
200-250
150-200
100-150
50-100
0-50
-50-0
-100--50
C
4NQO
Concentration (µg/ml)
40
20
10
5
2.5
1.25
0.625
0.3125
0.15625
0.078125
1 2 3 4 5 6 7 8 9 10 11 12
Day
LUM (4NQO/CIP %)
250-300
200-250
150-200
100-150
50-100
0-50
-50-0
-100--50

Figure 4.5: Kinetics of Wt::p*recA-lux* induction in response to known DNA-damaging agents. Induction of *recA* as a measure of luminescence (reported as % luminescence) in response to MMC (**A**), NFZ (**B**), and 4NQO (**C**). Each antimicrobial was tested at 10 different concentrations over a 12-day period. Data were normalized to CIP, which represents a true inducer. MMC strongly induced *recA*, NFZ displayed a delayed response, while 4NQO only exhibited a mild initial response. The MIC_{90} of each drug is indicated by the asterisk (★). Data are representative of at least 3 biological replicates.

In general, *radA* was induced similarly to *recA* by the same DNA damaging agents (Figure 4.6). MMC exhibited the greatest induction of all antimicrobials assayed, as with Wt::p*recA-lux.* However, exponential induction was observed from 24 hr of exposure, reaching a maximum at day 7, and followed by a gradual decline to day 12 (Figure 4.6B). Again, significant induction by NFZ was delayed until day 5, followed by a gradual decrease from day 8 (Figure 4.6C). 4NQO exhibited moderate induction initially, as observed for Wt::p*recA-lux*, and then decreased between days 5 and 7. Unlike Wt::p*recA-lux*, the *radA* reporter exhibited moderate induction at the lower concentrations (≥ ¼ × MIC_{90}) of drug up to day 12 (Figure 4.6D). This indicates that the RecA-ND mechanism may play a role in remediation of DNA damage induced by 4NQO specifically, in a concentration and time-dependent manner.

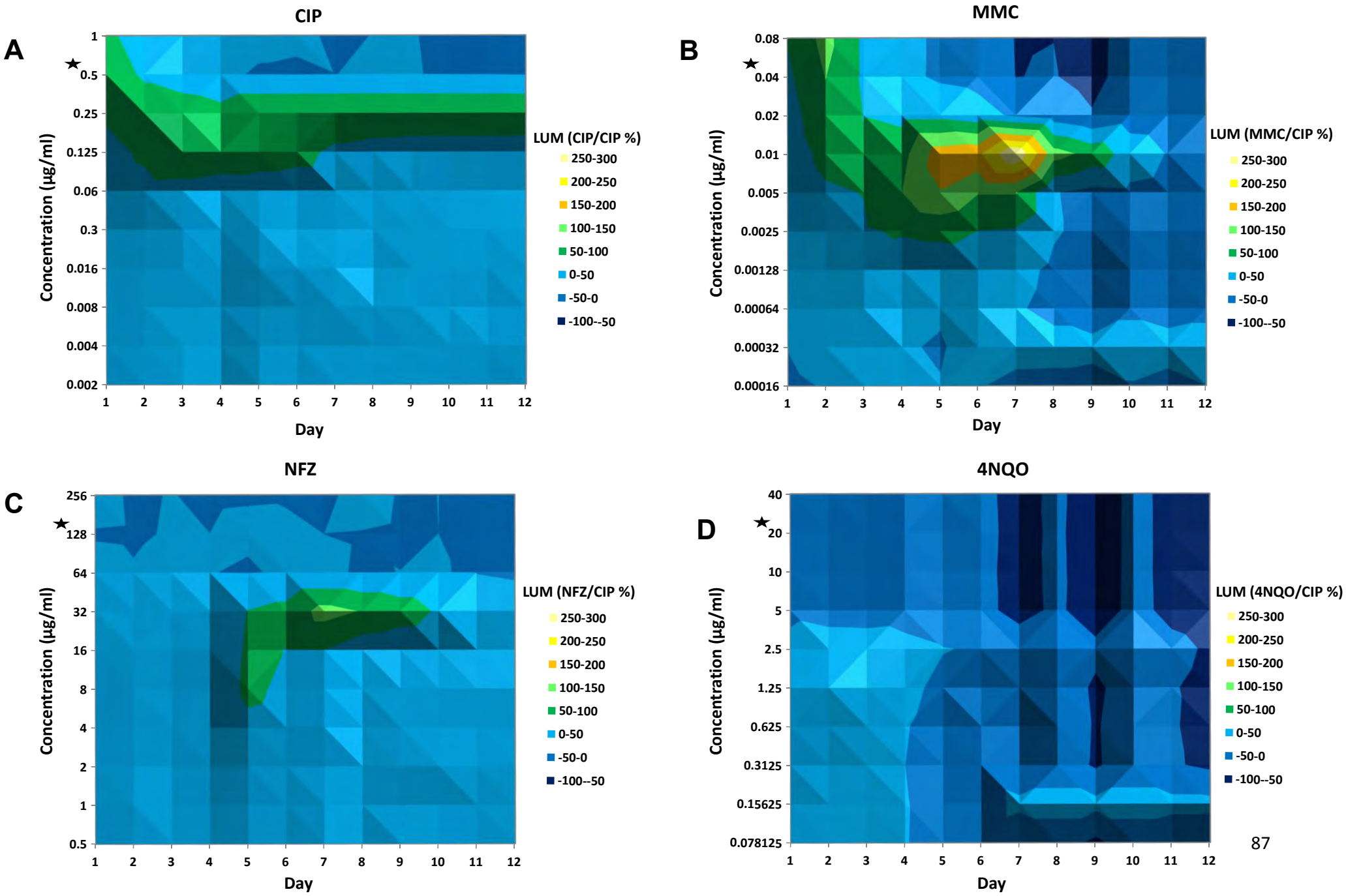
A
CIP
Concentration (µg/ml)
1
0.5
0.25
0.125
0.06
0.3
0.016
0.008
0.004
0.002
1 2 3 4 5 6 7 8 9 10 11 12
Day
LUM (CIP/CIP %)
250-300
200-250
150-200
100-150
50-100
0-50
-50-0
-100--50
B
MMC
Concentration (µg/ml)
0.08
0.04
0.02
0.01
0.005
0.0025
0.00128
0.00064
0.00032
0.00016
1 2 3 4 5 6 7 8 9 10 11 12
Day
LUM (MMC/CIP %)
250-300
200-250
150-200
100-150
50-100
0-50
-50-0
-100--50
C
NFZ
Concentration (µg/ml)
256
128
64
32
16
8
4
2
1
0.5
1 2 3 4 5 6 7 8 9 10 11 12
Day
LUM (NFZ/CIP %)
250-300
200-250
150-200
100-150
50-100
0-50
-50-0
-100--50
D
4NQO
Concentration (µg/ml)
40
20
10
5
2.5
1.25
0.625
0.3125
0.15625
0.078125
1 2 3 4 5 6 7 8 9 10 11 12
Day
LUM (4NQO/CIP %)
250-300
200-250
150-200
100-150
50-100
0-50
-50-0
-100--50

Figure 4.6: Kinetics of Wt::p*radA-lux* induction in response to known DNA-damaging agents. Induction of *radA* as a measure of luminescence (reported as % luminescence) in response to CIP (**A**), MMC (**B**), NFZ (**C**) and 4NQO (**D**). Each antimicrobial was tested at 10 different concentrations over a 12-day period. Data were normalized to CIP, which represents a true inducer. MMC strongly induced *radA*, NFZ displayd a delayed response and 4NQO exhibited a mild initial response. The MIC_{90} of each drug is indicated by the asterisk (★). Data are representative of at least 3 biological replicates.

To confirm that induction of luminescence was restricted to DNA-damaging agents, various antimicrobials of different classes were tested that were not expected to induce a DNA damage response, (Figure 4.7). These included INH (cell wall inhibitor), RIF (transcriptional inhibitor), FA (protein synthesis inhibitor) and DCS (cell wall inhibitor which is cidal against mycobacteria), all of which exhibited low to no (< 20% to < 0%, raw data not shown) induction (Figure 4.7, and Wt::p*radA-lux*, data not shown). This is an important result since it indicates that antibiotic-mediated cell death (or stasis) does not cause an increase in luminescence signal, and so eliminates the possibility that cell death (or stasis) might result in the erroneous assignment of an unknown compound as a "genotoxin". That is, it suggests that the reporter assay specifically detects compounds whose direct MoA involves damaging (myco)bacterial DNA.

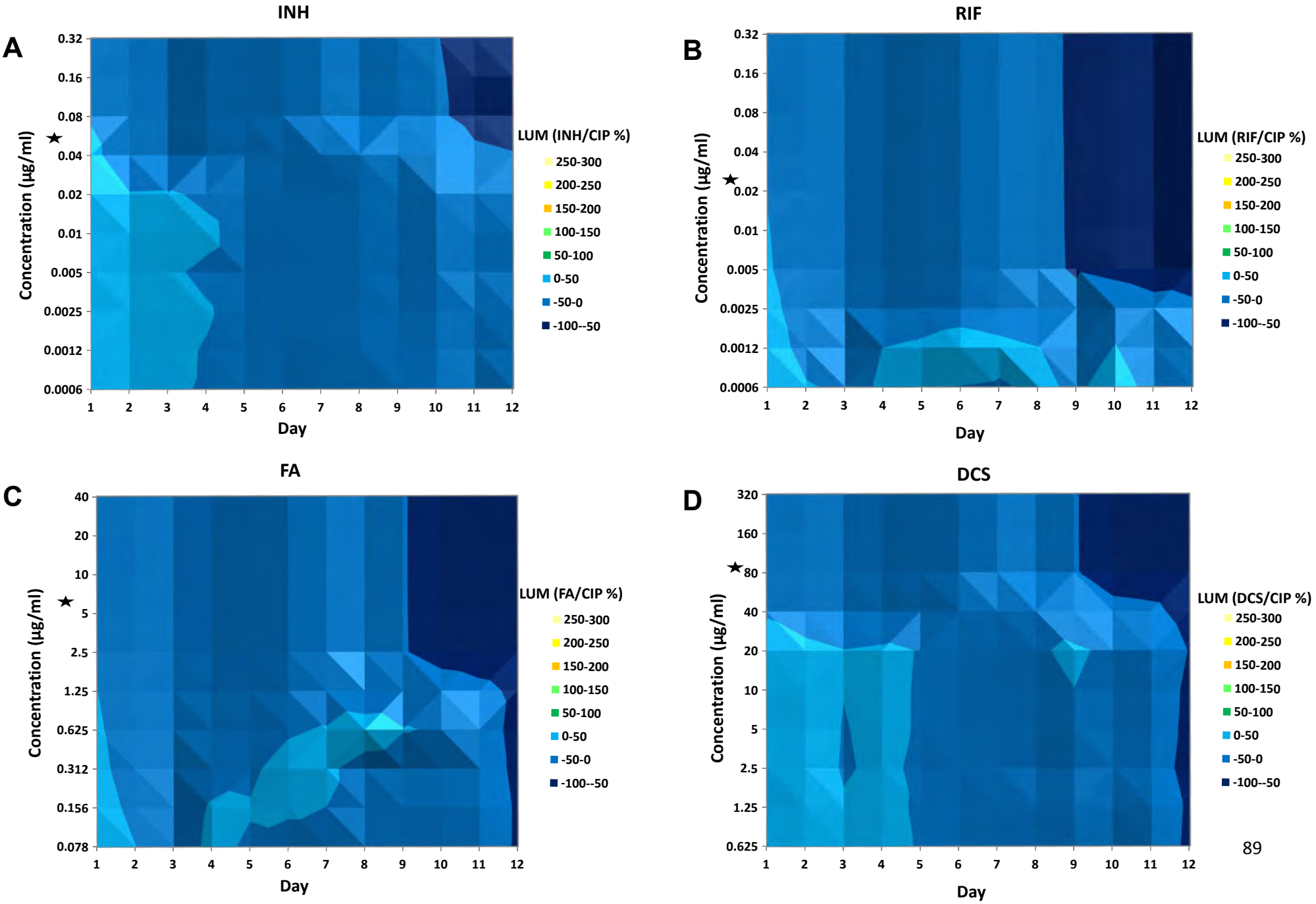
A
INH
Concentration (µg/ml)
0.32
0.16
0.08
0.04
0.02
0.01
0.005
0.0025
0.0012
0.0006
1 2 3 4 5 6 7 8 9 10 11 12
Day
LUM (INH/CIP %)
250-300
200-250
150-200
100-150
50-100
0-50
-50-0
-100--50
B
RIF
Concentration (µg/ml)
0.32
0.16
0.08
0.04
0.02
0.01
0.005
0.0025
0.0012
0.0006
1 2 3 4 5 6 7 8 9 10 11 12
Day
LUM (RIF/CIP %)
250-300
200-250
150-200
100-150
50-100
0-50
-50-0
-100--50
C
FA
Concentration (µg/ml)
40
20
10
5
2.5
1.25
0.625
0.312
0.156
0.078
1 2 3 4 5 6 7 8 9 10 11 12
Day
LUM (FA/CIP %)
250-300
200-250
150-200
100-150
50-100
0-50
-50-0
-100--50
D
DCS
Concentration (µg/ml)
320
160
80
40
20
10
5
2.5
1.25
0.625
1 2 3 4 5 6 7 8 9 10 11 12
Day
LUM (DCS/CIP %)
250-300
200-250
150-200
100-150
50-100
0-50
-50-0
-100--50

Figure 4.7: Kinetics of Wt::p*recA-lux* induction in response to antimicrobials with various MoAs . Induction of *recA* as a measure of luminescence (reported as % luminescence) in response to INH (**A**), RIF (**B**), FA (**C**) and DCS (**D**). Each antimicrobial was tested at 10 different concentrations over a 12-day period. Data were normalized to CIP, which represents a true inducer. All four antimicrobials tested displayed low to no induction of *recA*. The MIC_{90} of each drug is indicated by the asterisk (★). Data are representative of at least 3 biological replicates.

In addition, the kinetic profile of 5-FU, an antimicrobial agent with a complex MoA (Singh *et al.,* 2015), was evaluated (Figure 4.8). Interestingly, delayed induction was observed between days 3 and 7 and at day 6 for Wt::p*recA-lux* and Wt::p*radA-lux*, respectively. In addition, *recA* is induced significantly more than *radA*, suggesting that the LexA/RecA-dependent SOS pathway may be the governing response to 5-FU-induce DNA damage. The MoA of 5-FU was recently elucidated through an extended and multi-pronged approach which established that DNA damage is a minor component of a complex mechanism that is dominated by cell wall inhibition (Singh *et al.,* 2015). It is encouraging that the results of the luminescence assay suggest the possibility that a simple (and rapid) bioreporter might have provided early insight into the role of genotoxicity as one component of the MoA of 5-FU.

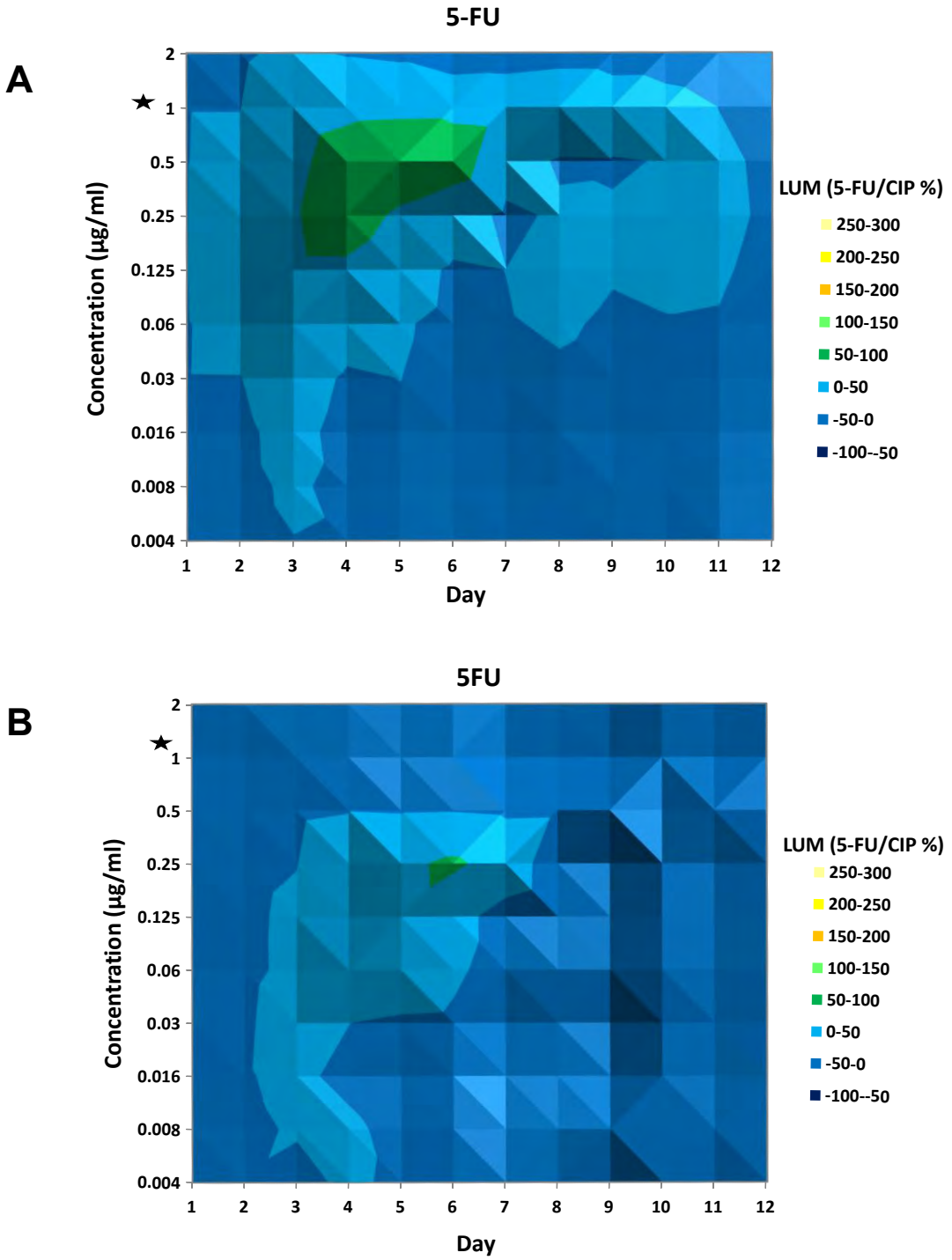

Figure 4.8: Kinetics in response to 5-FU. Induction of *recA* (A) and *radA* (B) as a measure of luminescence in response to 5-FU at 10 different concentrations over a 12-day period. Data were normalized to CIP. In both strains, the response to treatment was delayed, although *recA* was induced significantly more than *radA*. The MIC_{90} is indicated by the asterisk (★). Data are representative of at least 3 biological replicates, within which, 5-FU was tested in technical duplicate.

4.4.3 Use of auto-bioluminescent reporter strains as screening tools

Following validation of the auto-luminescent reporter strains, we selected two novel compounds of unknown MoA for assessment in the assays. The compounds, which had been synthesized as part of a medicinal chemistry programme at UCT, possessed structural and physicochemical properties suggesting the potential to act as DNA intercalators. The results of the assay suggest, however, that the compounds are not genotoxic: no to low luminescence (< 20% to < 0%, raw data not shown) was observed throughout the 12 day exposure (Figure 4.9), consistent with the profile observed for known non-inducers (Figure 4.7).

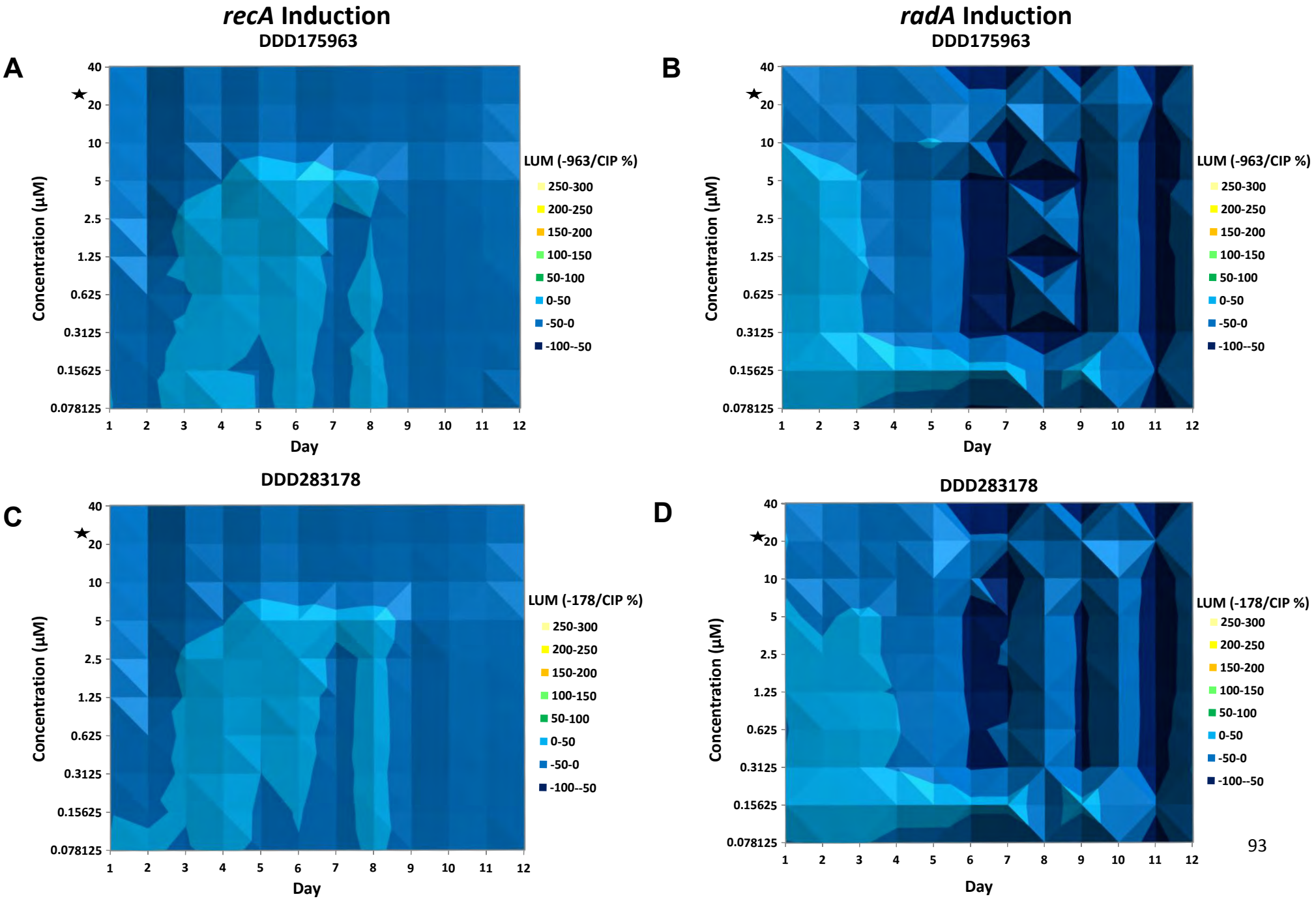
A
recA Induction
DDD175963
Concentration (µM)
40
20
10
5
2.5
1.25
0.625
0.3125
0.15625
0.078125
1 2 3 4 5 6 7 8 9 10 11 12
Day
LUM (-963/CIP %)
250-300
200-250
150-200
100-150
50-100
0-50
-50-0
-100--50
B
radA Induction
DDD175963
C
DDD283178
LUM (-178/CIP %)
D
DDD283178

Figure 4.9: Kinetics in response to novel antimicrobials. Induction of *recA* (A and C) and *radA* (B and D) as a measure of luminescence in response to 2 novel compounds at 10 different concentrations over a 12-day period Data were normalized to CIP, which represents a true inducer. The kinetic profiles suggested the neither compound induced the DNA damage response. The MIC_{90} of each drug is indicated by the asterisk (★). Data are representative of at least 3 biological replicates.

4.5 Discussion

The success of whole-cell screening in TB drug discovery is evident in the fact that all novel chemical entities discovered in the last 10 years have been identified through this approach (Lechartier *et al.,* 2014). Critically, whole-cell screening circumvents the risk (substantial in the case of *Mtb* which has a notoriously complex and impermeable cell wall; (Jackson 2014)]) of failing to convert (biochemical) target inhibition into (bacterial) growth inhibition (or death) - something which the target-driven approach is unable to achieve. On the other hand, an obvious drawback of the whole-cell screening approach is that it does not provide information regarding the MoA and possible host toxicity, both of which are especially relevant to TB chemotherapy given the prolonged duration of treatment (Balganesh *et al.,* 2008).

The identification of the molecular target/ MoA is also critical in prioritizing and optimizing lead chemical series during early stage drug discovery. The advances in WGS technology have augmented the whole-cell screening approach by enabling more rapid target identification through the identification of resistance-conferring mutations (Lechartier *et al.,* 2014). However, mechanisms of resistance do not always provide immediate insight in to the mechanism of action (Grzegorzewicz *et al.,* 2012; Singh *et al.,* 2014c). In addition, and from a practical perspective, the long generation time of *Mtb* (~24 hr) impedes the drug discovery process as extended incubation periods on solid agar medium (5 – 6 weeks for resistant mutants) are required (Sharma *et al.,* 2014). Reporter strains are an alternative approach that provides a rapid, sensitive real-time readout of the response to antibiotics.

In this study, auto-luminescent DNA-damage reporter strains that allow for the identification of compounds whose MoA includes the induction of genotoxic stress in *Mtb*, were developed and validated. In addition, by exploiting the bacterial *lux* system, a bioreporter was developed, that enables the real-time monitoring and elucidation of the

kinetics of the DNA-damage response in a concentration- and time-dependent manner over ~12 days. In general, *recA* was induced to higher levels than *radA* (Figure 4.3), suggesting a differential promoter strength between *recA* and *radA*, consistent with dd-PCR data (Chapter 3, Figure 3.10), whereby *recA* expression is higher than *radA*, both in uninduced and MMC-induced conditions, in Wt. As expression of *recA* is driven off two different promoters (Gopaul *et al.,* 2003), induced by the SOS and RecA-ND mechanisms respectively, the higher *recA* expression suggests an additive effect of both responses. Fusion of the *lux* operon to various genes encoding proteins that are emerging as attractive drug targets may provide more insight into the dynamics of the *Mtb* damage response. These could include targets such as DnaE2, that is regulated by the SOS mechanism, or the *clgR* transcriptional regulator involved in regulation of not only the Clp protease system, but also the RecA-ND mechanism (Boshoff *et al.,* 2003; Wang *et al.,* 2011; McGillivray *et al.,* 2014).

For antimicrobials identified as "true" DNA-damaging agents (CIP, MMC and NFZ), significant induction (100% or more) was observed at sub-inhibitory concentrations in both reporter strains. Therefore, for future incorporation of these reporters into a drug discovery programme – either as frontline HTS of novel compounds or as part of the downstream SAR and target identification process – it is suggested that MMC and INH be included as the positive and negative controls, respectively.

There are important parameters to be considered with this assay including the growth phase and concentration of cells used to inoculate the 96-well microtitre plate, as has been reported in previously (Andreu *et al.,* 2010). An inverse correlation between luminescence and cell density was observed, and is likely attributable to a decrease in metabolic activity as cells approach stationary phase, and a concomitant decrease in the availability of the $FMNH_2$ and ATP substrates which are essential for Lux activity (Andreu *et al.,* 2010). This feature may limit the use of these strains to screen novel compounds against non- or slowly-replicating *Mtb*. In addition, we observed loss of auto-luminescence at the passage 6 – passage 8 generations, following successive rounds of propagation. This could be attributable to the presence of *luxD*, the expression of which has been suggested to be toxic to mycobacteria (Andreu *et al.,* 2010). For this reason, precautions were taken during the development of this assay to minimize the potential toxic effects of the reporter itself.

The response to 4NQO is interesting in that, like NFZ, it forms adducts at the N^2 -position of deoxyguanosine (dG) (Jarosz *et al.,* 2007), yet its kinetic profile, both *recA* and *radA* was different from NFZ. TLS across the sites of damaged DNA has been shown to bypass certain N^2-dG adducts efficiently and accurately in *E. coli*. In *Mtb,* the SOS response-mediate polymerase DnaE2 mediates TLS, therefore these agents are expected to induce *recA,* but not *radA*. In the case of 4NQO the absence of *recA* induction suggests that significant genotoxic stress may not accumulate with this agent, as not much is known about 4NQO penetration into the *Mtb* cell. Alternatively, it is possible that by normalizing data to CIP, the threshold set to identify "true" inducers may be too high. Continued optimization of this assay may lend some insight into these questions.

The apparent delayed response to 5-FU suggested by the reporter assays is of particular interest. Recently, the complex MoA of 5-FU was elucidated, and shown to involve the accumulation of the downstream metabolites of 5-FU which exert toxic effects on various cellular processes including cell envelope biogenesis, RNA and DNA synthesis and thymidylate synthesis (Singh *et al.,* 2014c). Importantly, this accumulation was shown to occur following extended periods of 5-FU treatment. Analysis of the Lux strains treated with 5-FU show comparable data, in which *recA* and *radA* are induced between days 3 and 7 (*recA*) and at day 6 (*radA*), respectively. This suggests the possibility for a reporter-based, real-time assay to give early indication of complex (and late) MoAs. Furthermore, the delayed induction of 5-FU and its MoA has been validated with a Wt::p*ini-lux* reporter strain that measures changes to cell wall metabolism (Moosa, Warner, unpublished).

In general, for quantitative gene expression experiments, *Mtb* is treated ≤ 24 hr with an antimicrobial agent. However, if such conditions were imposed on NFZ-treated cultures, the results may have been misleading. Thus, the insight into the time-dependent effects of antimicrobial action provided by the kinetic profiles generated with the Lux assay may provide further information to aid the design of currently available protocols. In addition, it might enable the inclusion of "late genotoxicity" (or equivalent stress on an essential metabolic pathway) as a desirable criterion in compound triage algorithms.

As the bioluminescent reaction requires $FMNH_2$ and production of endogenous reaction substrate, only viable cells are expected to luminesce (Sharma *et al.,* 2014). Viability of cells in this assay is therefore expected to affect the RLU readout in a concentration-dependent

manner. This is consistent with the kinetic data, in which maximum luminescence tended to correlate with compound MIC_{90}. Nevertheless, the observation that exposure to a cidal (and lytic) compound such as D-cycloserine did not result in detectable autoluminescence suggests that the assay is robust against false positive assignments of genotoxicity. Correlation of CFU values with luminescence should be explored as a rapid tool to allow cidal and static antimicrobials to be differentiated. Furthermore expression of *recA* and *radA* needs to be validated with protein expression levels.

In conclusion, autobioluminescent reporter strains are useful tools for drug discovery platforms as they allow for the identification of pathway-specific inhibitors with high sensitivity. The *lexA*$^{ind-}$::*lux* strains are actively being pursued, as the majority of genes in *Mtb* are regulated by an alternate, RecA-ND mechanism (Rand *et al.,* 2003; Gamulin *et al.,* 2004; Smollett *et al.,* 2012). As both *recA* and *radA* are expected to be fully inducible in the strains reported in this study, the attraction lies in the possibility of identifying novel compounds that induce *radA*, but not *recA,* suggesting a MoA specific for the RecA-ND mechanism.

Chapter 5: The identification of novel efflux pump inhibitors by *in vitro* and *ex vivo* evaluation of potential synergistic interactions

5.1 Introduction

Efflux pumps are membrane-associated proteins or transporter complexes that actively extrude toxic compounds, including antimicrobials. Since their initial report in *E. coli* (Ball *et al.,* 1980; McMurry *et al.,* 1980), the significance of efflux-mediated drug resistance has been described in a wide range of organisms, and for almost all antimicrobial classes (Zechini & Versace 2009; Szumowski *et al.,* 2013). Efflux pumps may select for a single substrate or may be non-selective, conferring a multidrug resistant phenotype (Zechini & Versace 2009).

Gram-positive bacteria encode efflux pumps belonging to the MFS (major facilitator superfamily), ABC (ATP-binding cassette), SMR (small multidrug resistance) and the multidrug and toxic compound extrusion (MATE) families (Li & Nikaido 2009). *Mycobacterium tuberculosis* (*Mtb*) is unique in that transporters belonging to the MATE family have not been identified (Da Silva *et al.,* 2011b). However, the *Mtb* genome encodes 13 putative RND (resistance-nodulation division)-type transporters which are usually associated with Gram-negative bacteria. These are designated MmpL proteins (mycobacterial membrane proteins, large) (Cole *et al.,* 1998; Li & Nikaido 2009). In fact, *Mtb* has the largest representation of RND-type transporters compared to all prokaryotes surveyed, and these are believed to play a significant role in the extrusion of lipids and other cell envelope constituents (Sarathy *et al.,* 2012). MDR efflux pumps have significant clinical implications; MFS efflux pumps are associated with fluoroquinolone (*Rv1634*, *Rv1258c*, *Rv2686c*, *Rv2687c*) and RIF resistance (RIF^R) (*Rv1258c*); the RND-like pump *mmpl7* is associated with INH resistance (INH^R); and the ABC efflux pump, DrrAB, is involved in resistance to Tet, ETH, macrolides, aminoglycosides, and chloramphenicol (Zechini & Versace 2009).

Current strategies used to counteract efflux-mediated resistance include either the development of new antimicrobials that overcome the efflux systems (Lee *et al.,* 2014) or the development and implementation of efflux pump inhibitors (EPIs) or ffflux inhibitors (EIs) (Amaral *et al.,* 2007; Sharma *et al.,* 2010; Adams *et al.,* 2014). Different approaches include improving the structural design of existing antimicrobials to reduce/avoid their efflux (Lee et al., 2014), or blocking pump function (Amaral *et al.,* 2007; Zechini & Versace

2009; Adams *et al.,* 2014). The recent discovery of a new class of antituberculosis agents called spectinamides that circumvent intrinsic efflux pump-mediated resistance, provides an elegant example of the clever use of medicinal chemistry in evading an innate biological function as part of the continued search for novel antimicrobials (Lee *et al.,* 2014). The development of EPIs provides an alternative approach to improve clinical efficacy of currently available antimicrobials, as a single EPI may be active against MDR pumps and can be used as adjunct therapy (Zechini & Versace 2009). The physiological role of efflux systems is complex and is associated with bacterial metabolism, physiology, and pathogenicity. Therefore inhibition of efflux systems may directly affect bacterial virulence *in vivo* (Zechini & Versace 2009) despite the fact that efflux pumps are generally not included among essential gene lists *in vitro* (Sassetti et al., 2003; Griffin et al., 2011).

Previously, it was shown that *Mtb* develops efflux pump-mediated tolerance to both first-line anti-TB antibiotics, RIF and INH, during macrophage residence (Adams *et al.,* 2011). Subsequent work then demonstrated that macrophage-induced RIF tolerance could be reversed with the addition of the EPI verapamil (VER) (Adams *et al.,* 2011). Interestingly, macrophage-induced INH tolerance was not inhibited with this EPI. Consequently, the efflux pump Rv1258c, which has been implicated in spectinomycin resistance (SPC^R), was found to mediate tolerance of RIF, but not INH (Adams *et al.,* 2011; Lee *et al.,* 2014). EPIs have also been shown to increase the antibiotic susceptibilities of MDR *Mtb* strains *in vitro*, and co-administration of VER, INH, RIF and pyrazinamide (PZA) to mice infected with MDR-TB strains reduced pulmonary bacillary loads (Louw *et al.,* 2011). The same study provided evidence that susceptibility of a RIF mono-resistant *Mtb* strain to one antimicrobial (OFX) was reduced when exposed to another antimicrobial (RIF). However, upon introduction of the EPIs, VER or reserpine (RES), susceptibility to both RIF and OFX was restored. More recent work has evaluated the effect of EPIs on macrophage-induced tolerance to second and third-line anti-TB drugs used to treat MDR- and XDR-TB. Interestingly, macrophage-induced tolerance developed broadly, including to the newer antimicrobials MOX, PA-824 and BDQ. The addition of VER reduced tolerance to MOX and BDQ, while the VER metabolite, norverapamil (NOR), and various derivatives significantly reduced tolerance to RIF and INH (Adams *et al.,* 2014). Thus, given the mounting evidence implicating the clinical significance of efflux pumps, the utilization of EPIs has become increasingly attractive as

part of the current effort to develop novel regimens for the eradication of drug resistant strains of TB.

5.2 Aims and objectives

Antimicrobial therapy with an EPI is, in effect, a form of combination therapy. Therefore, to maximize the synergy between the two agents, it is imperative that novel EPI's are tested in combination from the initial *in vitro* stages of development. With the increasing attractiveness of EPIs, there is likely to be a significant increase in the number of novel EPIs that will require rapid and reliable analyses in *in vitro* and *ex vivo* assays.

In this context, this study aimed to evaluate the interactions between pairwise combinations of selected antibiotics and efflux pump inhibitors (EPIs) *in vitro* and *ex vivo*, and to identify a novel VER-analogue with improved efficacy against *Mtb*. The specific objectives included:

1. The development and validation of an *in vitro* assay in which novel EPIs can be tested in combination with current/ novel antimicrobials.
2. The identification and development of candidate EPI(s) by *ex vivo* evaluation.

5.3 Materials and Methods

5.3.1 Antimicrobial agents and efflux pump inhibitors (EPIs)

RIF, MOX, spectinomycin (SPC) and VER were purchased from Sigma Aldrich. BDQ was purchased from Asclepia MedChem Solutions (Belgium, www.asclepia.com), PA-824 was kindly provided by Dr. Helena. I. Boshoff (NIAID, NIH, Bethesda, Maryland, USA) and VER-analogues were provided as lyophilized pellets with data sheets including the mass and molecular weight of each compound (Singh, Kumar, Chibale, Department of Chemistry, UCT). For stock solutions, antimicrobials were all dissolved in the following solvents: MOX, SPC and VER in nuclease-free water (Qiagen); RIF, BDQ, PA-824 and analogues in DMSO (Sigma Aldrich). VER and analogues were prepared at 100mM stock concentrations. All stock solutions were stored at -20°C.

5.3.2 Checkerboard synergy assay

The fractional inhibitory concentration index (FICI) was determined in a 96-well plate format using an adaptation of the broth microdilution method, as described in Chapter 2, in which the antimicrobial agent (compound A) and the EPI (compound B), were 2-fold serially diluted across and down the plate, respectively (Ramon-Garcia *et al.,* 2011). Briefly, 50 µl media was added to every well in the plate, except Row 1 and 12 (minimum and maximum inhibition controls, respectively). Additional 50 µl media was added to row B3-B11, and column 2A-2H, and 100 µl to well B2. Antimicrobials were prepared at concentrations 400x MIC and EPIs at a concentration of 10mM. Two µl of EPI (compound B) was added to every well, B3-B11 and serially diluted (50 µl) to H (50 µl was discarded from H). 4µl of the same EPI (compound B) was added to well B2 and serially diluted (100 µl) down column 2 (100 µl was discarded form 2H). Finally, 2 µl of antimicrobial agent (compound A) was added to every well in row 3 and serially diluted (50 µl) from row 2 to row 3 until row 11 (50 µl was discarded from 11). *Mtb* culture was added to every well as described previously in Chapter 2. RIF at a final concentration of 0.2 µM (50 × MIC) was used for the maximum inhibition control, media only served as the minimum inhibition control and well A2 serves as a "no drug" control (Figure 6.1). The microtitre plates were stored in secondary containers and incubated at 37°C for 14 days, after which 10 µl of alamar blue (Celtic Molecular Diagnostics) was added to each well. After 24 hr of incubation, fluorescence was measured with a Fluostar Optima microplate reader (BMG Labtech) using excitation and emission wavelengths of 485 and 508 nm, respectively. The lowest concentration of drug that inhibited more than 90% of the bacterial population was considered to be the MIC_{90}.

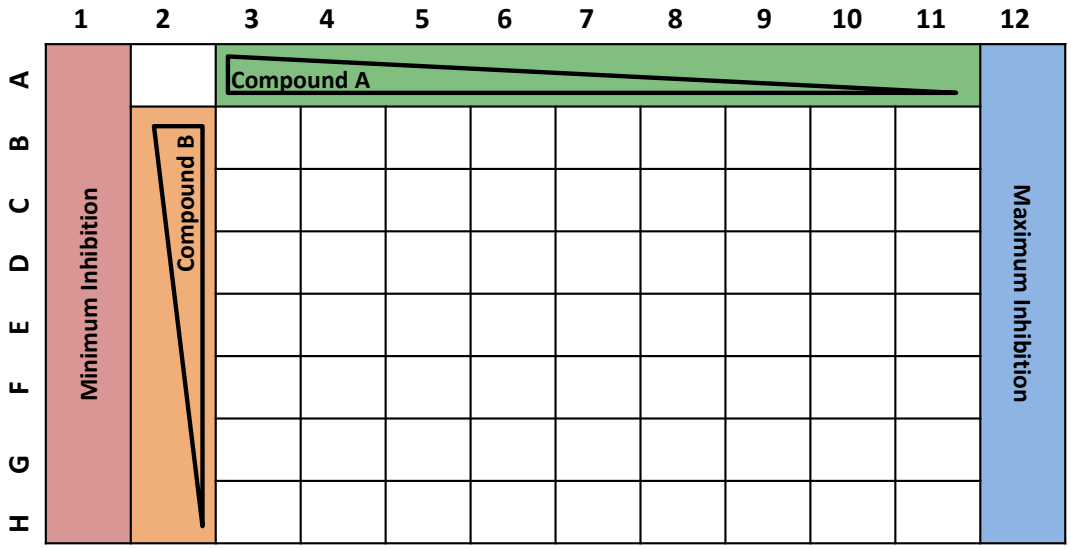

Figure 5.1: Checkerboard synergy assay plate layout in 96-well microtitre plates. Column 1 contains minimum inhibition control (no drug/EPI) and column 12 contains maximum inhibition control (rifampicin). The drug (compound A) was 2-fold serially diluted across the plate (column 3 – 11) and the EPI (compound B) was 2-fold serially diluted down the plate (row B – H). Well A2 serves as the "no drug" control.

The fractional inhibitory concentration (FIC) for each compound was calculated as follows: FIC_A (MIC_{90} of compound "A" in the presence of compound "B")/ (MIC_{90} of compound "A" alone). Similarly, the FIC_B for compound "B" was calculated. Synergy curves were plotted using Microsoft Excel 2010. The FICI was calculated as FIC_A plus FIC_B. Synergy was defined by FICI values of ≤ 0.5, antagonism by FICI values of ≥ 4.0, and no interaction by FICI values from 0.5 to 4.0 according to the recommended classification (Odds 2003). Checkerboard synergy assays for each reported combination were performed in triplicate.

5.3.3 Macrophage cytotoxicity assay

Frozen stocks of macrophage THP-1 cells (ATCC TIB-202) were thawed in RPMI medium (Sigma-Aldrich) supplemented with 10% fetal bovine serum (FBS). Cells were passaged only 5 times and maintained without antibiotics. Four thousand cells per well were allowed to differentiate in RPMI medium containing 200nM phorbol myristate acetate (PMA), and 10% FBS and left to adhere to the 96-well flat-bottom microtiter plate (PGRE655180, Lasec, SA) for 24 hr. Two-fold serial dilutions of EPIs were performed in RPMI medium containing 10% FBS and drug (at MIC_{90} concentrations) to a final volume of 100 µl. After cell differentiation,

medium was removed from the wells and 100 µl of EPI-drug-containing RPMI medium was added. Cells were incubated in the presence of the EPI-drug for 72 hr, after which 20 µl of alamar blue (Celtic Molecular Diagnostics) was added to each well. After 24 hr of incubation, fluorescence was measured with a Fluostar Optima microplate reader (BMG Labtech) using excitation and emission wavelengths of 485 and 508 nm, respectively. The IC_{20} was considered as the lowest concentration of compound that inhibited the ≥ 20% viability of the macrophages. EPIs with an *in vitro* FIC smaller than the macrophage toxicity concentration were analyzed further in *ex vivo* checkerboard synergy assays with RIF or BDQ (as described by the *in vitro* checkerboard synergy assay). Raw relative fluorescent units (RFU) data was provided by the MARS Data Analysis Software. All RFUs were normalized to the maximum and minimum fluorescent controls. Data were plotted as 3D surface charts (Microsoft Excel 2010).

5.4 Results

5.4.1 Development and validation of the checkerboard synergy assay for *in vitro* evaluation of EPI efficacy.

VER is a well-characterized compound and is often chosen as the preferred EPI (Louw *et al.,* 2011; Balganesh *et al.,* 2012a; Adams *et al.,* 2014). Adams *et al.,* 2011 reported that macrophage-induced RIF tolerance was reversed with the addition of this EPI. Therefore, the checkerboard synergy assay was selected to measure the interaction between RIF and VER. To confirm the reported potentiation of RIF efficacy in the presence of VER, the fractional inhibitory concentration (FIC) of each compound was determined in the *in vitro* assay (Figure 5.2).

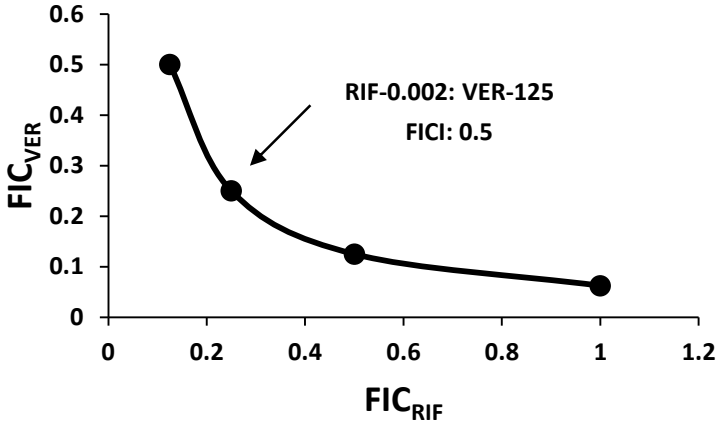

Figure 5.2: A concave FIC curve indicates a synergistic relationship between VER and RIF. The closest point to the intersection of the axes (zero) is the most effective combination for inhibiting bacterial growth, as indicated by the FICI. The concentrations (µM) of each compound required to achieve this effect are indicated. Data are representative of at least 3 biological replicates.

Overexpression of the tap-like efflux pump, *Rv1258c*, is associated with RIF resistance (Siddiqi *et al.,* 2004; Sharma *et al.,* 2010). The ability of VER to sensitize a *Rv1258c*-overexpressing strain to RIF has driven clinical interest in synergism between the two compounds. In addition, deletion of this efflux pump has recently been reported to reduce intrinsic SPC resistance (Ramon-Garcia *et al.,* 2011; Lee *et al.,* 2014). In the absence of the overexpressing strain, the checkerboard synergy assay was applied to VER and SPC. The compounds exhibited a significant synergistic interaction, thereby validating the specificity of this assay by recapitulating previous observations (Lee *et al.,* 2014) that elimination of *Rv1258c* function potentiates the activity of SPC (Figure .5.3).

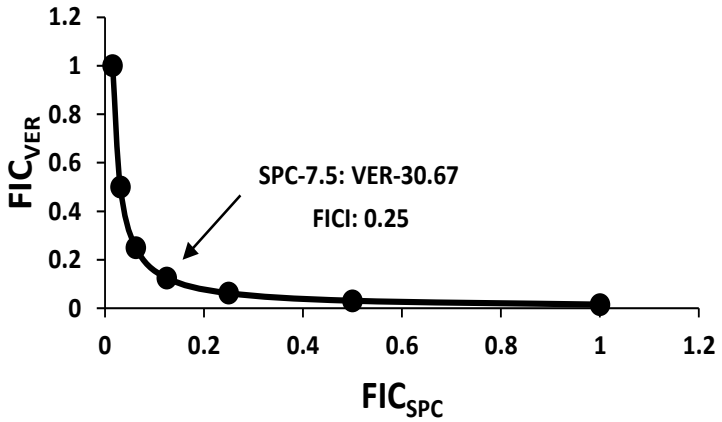

Figure 5.3: A concave FIC curve indicates a synergistic relationship between VER and SPC. The closest point to the intersection of the axes (zero) is the most effective combination for inhibiting bacterial growth, as indicated by the FICI. The concentrations (μM) of each compound required to achieve this effect are indicated. Data are representative of at least 3 biological replicates.

5.4.2 Application of the checkerboard assay in evaluating novel VER analogues.

In total, 37 different VER analogues were synthesized by colleagues in the Department of Chemistry, UCT, and screened *in vitro* in combination with RIF against *Mtb* H37Rv. RIF was selected as the antimicrobial as it is a frontline anti-TB drug, whereas SPC has not been established for use in the treatment of TB. The checkerboard synergy assay was utilized to evaluate the effect of 21 VER derivatives on the susceptibility of *Mtb* to RIF (Singh *et al.,* 2014a). The commercially available VER-analogue, NOR, was synthesized under the ID MKV1/7a. The majority of the analogues were inactive (MIC_{90} ≥ 500 µM) on their own and either had no effect on susceptibility to RIF, or reduced the MIC_{90} by 2-fold, which was considered insignificant for this study (Table 5.1, structures in appendix 3). Furthermore, these inactive compounds exhibited additive/no effect profiles, as indicated by the FICI. However, analogues MKV4, KSV10, MKV8 and MKV9 (Table. 5.2) reduced the MIC_{90} of RIF by 4-fold, with MKV4 exhibiting the only synergistic interaction, indicated by the FICI of 0.3. Although KSV21, also reduced the MIC_{90} of RIF by 4-fold, it displayed the highest FICI of 1.25 and was therefore not included for further investigation. Furthermore, these data suggested that fold reduction in RIF MIC_{90}, does not necessarily correlate with FICI.

Table 5.1: *In vitro* combinatorial evaluation of 21 VER-analogues with RIF against *Mtb*†

Analogue ID/ Published ID**	MIC_{90} (µM)			Fold reduction of RIF MIC★	FICI
	Analogue	Analogue (in combination with RIF)	RIF (in combination with analogue)		
MKV1/7a	500	31.25	0.004	2	0.56
MKV2/7b	1000	NC	0.008	NC	1.0
MKV3/7c	500	250	0.008	NC	0.78
MKV4/7d	1000	31.25	0.002	4	0.3
MKV5/7e	125	31.25	0.004	2	0.75
MKV11/12a	> 1000	NC	0.008	NC	ND
MKV10/12b	> 1000	NC	0.008	NC	ND
KSV5/14a	1000	500	0.004	2	1.0
KSV4/14b	1000	500	0.008	NC	1.5
KSV11/14c	1000	NC	0.008	NC	1.5
KSV8/14d	500	250	0.004	2	1.0
KSV14/14e	250	125	0.004	2	1.0
KSV7/14f	250	62.5	0.004	2	0.75
KSV10/14g	250	125	0.002	4	0.75
KSV12/14h	62.5	31.25	0.008	NC	1.5
MKV6/17a	1000	500	0.004	2	1.0
MKV7/17b	1000	500	0.004	2	1.0
MKV8/17c	1000	250	0.002	4	0.75
MKV9/17d	500	125	0.002	4	0.75
KSV19/17e	125	62.5	0.004	2	1.0
KSV21/17f	62.5	62.5	0.002	4	1.25

★ RIF MIC_{90} against *Mtb* is 0.008 µM; NC-No change; ND-Not Done as FIC of EPI could not be determined.

†Data are representative of 3 biological replicates.

**Published ID (Singh *et al.,* 2014a)

Table 5.3: Structures of VER and analogues. Exploratory SAR of VER included replacement of the methyl group on the tertiary nitrogen with a benzyl group (MKV4); replacement of the isopropyl group at the stereogenic carbon centre with an ethyl (MKV8) or propyl (MKV9) group; and replacement of the aminoethyl aromatic group with a heterocyclic group (KSV10) (Singh *et al.,* 2014a).

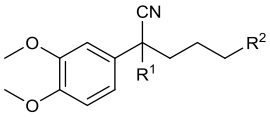

Compound ID	R^1	R^2
VER	$CH(CH_3)_2$	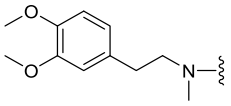
NOR	$CH(CH_3)_2$	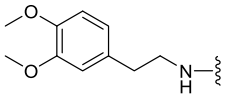
MKV4	$CH(CH_3)_2$	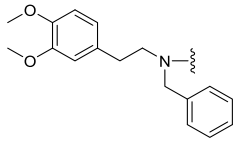
MKV8	CH_2CH_3	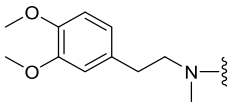
MKV9	$(CH_2)_2CH_3$	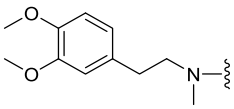
KSV10	$CH(CH_3)_2$	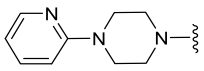

Preliminary combinatorial evaluation with the remaining 16 analogues indicated that the majority were inactive (MIC_{90} > 1000 µM) on their own and either had no effect on susceptibility to RIF, or reduced the MIC_{90} by only 2-fold (Table 5.4, structures in appendix 3). However, 3 potential candidates (KSV43, KSV44 and MKVB1) were identified that exhibited a synergistic interaction with RIF, with KSV44 reducing the MIC_{90} of RIF by 16-fold (Singh, Kumar, Chibale, unpublished). The analogues HEPI-04X and HEPI-06 are hybrid compounds in which the dimethoxyphenyl group of VER has been replaced with a chemosensitizer. This structural modification may explain the potent anti-mycobacterial activity of these compounds on their own compared to VER (MIC_{90} of 500 µM) and all other analogues tested in this study.

Table 5.4: *In vitro* combinatorial evaluation of 16 VER-analogues with RIF against *Mtb*†

Analogue ID	Analogue	MIC_{90} (µM)		Fold reduction of RIF MIC★	FICI
		Analogue (in combination with RIF)	RIF (in combination with analogue)		
HEPI-04X	< 15.625	NC	NC	NC	ND
HEPI-06	< 15.625	NC	NC	NC	ND
KSV-43	250	31.25	0.001	4	0.4
KSV-44	250	62.5	0.00025	16	0.3
MKV-R1	1000	500	0.001	4	0.8
MKV-R2	250	125	0.002	2	0.6
MKV-B1	500	125	0.001	4	0.5
MKV-B2	> 1000	NC	NC	NC	ND
MKV-B3	> 1000	NC	NC	NC	ND
MKV-B4	> 1000	NC	NC	NC	ND
MKV-B5	> 1000	NC	NC	NC	ND
MKV-B6	> 1000	62.5	0.002	2	ND
MKV-B8	500	250	0.002	2	1.0
MKV-B9	> 1000	NC	NC	NC	ND
MKV-B10	> 1000	62.5	0.002	2	ND
MKV-B11	> 1000	31.25	0.002	2	ND

★ RIF MIC_{90} against *Mtb* is 0.004 µM, NC-No change; ND-Not Done as FIC of EPI could not be determined.

†Data are from a single experiment only, owing to limited compound availability

5.4.3 Validation of VER-potentiation of newer anti-TB drugs.

During the course of this study, VER was reported to reduce tolerance to BDQ, MOX, and PA-824 (Adams *et al.,* 2014). *In vitro* data from this study partially concurred with these reports, in that activity of BDQ, but not MOX, was potentiated by VER (Figure 6.3A and B). Moreover, the combination of VER and PA-824 tended towards antagonistic: the shape of the FIC curve was convex, although the FICI of 2.5 did not fulfil the strict requirements for classification of the combination as truly antagonistic (Odds 2003). This VER/PA-824 interaction, as well as the additive effect of VER and MOX, is in contrast to recent reports (Adams *et al.,* 2014), and suggests that reported EPI-potentiation of MOX and PA-824 may be a macrophage-specific phenomenon.

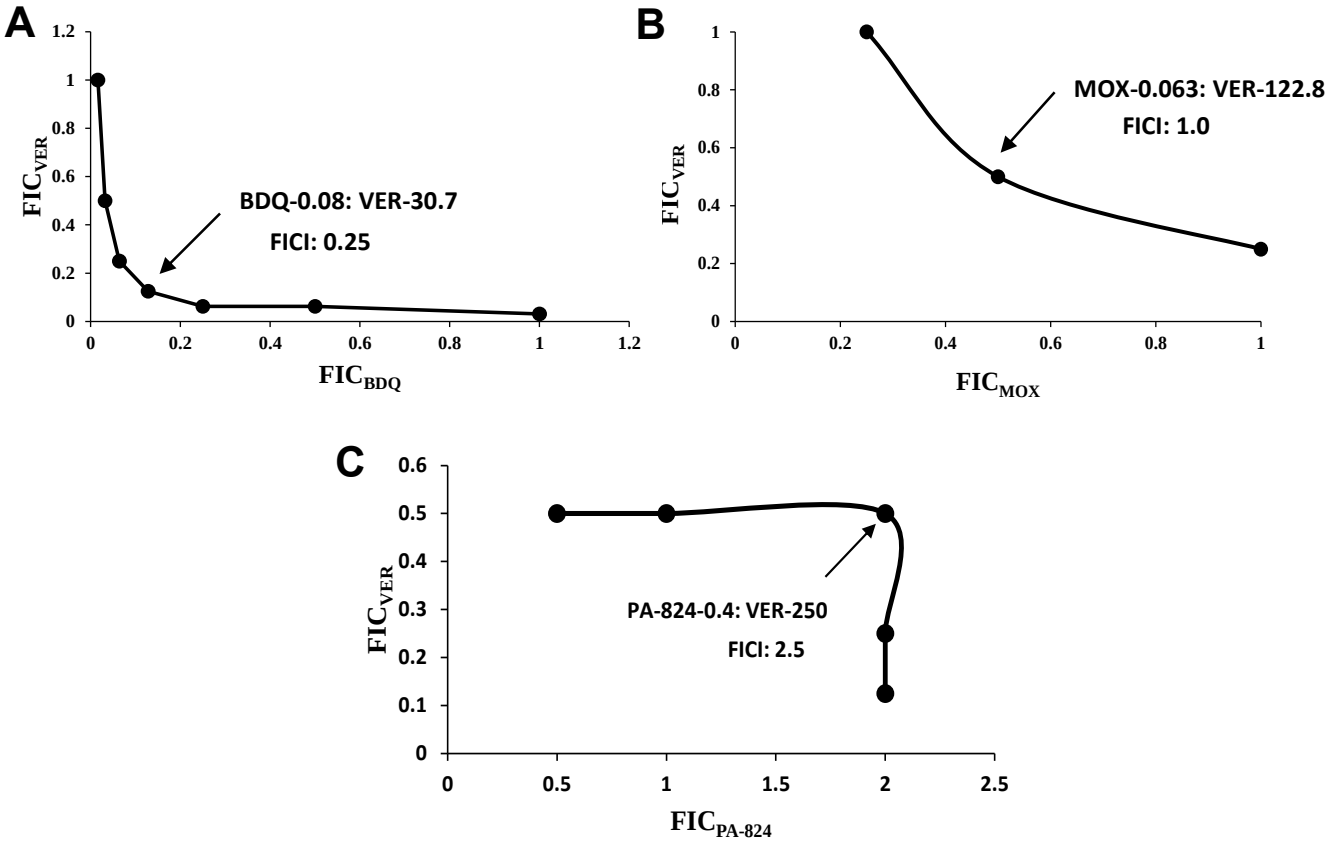

Figure 5.4: Interactions between newer antimicrobials and VER. The concave curve of VER vs. BDQ indicates a synergistic effect (**A**). VER vs. MOX indicates no interaction/ additive effect (**B**). The convex curve of VER vs. PA-824 suggests antagonism (**C**). The closest point to the intersection of the axes (zero) is the most effective combination for achieving the interaction (synergism/ additive/ antagonism), as indicated by the FICI. The concentrations (μM) of each compound required to achieve this effect are indicated. Data are representative of at least 3 biological replicates.

5.4.4 Identification of novel EPIs with *in vitro* efficacy against newer anti-TB drugs.

Since several VER-analogues showed comparable activity relative to VER in terms of their potentiation of RIF efficacy against *Mtb* (Table 5.5), a select panel of analogues was chosen for further investigation in combination with newer anti-TB drugs (Table 6.3). MKV4 significantly reduced the MIC_{90} of BDQ by 16-fold, with a synergistic interaction, FICI 0.38, slightly worse than that of VER and BDQ, FICI 0.25. Interestingly, MKV9 reduced the MIC_{90} of BDQ by 32-fold, but displayed the same synergistic interaction as VER. In general, VER and its analogues did not synergize with MOX; instead, the interaction was additive.

Table 5.5*: In vitro* combinatorial evaluation of VER and associated analogues with BDQ or MOX against *Mtb*[⋆]

Compound ID	Analogue MIC_{90} (µM)	BDQ			MOX		
		MIC_{90}(with analogue, µM)	Fold reduction	FICI	MIC_{90} (with analogue, µM)	Fold reduction	FICI
VER	500	0.14	8	0.25	0.14	4	1.0
NOR	500	0.28	4	0.38	0.07	8	0.75
MKV4	1000	0.07	16	0.38	0.14	2	1.0
MKV8	1000	0.14	8	0.25	0.035	8	0.49
MKV9	500	0.035	32	0.25	0.035	8	0.49
KSV10	500	0.28	4	0.38	0.14	2	0.75

[⋆] Data are representative of 3 biological replicates

5.4.5 Identification of a novel, non-cytotoxic EPI.

The mammalian cell toxicity profiles of the EPIs were evaluated against the monocyte-like cell line, THP-1. Compounds were initially tested for cytotoxic effects individually and MKV4 was found to be 2-fold less toxic than the parent EPI, VER (Table 5.6). As MKV4 was the only EPI with an *in vitro* FIC lower than the THP-1 IC_{20}, it was selected for further analysis in *ex vivo* checkerboard synergy assays (Ramón-García *et al.,* 2011) with RIF or BDQ, and compared to the cytotoxicity profiles of VER and NOR (Figure 5.5). RIF and BDQ were selected as they demonstrated the most significant *in vitro* interactions with MKV4. When compared to the cytotoxicity profile on its own (Table 5.6), MKV4 was less cytotoxic in combination with RIF ($IC_{20} \leq 500$ µM) and remained the same in combination with BDQ (IC_{20} < 250 µM). However, MKV4 was the least cytotoxic EPI compared to VER (IC_{20} < 62.5 µM) and NOR, which was the most cytotoxic (IC_{20} < 62.5 µM). In general, MKV4 was 4-fold less toxic in combination with RIF, than VER with RIF and 2-fold less toxic in combination with BDQ, than VER and BDQ.

Table 5.6: *Ex vivo* activity of VER, associated analogues and various antimicrobials against THP-1 macrophages.

Compound	IC_{20} (µM)★
VER	125
NOR	< 62.5
MKV4	250
MKV8	< 62.5
MKV9	< 62.5
KSV10	< 62.5
RIF	0.4
BDQ	56.2
MOX	< 90
RIF + VER	< 62.5
BDQ + NOR	< 62.5
RIF + NOR	< 62.5
BDQ +NOR	< 62.5
RIF + MKV4	≤ 500
BDQ + MKV4	< 250 µM

★IC_{20} – Inhibitory concentration, the lowest concentration of compound at which ≥ 20% THP-1 cytotoxicity is observed. Data are representative of 2 biological replicates.

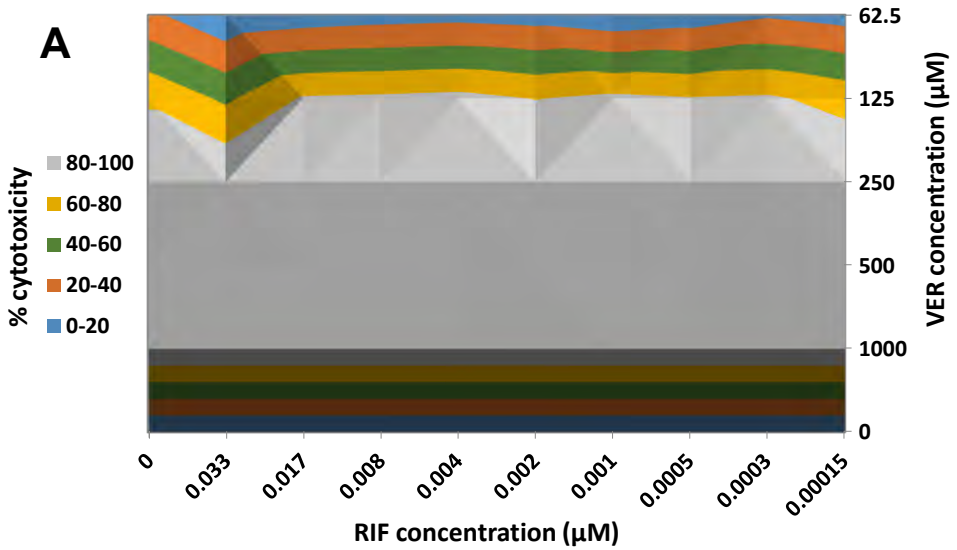
A
% cytotoxicity
80-100
60-80
40-60
20-40
0-20
62.5
125
250
500
1000
0
VER concentration (µM)
0
0.033
0.017
0.008
0.004
0.002
0.001
0.0005
0.0003
0.00015
RIF concentration (µM)

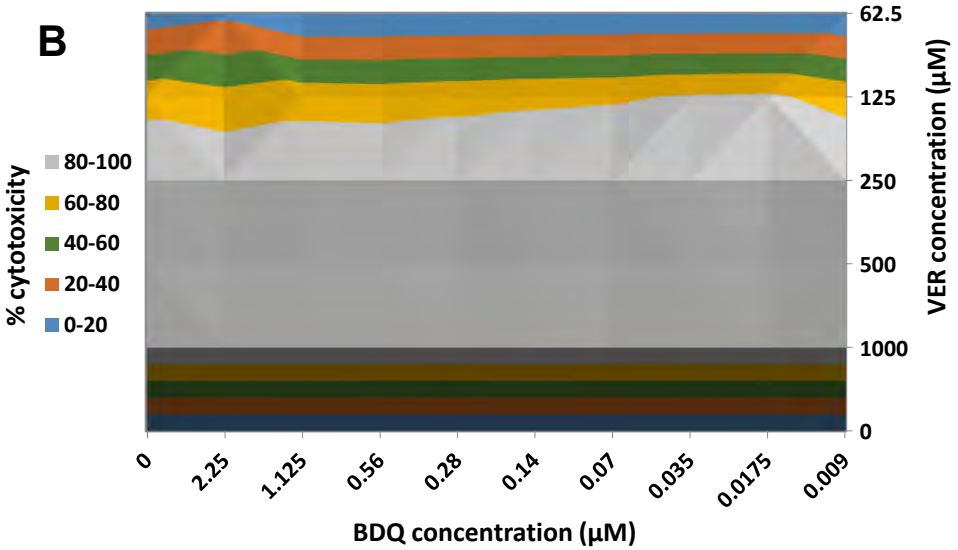
B
% cytotoxicity
80-100
60-80
40-60
20-40
0-20
62.5
125
250
500
1000
0
VER concentration (µM)
0
2.25
1.125
0.56
0.28
0.14
0.07
0.035
0.0175
0.009
BDQ concentration (µM)

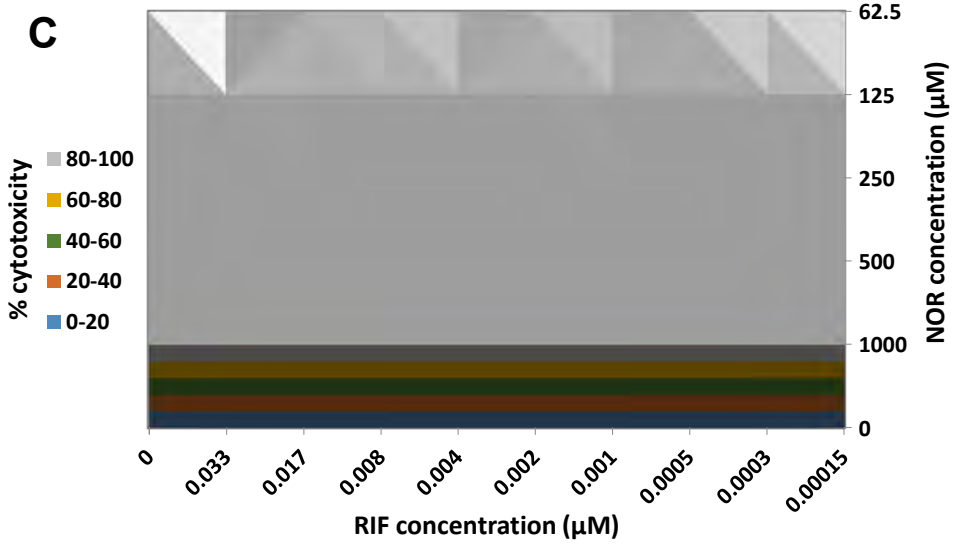
C
% cytotoxicity
80-100
60-80
40-60
20-40
0-20
62.5
125
250
500
1000
0
NOR concentration (µM)
0
0.033
0.017
0.008
0.004
0.002
0.001
0.0005
0.0003
0.00015
RIF concentration (µM)

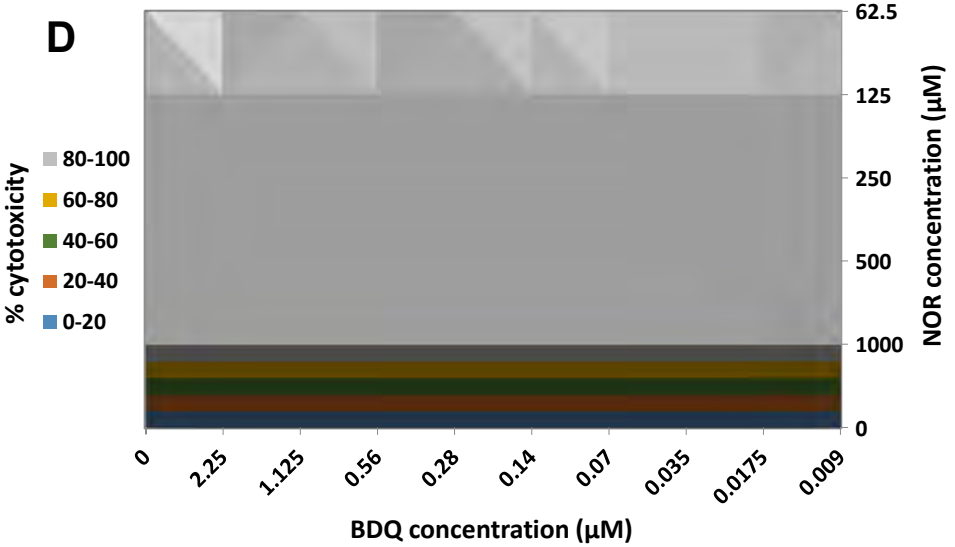
D
% cytotoxicity
80-100
60-80
40-60
20-40
0-20
62.5
125
250
500
1000
0
NOR concentration (µM)
0
2.25
1.125
0.56
0.28
0.14
0.07
0.035
0.0175
0.009
BDQ concentration (µM)

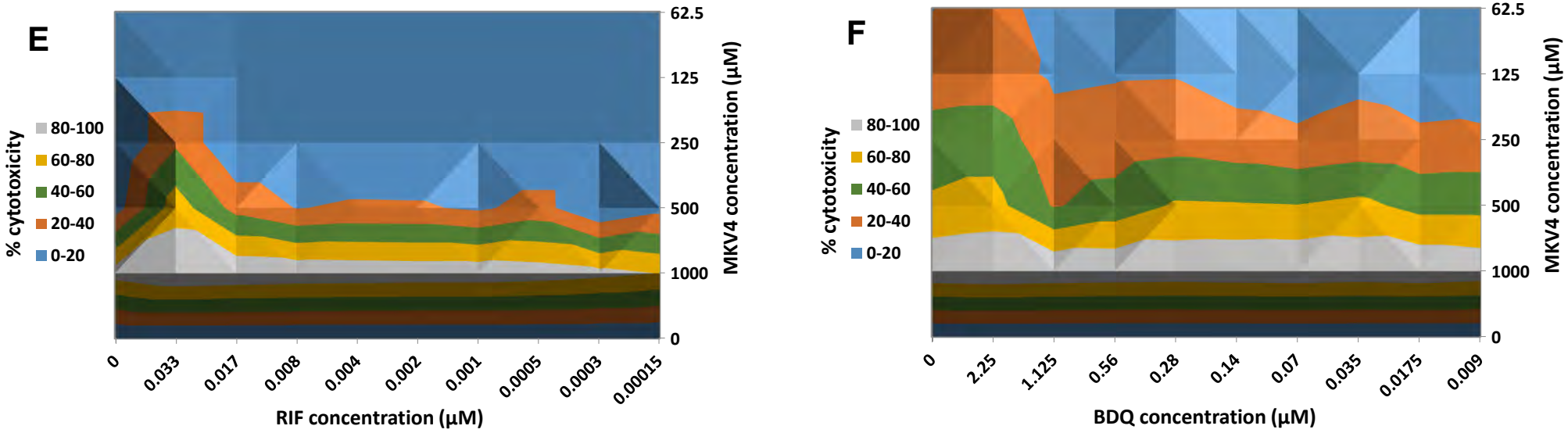

Figure 5.5: The analogue MKV4 is less toxic to THP-1 cells than its parent compound VER. 3D surface plots depicting % cytotoxicity of EPIs in combination with antimicrobials**.** The percentage (%) cytotoxicity of VER (**A**), NOR (**C**) and MKV4 (**E**) in combination with either RIF or BDQ. VER was cytotoxic in combination with either antimicrobial at concentrations < 62.5 µM (**A – B**). NOR was cytotoxic at all concentrations tested and was the most cytotoxic EPI (IC_{20} > 62.5 µM) (**C –D**). In general, MKV4 displayed the least cytotoxic profile, and was not toxic at concentrations ≤ 500 µM when used in combination with RIF and was not toxic at concentrations < 250 µM when used in combination with BDQ (**E – F**). Data are representative of 2 biological replicates.

5.5 Discussion

Efflux pumps contribute directly to intrinsic resistance, and indirectly by providing a "window" for the emergence of high-level resistance through drug-target mutations (high-level, adaptive resistance mechanisms). In addition, overexpression of – or mutations within – efflux pumps may result in antimicrobial resistance, as the drug is extruded more efficiently and the intracellular concentration of the drug decreases to sub-inhibitory concentrations, thus inducing genetic resistance (Figure 5.6) (Piddock 2006; Zechini & Versace 2009).

The activity of efflux pumps can either be inhibited indirectly, by targeting the driving force of the mechanism, or directly, by blocking pump activity by competitive or non-competitive binding of substrates (Zechini & Versace 2009). The inhibition of the proton motive force dependent pump involves direct interaction with the pump and a reduction in the trans-membrane potential. Compounds that affect the energy level of the bacterial membrane such as carbonylcyanide *m*-chlorophenylhydrazone (CCCP), valinomycin and dinitrophenol (DNP) are known as efflux inhibitors (EIs). The peptidomimetic phenylalaninearginyl β-naphthylamide (PAβN) is the most widely studied compound in the second category, known as efflux pump inhibitors (EPIs), and is itself a substrate of efflux pumps, acting as a competitive inhibitor. The identification and development of EPIs is an interesting approach to retard the emergence of drug resistance by increasing drug efficacy. To date, VER, a calcium channel blocker long in clinical use, is the most promising inhibitor and is often chosen as the preferred inhibitor over other candidates such as piperine and reserpine (Balganesh *et al.,* 2012a; Adams *et al.,* 2014). VER can potentiate the efficacy of multiple antimicrobials *in vitro*, inhibit tolerance *ex vivo*, has well-characterized pharmacokinetic profiles in dog and rabbit models, and is significantly concentrated in the lung (Schwartz *et al.,* 1986; Solans *et al.,* 2000; Louw *et al.,* 2011; Adams *et al.,* 2014; Gupta *et al.,* 2014). Thus, the discovery and development of novel VER analogues with improved safety, tolerability and the mechanism to enhance the efficacy of multiple antimicrobials is of significant importance.

An *in vitro* assay was developed based on the checkerboard synergy assay in order to identify novel VER analogues. If the EPI also reduces the viability of *Mtb*, the observed effect

may be due to mechanisms other than efflux inhibition, depending on the concentration used, which in turn, may result in the EPI itself as a substrate of the intended efflux pump (Viveiros *et al.,* 2012). Therefore, the aim was to find compounds which are relatively inactive on their own but, when applied in combination with an antimicrobial, have the ability to potentiate efficacy. In addition, a variation of the same assay was used in *ex vivo* assessments to identify compounds that were not cytotoxic at the concentrations required for the desired *in vitro* synergistic effects.

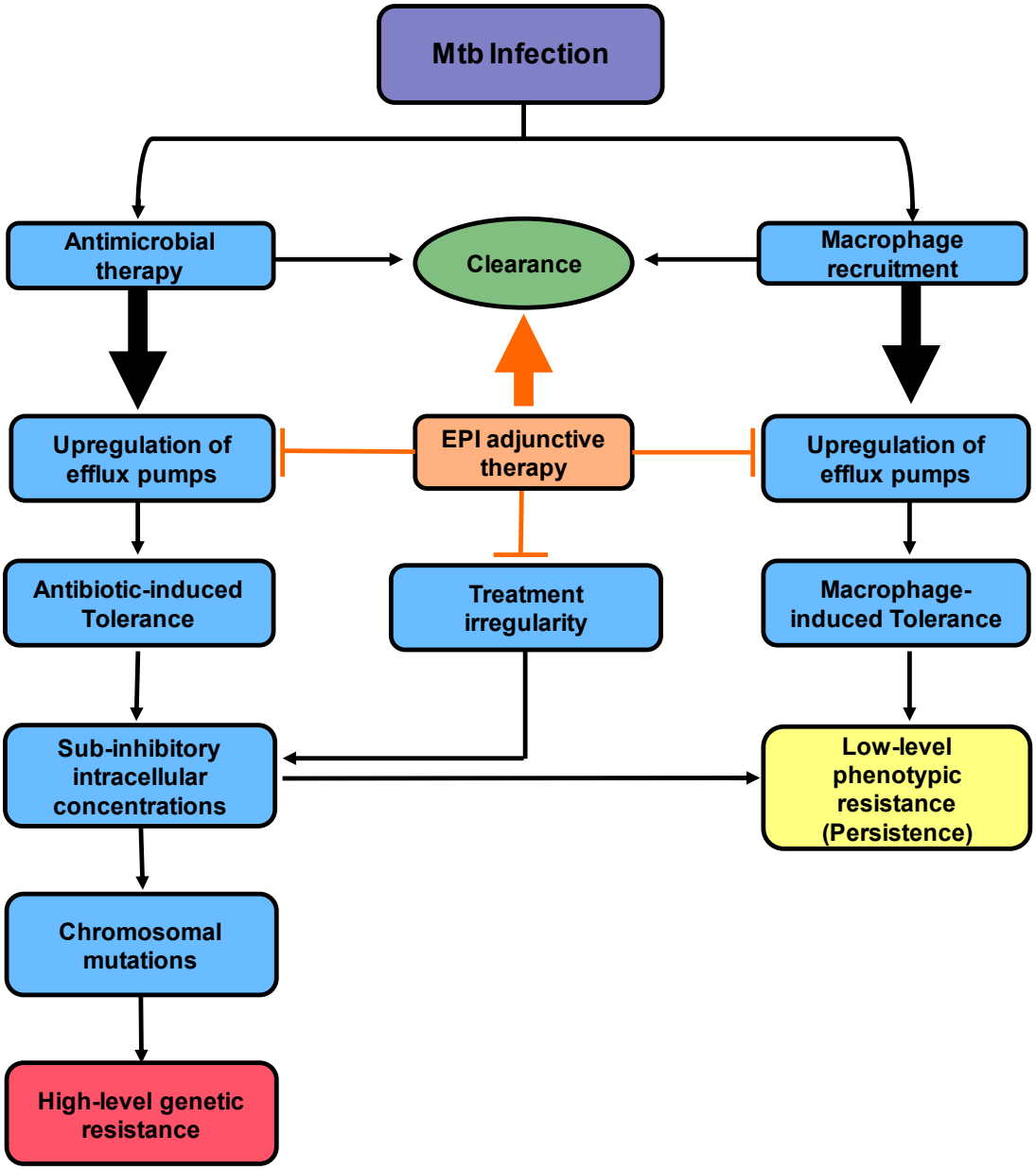

Figure 5.6: Adjunct therapy with efflux pump inhibitors (EPIs) perpetuates clearance of infection and prevents the emergence of drug resistance and persistence. Following infection, macrophages are recruited to phagocytose the bacilli. Both macrophage residence and antimicrobial therapy induce the upregulation of efflux pumps which render the bacilli tolerant to antibiotic treatment (Adams *et al.,* 2011). This results in low-level phenotypic antibiotic resistance, a phenomenon known as persistence. In addition, the active extrusion decreases the intracellular concentration of the antibiotics to sub-inhibitory levels, driving the emergence of target chromosomal mutations and subsequently accelerates the progression to high-level genetic resistance (Da Silva *et al.,* 2011b; Viveiros *et al.,* 2012). In addition, external factors that impact the emergence of resistant *Mtb* strains include treatment irregularities such as insufficient dosage, inadequate prescription and/or patient non-adherence. The use of EPI adjunct therapy has the potential to eliminate the emergence of antibiotic-tolerant populations, subsequent genetically resistant populations and possibly salvage control over treatment irregularities (Viveiros *et al.,* 2012; Adams *et al.,* 2014; Lechartier *et al.,* 2014; Zumla *et al.,* 2014).

Using this approach, a candidate VER analogue (designated MKV4) was identified with equivalent *in vitro* synergistic effects to VER when used in combination with various antimicrobials. Although MKV4 was only 2-fold less toxic than VER against THP-1 cells on its own, in combination with RIF, it was 4-fold less toxic. Considering that potential antimicrobial therapy with an EPI is a form of combination therapy, this observation may be of some significance.

The *in vivo* profiles of this candidate EPI remain to be determined. In addition, as this study is currently in progress, further investigation of MKV-B2, KSV43 and KSV44, which displayed attractive FICI values in combination with RIF, is underway. It is hoped that a continuous supply of compounds in the EPI pipeline may yield a successful clinical candidate. In addition, evaluation of candidates against a RIF mono-resistant *Mtb* H37Rv strain may progress certain analogues further if restoration to RIF susceptibility is validated.

Chapter 6: Circumvention of mycothiol-mediated intrinsic resistance

6.1 Introduction

Bacterial thiols function both as redox buffer systems and as substrates in detoxification pathways to maintain the cell's intracellular reducing environment and protect against damage by xenobiotics (oxidizing agents, alkylating agents and antibiotics). Mycothiol (MSH) is the major thiol in the genus *Mycobacterium* and is present in the cell in significant amounts (Newton *et al.,* 2008). The essentiality of MSH in *Mtb* remains controversial, mainly due to conflicting reports on the capacity of the bacillus to tolerate deletion of specific genes (*mshA* in particular) involved in MSH biosynthesis (Sareen *et al.,* 2003; Vilchèze *et al.,* 2008; Griffin *et al.,* 2011). Regardless of this controversy, MSH has an established role in tolerance of oxidative and other stressed conditions, and contributes to the survival of bacilli within macrophages. MSH functions in the intrinsic resistance of *Mtb* by serving as a substrate for enzymes involved in antibiotic detoxification (Rawat & Av-Gay 2007; Jothivasan & Hamilton 2008; Newton *et al.,* 2008). Decreased levels of MSH have been shown to increase susceptibility of *Mtb* to RIF, STR and ERY (Table 6.1) (Hayward *et al.,* 2004). However, resistance to INH and ethionamide (ETH) (both pro-drugs that share a common target, *inhA*) has also been associated with decreased MSH levels (Vilchèze *et al.,* 2011).

The defined role of MSH in antibiotic detoxification identifies this pathway as integral to *Mtb*'s intrinsic resistome. Enzymes involved in MSH-dependent detoxification and/or enzymes involved in MSH biosynthesis contribute to this pathway. MSH-dependent enzymes include Mtr (NADPH-dependent flavoenzyme), Mrx1 (oxidoreductase), MST (mycothiol-*S*-transferase) and Mca (metalloenzyme). Mtr (mycothione reductase) is an MSH disulphide reductase and is a key component of the cellular thiol redox buffer system in *Mtb* responsible for maintaining MSH in its reduced form via reduction of mycothione (MSSM) (Patel & Blanchard 2001). MSH is critically dependent on functional Mtr, as it is only capable of protecting mycobacteria against oxidative damage in its reduced form. Thus, loss of Mtr is expected to reduce MSH levels and thereby sensitize mycobacteria to ROS and RNS. Studies utilizing various techniques (RNA antisense, transposon mutagenesis and a combination of high-density mutagenesis and deep sequencing) have identified *mtr* as essential *in vitro* (Sassetti *et al.,* 2003; Hayward *et al.,* 2004; Griffin *et al.,* 2011). Upon oxidation of MSH, MSSM is formed, but it is rapidly reduced to MSH in an NADPH-dependent manner by MTR,

thereby maintaining the intracellular MSH/MSSM ratio that is essential in preserving a reduced intracellular environment crucial for various biological processes (Hayward *et al.,* 2004). In addition, there exists a well-established MSH-dependent pathway for the detoxification of electrophilic xenobiotics (such as INH) in which the mycothiol-*S*-transferase (MST) enzyme and the metalloenzyme, Mca, are central components. Following entry into the cell, MST catalyzes the conjugation of the electrophilic xenobiotic to the free thiol group on MSH, yielding mycothiol-*S*-conjugates which are then cleaved by an S-conjugate amidase (Mca) to form a hydrophobic mercapturic acid which is released from the cell and the intermediate 1-*O*-(2-amino-2-deoxy-α-D-glucopyranosyl)-D-*myo*-inositol (GlcN-Ins), which is recycled back into the MSH biosynthetic pathway. In *Msm*, MST has reasonable activity with MMC as a substrate, suggesting a possible role for MST in the detoxification of antibiotics; consistent with this notion, increased sensitivity to RIF and ERY has been observed where *mca* is mutated (Hernick 2013).

The MSH biosynthetic pathway is complex: MSH is synthesized from glucose-6-phosphate in six steps by the enzymes myo-inositol-1-phosphate synthase (MIPS; inositol synthase), MshA (glycosyl transferase), MshA2 (phosphatase), MshB (deacetylase), MshC (ligase) and MshD (synthase) (Hernick 2013). In *Mtb*, *mshC* is the only essential gene confirmed by transposon mutagenesis (Sassetti *et al.,* 2003; Newton *et al.,* 2005; Griffin *et al.,* 2011).

Table 6.1: Summary of enzymes involved in mycothiol biosynthesis and phenotypes of genetic mutants. Comparative analyses of the five mycothiol biosynthetic genes and the effect of mutations/ deletions corresponding with each enzyme in either *Msm* or *Mtb*.

Gene	Protein Function	*Msm* mutant	*Mtb* mutant	MSH levels in mutants	Reference
mshA	MSH glycosyltransferase	G32D Mutation: Slower cell growth;↑ sensitivity to ROS and RNS; alkylating agents; RIF, STR and ERY; resistance to INH and ETH	Essentiality initially controversial: Δ*mshA* only viable in presence of catalase - INH and ETH co-resistance; *in vitro* essential	*Msm*: < 0.01 µmol/g *Mtb*: undetectable levels	(Buchmeier *et al.,* 2006; Vilchèze *et al.,* 2008; Griffin *et al.,* 2011; Xu *et al.,* 2011)
(mshA2)	MSH phosphatase	Identity of gene encoding MshA2 remains unknown: Possibly *impC* (Rv3137)- essential			(Movahedzadeh *et al.,* 2010; Griffin *et al.,* 2011)
mshB	MSH deacetylase	Δ*mshB* - compensated by MCA; slight resistance to INH and resistance to ETH; ↑ sensitivity to RIF	Δ*mshB* : log-phase cultures display ↑ sensitivity to RIF	*Msm*: ~10% of Wt levels *Mtb*: ~20% Wt levels (exponential growth) Increases 20-fold – higher than Wt levels (stationary phase)	(Buchmeier *et al.,* 2006; Xu *et al.,* 2011)
mshC	MSH ligase	Transposon insertion:↑ sensitivity to alkylating and oxidizing agents; RIF and ERY; resistance to INH and ETA	Essential	*Msm*: <0.004 µmol/g dry weight	(Rawat *et al.,* 2002; Sareen *et al.,* 2003; Vilchèze *et al.,* 2008; Xu *et al.,* 2011)
mshD	MSH synthase	Transposon insertion: altered thiol content; No effect on sensitivity to oxidizing agents or antibiotic resistance – compensated by MCA and MTR	Δ*mshD*: ↑ sensitivity to hydrogen peroxide. Essential for growth in macrophages	*Msm*: 0.12 µmol/g dry weight *Mtb*: ~1% Wt levels (exponential phase) Increase 8-fold (stationary phase)	(Newton *et al.,* 2005; Xu *et al.,* 2011)

*Wt levels of MSH are 10 ± 3 µmol/g dry weight in *Msm*, 10 – 20 nmol/109 cells for exponential-phase *Mtb* and 30 – 40 nmol/109 cells for stationary-phase *Mtb* (Newton *et al.,* 2008).

6.2 Aims and objectives

Inducible gene expression systems offer a useful approach for studying gene function and have been validated as tools to identify inhibitors of prioritized drug targets in *Mtb* (Ehrt *et al.,* 2005; Gandotra *et al.,* 2007). These systems allow the expression of a single target gene to be silenced, either by addition (Tet-OFF system) or by removal of tetracycline (Tet-ON system).

As the efficacy of various antimicrobials is mitigated by MSH, the overall aim of this study was to generate an *Mtb* mutant in which MSH production could be conditionally depleted, sensitizing *Mtb* to certain antimicrobials. The specific objectives included:

1. Generation of an *Mtb* mutant strain in which expression of *mshC* is regulated using a conditional expression system based on the tetracycline (Tet)-regulatable promoter element (Ehrt *et al.,* 2005).
2. Phenotypic and transcriptional validation of anhydrotetracycline (ATC)-dependent regulation of *mshC*.

6.3 Materials and Methods

6.3.1 Mycobacterial strains, plasmids, and probes

The strains used in this study are detailed in Table 6.2, plasmids are listed in Table 3.3, and primers in Table 6.4.

Table 6.2: Strains used in this study

Strain	Description/ Genotype	Reference/ Source
Mtb		
H37RvMA (Wt)	Virulent reference laboratory strain of *Mtb* ATCC 27294	(Ioerger *et al.,* 2010)
mshC-SCO	H37RvMA derivative in which expression of *mshC* is controlled by P_{myc1}tetO, HYG^R	This study
⋆*mshC* Tet-ONs	Derivative of *mshC*-SCO harbouring pGMCK3-0X21-T10 integrated at the L5 *attB* site, HYG^R, KAN^R	This study
⋆*mshC* Tet-ONm	Derivative of *mshC*-SCO harbouring pGMCK3-0X38-T10 integrated at the L5 *attB* site, HYG^R, KAN^R	This study
mshC Tet-OFF	Derivative of *mshC*-SCO harbouring pGMCK3-0X38-T10 integrated at the L5 *attB* site, HYG^R, KAN^R	This study

⋆ Strains were generated but not characterized.

Table 6.3: Plasmids used in this study

Plasmid	Description	Reference/ Source
pSE100	*E. coli-Mycobacterium* shuttle vector carrying P_{myc1}tetO; HYG^R	(Guo *et al.,* 2007)
pGMCK3-0X21-T10	L5-based integration vector harbouring modified P*smyc*-tetR; KAN^R	(Klotzsche *et al.,* 2009)
pGMCK3-0X38-T10	L5-based integration vector harbouring modified P*smyc*-tetR; KAN^R	(Klotzsche *et al.,* 2009)
pGMCK3-0X38-T28	L5-based integration vector harbouring modified P*smyc*-tetR r1.7; KAN^R	(Klotzsche *et al.,* 2009)
pGA-0XP15-intL5	Suicide vector harbouring L5 integrase; AMP^R	(Klotzsche *et al.,* 2009)
p*mshC*-SCO	Suicide plasmid for generating *mshC*-SCO. pSE100 derivative in which the mycobacterial origin of replication was replaced by the first 714 bp of *mshC,* HYG^R	This study
pTT1B::Gm	Derivative of pTT1B, a Tweety-based integration vector; GEN^R	(Abrahams *et al.,* 2012)
★pTTB::*2129*c	pTT1B::Gm derivative harbouring *Rv2129c*; used for genetic complementation of *mshC* conditional mutant; GEN^R	This study

★ Plasmid was generated but not used.

Table 6.4: Primers used in this study

Name	Sequence 5'-3'	Comments ★
*mshC*F	GCATGCTTTAGAGTCGAGGAC	725 bp; 5' end of *mshC i*ncluding the ribosomal binding site with introduced *Sph*I and *Not*I sites, respectively; probe for southern blot
*mshC*R	GCGGCCGCTCAGACATGCCA	
Rv2131F	TCTAGAGGGCCAAAGGG	307 bp; amplification of the 5'-region flanking *mshC* for construction of p2129c-Comp; introduced *Xba*I site in forward primer
Rv2131_SOER	AACGTACCGCCGCGCCGGGTC	
Rv2129_SOEF	CCGGCGCGGCGGTACGTTTTC	934 bp; amplification of the 3'-region flanking *mshC* for construction of pTTB::*2129*c; introduced *Xba*I site in reverse primer
Rv2129R	TCTAGAGAATCGAGCGCG	

★Restriction sites are underlined.

6.3.2 Construction of plasmids

The integrative plasmid p*mshC*-SCO was constructed by PCR amplification of the ribosomal binding site and first 705 bp of *mshC*. Following restriction with *Sph*I and *Not*I, the PCR product was cloned into pSE100 (Guo *et al.,* 2007).

For the complementation construct, pTTB::*2129c*, PCR amplification of the operon encoding *mshC,* but possessing an in-frame deletion of the target gene, was performed by the splice-by-overlap-extension method (Ho *et al.,* 1989). Briefly, in the first-round of PCR, two fragments flanking *mshC* were amplified. These fragments contained overlapping extensions and were combined, following purification, and used as a template in a second-round of PCR. The full length PCR product was digested with *Xba*I and cloned into *Xba*I-linearized pTT1B::Gm.

6.3.3 Construction and genotypic characterization of promoter-replacement mutants

The suicide plasmid p*mshC*-SCO was electroporated into *Mtb* H37RvMA, and transformants selected on 7H10/OADC agar plates containing HYG. Following incubation at 37 °C for 21 days, colonies were isolated and grown to mid-logarithmic phase in 7H9/OADC liquid medium, cells harvested and genomic DNA isolated. The site-specificity of homologous recombination was confirmed by Southern blot analysis. To generate conditional mutants, plasmids pGMCK3-0X21-T10, pGMCK3-0X38-T10 and pGMCK3-0X38-T28, were co-electroporated with pGA0XP15-intL5 in order to facilitate transient integrase expression into the SCO recombinants (Klotzsche *et al.,* 2009). In addition, the complementation construct pTTB::*2129c*, was co-electroporated with the TetR-expressing plasmids. Transformants were selected on 7H10/OADC agar plates supplemented with HYG, KAN, and GEN, where required, with or without ATC (500 ng/ml). To avoid the inactivation of inducer, all cultures containing ATC were grown in the dark and exposure to light was minimized.

6.3.4 ATC-dependent growth in liquid and on solid media

To assess the effect of ATC on growth in liquid medium, cells were inoculated at a final OD_{600} of 0.005 into 20 ml 7H9/OADC containing the appropriate antibiotic (unsupplemented – Wt; HYG – *mshC*-SCO; and HYG, KAN – *mshC* Tet-OFF) and/or ATC: Wt and *mshC*-SCO – 500 ng/ml and *mshC* Tet-OFF – 500, 250, 125 and 62.5 ng/ml. Cultures were incubated at 37°C and OD_{600} was measured every 24 hr.

To assess the growth effect on solid medium, Wt, *mshc*-SCO and *mshC* Tet-OFF cultures were initially grown in 7H9/OADC medium to an OD_{600} of 0.5 then serially diluted 2-fold, before spotting on 7H10/OADC agar plates on the following combinations: unsupplemented – Wt, HYG – *mshC*-SCO and HYG, KAN – *mshC* Tet-OFF in addition to 7H10/OADC agar supplemented with ATC at 500, 250, 125 and 62.5 ng/ml.

6.3.5 Antimicrobial agents

Anhydrotetracycline (ATC); RIF; INH; STR; plumbagin (PMB) and oxyphenbutazone (OPB) were purchased from Sigma Aldrich. For stock solutions, antimicrobials were all dissolved in the following solvents: ATC in 70% ethanol; INH and STR in nuclease-free water (Qiagen) and RIF, PMB and OPB in DMSO. Antimicrobial stock solutions were stored at 4°C, with the exceptions of PMB and OPB that were stored at -20°C.

6.3.6 Checkerboard synergy assay

To evaluate ATC-dependent depletion, the checkerboard assay was adopted, as described above (Chapter 5). The antimicrobial agent (compound A) and ATC (compound B), were 2-fold serially diluted across and down the plate, respectively (Ramon-Garcia *et al.,* 2011). The starting concentrations of antimicrobials were prepared to 4 × MIC and ATC at a concentration 100 µg/ml.

6.3.7 Quantitative RT-PCR of *Mtb* genes in response to ATC treatment

Primers and probes used for droplet digital PCR (dd-PCR; BioRad) were designed using the Primer3 programme (http://frodo.wi.mit.edu/cgi-bin/primer3/primer3_www.cgi) (Table 6.5). All primers were designed to amplify DNA fragments internal to the coding sequence of the relevant genes with a standard annealing temperature (60°C).

Table 6.5: Primers and probes used for dd-PCR in this study

Gene	Primer 5'-3'		Probe 5'-3' ⋆
mshC	Rv2130RTF	GCGGCCTCGACATCCA	CGGTGGTAGCGATC (FAM)
	Rv2130RTR	ACTCGTGGTGCGGAAAGAT	
sigA	sigARTF	CGAGCCGATCTCGTTGGA	ACGAGGGCGACAGC (VIC)
	sigARTR	TTCGATGAAATCGCCAAGCT	

⋆ TaqMan minor groove binder (MGB) probes were either labeled with 6- carboxyfluorescein (FAM) or with 4,7,2'-trichloro-7'-phenyl-6- carboxyfluorescein (VIC).

6.4 Results

6.4.1 Disruption of *Mtb* mycothiol production by conditional regulation of *mshC.*

To generate a conditional mutant of *Mtb*, a two-step method was used in which the native promoter of the target gene, *Rv2130c* (*mshC*), was first replaced with a Tet-regulatable promoter element by SCO homologous recombination. Thereafter, plasmids expressing Tet repressors (TetRs) were introduced as per established protocols (Abrahams *et al.,* 2012). The integrity of the *mshC*-SCO was confirmed by Southern blot (Figure 6.1), after which plasmids harbouring either the forward (TetR) or reverse (rev-TetR) tetracycline repressor was used to generate conditional mutants in the Tet-ON (intermediate and strong) and Tet-OFF configurations, respectively.

When generating promoter-replacement mutants the chromosomal arrangement of the gene under investigation is key. Expression of co-regulated genes downstream of the target gene may be affected by placement of the Tet-promoter upstream of a gene present in an operon (Abrahams *et al.,* 2012). According to TBDB (http://www.tbdb.org/), the Pearson Correlation Coefficient for the gene pair *Rv2129c – Rv2130c* (*mshC*) is 0.23974, which indicates a relatively insignificant chance that the genes constitute an operon (strongest positive correlation is 1.0). As *Rv2129c* is characterized as a non-essential hypothetical protein, is not significantly operonic with *mshC*, a complementation strain was omitted from this study (Sassetti *et al.,* 2003; Griffin *et al.,* 2011).

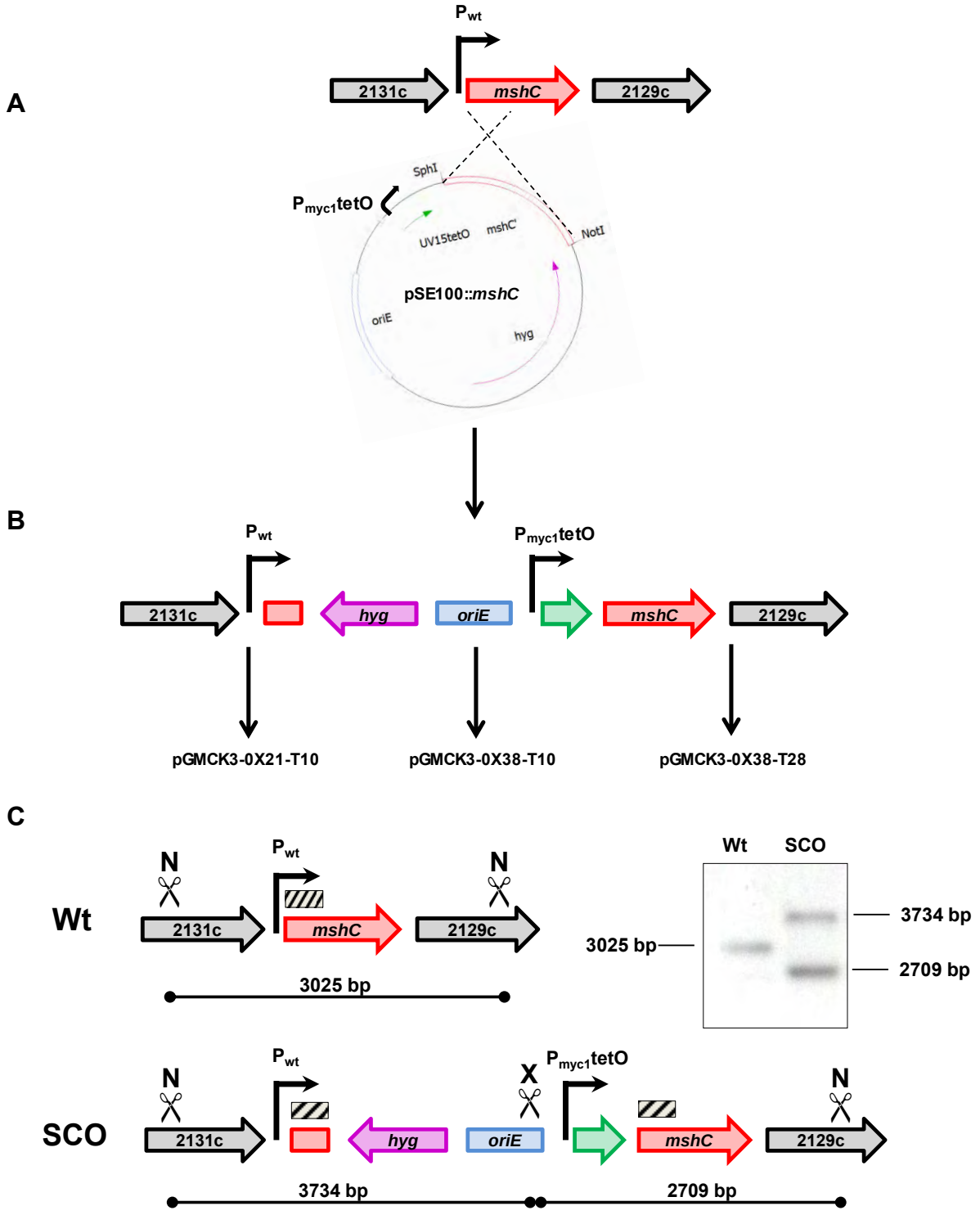

Figure 6.1: Schematic overview of the construction of *Mtb mshC* conditional mutants. (A) The pSE100 suicide plasmid habouring the 5' region of *mshC* (including the ribosomal binding site and first 704 bp of *mshC*). **(B)** Following homologous recombination, the SCO strain was generated in which *mshC* is under the control of the ATC-regulatable promoter-operator element, $P_{myc1}tetO$. Subsequently, plasmids expressing TetRs were introduced into the SCO to generate conditional mutants in the Tet-ON (intermediate and strong) and Tet-OFF configurations. **(C)** Genotypic verification of the *mshC*-SCO strain. Schematic illustration of the Southern blot strategy in which *Nco*I-*Xba*I digested genomic DNA hybridized to the 725 bp probe (truncated 5' *mshC* PCR product), depicted as the lined box (not drawn to scale).

6.4.2 Growth of the *mshC* conditional mutant cannot be modulated with ATC.

In the Tet-OFF strain, reverse TetR binds to the *tet* operator (*tetO*) in the presence of ATC, repressing gene transcription (Klotzsche *et al.,* 2009). The Tet-OFF strain is advantageous under certain conditions, such as hypoxia, when ATC cannot be easily depleted (Klotzsche *et al.,* 2009). Following electroporation of the SCO with the Tet repressors (TetR), only the *mshC* Tet-OFF strain was selected for further characterization. The mutant was evaluated for ATC-dependent growth in liquid and on solid media. In liquid medium, a slight growth impairment of *mshC* Tet-OFF was observed in the presence of ATC at all concentrations tested (500, 250, 125 and 62.5 ng/ml), compared to growth in the absence of ATC (Figure 6.2). Furthermore, *mshC* Tet-OFF (with and without ATC) exhibited a definite growth defect when compared to the control strains, Wt *Mtb* and *mshC*-SCO. The presence of ATC slightly reduced the growth of Wt, and the *mshC*-SCO (with and without ATC) grew at a slightly, but reproducibly, slower rate than Wt, although it could not be considered significant. On solid medium, the Tet-OFF strain exhibited equivalent growth kinetics in the absence and presence of ATC at all concentrations tested (Figure 6.3). In addition, the mutant strain grew comparably to the control strains, Wt and *mshC*-SCO, both with and without ATC. Importantly, the concentrations of ATC used in this study did not have a growth effect on Wt or *mshC*-SCO.

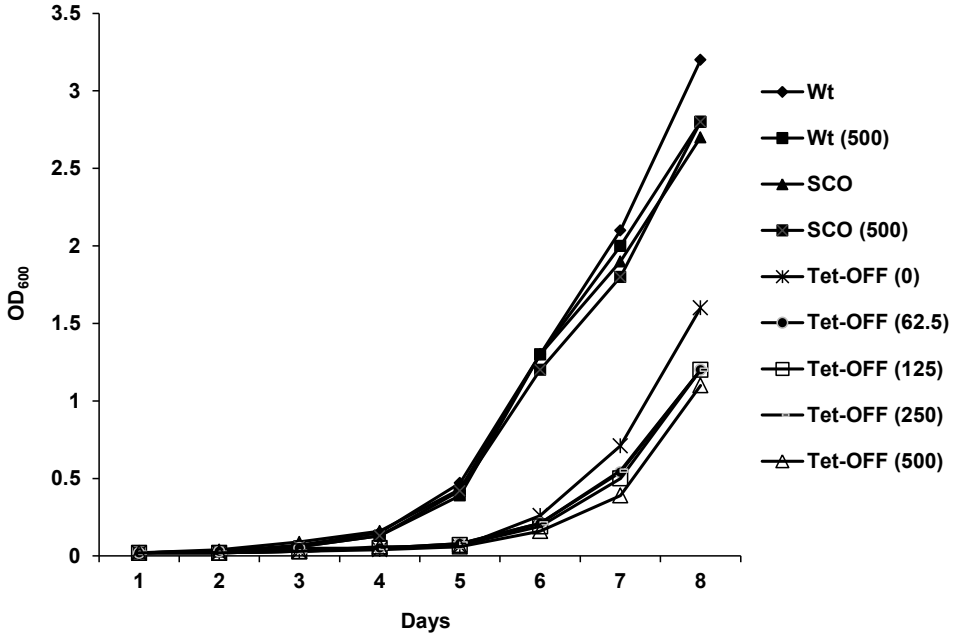

Figure 6.2: The *mshC* Tet-OFF strain is not ATC-regulated in liquid medium. Growth of *mshC* Tet-OFF in 7H9 medium in the absence or presence of ATC at the indicated concentrations. The parental Wt and *mshC*-SCO strains were included as controls. Data are from a representative experiment performed in duplicate. The numbers in parentheses represent the concentration of ATC (ng/ml).

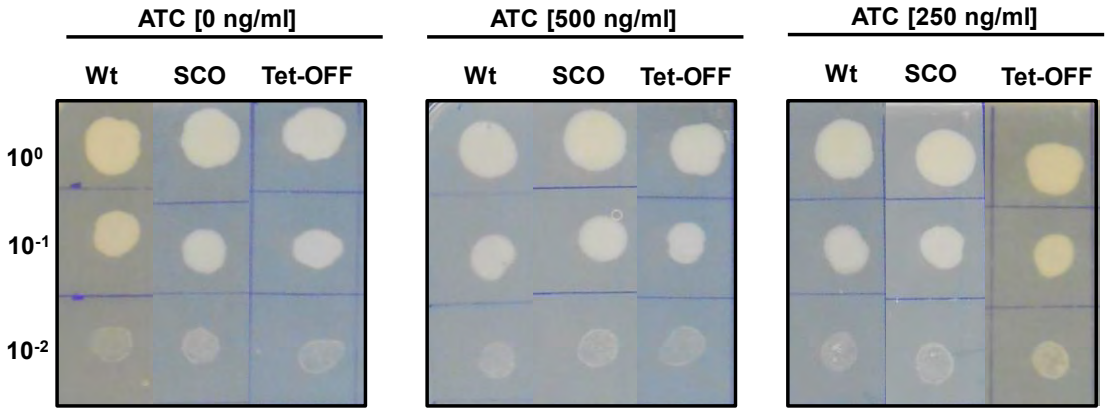

Figure 6.3: The *mshC* Tet-OFF strain does not display ATC-dependent growth regulation on solid medium. Strains were grown to mid-log phase and equivalent numbers of cells spotted on plates containing no ATC or ATC at concentrations of 500 ng/ml or 250 ng/ml. Cultures were also spotted onto plates containing ATC at 125 ng/ml and 62.5 ng/ml (data not shown). Data are from a representative experiment performed in duplicate.

6.4.3 Phenotypic characterization of *mshC* Tet-OFF.

In general, depletion or elimination of mycothiol (MSH) is associated with increased sensitivity to RIF, STR and ERY as well as oxidizing and alkylating agents. In addition, resistance to INH and ETH has been reported in these mutants (summarized in Table 6.1). To determine the potential impact of *mshC* depletion on antibiotic susceptibilty, the *mshC* Tet-OFF mutant was exposed to a subset of these agents and the MIC compared to that observed for Wt. As depletion of a target transcript has been shown to be ATC concentration-dependent (Abrahams *et al.,* 2012), the checkerboard synergy assay was adopted to examine the effect of a range of concentrations of both ATC and the antimicrobial agent against *mshC* Tet-OFF and Wt. There was no change in susceptibility to the antimycobacterial agents RIF, STR and INH in the *mshC* Tet-OFF strain in the presence of ATC. This suggests that MSH was not depleted sufficiently to render the cells hypersensitive to antibiotics (Table 6.6).

Table 6.6: The susceptibility of Wt and *mshC* Tet-OFF to antimycobacterial agents**:** A checkerboard synergy assay was used to evaluate the effect of ATC on susceptibility to RIF, STR and INH. Values indicate the minimum inhibitory concentration (MIC_{90}) – µg/ml.

	Wt	**Tet-OFF**
RIF	0.004	0.004
RIF + ATC	NC	NC
STR	0.625	0.625
STR + ATC	NC	NC
INH	0.08	0.08
INH + ATC	NC	NC

* NC-No change; Data are from a representative experiment performed in triplicate.

Furthermore, susceptibility to the oxidizing agents, plumbagin (PMB) and oxyphenbutazone (OPB), was evaluated. Interestingly, the *mshC* Tet-OFF strain displayed increased susceptibility to PMB with increasing concentrations of ATC (Figure 6.4). However an equivalent effect was observed against Wt, suggesting the synergistic effect of ATC and PMB is an *mshC*-independent outcome. There was no change in susceptibility to OPB in the *mshC* Tet-OFF strain in the presence of ATC and an equivalent effect was observed in Wt (Figure 6.4). Together, these data suggested that *mshC* was not regulated by ATC in the Tet-OFF strain.

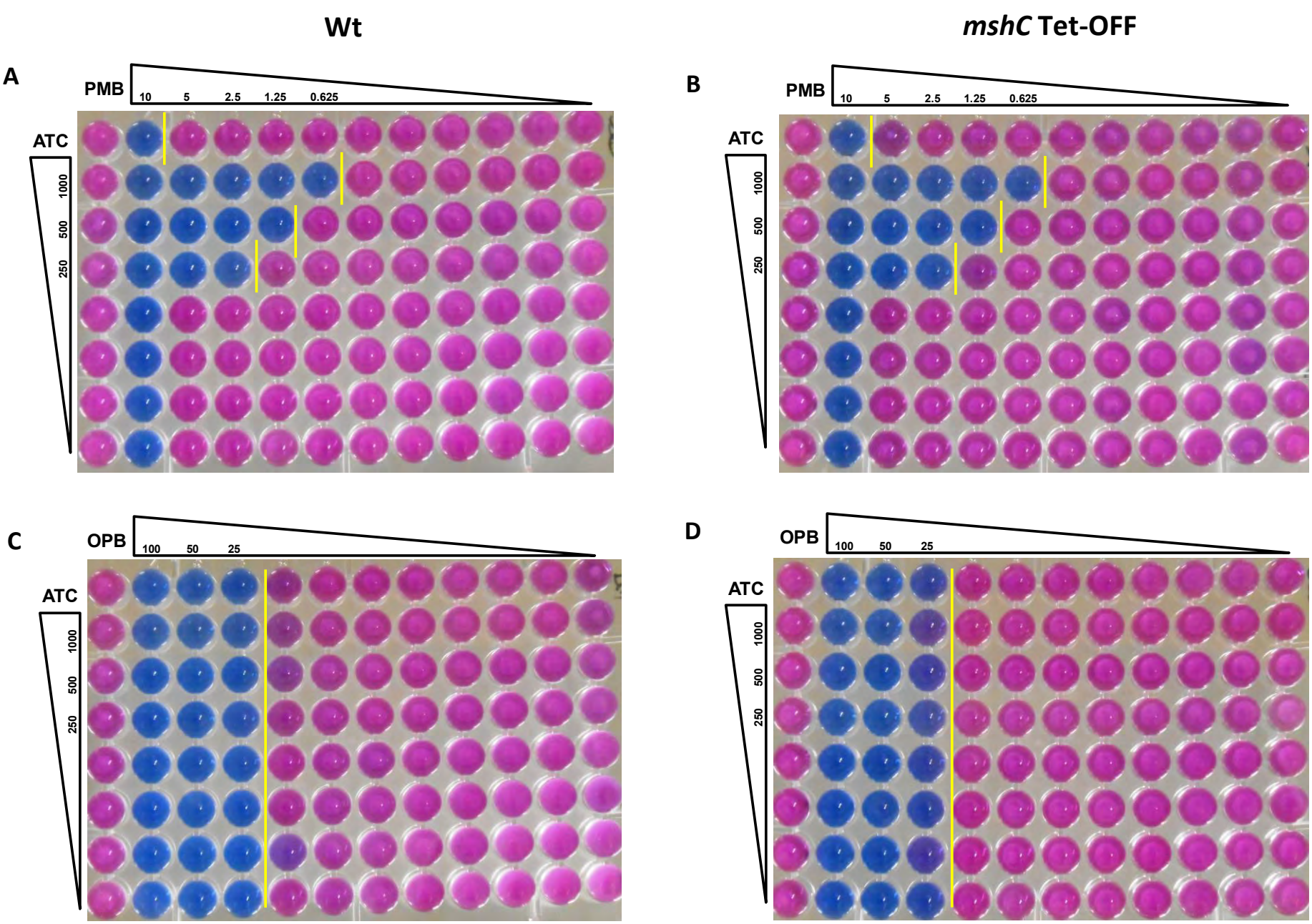
Wt
mshC Tet-OFF
A
PMB
10
5
2.5
1.25
0.625
ATC
1000
500
250
B
PMB
10
5
2.5
1.25
0.625
ATC
1000
500
250
C
OPB
100
50
25
ATC
1000
500
250
D
OPB
100
50
25
ATC
1000
500
250

Figure 6.4: The susceptibility of Wt and *mshC* Tet-OFF to oxidizing agents. A chequerboard synergy assay shows increased susceptibility of Wt (**A** and **C**) and *mshC* Tet-OFF (**B** and **D**) to plumbagin (PMB) in the presence of ATC at various concentrations. ATC has no effect on the susceptibility of Wt or *mshC* Tet-OFF to oxyphenbutazone (OPB). Bacterial viability was measured by the addition of alamar blue by which a transition from blue to pink colour indicates growth. The yellow line represents the minimum inhibitory concentration (MIC_{90}). ATC concentrations are presented as ng/ml while oxidizing agents are in µg/ml. Data are from a representative experiment performed in triplicate.

6.4.4 MshC is not ATC-regulated in the *mshC* Tet-OFF strain

The lack of an ATC-dependent effect on the growth and phenotype of *mshC* Tet-OFF suggested that mycothiol biosynthesis was not sufficiently depleted. To investigate the effect of ATC treatment on target gene expression, droplet digital PCR (dd-PCR) was used to analyse the expression levels of *mshC* in response to ATC treatment (250 ng/ml [Figure 6.5)]). No change to *mshC* expression was observed upon treatment with ATC in *mshC* Tet-OFF. As a control, and to validate ATC as an inducer, the expression of *coaBC* in a *coaBC* Tet-OFF strain (Evans and Mizrahi, unpublished) was evaluated. Additionally, expression of *mshC* was upregulated 2.5 fold in *mshC*-SCO relative to Wt, suggesting that the $P_{myc1tetO}$ is significantly stronger than the Wt promoter. Finally, ATC at a concentration of 250 ng/ml did not have an effect on *mshC* expression in Wt or *mshC*-SCO strain.

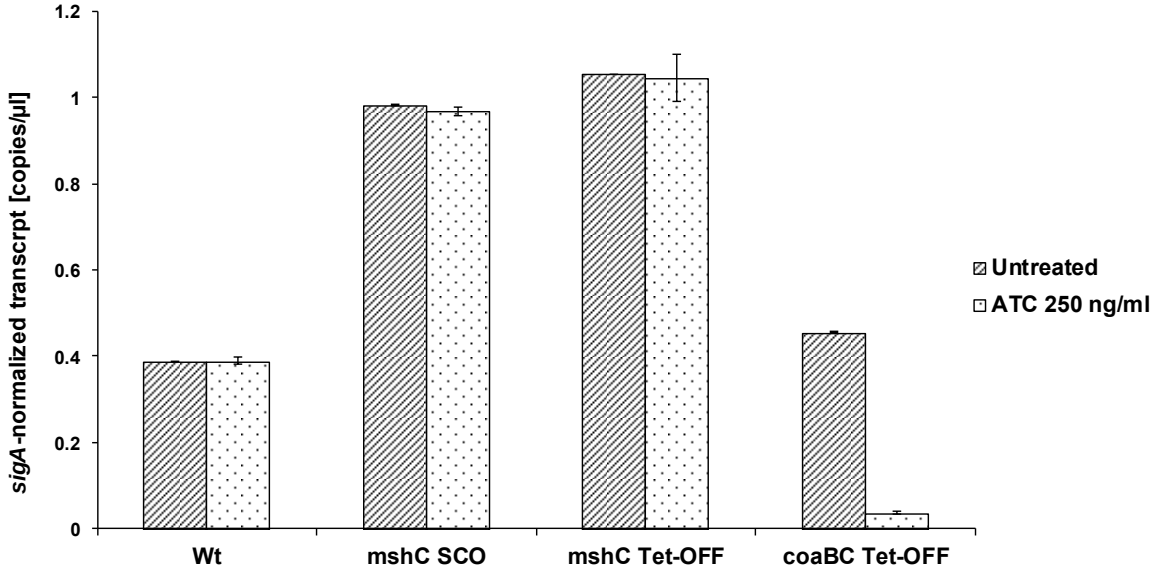

Figure 6.5: Transcriptional response of *mshC* to ATC treatment. A. dd-PCR analysis of *mshC* expression in *Mtb* Wt, *mshC*-SCO and *mshC* Tet-OFF treated with ATC (250 ng/ml for 24 hr), or untreated. Similarly, *coaBC* expression was evaluated as a positive control. The results represent the average with standard deviation (SD) of two biological replicates, for each of which two technical replicates were performed.

6.5. Discussion

The ability to conditionally regulate the expression of essential genes with a simple inducer is extremely useful to examine the contribution of the target gene or other components of the same pathway (Abrahams *et al.,* 2012; Park *et al.,* 2014). In mycobacteria, several groups have reported the use of Tet-based systems for the conditional regulation of essential genes *in vitro* as well as for characterization during infection in animal models (Carroll *et al.,* 2005; Ehrt *et al.,* 2005; Hernandez-Abanto *et al.,* 2006; Boldrin *et al.,* 2010).

In this study, to evaluate MSH-mediated fortification, application of the Tet-based conditional expression system to *mshC* was attempted. Although it was possible to generate an SCO mutant in which the native gene was placed under the control of a Tet-regulatable promoter, ATC-dependent regulation was not observed following introduction of the reverse Tet repressors (RevTetR). For different genes the level of expression at which growth impairment manifests is different; that said, the lack of regulation observed in the *mshC* Tet-OFF strain was intriguing, especially since genes with naturally low expression levels are expected to be unresponsive (Carroll *et al.,* 2005). In addition, the concentration of ATC appears to play an important role due to the presence of multidrug efflux pumps in *Mtb* that actively extrude the inducer.

Although the range of concentrations of ATC tested did not elicit a clear phenotype, it may be worthwhile to optimize the concentration as suggested previously (Carroll *et al.,* 2005). Furthermore, the propensity of certain strains to lose Tet regulation when propagated *in vitro* has been previously reported and may possibly explain the phenotype observed in this study, although care was taken to not propagate beyond 5 generations (Abrahams *et al.,* 2012). Furthermore, validating the behaviour of this strain in response to ATC was especially challenging since, unlike auxotrophs (Abrahams *et al.,* 2012), this strain could not be stabilized by supplementation. Although we generated two Tet-ON strains in which Wt TetR were expressed from strong (S) and intermediate (M) mycobacterial promoters, these were not selected for further characterization. The disadvantage of the Tet-ON strains is that the inducer needs to be removed in order to silence the gene, and this can be challenging depending on the nature of the assay as well as the nature of the target gene.

Mycothiol has been advocated as a drug target. The first MSH biosynthesis inhibitor identified, NTF1836, was initially found in a screen for inhibitors of the native *Mtb* MshC. This compound was optimized and demonstrated activity against non-replicating *Mtb* (Newton *et al.,* 2006; Newton *et al.,* 2011). In addition, in a separate screen, two quinaldinium derivatives were recently identified which exhibit micromolar inhibition of MshC (Gutierrez-Lugo *et al.,* 2009). Its defined role in the survival and adaptation of mycobacteria to oxidative stress promotes MshC as a drug target (Hayward *et al.,* 2004). However, the resistance to INH and ETH associated with mycothiol depletion is of definite concern. Together with RIF, INH is the foundation of the current regimen for the treatment of susceptible tuberculosis (TB). Therefore, in addition to prophylactic treatment to prevent progression from latent to active TB, it is unlikely that an MshC inhibitor will be administered concurrently with either INH or ETH or any other novel drug that may target *inhA*. Additionally, it has been suggested that functional defects in the mycothiol pathway may result in low level INH resistance or later development of high-level mono- resistance (Hayward *et al.,* 2004).

The ultimate generation of a “knock-up” mutant in turn suggests that a Tet-based conditional expression system is not applicable to this gene. This is not a new observation: this approach has previously been shown to result in differential regulation of essential genes (Abrahams *et al*., 2012 and Evans and Mizrahi, unpublished).

Chapter 7: General Conclusion

It is now generally accepted that the molecular mechanisms that perpetuate antibiotic resistance in the clinical setting are not limited to a single resistance mechanism, but to an amalgamation between intrinsic and genetic resistance mechanisms (Viveiros *et al.,* 2012). These include the low permeability of the mycolic acid-containing cell wall, the operation of various antibiotic-modifying or -inactivating systems, and the activity of efflux pumps.(Louw *et al.,* 2009; da Silva *et al.,* 2011a; Balganesh *et al.,* 2012b) Subsequently, intrinsic resistance mechanisms limit the antibiotics available for treatment and drive the emergence of strains with high levels of antibiotic resistance. This study aimed to investigate the role of various components of the "intrinsic resistome" that limit the efficacy of antitubercular agents.

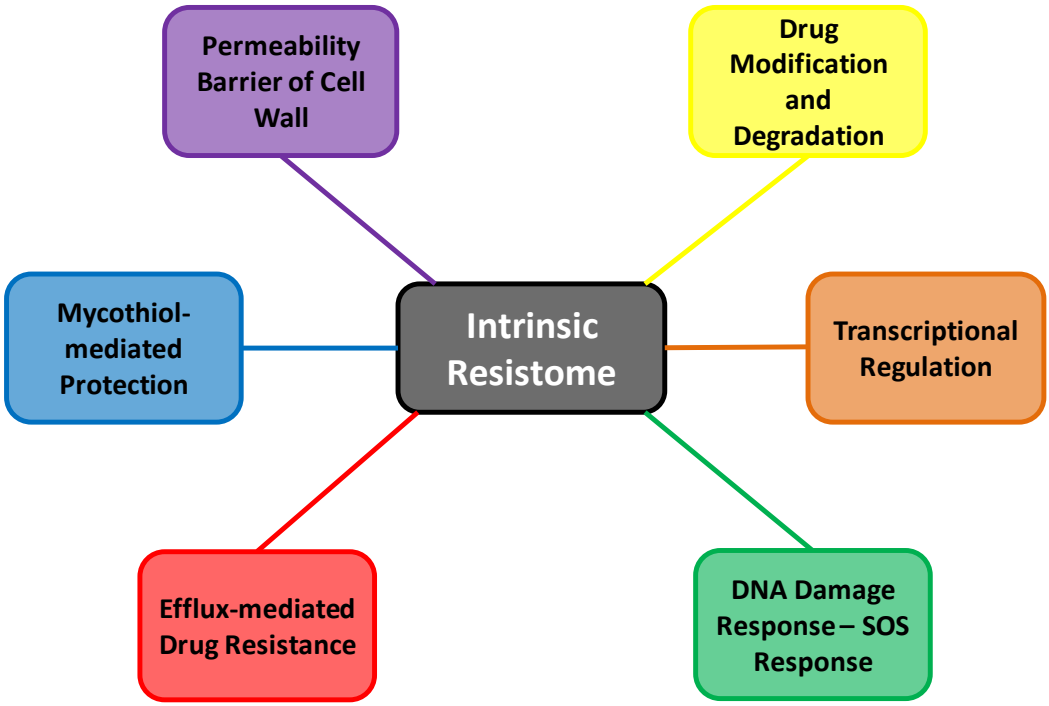

Figure 7.1: Mechanisms that contribute to the mycobacterial intrinsic resistome. The individual mechanisms that contribute to *Mtb*'s intrinsic resistance do not function as discrete mechanisms, but rather a coordinated interplay of one or more mechanisms to form an intricate, dynamic network termed the intrinsic resistome. These intrinsic mechanisms include the permeability barrier of the mycobacterial cell wall, mycothiol-mediated protection, transcriptional regulation of multidrug resistance, the SOS response, drug modification and degradation and efflux-mediated resistance. The intrinsic resistome thus presents a formidable opponent in the quest for the discovery and development of novel antituberculosis drugs and limits currently available drugs by driving the emergence of strains with high levels of antibiotic resistance.

Several lines of evidence implicate the SOS response in intrinsic resistance to antibiotics through its role in adaptive mutagenesis (Drlica & Zhao 1997; Miller *et al.,* 2004; Cirz & Romesberg 2007; Kohanski *et al.,* 2007). Mycobacteria are intriguing in that there are two mechanisms associated with the regulation of DNA repair genes: a small number of genes are regulated by the classic SOS or RecA/LexA-dependent mechanism (referred to as the SOS response), while a larger subset of genes are regulated by an alternate, RecA/LexA-independent mechanism (referred to as the RecA-ND mechanism/response) (Figure 3.2) (Durbach *et al.,* 1997; Rand *et al.,* 2003; Gamulin *et al.,* 2004; Smollett *et al.,* 2012). Given the existence of an alternative DNA damage response in mycobacteria (Rand *et al.,* 2003; Gamulin *et al.,* 2004), corresponding *Mtb* and *Msm lexA*$^{Ind-}$ (SOS-uninducible) mutants were generated to evaluate how the SOS pathway specifically contributes to antibiotic-mediated DNA damage tolerance and induced mutagenesis. This study is the first to report the construction of *lexA*$^{Ind-}$ mutants in both *Msm* and *Mtb*. However, inactivation of the SOS response still renders a fully functional RecA-ND response. Thus, error-prone damage tolerance (TLS) is compromised in these strains, but error-free DNA repair (BER/NER) and repair of double-strand breaks (DSBs, HR/NHEJ) remains functional. Furthermore, *Mtb* auto-bioluminescent reporter strains were generated by introducing the *lux* operon downstream of the *recA* or *radA* promoters. Analysis of a panel of antimicrobials against these strains allowed for the identification of true DNA-damaging agents and the evaluation of the kinetics of the DNA-damage response, in a concentration- and time-dependent manner.

Efflux pumps contribute directly to intrinsic resistance, and indirectly by providing a "window" for the emergence of high-level resistance through drug-target mutations (high-level, adaptive resistance mechanisms). In addition, overexpression of – or mutations within – efflux pumps may result in antimicrobial resistance, as the drug is extruded more efficiently and the intracellular concentration of the drug decreases to sub-inhibitory concentrations, thus inducing genetic resistance (Piddock 2006; Zechini & Versace 2009). Current strategies used to counteract efflux-mediated resistance include the search of either new antibiotics that overcome the efflux systems or efflux pump inhibitors (EPIs). Utilization of EPIs has become increasing attractive, given the mounting evidence implicating the clinical significance of efflux pumps. Ultimately, antimicrobial therapy with an EPI is a combination therapy. Therefore to maximize the synergy between the two

agents, it is imperative that novel EPI's are tested in combination from the *in vitro* stages of development. With the increasing attractiveness of EPIs a deluge of novel EPIs are predicted, that will require rapid and reliable analyses in *in vitro* and *ex vivo* assays. In this context, an *in vitro* assay has been established in which novel EPIs can be tested in combination with current/ novel antimicrobials, to indicate efficacy of the prospective EPI in downstream applications (*ex vivo* and *in vivo*). Using this approach, various candidates have been identified and it is hoped that a continuous supply of compounds in the EPI pipeline may yield a successful clinical candidate.

MSH has an established role in tolerance of oxidative and other stressed conditions, and contributes to the survival of bacilli within macrophages. MSH functions in the intrinsic resistance of *Mtb* by serving as a substrate for enzymes involved in antibiotic detoxification (Rawat & Av-Gay 2007; Jothivasan & Hamilton 2008; Newton *et al.,* 2008). The attempt to disrupt MSH production by conditionally knocking-down expression of the essential gene, *mshC,* was futile, highlighting the difficulties of knocking down a pathway in which the essentiality of the gene(s) involved remain contraversial.

In conclusion, *Mtb* has a multitude of inherent mechanisms to subvert the effects of antimicrobial treatment. This study has contributed to the understanding of certain aspects of the intrinsic resistome and in doing so, established tools, such as the autobiolumiscent reporter assay for early identification of DNA-damaging agents and the chequerboard synergy assay for rapid identification of novel EPIs, that can be used in future drug discovery programmes.

Appendices

Appendix 1: List of abbreviations

2TY	Tryptone Yeast broth
4NQO	4-nitroquinoline-1-oxide
5-FU	5-fluorouracil
AAC	Aminoglycoside acetyltransferases
ABC	ATP-binding cassette
AMP	Ampicillin
ANT	Aminoglycoside nucleotransferases
APH	Aminoglycoside phosphotransferases
ARV	Anti-retroviral
ATC	Anhydrotetracycline
BCG	Bacille Calmette-Guérin
BDQ	Bedaquiline
BER	Base excision repiar
bp	Base pair
CCP	Cell-penetrating peptides
cDNA	Complementary DNA
CEM	Cryo-electron microscopy
CET	Cryo-electron tomography
CFU	Colony forming unit
CIP	Ciprofoxacin
CTAB	Cetyltrimethylammonium bromide
DAGS	Diacyl gycerols
DCS	D-cycloserine
dd-PCR	digital droplet PCR
DEPC	Diethylpyrocarbonate
dG	Deoxyguanosine
DMSO	Dimethylsulphoxide
DNA	Deoxyribonucleic acid
dNTP	Deoxynucleotide triphosphate
DOTS	Directly Observed Therapy – Short Course
DSBs	Double-strand breaks
EDTA	Ethylenediaminetetraacetic acid
EMB	Ethambutol
EPI	Efflux pump inhibitor
ERY	Erythromycin
ETH	Ethionamide
FA	Fusidic acid
FAM	6-carboxyfluorescein
FBS	Fetal bovine serum
FDA	US Food and Drug Administration
FIC	Fractional inhibitory concentration
FICI	Fractional inhibitory concentration index

$FMNH_2$	Riboflavin phosphate
g	Gravitational force
GAT	Gatifloxacin
GEN	Gentamycin
HCL	Hydrochloric acid
HIV	Human Immunodeficiency Virus
HK	Histidine kinase
HTS	High throughput screening
HYG	Hygromycin
IC_{20}	Inhibitory concentration
INH	Isoniazid
IPT	INH preventive therapy
IRIS	Immune Reconstitution Inflammatory Syndrome
KAN	Kanamycin
LA	Luria-Bertani agar
LB	Luria-Bertani broth
LEV	Levofloxacin
LTBI	Latent tuberculosis infection
mAGP	Mycolyl arabinogalactan–peptidoglycan
MALDI	Matrix-assisted laser desorption/ionization
MALDI-MSI	MALDI- mass spectrometry imaging
MATE	Multidrug and toxic compound extrusion
MDR	Multidrug resistant
MFS	Major facilitator superfamily
MIC_{90}	Minimum Inhibitory Concentration
MMC	Mitomycin C
MMR	Mismatch repair
MoA	Mechanism of action
MOX	Moxifloxacin
MSH	Mycothiol
Msm	*Mycobacterium smegmatis*
MSSM	Mycothione
Mtb	*Mycobacterium tuberculosis*
NAG	N-acetyl glucosamine
NaOH	Sodium hydroxide
NaOH	Sodium chloride
NER	Nucleotide excision repair
NFZ	Nitrofurazone
NHEJ	Nonhomologous end-joining
NOR	Norfloxacin
NOV	Novobiocin
OADC	Oleic acid-albumin-dextrose-catalase
OFX	Ofloxacin
$OH^{\cdot}$	Hydroxyl radical
OMP	Outer membrane protein
OPB	Oxyphenbutazone
PAS	Para-aminosalysilic acid

PBP	Penicillin binding proteins
PCR	Polymerase Chain Reaction
PD	Pharmacodynamics
PDIM	Phthiocerol dimycocerosate
PET	Positron emission tomography
PGL	Phenolic glycolipids
PIMS	Phosphatidylinositol mannosides
PK	Pharmacokinetic
PMA	Phorbol myristate acetate
PMB	Plumbagin
PZA	Pyrazinamide
RecA-ND	RecA/LexA-independent mechanism
RecA-NDp	RecA/LexA-independent promoter
RevTetR	Reverse Tet repressor
RIF	Rifampicin
RLU	Relative Luminescence Units
RMS	Reverse micellar solution
RNA	Ribonucleic acid
RND	Resistance-nodulation division
RNS	Reactive nitrogen species
ROS	Reactive oxygen species
SAR	Structure-activity relationship
SCO	Single crossover
SD	Standard deviation
sdH_2O	Sterile distilled water
SMR	Small multidrug resistance
SNPs	Single nucleotide polymorphisms
SPC	Spectinomycin
ssDNA	Single-stranded DNA
STM	Streptomycin
Suc	Sucrose
TAGS	Triacylglycerols
TB	Tuberculosis
TbI	Transformation Buffer I
TbII	Transformation Buffer II
TB-WCS	Target-based whole-cell screening
TE	Tris-EDTA
Tet	Tetracycline
TetR	Tet-repressor
TF	Transcription factor
TLS	Translesion synthesis
Tris	Tris(hydroxymethyl)aminomethane
UCT	University of Cape Town
UV	Ultraviolet
v/v	Volume per volume
v/w	Weight per volume
VAN	Vancomycin

VER	Verapamil
VIC	4,7,20-trichloro-7'-phenyl-6-carboxyfluorescein
WGS	Whole-genome sequencing
Wt	Wild-type
XDR	Extensively Drug Resistant
X-gal	5-bromo-4-chloro-3-indolyl-D-thiogalactopyranoside
γ	gamma

Appendix 2: Culture media

All media were made to a final volume of 1L with distilled water. Media were sterilized by autoclaving at 121°C for 15 min.

Luria-Bertani Agar

10 g tryptone, 10 g NaCl, 5 g yeast extract, 15 g bacteriological agar

Luria-Bertani Broth

10 g tryptone broth, 10 g NaCl, 5 g yeast extract

2TY

5 g NaCl, 10 g yeast extract, 16 g tryptone

7H10/OADC Agar

19 g Middlebrook 7H10 agar powder (DifcoTM, USA), 5 ml glycerol (Merck, Germany)

100 ml Middlebrook OADC Enrichment (BD Microbiology Systems, USA) added after autoclaving.

7H9/OADC Liquid

4.7 g Middlebrook 7H9 broth powder (DifcoTM, USA), 2 ml glycerol (Merck, Germany)

100 ml OADC Middlebrook OADC Enrichment (BD Microbiology Systems, USA) added after autoclaving.

Appendix 3: Chemical Structures

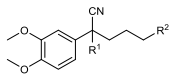

Analogue ID/ Published ID**	R^1	R^2
VER	$CH(CH_3)_2$	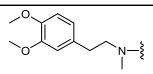
MKV1/ 7a	$CH(CH_3)_2$	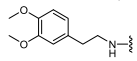
MKV2/ 7b	$CH(CH_3)_2$	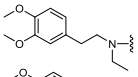
MKV3/ 7c	$CH(CH_3)_2$	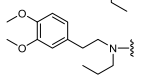
MKV4/ 7d	$CH(CH_3)_2$	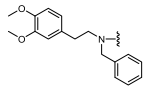
MKV5/ 7e	$CH(CH_3)_2$	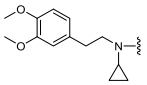
MKV11/ 12a	$CH(CH_3)_2$	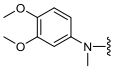
MKV10/ 12b	$CH(CH_3)_2$	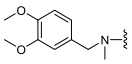
KSV5/ 14a	$CH(CH_3)_2$	
KSV4/ 14b	$CH(CH_3)_2$	
(KSV11/ 14c	$CH(CH_3)_2$	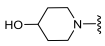
KSV8/ 14d	$CH(CH_3)_2$	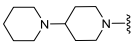
KSV14/ 14e	$CH(CH_3)_2$	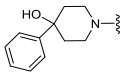
KSV7/ 14f	$CH(CH_3)_2$	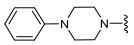
KSV10/ 14g	$CH(CH_3)_2$	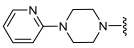
KSV12/ 14h	$CH(CH_3)_2$	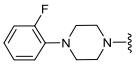
MKV6/17a	H	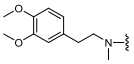
MKV7/ 17b	CH_3	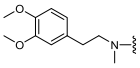
MKV8/ 17c	CH_2CH_3	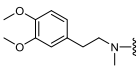
MKV9/ 17d	$(CH_2)_2CH_3$	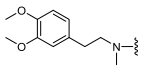
KSV19/ 17e		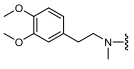
KSV21/ 17f		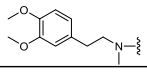

** Singh *et al.,* 2014a

Analogue ID	Structure
HEPI-04X	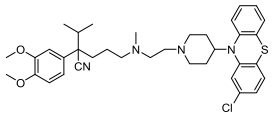
HEPI-06	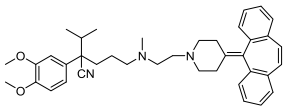
KSV-43	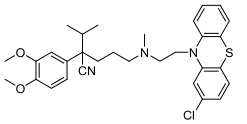
KSV-44	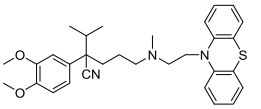
MKV-R1	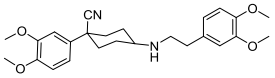
MKV-R2	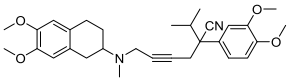
MKV-B1	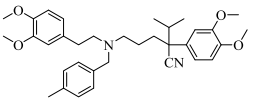
MKV-B2	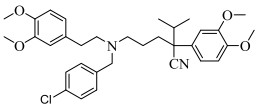
MKV-B3	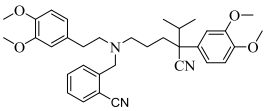
MKV-B4	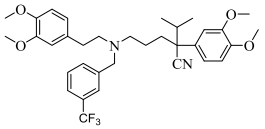
MKV-B5	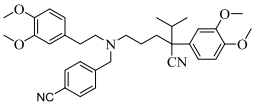
MKV-B6	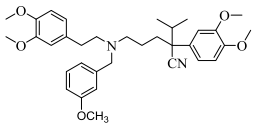
MKV-B8	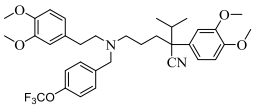
MKV-B9	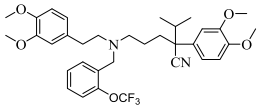
MKV-B10	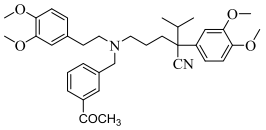
MKV-B11	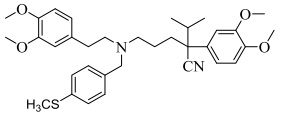

References

Abella, M., Erill, I., Jara, M., Mazón, G., Campoy, S. and Barbé, J. (2004). Widespread distribution of a *lexA*-regulated DNA damage-inducible multiple gene cassette in the Proteobacteria phylum. *Molecular Microbiology* 54(1): 212-222.

Abrahams, G. L., Kumar, A., Savvi, S., Hung, A. W., Wen, S., Abell, C., Barry III, C. E., Sherman, D. R., Boshoff, H. I. and Mizrahi, V. (2012). Pathway-Selective Sensitization of *Mycobacterium tuberculosis* for Target-Based Whole-Cell Screening. *Chemistry & Biology* 19(7): 844-854.

Adams, K. N., Szumowski, J. D. and Ramakrishnan, L. (2014). Verapamil, and its metabolite norverapamil, inhibit macrophage-induced, bacterial efflux pump-mediated tolerance to multiple anti-tubercular drugs. *Journal of Infectious Diseases* 210(3): 456-466.

Adams, K. N., Takaki, K., Connolly, L. E., Wiedenhoft, H., Winglee, K., Humbert, O., Edelstein, P. H., Cosma, C. L. and Ramakrishnan, L. (2011). Drug tolerance in replicating mycobacteria mediated by a macrophage-induced efflux mechanism. *Cell* 145(1): 39-53.

Al-Attiyah, R., El-Shazly, A. and Mustafa, A. (2006). Assessment of *in vitro* immunity to *Mycobacterium tuberculosis* in a human peripheral blood infection model using a luciferase reporter construct of *M. tuberculosis* H37Rv. *Clinical & Experimental Immunology* 145(3): 520-527.

Alland, D., Steyn, A. J., Weisbrod, T., Aldrich, K. and Jacobs, W. R. (2000). Characterization of the *Mycobacterium tuberculosis iniBAC* promoter, a promoter that responds to cell wall biosynthesis inhibition. *Journal of Bacteriology* 182(7): 1802-1811.

Amaral, L., Martins, M. and Viveiros, M. (2007). Enhanced killing of intracellular multidrug-resistant *Mycobacterium tuberculosis* by compounds that affect the activity of efflux pumps. *Journal of Antimicrobial Chemotherapy* 59(6): 1237-1246.

Andersen, P. and Kaufmann, S. H. (2014). Novel Vaccination Strategies against Tuberculosis. *Cold Spring Harbor perspectives in medicine* 4(6): a018523.

Andreu, N., Fletcher, T., Krishnan, N., Wiles, S. and Robertson, B. D. (2012). Rapid measurement of antituberculosis drug activity in vitro and in macrophages using bioluminescence. *Journal of Antimicrobial Chemotherapy* 67(2): 404-414.

Andreu, N., Zelmer, A., Fletcher, T., Elkington, P. T., Ward, T. H., Ripoll, J., Parish, T., Bancroft, G. J., Schaible, U. and Robertson, B. D. (2010). Optimisation of bioluminescent reporters for use with mycobacteria. *PloS One* 5(5): e10777.

Andrew, P. W. and Roberts, I. (1993). Construction of a bioluminescent mycobacterium and its use for assay of antimycobacterial agents. *Journal of clinical microbiology* 31(9): 2251-2254.

Babbar, N. and Gerner, E. W. (2011). Targeting polyamines and inflammation for cancer prevention. *Clinical Cancer Prevention*, Springer: 49-64.

Balganesh, M., Dinesh, N., Sharma, S., Kuruppath, S., Nair, A. V. and Sharma, U. (2012a). Efflux pumps of *Mycobacterium tuberculosis* play a significant role in antituberculosis activity of potential drug candidates. *Antimicrobial Agents and Chemotherapy* 56(5): 2643-2651.

Balganesh, M., Dinesh, N., Sharma, S., Kuruppath, S., Nair, A. V. and Sharma, U. (2012b). Efflux pumps of Mycobacterium tuberculosis play a significant role in antituberculosis activity of potential drug candidates. *Antimicrob Agents Chemother* 56(5): 2643-2651.

Balganesh, T. S., Alzari, P. M. and Cole, S. T. (2008). Rising standards for tuberculosis drug development. *Trends in pharmacological sciences* 29(11): 576-581.

Ball, P., Shales, S. and Chopra, I. (1980). Plasmid-mediated tetracycline resistance in *Escherichia coli* involves increased efflux of the antibiotic. *Biochemical and biophysical research communications* 93(1): 74-81.

Bansal-Mutalik, R. and Nikaido, H. (2014). Mycobacterial outer membrane is a lipid bilayer and the inner membrane is unusually rich in diacyl phosphatidylinositol dimannosides. *Proc Natl Acad Sci U S A* 111(13): 4958-4963.

Barkan, D., Liu, Z., Sacchettini, J. C. and Glickman, M. S. (2009). Mycolic acid cyclopropanation is essential for viability, drug resistance, and cell wall integrity of *Mycobacterium tuberculosis*. *Chemistry and Biology* 16(5): 499-509.

Boldrin, F., Casonato, S., Dainese, E., Sala, C., Dhar, N., Palù, G., Riccardi, G., Cole, S. T. and Manganelli, R. (2010). Development of a repressible mycobacterial promoter system based on two transcriptional repressors. *Nucleic Acids Research* 38(12): e134-e134.

Boshoff, H. I., Barry, C. E. and Mizrahi, V. (2004a). Mutational dynamics in *Mycobacterium tuberculosis*: implications for the evolution of drug resistance: pathogen genomics. *South African journal of science* 100(9 & 10): p. 471-474.

Boshoff, H. I. and Barry III, C. E. (2006). Is the mycobacterial cell wall a hopeless drug target for latent tuberculosis? *Drug Discovery Today: Disease Mechanisms* 3(2): 237-245.

Boshoff, H. I., Myers, T. G., Copp, B. R., McNeil, M. R., Wilson, M. A. and Barry, C. E. (2004b). The transcriptional responses of *Mycobacterium tuberculosis* to inhibitors of metabolism novel insights into drug mechanisms of action. *Journal of Biological Chemistry* 279(38): 40174-40184.

Boshoff, H. I., Reed, M. B., Barry III, C. E. and Mizrahi, V. (2003). DnaE2 Polymerase Contributes to In Vivo Survival and the Emergence of Drug Resistance in *Mycobacterium tuberculosis*. *Cell* 113(2): 183-193.

Bowman, J. and Ghosh, P. (2014). A complex regulatory network controlling intrinsic multidrug resistance in *Mycobacterium smegmatis*. *Molecular Microbiology* 91(1): 121-134.

Brennan, P. J. (2003). Structure, function, and biogenesis of the cell wall of *Mycobacterium tuberculosis*. *Tuberculosis (Edinb)* 83(1-3): 91-97.

Brooks, P. C., Dawson, L. F., Rand, L. and Davis, E. O. (2006). The mycobacterium-specific gene *Rv2719c* is DNA damage inducible independently of RecA. *Journal of Bacteriology* 188(16): 6034-6038.

Brynildsen, M. P., Winkler, J. A., Spina, C. S., MacDonald, I. C. and Collins, J. J. (2013). Potentiating antibacterial activity by predictably enhancing endogenous microbial ROS production. *Nature biotechnology* 31(2): 160-165.

Buchmeier, N. A., Newton, G. L. and Fahey, R. C. (2006). A mycothiol synthase mutant of *Mycobacterium tuberculosis* has an altered thiol-disulfide content and limited tolerance to stress. *Journal of Bacteriology* 188(17): 6245-6252.

Burian, J., Ramón-García, S., Sweet, G., Gómez-Velasco, A., Av-Gay, Y. and Thompson, C. J. (2012). The mycobacterial transcriptional regulator *whiB7* gene links redox homeostasis and intrinsic antibiotic resistance. *Journal of Biological Chemistry* 287(1): 299-310.

Butala, M., Žgur-Bertok, D. and Busby, S. J. (2009). The bacterial LexA transcriptional repressor. *Cellular and Molecular Life Sciences* 66(1): 82-93.

Camacho, L. R., Constant, P., Raynaud, C., Lanéelle, M.-A., Triccas, J. A., Gicquel, B., Daffé, M. and Guilhot, C. (2001). Analysis of the Phthiocerol Dimycocerosate Locus of *Mycobacterium tuberculosis*: Evidence that this ;lipid is involved in the cell wall permeability barrier. *Journal of Biological Chemistry* 276(23): 19845-19854.

Carroll, P., Muttucumaru, D. N. and Parish, T. (2005). Use of a tetracycline-inducible system for conditional expression in *Mycobacterium tuberculosis* and *Mycobacterium smegmatis*. *Applied and Environmental Microbiology* 71(6): 3077-3084.

Carvalho, R., de Sonneville, J., Stockhammer, O. W., Savage, N. D., Veneman, W. J., Ottenhoff, T. H., Dirks, R. P., Meijer, A. H. and Spaink, H. P. (2011). A high-throughput screen for tuberculosis progression. *PloS One* 6(2): e16779.

Chambers, H. F., Moreau, D., Yajko, D., Miick, C., Wagner, C., Hackbarth, C., Kocagöz, S., Rosenberg, E., Hadley, W. and Nikaido, H. (1995). Can penicillins and other beta-lactam antibiotics be used to treat tuberculosis? *Antimicrobial Agents and Chemotherapy* 39(12): 2620-2624.

Chao, M. C. and Rubin, E. J. (2010). Letting sleeping dos lie: does dormancy play a role in tuberculosis? *Annual Review of Microbiology* 64: 293-311.

Chapman, G. B., Hanks, J. H. and Wallace, J. H. (1959). An electron microscope study of the disposition and fine structure of *Mycobacterium lepraemurium* in mouse spleen. *Journal of Bacteriology* 77(2): 205-211.

Chatterjee, D. (1997). The mycobacterial cell wall: structure, biosynthesis and sites of drug action. *Current Opinion in Chemical Biology* 1(4): 579-588.

Chauhan, A., Lofton, H., Maloney, E., Moore, J., Fol, M., Madiraju, M. V. and Rajagopalan, M. (2006). Interference of *Mycobacterium tuberculosis* cell division by *Rv2719*c, a cell wall hydrolase. *Molecular Microbiology* 62(1): 132-147.

Chavadi, S. S., Edupuganti, U. R., Vergnolle, O., Fatima, I., Singh, S. M., Soll, C. E. and Quadri, L. E. (2011). Inactivation of *tesA* reduces cell wall lipid production and increases drug susceptibility in mycobacteria. *Journal of Biological Chemistry* 286(28): 24616-24625.

Cirz, R. T. and Romesberg, F. E. (2007). Controlling mutation: intervening in evolution as a therapeutic strategy. *Critical Reviews in Biochemistry and Molecular Biology* 42(5): 341-354.

Cohen, N. R., Lobritz, M. A. and Collins, J. J. (2013). Microbial persistence and the road to drug resistance. *Cell Host & Microbe* 13(6): 632-642.

Colangeli, R., Haq, A., Arcus, V., Summers, E., Magliozzo, R., McBride, A., Mitra, A., Radjainia, M., Khajo, A. and Jacobs, W. (2009). The multifunctional histone-like protein Lsr2 protects mycobacteria against reactive oxygen intermediates. *Proceedings of the National Academy of Sciences* 106(11): 4414-4418.

Colangeli, R., Helb, D., Vilchèze, C., Hazbón, M. H., Lee, C.-G., Safi, H., Sayers, B., Sardone, I., Jones, M. B. and Fleischmann, R. D. (2007). Transcriptional regulation of multi-drug tolerance and antibiotic-induced responses by the histone-like protein Lsr2 in *M. tuberculosis*. *PLoS Pathogens* 3(6): e87.

Cole, S., Brosch, R., Parkhill, J., Garnier, T., Churcher, C., Harris, D., Gordon, S., Eiglmeier, K., Gas, S. and Barry, C. r. (1998). Deciphering the biology of *Mycobacterium tuberculosis* from the complete genome sequence. *Nature* 393(6685): 537-544.

Collins, L. and Franzblau, S. G. (1997). Microplate alamar blue assay versus BACTEC 460 system for high-throughput screening of compounds against *Mycobacterium tuberculosis* and *Mycobacterium avium*. *Antimicrobial Agents and Chemotherapy* 41(5): 1004-1009.

Collins, L., Torrero, M. and Franzblau, S. (1998). Green Fluorescent Protein Reporter Microplate Assay for High-Throughput Screening of Compounds against *Mycobacterium tuberculosis*. *Antimicrobial Agents and Chemotherapy* 42(2): 344-347.

Connolly, L. E., Edelstein, P. H. and Ramakrishnan, L. (2007). Why is long-term therapy required to cure tuberculosis? *PLoS Medicine* 4(3): e120.

Cooksey, R., Crawford, J., Jacobs, W. and Shinnick, T. (1993). A rapid method for screening antimicrobial agents for activities against a strain of *Mycobacterium tuberculosis* expressing firefly luciferase. *Antimicrobial Agents and Chemotherapy* 37(6): 1348-1352.

Courcelle, J., Khodursky, A., Peter, B., Brown, P. O. and Hanawalt, P. C. (2001). Comparative gene expression profiles following UV exposure in wild-type and SOS-deficient *Escherichia coli*. *Genetics* 158(1): 41-64.

Cox, M. M. (2003). The bacterial RecA protein as a motor protein. *Annual Reviews in Microbiology* 57(1): 551-577.

Cox, M. M. (2007). Regulation of bacterial RecA protein function. *Critical Reviews in Biochemistry and Molecular Biology* 42(1): 41-63.

Cox, M. M., Goodman, M. F., Kreuzer, K. N., Sherratt, D. J., Sandler, S. J. and Marians, K. J. (2000). The importance of repairing stalled replication forks. *Nature* 404(6773): 37-41.

Coxon, G. D., Cooper, C. B., Gillespie, S. H. and McHugh, T. D. (2012). Strategies and challenges involved in the discovery of new chemical entities during early-stage tuberculosis drug discovery. *Journal of Infectious Diseases*: jis191.

da Silva, P. E., Von Groll, A., Martin, A. and Palomino, J. C. (2011a). Efflux as a mechanism for drug resistance in Mycobacterium tuberculosis. *FEMS Immunol Med Microbiol* 63(1): 1-9.

Da Silva, P. E. A. and Palomino, J. C. (2011). Molecular basis and mechanisms of drug resistance in *Mycobacterium tuberculosis*: classical and new drugs. *Journal of Antimicrobial Chemotherapy* 66(7): 1417-1430.

Da Silva, P. E. A., Von Groll, A., Martin, A. and Palomino, J. C. (2011b). Efflux as a mechanism for drug resistance in *Mycobacterium tuberculosis*. *FEMS Immunology & Medical Microbiology* 63(1): 1-9.

Dabbs, E. R., Yazawa, K., Mikami, Y., Miyaji, M., Morisaki, N., Iwasaki, S. and Furihata, K. (1995). Ribosylation by mycobacterial strains as a new mechanism of rifampin inactivation. *Antimicrobial Agents and Chemotherapy* 39(4): 1007-1009.

Daffe, M. and Etienne, G. (1999). The capsule of *Mycobacterium tuberculosis* and its implications for pathogenicity. *Tubercle and Lung Disease* 79(3): 153-169.

Danilchanka, O., Pavlenok, M. and Niederweis, M. (2008). Role of porins for uptake of antibiotics by *Mycobacterium smegmatis*. *Antimicrobial Agents and Chemotherapy* 52(9): 3127-3134.

Darby, C. M., Ingólfsson, H. I., Jiang, X., Shen, C., Sun, M., Zhao, N., Burns, K., Liu, G., Ehrt, S. and Warren, J. D. (2013). Whole cell screen for inhibitors of pH homeostasis in *Mycobacterium tuberculosis*. *PloS One* 8(7): e68942.

Dartois, V. (2014). The path of anti-tuberculosis drugs: from blood to lesions to mycobacterial cells. *Nature Reviews Microbiology* 12(3): 159-167.

Darwin, K. H. and Nathan, C. F. (2005). Role for nucleotide excision repair in virulence of *Mycobacterium tuberculosis*. *Infection and Immunity* 73(8): 4581-4587.

Datta, A. K. (1995). Efficient amplification using 'megaprimer'by asymmetric polymerase chain reaction. *Nucleic Acids Research* 23(21): 4530-4531.

Davis, E. O., Springer, B., Gopaul, K. K., Papavinasasundaram, K., Sander, P. and Böttger, E. C. (2002). DNA damage induction of *recA* in *Mycobacterium tuberculosis* independently of RecA and LexA. *Molecular Microbiology* 46(3): 791-800.

Davis, T. D., Gerry, C. J. and Tan, D. S. (2014). General Platform for Systematic Quantitative Evaluation of Small-Molecule Permeability in Bacteria. *ACS Chemical Biology*.

DeVito, J. A., Mills, J. A., Liu, V. G., Agarwal, A., Sizemore, C. F., Yao, Z., Stoughton, D. M., Cappiello, M. G., Barbosa, M. D. and Foster, L. A. (2002). An array of target-specific screening strains for antibacterial discovery. *Nature Biotechnology* 20(5): 478-483.

Draker, K.-A., Boehr, D. D., Elowe, N. H., Noga, T. J. and Wright, G. D. (2003). Functional annotation of putative aminoglycoside antibiotic modifying proteins in *Mycobacterium tuberculosis* H37Rv. *The Journal of Antibiotics* 56(2): 135-142.

Drews, J. (2000). Drug discovery: a historical perspective. *Science* 287(5460): 1960-1964.

Drlica, K., Malik, M., Kerns, R. J. and Zhao, X. (2008). Quinolone-mediated bacterial death. *Antimicrobial Agents and Chemotherapy* 52(2): 385-392.

Drlica, K. and Zhao, X. (1997). DNA gyrase, topoisomerase IV, and the 4-quinolones. *Microbiology and Molecular Biology Reviews* 61(3): 377-392.

Durbach, S. I., Andersen, S. J. and Mizrahi, V. (1997). SOS induction in mycobacteria: analysis of the DNA binding activity of a LexA like repressor and its role in DNA damage induction of the recA gene from *Mycobacterium smegmatis*. *Molecular Microbiology* 26(4): 643-653.

Dwyer, D. J., Belenky, P. A., Yang, J. H., MacDonald, I. C., Martell, J. D., Takahashi, N., Chan, C. T., Lobritz, M. A., Braff, D. and Schwarz, E. G. (2014). Antibiotics induce redox-related physiological alterations as part of their lethality. *Proceedings of the National Academy of Sciences* 111(20): E2100-E2109.

Dwyer, D. J., Kohanski, M. A., Hayete, B. and Collins, J. J. (2007). Gyrase inhibitors induce an oxidative damage cellular death pathway in *Escherichia coli*. *Molecular Systems Biology* 3(1).

Dye, C. and Williams, B. G. (2000). Criteria for the control of drug-resistant tuberculosis. *Proceedings of the National Academy of Sciences* 97(14): 8180-8185.

Ehrt, S., Guo, X. V., Hickey, C. M., Ryou, M., Monteleone, M., Riley, L. W. and Schnappinger, D. (2005). Controlling gene expression in mycobacteria with anhydrotetracycline and Tet repressor. *Nucleic Acids Research* 33(2): e21-e21.

Engelhardt, H., Heinz, C. and Niederweis, M. (2002). A Tetrameric Porin Limits the Cell Wall Permeability of *Mycobacterium smegmatis*. *Journal of Biological Chemistry* 277(40): 37567-37572.

Erill, I., Campoy, S. and Barbé, J. (2007). Aeons of distress: an evolutionary perspective on the bacterial SOS response. *FEMS Microbiology Reviews* 31(6): 637-656.

Estorninho, M., Smith, H., Thole, J., Harders-Westerveen, J., Kierzek, A., Butler, R. E., Neyrolles, O. and Stewart, G. R. (2010). ClgR regulation of chaperone and protease systems is essential for *Mycobacterium tuberculosis* parasitism of the macrophage. *Microbiology* 156(11): 3445-3455.

Etienne, G., Laval, F., Villeneuve, C., Dinadayala, P., Abouwarda, A., Zerbib, D., Galamba, A. and Daffé, M. (2005). The cell envelope structure and properties of *Mycobacterium smegmatis* mc2155: is there a clue for the unique transformability of the strain? *Microbiology* 151(6): 2075-2086.

Fan, J., de Jonge, B. L., MacCormack, K., Sriram, S., McLaughlin, R. E., Plant, H., Preston, M., Fleming, P. R., Albert, R. and Foulk, M. (2014). A Novel High-Throughput Cell-Based Assay Aimed at Identifying Inhibitors of DNA Metabolism in Bacteria. *Antimicrobial Agents and Chemotherapy* 58(12): 7264-7272.

Ferreras, J. A., Stirrett, K. L., Lu, X., Ryu, J.-S., Soll, C. E., Tan, D. S. and Quadri, L. E. (2008). Mycobacterial phenolic glycolipid virulence factor biosynthesis: mechanism and small-molecule inhibition of polyketide chain initiation. *Chemistry & Biology* 15(1): 51-61.

Fine, P. E. (1995). Variation in protection by BCG: implications of and for heterologous immunity. *The Lancet* 346(8986): 1339-1345.

Fol, M., Chauhan, A., Nair, N. K., Maloney, E., Moomey, M., Jagannath, C., Madiraju, M. V. and Rajagopalan, M. (2006). Modulation of *Mycobacterium tuberculosis* proliferation by MtrA, an essential two-component response regulator. *Molecular Microbiology* 60(3): 643-657.

Foster, P. L. (2007). Stress-induced mutagenesis in bacteria. *Critical Reviews in Biochemistry and Molecular Biology* 42(5): 373-397.

Foti, J. J., Devadoss, B., Winkler, J. A., Collins, J. J. and Walker, G. C. (2012). Oxidation of the guanine nucleotide pool underlies cell death by bactericidal antibiotics. *Science* 336(6079): 315-319.

Franzblau, S. G., DeGroote, M. A., Cho, S. H., Andries, K., Nuermberger, E., Orme, I. M., Mdluli, K., Angulo-Barturen, I., Dick, T. and Dartois, V. (2012). Comprehensive analysis of methods used for the evaluation of compounds against *Mycobacterium tuberculosis*. *Tuberculosis* 92(6): 453-488.

Friedberg, E. C., Wagner, R. and Radman, M. (2002). Specialized DNA polymerases, cellular survival, and the genesis of mutations. *Science* 296(5573): 1627-1630.

Fu, L. M. and Fu-Liu, C. S. (2007). The gene expression data of *Mycobacterium tuberculosis* based on Affymetrix gene chips provide insight into regulatory and hypothetical genes. *BMC Microbiology* 7(1): 37.

Gamulin, V., Cetkovic, H. and Ahel, I. (2004). Identification of a promoter motif regulating the major DNA damage response mechanism of *Mycobacterium tuberculosis*. *FEMS Microbiology Letters* 238(1): 57-63.

Gandhi, N. R., Moll, A., Sturm, A. W., Pawinski, R., Govender, T., Lalloo, U., Zeller, K., Andrews, J. and Friedland, G. (2006). Extensively drug-resistant tuberculosis as a cause of death in patients co-infected with tuberculosis and HIV in a rural area of South Africa. *The Lancet* 368(9547): 1575-1580.

Gandotra, S., Schnappinger, D., Monteleone, M., Hillen, W. and Ehrt, S. (2007). *In vivo* gene silencing identifies the *Mycobacterium tuberculosis* proteasome as essential for the bacteria to persist in mice. *Nature Medicine* 13(12): 1515-1520.

García, A., Bocanegra-García, V., Palma-Nicolás, J. P. and Rivera, G. (2012). Recent advances in antitubercular natural products. *European journal of medicinal chemistry* 49: 1-23.

Gebhardt, H., Meniche, X., Tropis, M., Kramer, R., Daffe, M. and Morbach, S. (2007). The key role of the mycolic acid content in the functionality of the cell wall permeability barrier in *Corynebacterineae*. *Microbiology* 153(Pt 5): 1424-1434.

Geiman, D. E., Raghunand, T. R., Agarwal, N. and Bishai, W. R. (2006). Differential gene expression in response to exposure to antimycobacterial agents and other stress conditions among seven *Mycobacterium tuberculosis whiB*-like genes. *Antimicrobial Agents and Chemotherapy* 50(8): 2836-2841.

George, K. M., Yuan, Y., Sherman, D. R. and Barry, C. E. (1995). The biosynthesis of cyclopropanated mycolic acids in *Mycobacterium tuberculosis* Identification and functional analysis of CMAS-2. *Journal of Biological Chemistry* 270(45): 27292-27298.

Glickman, M. S., Cox, J. S. and Jacobs, W. R. (2000). A novel mycolic acid cyclopropane synthetase is required for cording, persistence, and virulence of *Mycobacterium tuberculosis*. *Molecular Cell* 5(4): 717-727.

Godfrey-Faussett, P. and Ayles, H. (2003). Can we control tuberculosis in high HIV prevalence settings? *Tuberculosis* 83(1): 68-76.

Goldman, R. C. (2013). Why are membrane targets discovered by phenotypic screens and genome sequencing in *Mycobacterium tuberculosis*? *Tuberculosis* 93(6): 569-588.

Goldman, R. C. and Scaglione, F. (2004). The macrolide-bacterium interaction and its biological basis. *Current Drug Targets-Infectious Disorders* 4(3): 241-260.

Goodman, M. F. (2002). Error-prone repair DNA polymerases in prokaryotes and eukaryotes. *Annual Review of Biochemistry* 71(1): 17-50.

Gopaul, K. K., Brooks, P. C., Prost, J.-F. and Davis, E. O. (2003). Characterization of the two Mycobacterium tuberculosis recA promoters. *Journal of Bacteriology* 185(20): 6005-6015.

Gordhan, B. G. and Parish, T. (2001). Gene Replacement using Pretreated DNA. *Mycobacterium tuberculosis Protocols*. T. Parish and N. G. Stoker. Otowa, New Jersey, Humana Press: 59-92.

Gorna, A., Bowater, R. and Dziadek, J. (2010). DNA repair systems and the pathogenesis of *Mycobacterium tuberculosis*: varying activities at different stages of infection. *Clinical Science* 119: 187-202.

Grant, S. S., Kaufmann, B. B., Chand, N. S., Haseley, N. and Hung, D. T. (2012). Eradication of bacterial persisters with antibiotic-generated hydroxyl radicals. *Proceedings of the National Academy of Sciences* 109(30): 12147-12152.

Griffin, J. E., Gawronski, J. D., DeJesus, M. A., Ioerger, T. R., Akerley, B. J. and Sassetti, C. M. (2011). High-resolution phenotypic profiling defines genes essential for mycobacterial growth and cholesterol catabolism. *PLoS Pathogens* 7(9): e1002251.

Grogan, D. W. and Cronan, J. E. (1997). Cyclopropane ring formation in membrane lipids of bacteria. *Microbiology and Molecular Biology Reviews* 61(4): 429-441.

Grzegorzewicz, A. E., Pham, H., Gundi, V. A., Scherman, M. S., North, E. J., Hess, T., Jones, V., Gruppo, V., Born, S. E., Kordulakova, J., Chavadi, S. S., Morisseau, C., Lenaerts, A. J., Lee, R. E., McNeil, M. R. and Jackson, M. (2012). Inhibition of mycolic acid transport across the *Mycobacterium tuberculosis* plasma membrane. *Nature Chemical Biology* 8(4): 334-341.

Guo, X. V., Monteleone, M., Klotzsche, M., Kamionka, A., Hillen, W., Braunstein, M., Ehrt, S. and Schnappinger, D. (2007). Silencing essential protein secretion in *Mycobacterium smegmatis* by using tetracycline repressors. *Journal of Bacteriology* 189(13): 4614-4623.

Gupta, R., Barkan, D., Redelman-Sidi, G., Shuman, S. and Glickman, M. S. (2011). Mycobacteria exploit three genetically distinct DNA double-strand break repair pathways. *Molecular Microbiology* 79(2): 316-330.

Gupta, S., Cohen, K. A., Winglee, K., Maiga, M., Diarra, B. and Bishai, W. R. (2014). Efflux inhibition with verapamil potentiates bedaquiline in *Mycobacterium tuberculosis*. *Antimicrobial Agents and Chemotherapy* 58(1): 574-576.

Gutierrez-Lugo, M.-T., Baker, H., Shiloach, J., Boshoff, H. and Bewley, C. A. (2009). Dequalinium, a new inhibitor of *Mycobacterium tuberculosis* mycothiol ligase identified by high-throughput screening. *Journal of Biomolecular Screening* 14(6): 643-652.

Guy, E. S. and Mallampalli, A. (2008). Review: Managing TB in the 21st century: existing and novel drug therapies. *Therapeutic Advances in Respiratory Disease* 2(6): 401-408.

Harding, C. V. and Boom, W. H. (2010). Regulation of antigen presentation by *Mycobacterium tuberculosis*: a role for Toll-like receptors. *Nature Reviews Microbiology* 8(4): 296-307.

Hare, J. M., Bradley, J. A., Lin, C.-l. and Elam, T. J. (2012). Diverse responses to UV light exposure in Acinetobacter include the capacity for DNA damage-induced mutagenesis in the opportunistic pathogens *Acinetobacter baumannii* and *Acinetobacter ursingii*. *Microbiology* 158(Pt 3): 601-611.

Hare, J. M., Perkins, S. N. and Gregg-Jolly, L. A. (2006). A constitutively expressed, truncated *umuDC* operon regulates the *recA*-dependent DNA damage induction of a gene in *Acinetobacter baylyi* strain ADP1. *Applied and Environmental Microbiology* 72(6): 4036-4043.

Hawn, T. R., Matheson, A. I., Maley, S. N. and Vandal, O. (2013). Host-directed therapeutics for tuberculosis: can we harness the host? *Microbiology and Molecular Biology Reviews* 77(4): 608-627.

Hayward, D., Wiid, I. and van Helden, P. (2004). Differential expression of mycothiol pathway genes: Are they affected by antituberculosis drugs? *IUBMB Life* 56(3): 131-138.

Hegde, S. S., Javid-Majd, F. and Blanchard, J. S. (2001). Overexpression and Mechanistic Analysis of Chromosomally Encoded Aminoglycoside 2'-N-Acetyltransferase (AAC (2')-Ic) from *Mycobacterium tuberculosis*. *Journal of Biological Chemistry* 276(49): 45876-45881.

Hernandez-Abanto, S. M., Woolwine, S. C., Jain, S. K. and Bishai, W. (2006). Tetracycline-inducible gene expression in mycobacteria within an animal host using modified Streptomyces tcp830 regulatory elements. *Archives of Microbiology* 186(6): 459-464.

Hernick, M. (2013). Mycothiol: a target for potentiation of rifampin and other antibiotics against *Mycobacterium tuberculosis*.

Hickey, M. J., Arain, T. M., Shawar, R. M., Humble, D. J., Langhorne, M. H., Morgenroth, J. N. and Stover, C. K. (1996). Luciferase *in vivo* expression technology: use of recombinant mycobacterial reporter strains to evaluate antimycobacterial activity in mice. *Antimicrobial Agents and Chemotherapy* 40(2): 400-407.

Hingley-Wilson, S. M., Sambandamurthy, V. K. and Jacobs, W. R. (2003). Survival perspectives from the world's most successful pathogen, *Mycobacterium tuberculosis*. *Nature immunology* 4(10): 949-955.

Ho, S. N., Hunt, H. D., Horton, R. M., Pullen, J. K. and Pease, L. R. (1989). Site-directed mutagenesis by overlap extension using the polymerase chain reaction. *Gene* 77(1): 51-59.

Hoffmann, C., Leis, A., Niederweis, M., Plitzko, J. M. and Engelhardt, H. (2008). Disclosure of the mycobacterial outer membrane: cryo-electron tomography and vitreous sections reveal the lipid bilayer structure. *Proceedings of the National Academy of Sciences* 105(10): 3963-3967.

Hugonnet, J.-E. and Blanchard, J. S. (2007). Irreversible inhibition of the *Mycobacterium tuberculosis* β-lactamase by clavulanate. *Biochemistry* 46(43): 11998-12004.

Hugonnet, J.-E., Tremblay, L. W., Boshoff, H. I., Barry, C. E. and Blanchard, J. S. (2009). Meropenem-clavulanate is effective against extensively drug-resistant *Mycobacterium tuberculosis*. *Science* 323(5918): 1215-1218.

Hutter, B., Fischer, C., Jacobi, A., Schaab, C. and Loferer, H. (2004). Panel of *Bacillus subtilis* reporter strains indicative of various modes of action. *Antimicrobial Agents and Chemotherapy* 48(7): 2588-2594.

Ioerger, T. R., Feng, Y., Ganesula, K., Chen, X., Dobos, K. M., Fortune, S., Jacobs, W. R., Mizrahi, V., Parish, T. and Rubin, E. (2010). Variation among genome sequences of H37Rv strains of *Mycobacterium tuberculosis* from multiple laboratories. *Journal of Bacteriology* 192(14): 3645-3653.

Ioerger, T. R., O'Malley, T., Liao, R., Guinn, K. M., Hickey, M. J., Mohaideen, N., Murphy, K. C., Boshoff, H. I., Mizrahi, V. and Rubin, E. J. (2013). Identification of new drug targets and resistance mechanisms in *Mycobacterium tuberculosis*. *PloS One* 8(9): e75245.

Jackson, M. (2014). The Mycobacterial Cell Envelope—Lipids. *Cold Spring Harbor Perspectives in Medicine*: a021105.

Janin, Y. L. (2007). Antituberculosis drugs: ten years of research. *Bioorganic & Medicinal Chemistry* 15(7): 2479-2513.

Janion, C. (2008). Inducible SOS response system of DNA repair and mutagenesis in *Escherichia coli*. *International Journal of Biological Sciences* 4(6): 338.

Jap, B. K. and Walian, P. J. (1996). Structure and functional mechanism of porins. *Physiological Reviews* 76(4): 1073-1088.

Jarlier, V. and Nikaido, H. (1990). Permeability barrier to hydrophilic solutes in *Mycobacterium chelonei*. *Journal of Bacteriology* 172(3): 1418-1423.

Jarosz, D. F., Godoy, V. G. and Walker, G. C. (2007). Proficient and accurate bypass of persistent DNA lesions by DinB DNA polymerases. *Cell Cycle* 6(7): 817-822.

Jawahar, M. (2004). Current trends in chemotherapy of tuberculosis. *Indian Journal of Medical Research* 120(Oct): 398-417.

Jothivasan, V. K. and Hamilton, C. J. (2008). Mycothiol: synthesis, biosynthesis and biological functions of the major low molecular weight thiol in actinomycetes. *Natural Product Reports* 25(6): 1091-1117.

Kammann, M., Laufs, J. r., Schell, J. and Gronenborn, B. (1989). Rapid insertional mutagenesis of DNA by polymerase chain reaction (PCR). *Nucleic Acids Research* 17(13): 5404.

Keren, I., Wu, Y., Inocencio, J., Mulcahy, L. R. and Lewis, K. (2013). Killing by bactericidal antibiotics does not depend on reactive oxygen species. *Science* 339(6124): 1213-1216.

Klotzsche, M., Ehrt, S. and Schnappinger, D. (2009). Improved tetracycline repressors for gene silencing in mycobacteria. *Nucleic Acids Research* 37(6): 1778-1788.

Koch, A., Mizrahi, V. and Warner, D. F. (2014). The impact of drug resistance on *Mycobacterium tuberculosis* physiology: what can we learn from rifampicin? *Emerging Microbes & Infections* 3(3): e17.

Kohanski, M. A., Dwyer, D. J., Hayete, B., Lawrence, C. A. and Collins, J. J. (2007). A common mechanism of cellular death induced by bactericidal antibiotics. *Cell* 130(5): 797-810.

Korkegian, A., Roberts, D. M., Blair, R. and Parish, T. (2014). Mutations in the essential arabinosyltransferase EmbC lead to alterations in *Mycobacterium tuberculosis* lipoarabinomannan. *Journal of Biological Chemistry* 289(51): 35172-35181.

Lambert, P. A. (2002). Cellular impermeability and uptake of biocides and antibiotics in gram-positive bacteria and mycobacteria. *Symp Ser Soc Appl Microbiol*(31): 46S-54S.

Larsen, M. H. (2000). Appendix 1. *Molecular Genetics of Mycobacteria*. G. F. Hatfull and W. R. Jacobs, Jr. Washington, D.C., ASM Press. : 313-320.

Lawn, S. D., Meintjes, G., McIlleron, H., Harries, A. D. and Wood, R. (2013). Management of HIV-associated tuberculosis in resource-limited settings: a state-of-the-art review. *BMC Medicine* 11(1): 253.

Lechartier, B., Rybniker, J., Zumla, A. and Cole, S. T. (2014). Tuberculosis drug discovery in the post-post-genomic era. *EMBO Molecular Medicine*.

Lee, R. E., Hurdle, J. G., Liu, J., Bruhn, D. F., Matt, T., Scherman, M. S., Vaddady, P. K., Zheng, Z., Qi, J. and Akbergenov, R. (2014). Spectinamides: a new class of semisynthetic antituberculosis agents that overcome native drug efflux. *Nature Medicine* 20(2): 152-158.

Lemassu, A., Ortalo-Magne, A., Bardou, F., Silve, G., Laneelle, M. A. and Daffe, M. (1996). Extracellular and surface-exposed polysaccharides of non-tuberculous mycobacteria. *Microbiology* 142 (Pt 6): 1513-1520.

Lewis, K. (2013). Platforms for antibiotic discovery. *Nature Reviews Drug Discovery* 12(5): 371-387.

Li, X.-Z. and Nikaido, H. (2009). Efflux-mediated drug resistance in bacteria. *Drugs* 69(12): 1555-1623.

Lienhardt, C., Glaziou, P., Uplekar, M. and LÃ, K. (2012). Global tuberculosis control: lessons learnt and future prospects. *Nature Reviews Microbiology* 10(6): 407-416.

Ling, L. L., Schneider, T., Peoples, A. J., Spoering, A. L., Engels, I., Conlon, B. P., Mueller, A., Schäberle, T. F., Hughes, D. E. and Epstein, S. (2015). A new antibiotic kills pathogens without detectable resistance. *Nature* 517(7535): 455-459.

Lipinski, C. A., Lombardo, F., Dominy, B. W. and Feeney, P. J. (2012). Experimental and computational approaches to estimate solubility and permeability in drug discovery and development settings. *Advanced Drug Delivery Reviews* 64: 4-17.

Liu, J., Barry, C. E., 3rd, Besra, G. S. and Nikaido, H. (1996). Mycolic acid structure determines the fluidity of the mycobacterial cell wall. *Journal of Biological Chemistry* 271(47): 29545-29551.

Liu, J. and Nikaido, H. (1999). A mutant of *Mycobacterium smegmatis* defective in the biosynthesis of mycolic acids accumulates meromycolates. *Proceedings of the National Academy of Sciences* 96(7): 4011-4016.

Liu, M., Hanks, T. S., Zhang, J., McClure, M. J., Siemsen, D. W., Elser, J. L., Quinn, M. T. and Lei, B. (2006). Defects in *ex vivo* and *in vivo* growth and sensitivity to osmotic stress of group A Streptococcus caused by interruption of response regulator gene *vicR*. *Microbiology* 152(4): 967-978.

Liu, Y. and Imlay, J. A. (2013). Cell death from antibiotics without the involvement of reactive oxygen species. *Science* 339(6124): 1210-1213.

Louw, G. E., Warren, R. M., Gey van Pittius, N. C., Leon, R., Jimenez, A., Hernandez-Pando, R., McEvoy, C. R., Grobbelaar, M., Murray, M. and van Helden, P. D. (2011). Rifampicin reduces susceptibility to ofloxacin in rifampicin-resistant *Mycobacterium tuberculosis* through efflux. *American Journal of Respiratory and Critical Care Medicine* 184(2): 269-276.

Louw, G. E., Warren, R. M., Gey van Pittius, N. C., McEvoy, C. R., Van Helden, P. D. and Victor, T. C. (2009). A balancing act: efflux/influx in mycobacterial drug resistance. *Antimicrob Agents Chemother* 53(8): 3181-3189.

Machowski, E. E., Barichievy, S., Springer, B., Durbach, S. I. and Mizrahi, V. (2007). In vitro analysis of rates and spectra of mutations in a polymorphic region of the Rv0746 PE_PGRS gene of *Mycobacterium tuberculosis*. *Journal of Bacteriology* 189(5): 2190-2195.

Mah, N., Perez-Iratxeta, C. and Andrade-Navarro, M. A. (2010). Outer membrane pore protein prediction in mycobacteria using genomic comparison. *Microbiology* 156(8): 2506-2515.

Malik, M., Zhao, X. and Drlica, K. (2006). Lethal fragmentation of bacterial chromosomes mediated by DNA gyrase and quinolones. *Molecular Microbiology* 61(3): 810-825.

Manjunatha, U. H., Boshoff, H., Dowd, C. S., Zhang, L., Albert, T. J., Norton, J. E., Daniels, L., Dick, T., Pang, S. S. and Barry, C. E. (2006). Identification of a nitroimidazo-oxazine-specific protein involved in PA-824 resistance in *Mycobacterium tuberculosis*. *Proceedings of the National Academy of Sciences of the United States of America* 103(2): 431-436.

Manjunatha, U. H. and Smith, P. W. (2014). Perspective: Challenges and Opportunities in TB drug discovery from phenotypic screening. *Bioorganic & Medicinal Chemistry*.

Martin, P. K., Li, T., Sun, D., Biek, D. P. and Schmid, M. B. (1999). Role in cell permeability of an essential two-component system in *Staphylococcus aureus*. *Journal of Bacteriology* 181(12): 3666-3673.

Mazloum, N., Stegman, M. A., Croteau, D. L., Van Houten, B., Kwon, N. S., Ling, Y., Dickinson, C., Venugopal, A., Towheed, M. A. and Nathan, C. (2011). Identification of a chemical that inhibits the mycobacterial UvrABC complex in nucleotide excision repair. *Biochemistry* 50(8): 1329-1335.

McGillivray, A., Golden, N. A. and Kaushal, D. (2014). The *Mycobacterium tuberculosis* Clp gene regulator is required for *in-vitro* reactivation from hypoxia-induced dormancy. *Journal of Biological Chemistry*: jbc. M114. 615534.

McMurry, L., Petrucci, R. E. and Levy, S. B. (1980). Active efflux of tetracycline encoded by four genetically different tetracycline resistance determinants in *Escherichia coli*. *Proceedings of the National Academy of Sciences* 77(7): 3974-3977.

Mdluli, K., Kaneko, T. and Upton, A. (2014). Tuberculosis drug discovery and emerging targets. *Annals of the New York Academy of Sciences* 1323(1): 56-75.

Mehra, S., Dutta, N. K., Mollenkopf, H.-J. and Kaushal, D. (2010). *Mycobacterium tuberculosis* MT2816 encodes a key stress-response regulator. *Journal of Infectious Diseases* 202(6): 943-953.

Meighen, E. A. (1991). Molecular biology of bacterial bioluminescence. *Microbiological Reviews* 55(1): 123-142.

Miller, C., Thomsen, L. E., Gaggero, C., Mosseri, R., Ingmer, H. and Cohen, S. N. (2004). SOS response induction by ß-lactams and bacterial defense against antibiotic lethality. *Science* 305(5690): 1629-1631.

Minch, K. J., Rustad, T. R., Peterson, E. J., Winkler, J., Reiss, D. J., Ma, S., Hickey, M., Brabant, W., Morrison, B. and Turkarslan, S. (2015). The DNA-binding network of *Mycobacterium tuberculosis*. *Nature Communications* 6.

Minnikin, D. E. (1982). Lipids: complex lipids, their chemistry, biosynthesis and roles. *The Biology of the Mycobacteria* 1: 95-184.

Mizrahi, V. and Andersen, S. J. (1998). DNA repair in *Mycobacterium tuberculosis*. What have we learnt from the genome sequence? *Molecular Microbiology* 29(6): 1331-1339.

Möker, N., Brocker, M., Schaffer, S., Krämer, R., Morbach, S. and Bott, M. (2004). Deletion of the genes encoding the MtrA–MtrB two-component system of *Corynebacterium glutamicum* has a strong influence on cell morphology, antibiotics susceptibility and expression of genes involved in osmoprotection. *Molecular Microbiology* 54(2): 420-438.

Morris, R. P., Nguyen, L., Gatfield, J., Visconti, K., Nguyen, K., Schnappinger, D., Ehrt, S., Liu, Y., Heifets, L. and Pieters, J. (2005). Ancestral antibiotic resistance in *Mycobacterium tuberculosis*. *Proceedings of the National Academy of Sciences of the United States of America* 102(34): 12200-12205.

Motiwala, A. S., Dai, Y., Jones-López, E. C., Hwang, S.-H., Lee, J. S., Cho, S. N., Via, L. E., Barry, C. E. and Alland, D. (2010). Mutations in extensively drug-resistant *Mycobacterium tuberculosis* that do not code for known drug-resistance mechanisms. *Journal of Infectious Diseases* 201(6): 881-888.

Movahedzadeh, F., Wheeler, P. R., Dinadayala, P., Av-Gay, Y., Parish, T., Daffé, M. and Stoker, N. G. (2010). Inositol monophosphate phosphatase genes of *Mycobacterium tuberculosis*. *BMC Microbiology* 10(1): 50.

Nagamachi, E., Shibuya, S. i., Hirai, Y., Matsushita, O., Tomochika, K. i. and Kanemasa, Y. (1991). Adaptational changes of fatty acid composition and the physical state of membrane lipids following the change of growth temperature in *Yersinia enterocolitica*. *Microbiology and Immunology* 35(12): 1085-1093.

Newman, D. J., Cragg, G. M. and Snader, K. M. (2003). Natural products as sources of new drugs over the period 1981-2002. *Journal of Natural Products* 66(7): 1022-1037.

NewTBDrugs.org (2015). Working Group On New TB Drugs. from http://www.newtbdrugs.org/pipeline.php.

Newton, G. L., Buchmeier, N. and Fahey, R. C. (2008). Biosynthesis and functions of mycothiol, the unique protective thiol of Actinobacteria. *Microbiology and Molecular Biology Reviews* 72(3): 471-494.

Newton, G. L., Buchmeier, N., La Clair, J. J. and Fahey, R. C. (2011). Evaluation of NTF1836 as an inhibitor of the mycothiol biosynthetic enzyme MshC in growing and non-replicating *Mycobacterium tuberculosis*. *Bioorganic & Medicinal Chemistry* 19(13): 3956-3964.

Newton, G. L., Ta, P., Bzymek, K. P. and Fahey, R. C. (2006). Biochemistry of the initial steps of mycothiol biosynthesis. *Journal of Biological Chemistry* 281(45): 33910-33920.

Newton, G. L., Ta, P. and Fahey, R. C. (2005). A mycothiol synthase mutant of *Mycobacterium smegmatis* produces novel thiols and has an altered thiol redox status. *Journal of Bacteriology* 187(21): 7309-7316.

Nguyen, H. T., Wolff, K. A., Cartabuke, R. H., Ogwang, S. and Nguyen, L. (2010). A lipoprotein modulates activity of the MtrAB two-component system to provide intrinsic multidrug resistance, cytokinetic control and cell wall homeostasis in *Mycobacterium*. *Molecular Microbiology* 76(2): 348-364.

Nguyen, L. and Thompson, C. J. (2006). Foundations of antibiotic resistance in bacterial physiology: the mycobacterial paradigm. *Trends in Microbiology* 14(7): 304-312.

Niederweis, M., Danilchanka, O., Huff, J., Hoffmann, C. and Engelhardt, H. (2010). Mycobacterial outer membranes: in search of proteins. *Trends in Microbiology* 18(3): 109-116.

Niederweis, M., Ehrt, S., Heinz, C., KloÈcker, U., Karosi, S., Swiderek, K. M., Riley, L. W. and Benz, R. (1999). Cloning of the *mspA* gene encoding a porin from *Mycobacterium smegmatis*. *Molecular Microbiology* 33(5): 933-945.

Nikaido, H. (1994). Prevention of drug access to bacterial targets: permeability barriers and active efflux. *Science* 264(5157): 382-388.

Nohmi, T. (2006). Environmental stress and lesion-bypass DNA polymerases. *Annual Review of Microbiology* 60: 231-253.

Noll, D. M., Mason, T. M. and Miller, P. S. (2006). Formation and repair of interstrand cross-links in DNA. *Chemical Reviews* 106(2): 277-301.

O'sullivan, D., Hinds, J., Butcher, P., Gillespie, S. and McHugh, T. (2008). *Mycobacterium tuberculosi*s DNA repair in response to subinhibitory concentrations of ciprofloxacin. *Journal of Antimicrobial Chemotherapy* 62(6): 1199-1202.

Odds, F. (2003). Synergy, antagonism, and what the chequerboard puts between them. *Journal of Antimicrobial Chemotherapy* 52(1): 1-1.

Ortalo-Magne, A., Dupont, M. A., Lemassu, A., Andersen, A. B., Gounon, P. and Daffe, M. (1995). Molecular composition of the outermost capsular material of the tubercle bacillus. *Microbiology* 141 (Pt 7): 1609-1620.

Parish, T. and Stoker, N. G. (2000). Use of a flexible cassette method to generate a double unmarked *Mycobacterium tuberculosis tlyA plcABC* mutant by gene replacement. *Microbiology* 146(8): 1969-1975.

Park, S. W., Casalena, D. E., Wilson, D. J., Dai, R., Nag, P. P., Liu, F., Boyce, J. P., Bittker, J. A., Schreiber, S. L. and Finzel, B. C. (2014). Target-Based Identification of Whole-Cell Active Inhibitors of Biotin Biosynthesis in *Mycobacterium tuberculosis*. *Chemistry & Biology*.

Patel, M. P. and Blanchard, J. S. (2001). *Mycobacterium tuberculosis* mycothione reductase: pH dependence of the kinetic parameters and kinetic isotope effects. *Biochemistry* 40(17): 5119-5126.

Payne, D. J., Gwynn, M. N., Holmes, D. J. and Pompliano, D. L. (2006). Drugs for bad bugs: confronting the challenges of antibacterial discovery. *Nature Reviews Drug Discovery* 6(1): 29-40.

Pennington, J. M. and Rosenberg, S. M. (2007). Spontaneous DNA breakage in single living *Escherichia coli* cells. *Nature Genetics* 39(6): 797-802.

Pepper, D. J., Meintjes, G. A., McIlleron, H. and Wilkinson, R. J. (2007). Combined therapy for tuberculosis and HIV-1: the challenge for drug discovery. *Drug Discovery Today* 12(21): 980-989.

Philalay, J. S., Palermo, C. O., Hauge, K. A., Rustad, T. R. and Cangelosi, G. A. (2004). Genes required for intrinsic multidrug resistance in *Mycobacterium avium*. *Antimicrobial Agents and Chemotherapy* 48(9): 3412-3418.

Philips, J. A. and Ernst, J. D. (2012). Tuberculosis pathogenesis and immunity. *Annual Review of Pathology: Mechanisms of Disease* 7: 353-384.

Piddock, L. J. (2006). Multidrug-resistance efflux pumps? not just for resistance. *Nature Reviews Microbiology* 4(8): 629-636.

Puech, V., Chami, M., Lemassu, A., Lanéelle, M.-A., Schiffler, B., Gounon, P., Bayan, N., Benz, R. and Daffé, M. (2001). Structure of the cell envelope of corynebacteria: importance of the non-covalently bound lipids in the formation of the cell wall permeability barrier and fracture plane. *Microbiology* 147(5): 1365-1382.

Pujals, S., Fernández-Carneado, J., López-Iglesias, C., Kogan, M. J. and Giralt, E. (2006). Mechanistic aspects of CPP-mediated intracellular drug delivery: relevance of CPP self-assembly. *Biochimica et Biophysica Acta (BBA)-Biomembranes* 1758(3): 264-279.

Radman, M. (1974). Phenomenology of an inducible mutagenic DNA repair pathway in *Escherichia coli*: SOS repair hypothesis. *Molecular and environmental aspects of mutagenesis*.

Ramon-Garcia, S., Ng, C., Anderson, H., Chao, J. D., Zheng, X., Pfeifer, T., Av-Gay, Y., Roberge, M. and Thompson, C. J. (2011). Synergistic drug combinations for tuberculosis therapy identified by a novel high-throughput screen. *Antimicrob Agents Chemother* 55(8): 3861-3869.

Ramón-García, S., Ng, C., Anderson, H., Chao, J. D., Zheng, X., Pfeifer, T., Av-Gay, Y., Roberge, M. and Thompson, C. J. (2011). Synergistic drug combinations for tuberculosis therapy identified by a novel high-throughput screen. *Antimicrobial Agents and Chemotherapy* 55(8): 3861-3869.

Rand, L., Hinds, J., Springer, B., Sander, P., Buxton, R. S. and Davis, E. O. (2003). The majority of inducible DNA repair genes in *Mycobacterium tuberculosis* are induced independently of RecA. *Molecular Microbiology* 50(3): 1031-1042.

Rastogi, N., Hellio, R. and David, H. L. (1991). A new insight into the mycobacterial cell envelope architecture by the localization of antigens in ultrathin sections. *Zentralblatt für Bakteriologie* 275(3): 287-302.

Rauch, P. J., Palmen, R., Burds, A. A., Gregg-Jolly, L. A., van der Zee, J. R. and Hellingwerf, K. J. (1996). The expression of the *Acinetobacter calcoaceticus recA* gene increases in response to DNA damage independently of RecA and of development of competence for natural transformation. *Microbiology* 142(4): 1025-1032.

Rawat, M. and Av-Gay, Y. (2007). Mycothiol-dependent proteins in actinomycetes. *FEMS Microbiology Reviews* 31(3): 278-292.

Rawat, M., Newton, G. L., Ko, M., Martinez, G. J., Fahey, R. C. and Av-Gay, Y. (2002). Mycothiol-deficient *Mycobacterium smegmatis* mutants are hypersensitive to alkylating agents, free radicals, and antibiotics. *Antimicrobial Agents and Chemotherapy* 46(11): 3348-3355.

Rawat, R., Whitty, A. and Tonge, P. J. (2003). The isoniazid-NAD adduct is a slow, tight-binding inhibitor of InhA, the *Mycobacterium tuberculosis* enoyl reductase: adduct affinity and drug resistance. *Proceedings of the National Academy of Sciences* 100(24): 13881-13886.

Raynaud, C., Papavinasasundaram, K., Speight, R. A., Springer, B., Sander, P., Böttger, E. C., Colston, M. J. and Draper, P. (2002). The functions of OmpATb, a pore-forming protein of *Mycobacterium tuberculosis*. *Molecular Microbiology* 46(1): 191-201.

Reed, M. B., Gagneux, S., DeRiemer, K., Small, P. M. and Barry, C. E. (2007). The W-Beijing lineage of *Mycobacterium tuberculosis* overproduces triglycerides and has the DosR dormancy regulon constitutively upregulated. *Journal of Bacteriology* 189(7): 2583-2589.

Rosche, W. A. and Foster, P. L. (2000). Determining mutation rates in bacterial populations. *Methods* 20(1): 4-17.

Rustad, T. R., Minch, K. J., Ma, S., Winkler, J. K., Hobbs, S., Hickey, M., Brabant, W., Turkarslan, S., Price, N. D. and Baliga, N. S. (2014). Mapping and manipulating the *Mycobacterium tuberculosis* transcriptome using a transcription factor overexpression-derived regulatory network. *Genome Biology* 15(11): 502.

Safi, H., Lingaraju, S., Amin, A., Kim, S., Jones, M., Holmes, M., McNeil, M., Peterson, S. N., Chatterjee, D. and Fleischmann, R. (2013). Evolution of high-level ethambutol-resistant tuberculosis through interacting mutations in decaprenylphosphoryl-[beta]-D-arabinose biosynthetic and utilization pathway genes. *Nature Genetics* 45(10): 1190-1197.

Sambrook, J., Fritsch, E. and Maniatis, T. (1989). Molecular cloning: a laboratory manual, Cold Spring Laboratory. *Cold Spring Harbor, NY. VIII. Appendix A. pBIND Vector Sequence (continued) A. pBIND Vector Sequence (continued) B. pBIND Vector Restriction Sites Enzyme# of Sites Location Dra I* 4(1857): 4877.

Sambrook, J. and Russell, D. (2001). Molecular Cloning: A Laboratory Manual 2001 3rd edn Cold Spring Harbor. *NY Cold Spring Harbor Laboratory*.

Sandgren, A., Strong, M., Muthukrishnan, P., Weiner, B. K., Church, G. M. and Murray, M. B. (2009). Tuberculosis drug resistance mutation database. *PLoS medicine* 6(2): e1000002.

Sani, M., Houben, E. N., Geurtsen, J., Pierson, J., de Punder, K., van Zon, M., Wever, B., Piersma, S. R., Jimenez, C. R., Daffe, M., Appelmelk, B. J., Bitter, W., van der Wel, N. and Peters, P. J. (2010). Direct visualization by cryo-EM of the mycobacterial capsular layer: a labile structure containing ESX-1-secreted proteins. *PLoS Pathog* 6(3): e1000794.

Sarathy, J. P., Dartois, V. and Lee, E. J. D. (2012). The Role of Transport Mechanisms in *Mycobacterium Tuberculosis* Drug Resistance and Tolerance. *Pharmaceuticals* 5(11): 1210-1235.

Sarathy, J. P., Lee, E. and Dartois, V. (2013). Polyamines inhibit porin-mediated fluoroquinolone uptake in mycobacteria. *PloS One* 8(6): e65806.

Sareen, D., Newton, G. L., Fahey, R. C. and Buchmeier, N. A. (2003). Mycothiol is essential for growth of *Mycobacterium tuberculosis* Erdman. *Journal of Bacteriology* 185(22): 6736-6740.

Sassetti, C. M., Boyd, D. H. and Rubin, E. J. (2003). Genes required for mycobacterial growth defined by high density mutagenesis. *Molecular Microbiology* 48(1): 77-84.

Schnappinger, D., Ehrt, S., Voskuil, M. I., Liu, Y., Mangan, J. A., Monahan, I. M., Dolganov, G., Efron, B., Butcher, P. D. and Nathan, C. (2003). Transcriptional adaptation of *Mycobacterium tuberculosis* within macrophages insights into the phagosomal environment. *The Journal of experimental medicine* 198(5): 693-704.

Schwartz, J., Todd, E., Abernethy, D. and Mitchell, J. (1986). Steady state verapamil tissue distribution in the dog: differing tissue accumulation. *Pharmacology* 32(6): 307-312.

Scorpio, A., Lindholm-Levy, P., Heifets, L., Gilman, R., Siddiqi, S., Cynamon, M. and Zhang, Y. (1997). Characterization of *pncA* mutations in pyrazinamide-resistant *Mycobacterium tuberculosis*. *Antimicrobial Agents and Chemotherapy* 41(3): 540-543.

Senadheera, M. D., Lee, A. W., Hung, D. C., Spatafora, G. A., Goodman, S. D. and Cvitkovitch, D. G. (2007). The Streptococcus mutans *vicX* gene product modulates *gtfB/C* expression, biofilm

formation, genetic competence, and oxidative stress tolerance. *Journal of Bacteriology* 189(4): 1451-1458.

Senaratne, R. H., Mobasheri, H., Papavinasasundaram, K., Jenner, P., Lea, E. J. and Draper, P. (1998). Expression of a Gene for a Porin-Like Protein of the OmpA Family from *Mycobacterium tuberculosis* H37Rv. *Journal of Bacteriology* 180(14): 3541-3547.

Sharma, S., Gelman, E., Narayan, C., Bhattacharjee, D., Achar, V., Humnabadkar, V., Balasubramanian, V., Ramachandran, V., Dhar, N. and Dinesh, N. (2014). Simple and Rapid Method To Determine Antimycobacterial Potency of Compounds by Using Autoluminescent *Mycobacterium tuberculosis*. *Antimicrobial Agents and Chemotherapy* 58(10): 5801-5808.

Sharma, S., Kumar, M., Sharma, S., Nargotra, A., Koul, S. and Khan, I. A. (2010). Piperine as an inhibitor of Rv1258c, a putative multidrug efflux pump of *Mycobacterium tuberculosis*. *Journal of Antimicrobial Chemotherapy*: dkq186.

Sharma, S., Mohan, A. and Kadhiravan, T. (2005). HIV-TB co-infection: epidemiology, diagnosis & management. *Indian Journal of Medical Research* 121(4): 550-567.

Sherrid, A. M., Rustad, T. R., Cangelosi, G. A. and Sherman, D. R. (2010). Characterization of a Clp protease gene regulator and the reaeration response in *Mycobacterium tuberculosis*. *PloS One* 5(7): e11622.

Siddiqi, N., Das, R., Pathak, N., Banerjee, S., Ahmed, N., Katoch, V. and Hasnain, S. (2004). *Mycobacterium tuberculosis* isolate with a distinct genomic identity overexpresses a tap-like efflux pump. *Infection* 32(2): 109-111.

Singh, A., Crossman, D. K., Mai, D., Guidry, L., Voskuil, M. I., Renfrow, M. B. and Steyn, A. J. (2009). *Mycobacterium tuberculosis* WhiB3 maintains redox homeostasis by regulating virulence lipid anabolism to modulate macrophage response. *PLoS Pathogens* 5(8): e1000545.

Singh, J. A., Upshur, R. and Padayatchi, N. (2007). XDR-TB in South Africa: no time for denial or complacency. *PLoS medicine* 4(1): e50.

Singh, K., Kumar, M., Pavadai, E., Naran, K., Warner, D. F., Ruminski, P. G. and Chibale, K. (2014a). Synthesis of new verapamil analogues and their evaluation in combination with rifampicin against *Mycobacterium tuberculosis* and molecular docking studies in the binding site of efflux protein Rv1258c. *Bioorganic & Medicinal Chemistry letters* 24(14): 2985-2990.

Singh, V., Biswas, R. K. and Singh, B. N. (2014b). Double Recombinant *Mycobacterium bovis* BCG Strain for Screening of Primary and Rationale-Based Antimycobacterial Compounds. *Antimicrobial Agents and Chemotherapy* 58(3): 1389-1396.

Singh, V., Brecik, M., Mukherjee, R., Evans, J. C., Svetlíková, Z., Blaško, J., Surade, S., Blackburn, J., Warner, D. F. and Mikušová, K. (2014c). The Complex Mechanism of Antimycobacterial Action of 5-Fluorouracil. *Chemistry & Biology*.

Slilaty, S. N. and Little, J. W. (1987). Lysine-156 and serine-119 are required for LexA repressor cleavage: a possible mechanism. *Proceedings of the National Academy of Sciences* 84(12): 3987-3991.

Smollett, K. L., Smith, K. M., Kahramanoglou, C., Arnvig, K. B., Buxton, R. S. and Davis, E. O. (2012). Global analysis of the regulon of the transcriptional repressor LexA, a key component of SOS response in *Mycobacterium tuberculosis*. *Journal of Biological Chemistry* 287(26): 22004-22014.

Snapper, S., Melton, R., Mustafa, S., Kieser, T. and WR Jr, J. (1990). Isolation and characterization of efficient plasmid transformation mutants of *Mycobacterium smegmatis*. *Molecular Microbiology* 4(11): 1911-1919.

Solans, C., Bregante, M., Aramayona, J., Fraile, L. and Garcia, M. (2000). Comparison of the pharmacokinetics of verapamil in the pregnant and non-pregnant rabbit: study of maternal and foetal tissue levels. *Xenobiotica* 30(1): 93-102.

Song, H., Huff, J., Janik, K., Walter, K., Keller, C., Ehlers, S., Bossmann, S. H. and Niederweis, M. (2011). Expression of the ompATb operon accelerates ammonia secretion and adaptation of *Mycobacterium tuberculosis* to acidic environments. *Molecular Microbiology* 80(4): 900-918.

Song, H., Sandie, R., Wang, Y., Andrade-Navarro, M. A. and Niederweis, M. (2008). Identification of outer membrane proteins of *Mycobacterium tuberculosis*. *Tuberculosis* 88(6): 526-544.

Sparr, C., Purkayastha, N., Kolesinska, B., Gengenbacher, M., Amulic, B., Matuschewski, K., Seebach, D. and Kamena, F. (2013). Improved efficacy of fosmidomycin against Plasmodium and Mycobacterium species by combination with the cell-penetrating peptide octaarginine. *Antimicrobial Agents and Chemotherapy* 57(10): 4689-4698.

Stahl, C., Kubetzko, S., Kaps, I., Seeber, S., Engelhardt, H. and Niederweis, M. (2001). MspA provides the main hydrophilic pathway through the cell wall of *Mycobacterium smegmatis*. *Molecular Microbiology* 40(2): 451-464.

Stallings, C. L. and Glickman, M. S. (2010). Is *Mycobacterium tuberculosis* stressed out? A critical assessment of the genetic evidence. *Microbes and Infection* 12(14): 1091-1101.

Starks, A. M., Gumusboga, A., Plikaytis, B. B., Shinnick, T. M. and Posey, J. E. (2009). Mutations at *embB* codon 306 are an important molecular indicator of ethambutol resistance in *Mycobacterium tuberculosi*s. *Antimicrobial Agents and Chemotherapy* 53(3): 1061-1066.

Stephan, J., Mailaender, C., Etienne, G., Daffé, M. and Niederweis, M. (2004). Multidrug resistance of a porin deletion mutant of *Mycobacterium smegmatis*. *Antimicrobial Agents and Chemotherapy* 48(11): 4163-4170.

Sun, R., Converse, P. J., Ko, C., Tyagi, S., Morrison, N. E. and Bishai, W. R. (2004). *Mycobacterium tuberculosis* ECF sigma factor sigC is required for lethality in mice and for the conditional expression of a defined gene set. *Molecular Microbiology* 52(1): 25-38.

Szumowski, J. D., Adams, K. N., Edelstein, P. H. and Ramakrishnan, L. (2013). Antimicrobial Efflux Pumps and *Mycobacterium Tuberculosis* Drug Tolerance: Evolutionary Considerations. *Pathogenesis of Mycobacterium tuberculosis and its Interaction with the Host Organism*, Springer: 81-108.

Tabor, C. W. and Tabor, H. (1985). Polyamines in microorganisms. *Microbiological Reviews* 49(1): 81.

Takiff, H. E., Salazar, L., Guerrero, C., Philipp, W., Huang, W. M., Kreiswirth, B., Cole, S. T., Jacobs, W. R. and Telenti, A. (1994). Cloning and nucleotide sequence of *Mycobacterium tuberculosis gyrA* and *gyrB* genes and detection of quinolone resistance mutations. *Antimicrobial Agents and Chemotherapy* 38(4): 773-780.

Tameris, M. D., Hatherill, M., Landry, B. S., Scriba, T. J., Snowden, M. A., Lockhart, S., Shea, J. E., McClain, J. B., Hussey, G. D. and Hanekom, W. A. (2013). Safety and efficacy of MVA85A, a new tuberculosis vaccine, in infants previously vaccinated with BCG: a randomised, placebo-controlled phase 2b trial. *The Lancet* 381(9871): 1021-1028.

Tanaka, Y., Yazawa, K., Dabbs, E. R., Nishikawa, K., Komaki, H., Mikami, Y., Miyaji, M., Morisaki, N. and Iwasaki, S. (1996). Different rifampicin inactivation mechanisms in Nocardia and related taxa. *Microbiology and Immunology* 40(1): 1-4.

Tarcsay, A. k. and Keserű, G. r. M. (2013). Contributions of Molecular Properties to Drug Promiscuity: Miniperspective. *Journal of medicinal chemistry* 56(5): 1789-1795.

Telenti, A., Imboden, P., Marchesi, F., Matter, L., Schopfer, K., Bodmer, T., Lowrie, D., Colston, M. and Cole, S. (1993). Detection of rifampicin-resistance mutations in *Mycobacterium tuberculosis*. *The Lancet* 341(8846): 647-651.

Teriete, P., Yao, Y., Kolodzik, A., Yu, J., Song, H., Niederweis, M. and Marassi, F. M. (2010). *Mycobacterium tuberculosis* Rv0899 adopts a mixed α/β-structure and does not form a transmembrane β-barrel. *Biochemistry* 49(13): 2768-2777.

Tomasz, M. (1995). Mitomycin C: small, fast and deadly (but very selective). *Chemistry & Biology* 2(9): 575-579.

Trauner, A., Borrell, S., Reither, K. and Gagneux, S. (2014). Evolution of drug resistance in tuberculosis: recent progress and implications for diagnosis and therapy. *Drugs* 74(10): 1063-1072.

Trias, J., Jarlier, V. and Benz, R. (1992). Porins in the cell wall of mycobacteria. *Science* 258(5087): 1479-1481.

Trunz, B. B., Fine, P. and Dye, C. (2006). Effect of BCG vaccination on childhood tuberculous meningitis and miliary tuberculosis worldwide: a meta-analysis and assessment of cost-effectiveness. *The Lancet* 367(9517): 1173-1180.

Tyagi, R., Lai, R. and Duggleby, R. G. (2004). A new approach to'megaprimer'polymerase chain reaction mutagenesis without an intermediate gel purification step. *BMC Biotechnology* 4(1): 2.

van Helden, P. D., Donald, P. R., Victor, T. C., Schaaf, H. S., Hoal, E. G., Walzl, G. and Warren, R. M. (2006). Antimicrobial resistance in tuberculosis: an international perspective.

Veber, D. F., Johnson, S. R., Cheng, H.-Y., Smith, B. R., Ward, K. W. and Kopple, K. D. (2002). Molecular properties that influence the oral bioavailability of drug candidates. *Journal of medicinal chemistry* 45(12): 2615-2623.

Vetting, M., Roderick, S., Hegde, S., Magnet, S. and Blanchard, J. (2003). What can structure tell us about in vivo function? The case of aminoglycoside-resistance genes. *Biochemical Society Transactions* 31(3): 520-522.

Vilchèze, C., Av-Gay, Y., Barnes, S. W., Larsen, M. H., Walker, J. R., Glynne, R. J. and Jacobs, W. R. (2011). Coresistance to isoniazid and ethionamide maps to mycothiol biosynthetic genes in *Mycobacterium bovis*. *Antimicrobial Agents and Chemotherapy* 55(9): 4422-4423.

Vilchèze, C., Av-Gay, Y., Attarian, R., Liu, Z., Hazbón, M. H., Colangeli, R., Chen, B., Liu, W., Alland, D. and Sacchettini, J. C. (2008). Mycothiol biosynthesis is essential for ethionamide susceptibility in *Mycobacterium tuberculosis*. *Molecular Microbiology* 69(5): 1316-1329.

Viveiros, M., Martins, M., Rodrigues, L., Machado, D., Couto, I., Ainsa, J. and Amaral, L. (2012). Inhibitors of mycobacterial efflux pumps as potential boosters for anti-tubercular drugs.

Walsh, C. (2003). Where will new antibiotics come from? *Nature Reviews Microbiology* 1(1): 65-70.

Wang, L., Slayden, R. A., Barry, C. E., 3rd and Liu, J. (2000). Cell wall structure of a mutant of *Mycobacterium smegmatis* defective in the biosynthesis of mycolic acids. *Journal of Biological Chemistry* 275(10): 7224-7229.

Wang, Y., Huang, Y., Xue, C., He, Y. and He, Z.-G. (2011). ClpR protein-like regulator specifically recognizes RecA protein-independent promoter motif and broadly regulates expression of DNA damage-inducible genes in mycobacteria. *Journal of Biological Chemistry* 286(36): 31159-31167.

Wards, B. J. and Collins, D. M. (1996). Electroporation at elevated temperatures substantially improves transformation efficiency of slow-growing mycobacteria. *FEMS Microbiology Letters* 145(1): 101-105.

Warner, D. F. (2010). The role of DNA repair in *M. tuberculosis* pathogenesis. *Drug Discovery Today: Disease Mechanisms* 7(1): e5-e11.

Warner, D. F. and Mizrahi, V. (2011). Making ends meet in mycobacteria. *Molecular Microbiology* 79(2): 283-287.

Warner, D. F., Ndwandwe, D. E., Abrahams, G. L., Kana, B. D., Machowski, E. E., Venclovas, Č. and Mizrahi, V. (2010). Essential roles for *imuA*'-and *imuB*-encoded accessory factors in DnaE2-dependent mutagenesis in *Mycobacterium tuberculosis*. *Proceedings of the National Academy of Sciences* 107(29): 13093-13098.

WHO (2014). *Global tuberculosis report.* Geneva: WHO, 2014, Available at http://www.who.int/tb/publications/global_report/en/ (accessed 10 November 2014)

Williams, K. J. and Duncan, K. (2007). Current strategies for identifying and validating targets for new treatment-shortening drugs for TB. *Current Molecular Medicine* 7(3): 297-307.

Wivagg, C. N., Bhattacharyya, R. P. and Hung, D. T. (2014). Mechanisms of β-lactam killing and resistance in the context of *Mycobacterium tuberculosis*. *The Journal of Antibiotics*.

Wright, G. D. (2005). Bacterial resistance to antibiotics: enzymatic degradation and modification. *Advanced Drug delivery Reviews* 57(10): 1451-1470.

Xu, X., Vilchèze, C., Av-Gay, Y., Gómez-Velasco, A. and Jacobs, W. R. (2011). Precise null deletion mutations of the mycothiol synthesis genes reveal their role in isoniazid and ethionamide resistance in *Mycobacterium smegmatis*. *Antimicrobial Agents and Chemotherapy* 55(7): 3133-3139.

Young, D. B., Gideon, H. P. and Wilkinson, R. J. (2009). Eliminating latent tuberculosis. *Trends in Microbiology* 17(5): 183-188.

Young, K., Jayasuriya, H., Ondeyka, J. G., Herath, K., Zhang, C., Kodali, S., Galgoci, A., Painter, R., Brown-Driver, V. and Yamamoto, R. (2006). Discovery of FabH/FabF inhibitors from natural products. *Antimicrobial Agents and Chemotherapy* 50(2): 519-526.

Yuan, Y., Zhu, Y., Crane, D. D. and Barry III, C. E. (1998). The effect of oxygenated mycolic acid composition on cell wall function and macrophage growth in *Mycobacterium tuberculosis*. *Molecular Microbiology* 29(6): 1449-1458.

Zahrt, T. C. and Deretic, V. (2000). An essential two-component signal transduction system in *Mycobacterium tuberculosis*. *Journal of Bacteriology* 182(13): 3832-3838.

Zapun, A., Contreras-Martel, C. and Vernet, T. (2008). Penicillin-binding proteins and β-lactam resistance. *FEMS Microbiology Reviews* 32(2): 361-385.

Zechini, B. and Versace, I. (2009). Inhibitors of multidrug resistant efflux systems in bacteria. *Recent Patents on Anti-Infective Drug Discovery* 4(1): 37-50.

Zhang, Y., Heym, B., Allen, B., Young, D. and Cole, S. (1992). The catalase—peroxidase gene and isoniazid resistance of *Mycobacterium tuberculosis*.

Zhang, Y. and Yew, W. (2009). Mechanisms of drug resistance in *Mycobacterium tuberculosis The International Journal of Tuberculosis and Lung Disease* 13(11): 1320-1330.

Zuber, B., Chami, M., Houssin, C., Dubochet, J., Griffiths, G. and Daffe, M. (2008). Direct visualization of the outer membrane of mycobacteria and corynebacteria in their native state. *Journal of Bacteriology* 190(16): 5672-5680.

Zumla, A. I., Gillespie, S. H., Hoelscher, M., Philips, P. P., Cole, S. T., Abubakar, I., McHugh, T. D., Schito, M., Maeurer, M. and Nunn, A. J. (2014). New antituberculosis drugs, regimens, and adjunct therapies: needs, advances, and future prospects. *The Lancet Infectious Diseases* 14(4): 327-340.